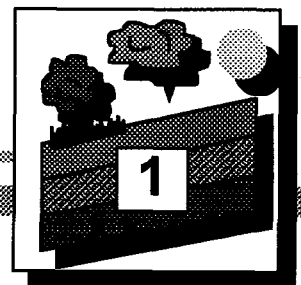
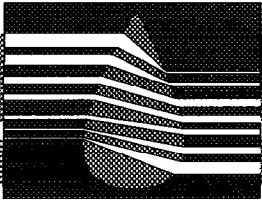


***ICARD WORKSHOP:
Dry Covers for Mine
Tailings and Waste Rock***

Dr. Ward Wilson
Dr. Michel Aubertin
Dr. Ernest Yanful

Vancouver - June 1, 1997



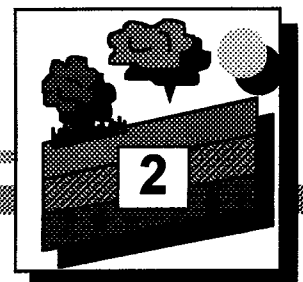


Decommissioning of Acid Generating Mine Waste

**Waste
Rock**



Tailings





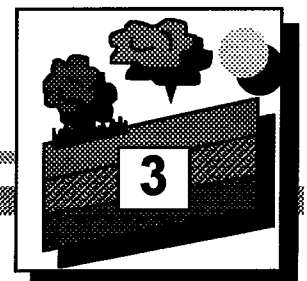
Short-Course Outline:

■ **1.0 Introduction (Wilson)**

- Design Objective and Philosophy
- Overview of Presentation
 - Design Principles
 - Material Characterization
 - Analyses Methods
 - Construction/Performance Monitoring

■ **2.0 Soil-Atmosphere Interactions (Wilson)**

- Introduction / Principles
- Design Concepts
- Case Study / Instrumentation
Slides

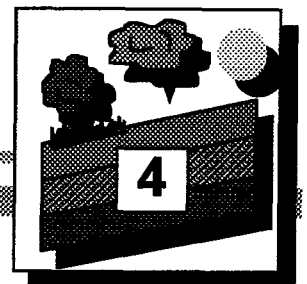




Outline (continued):

■ **3.0 Material Characterization /
Hydrogeologic Analyses
(Aubertin)**

- Introduction
- Unsaturated Flow in Porous Media
- Capillary Barrier Effects
- Applications
- Final Remarks

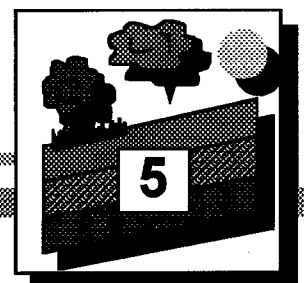


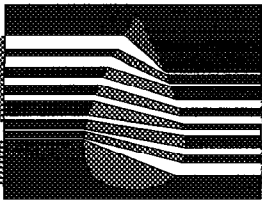


Outline (continued):

■ **4.0 Construction and Performance Monitoring of Covers (Yanful)**

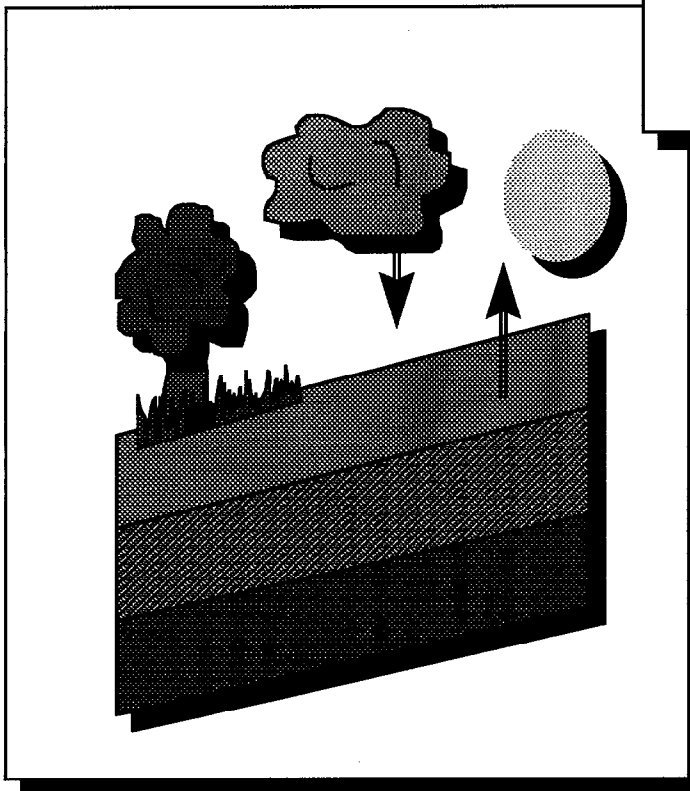
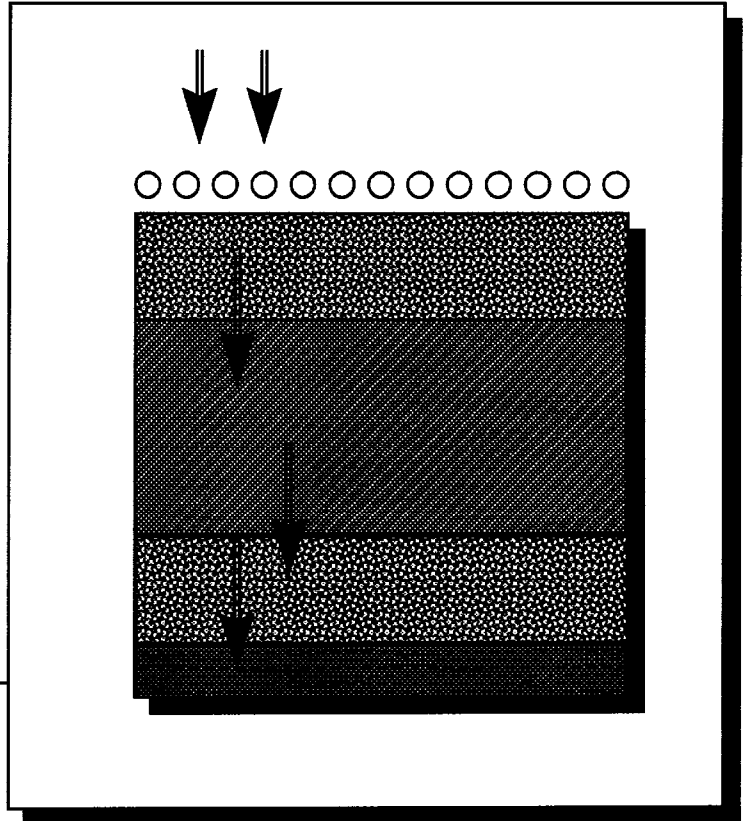
- Introduction
- Placement Requirements
- Definition of Problem Scale
- Material Selection and Inventory
- Cover Placement
- Performance Monitoring



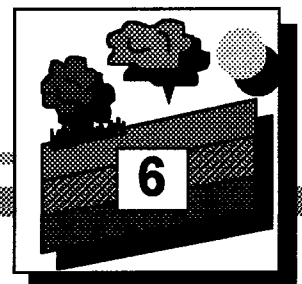


Design Philosophy

**Engineered
Structure**



**Engineered
System**





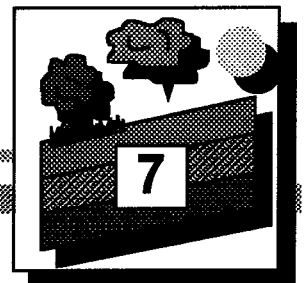
“Dry” Covers - Design Philosophy

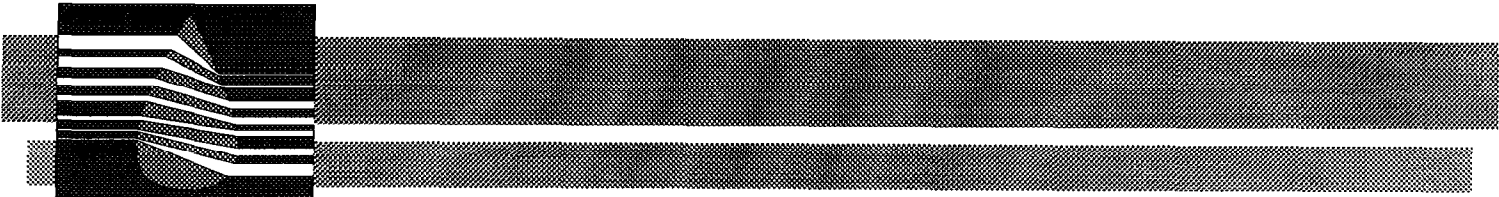
Engineered Structure

- Static
- Capillary
Barrier
- Steady State
- Engineered
Integrity
- Isolation

Engineered System

- Dynamic
- Soil /
Ecosystem
- Coupled
Transient
- Ecological
Stability
- Integration





Unsaturated Soils - Role of SWCC

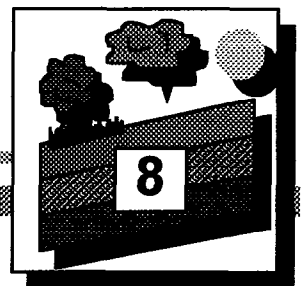
■ Relates Fundamental “States”

- Storage / Stress State
- Energy and Volume

■ Describes Distribution of Fluid Phase

■ Basis for Property Estimation

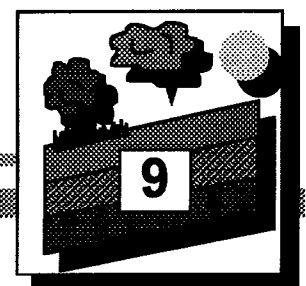
- Hydraulic Conductivity
- Shear Strength





Soil / Environmental Coupling

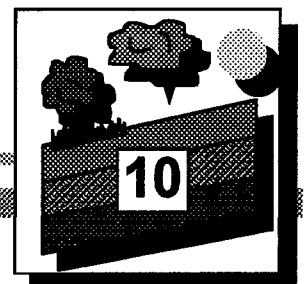
- Actual Evaporation
 - Soil / Climate
- Transpiration
 - Vegetation
 - Soil
 - Climate
- Freeze / Thaw
- Erosion / Stability





Characterization : SWCC and Hydraulic Conductivity

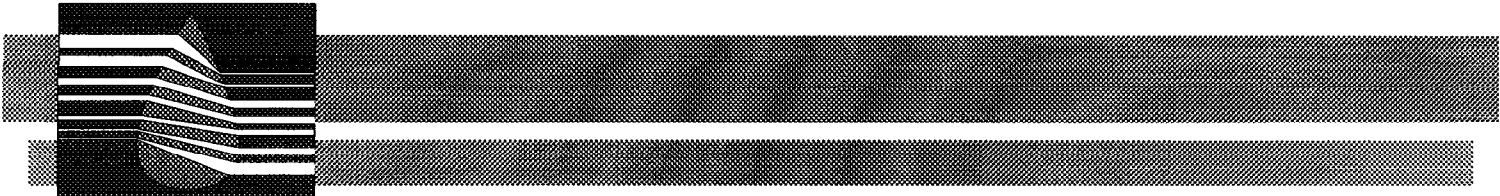
- All Materials (waste/soil)
- Insitu Conditions
(structure and stress state)
- Field Verification
- Effects of Weathering
(wet/dry, freeze/thaw,
vegetation)





Characterization: Environmental Influences

- Climate
 - Micro-Climatic Effects
- Vegetation
 - Root Depth
 - LAI
 - Species Data-Base



Design Methodology

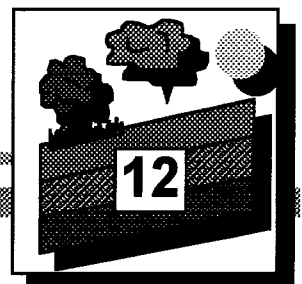
Empirical vs. Rational

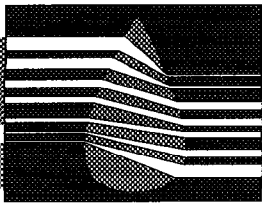
■ Empirical

- Prototype Based
- Experimentally Complex
- Analytically Simple

■ Rationale Design

- Theoretically Based
- Experimentally Simple
- Analytically Complex





ICARD SHORT COURSE:

THEORETICAL PRINCIPLES AND SOIL-ATMOSPHERE INTERACTIONS

**Dr. Ward Wilson,
Associate Professor**

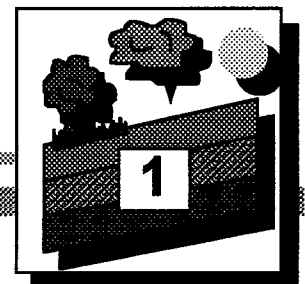
University of Saskatchewan

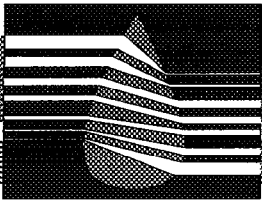
Tel.: 306-966-5373

Fax: 306-966-5427

E-mail: Ward_Wilson@engr.usask.ca

Vancouver - June 1, 1997





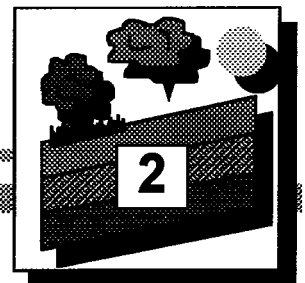
Short-Course Content:

II- THEORETICAL PRINCIPLES AND SOIL-ATMOSPHERE INTERACTIONS

PART I - Introduction
- Principles

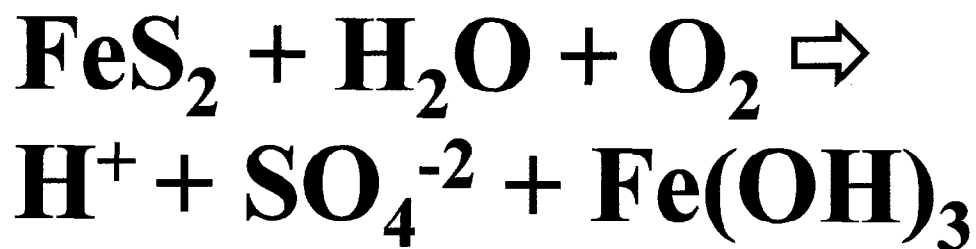
PART II - Design Concepts

PART III - Case Study
- Instrumentation Slides



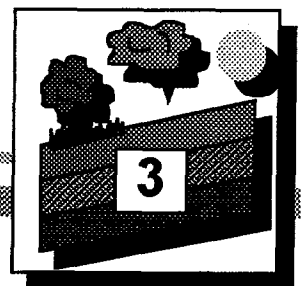


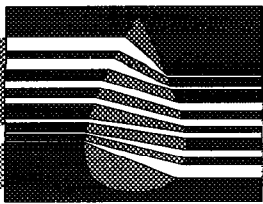
PART I - The Oxidation of Sulphide Minerals may be Summarized as follows:



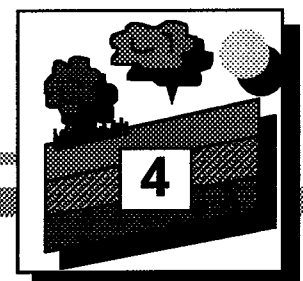
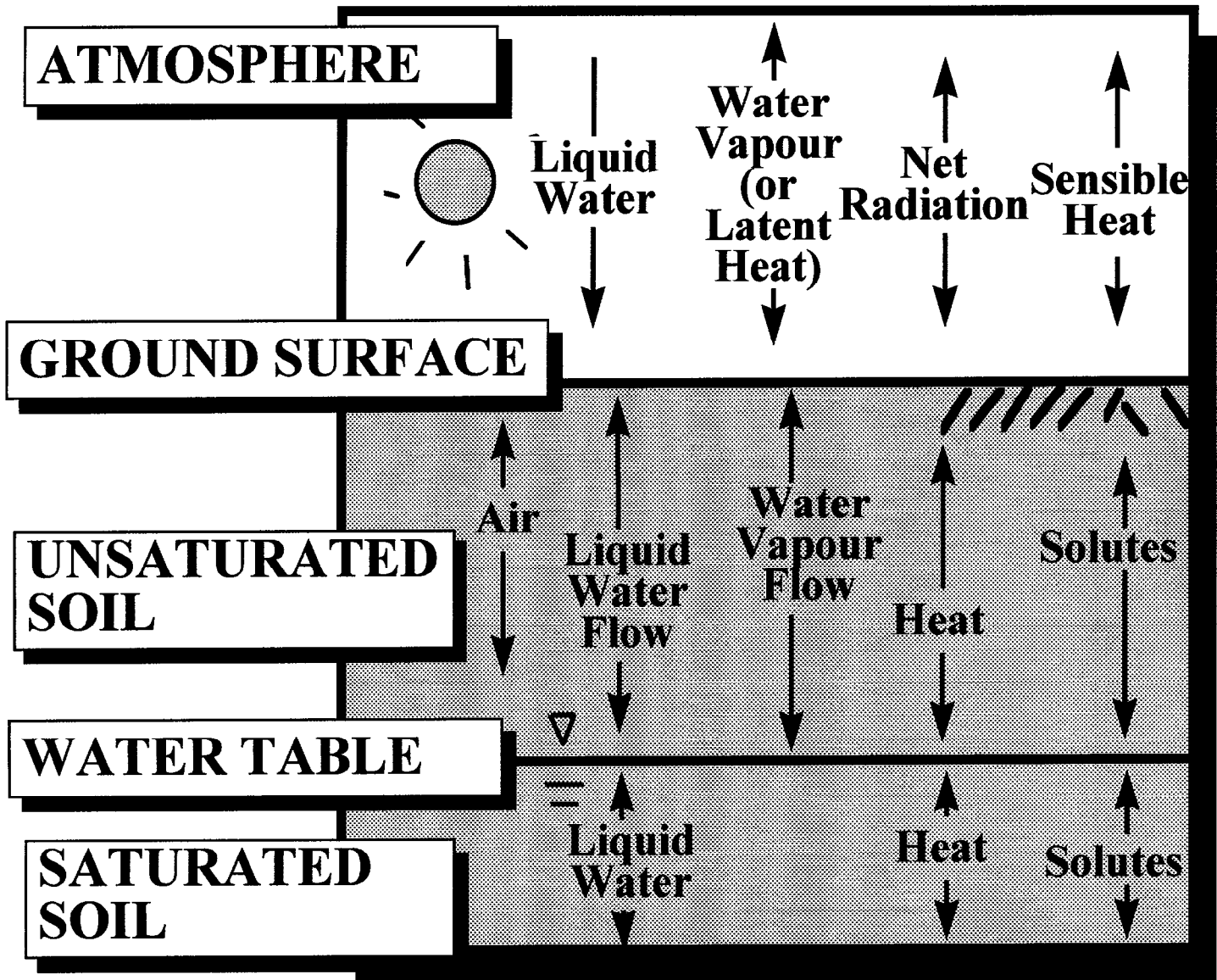
- This reaction may be controlled through the availability of two of the principle reactants:

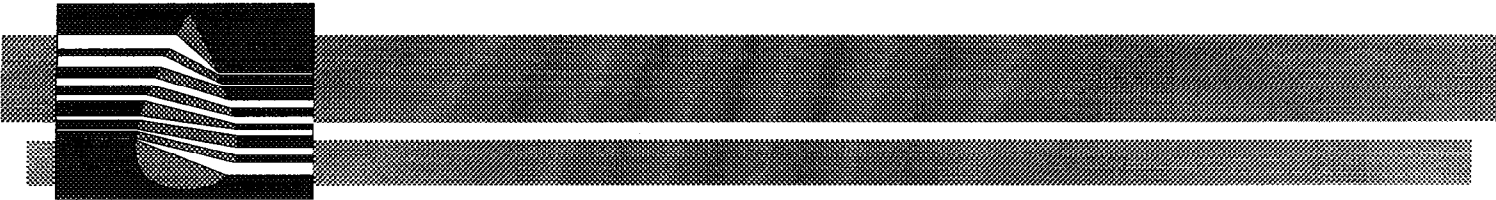
H₂O and O₂





Principles of Flow through Cover Systems





*The Flow of Water and
Oxygen through Tailings,
Waste Rock and Cover
Systems is a Function of the
Degree of Saturation of the
Porous Media*

Gas Flow:

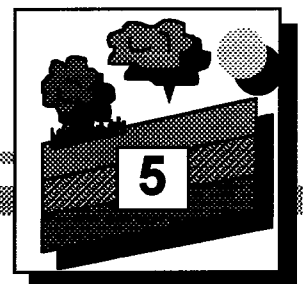
■ Fick's Law

■ $J = D_c \Delta C / \Delta x$

Liquid Flow:

■ Darcy's Law

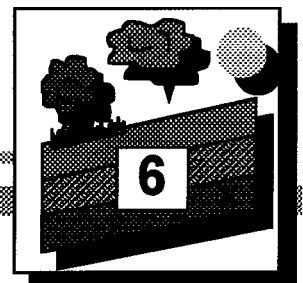
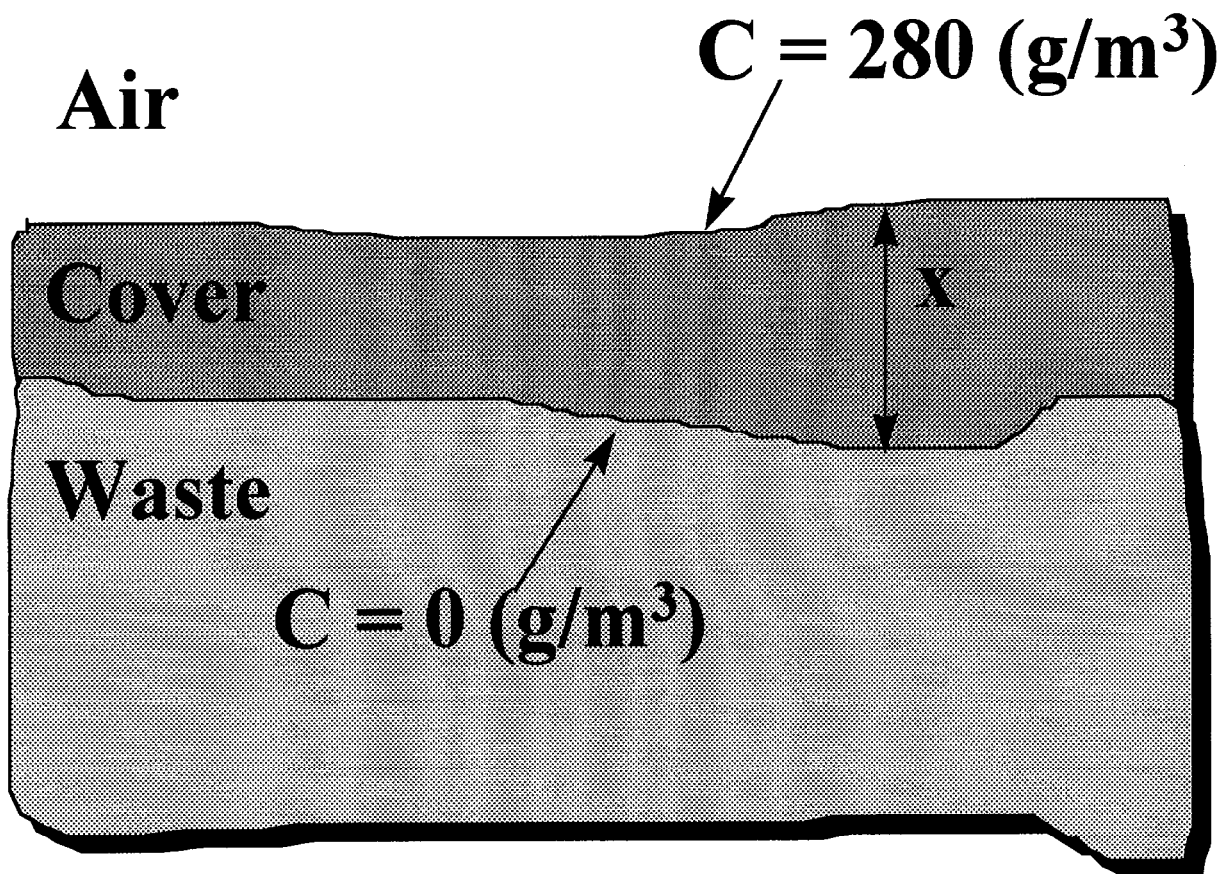
■ $q = k i$



Oxygen Diffusion in a Cover

■ Based on Fick's Law:

$$\text{Mass Flux, } J = D_c \Delta C / \Delta x$$





Darcy's Law: $Q = -kiA$

■ Where:

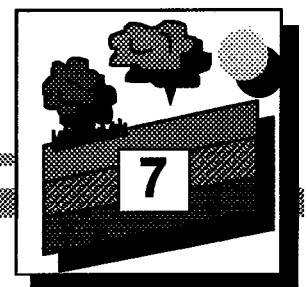
- Q = discharge (m^3)
- A = cross-sectional area
- i = hydraulic gradient = dh/dx
- k = coefficient of permeability

■ Saturated soils

- $k \sim$ constant

■ Unsaturated soils

- k = function of [S , θ , $(u_a - u_w)$]





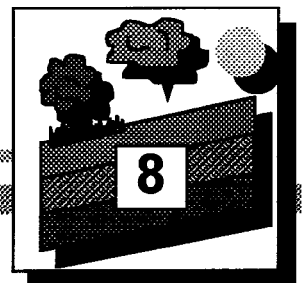
Flow / Storage in Unsaturated Soils

■ FLOW

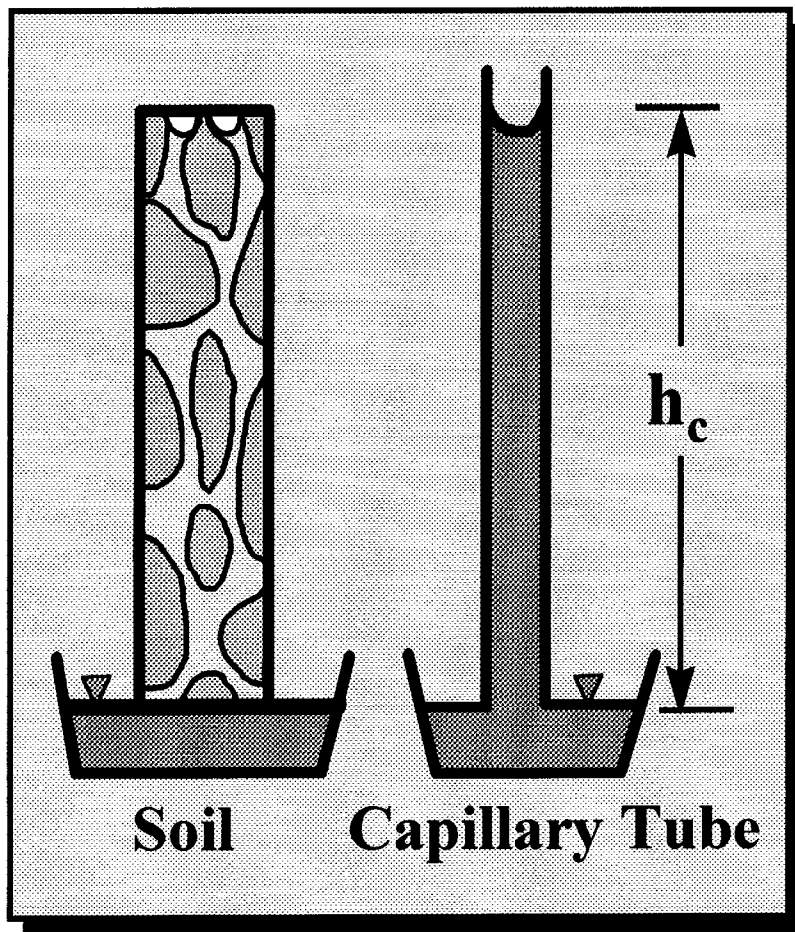
- Darcy's Law
(Hydraulic Conductivity)

■ STORAGE

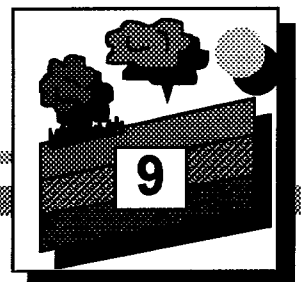
- Soil Water Characteristic
Curve (SWCC)



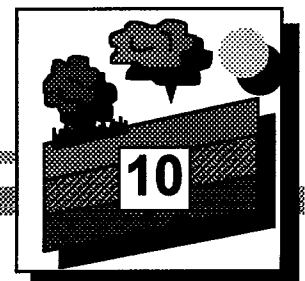
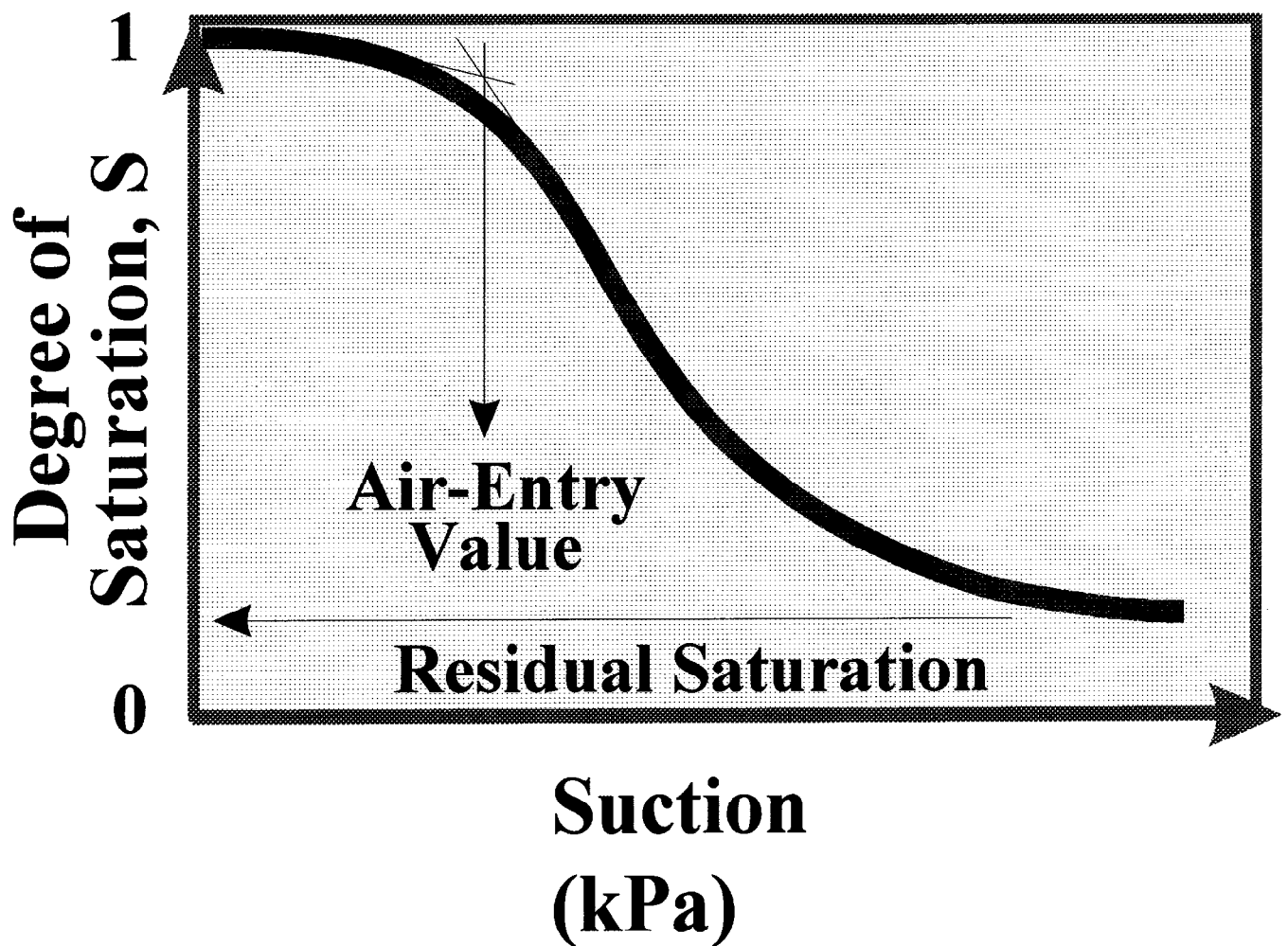
Capillary Model:



$$(u_a - u_w) = 2T_s / r$$



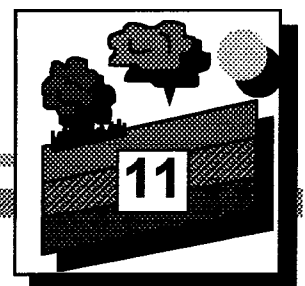
Soil-Water Characteristic Curve (SWCC)

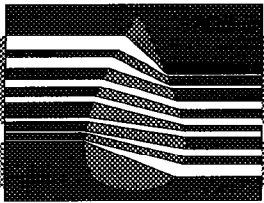




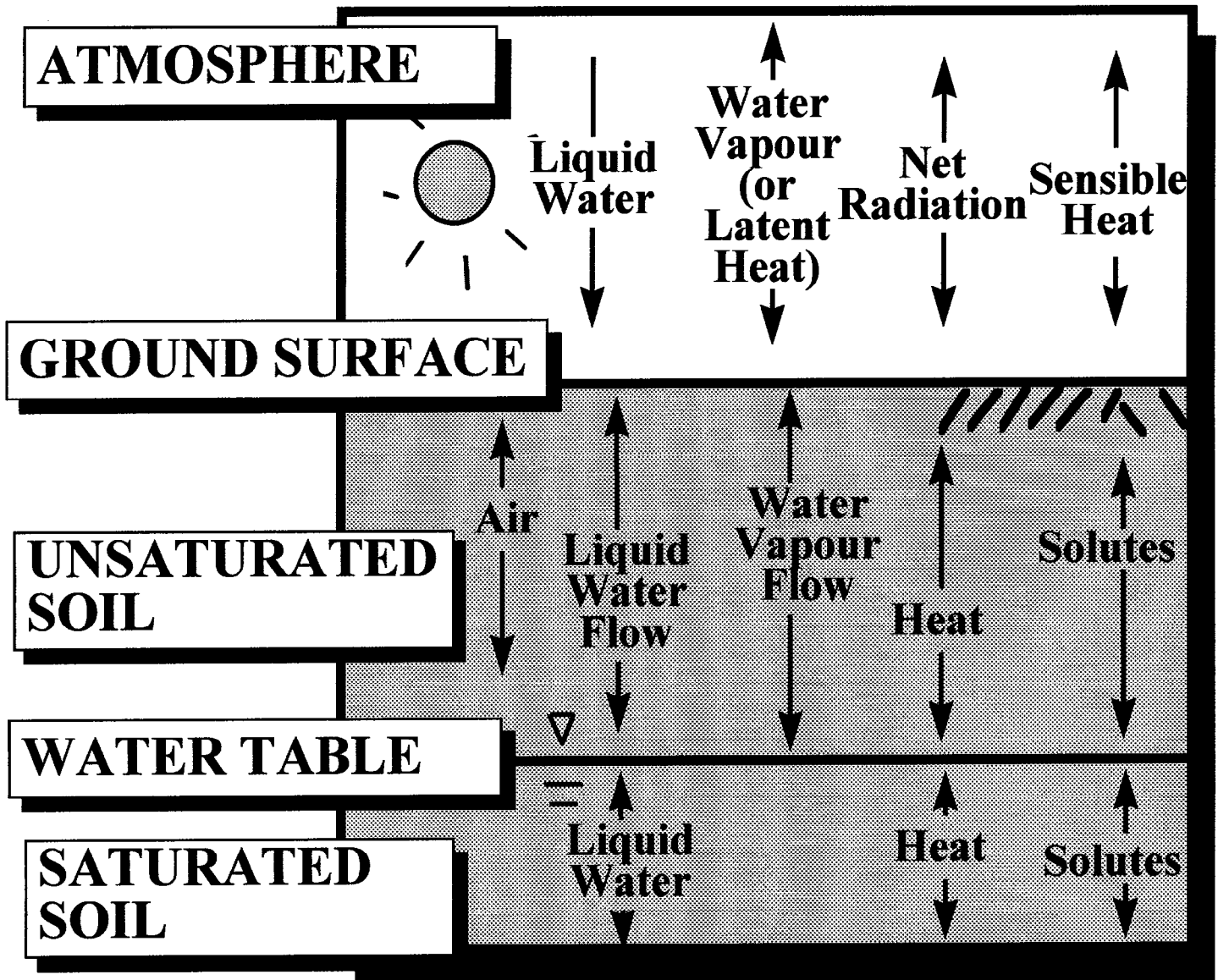
Part II - Design Concepts

- ① Design concepts for zero water flux covers
- ② Design concepts for oxygen limiting covers





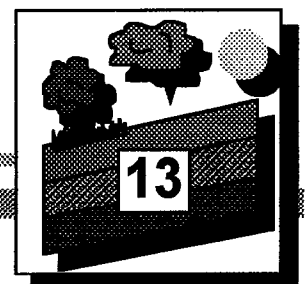
Design Concepts for Zero Water Flux Covers





Soil / Atmosphere Components

- Continuum across soil - atmosphere boundary
- Infiltration - mass transfer
- Evaporation - heat & mass transfer
- Soil properties
- Vegetation
- Runoff
- Oxygen diffusion

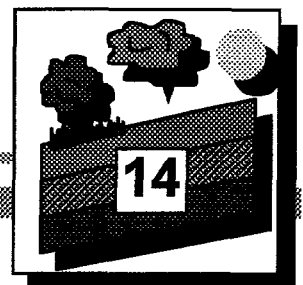




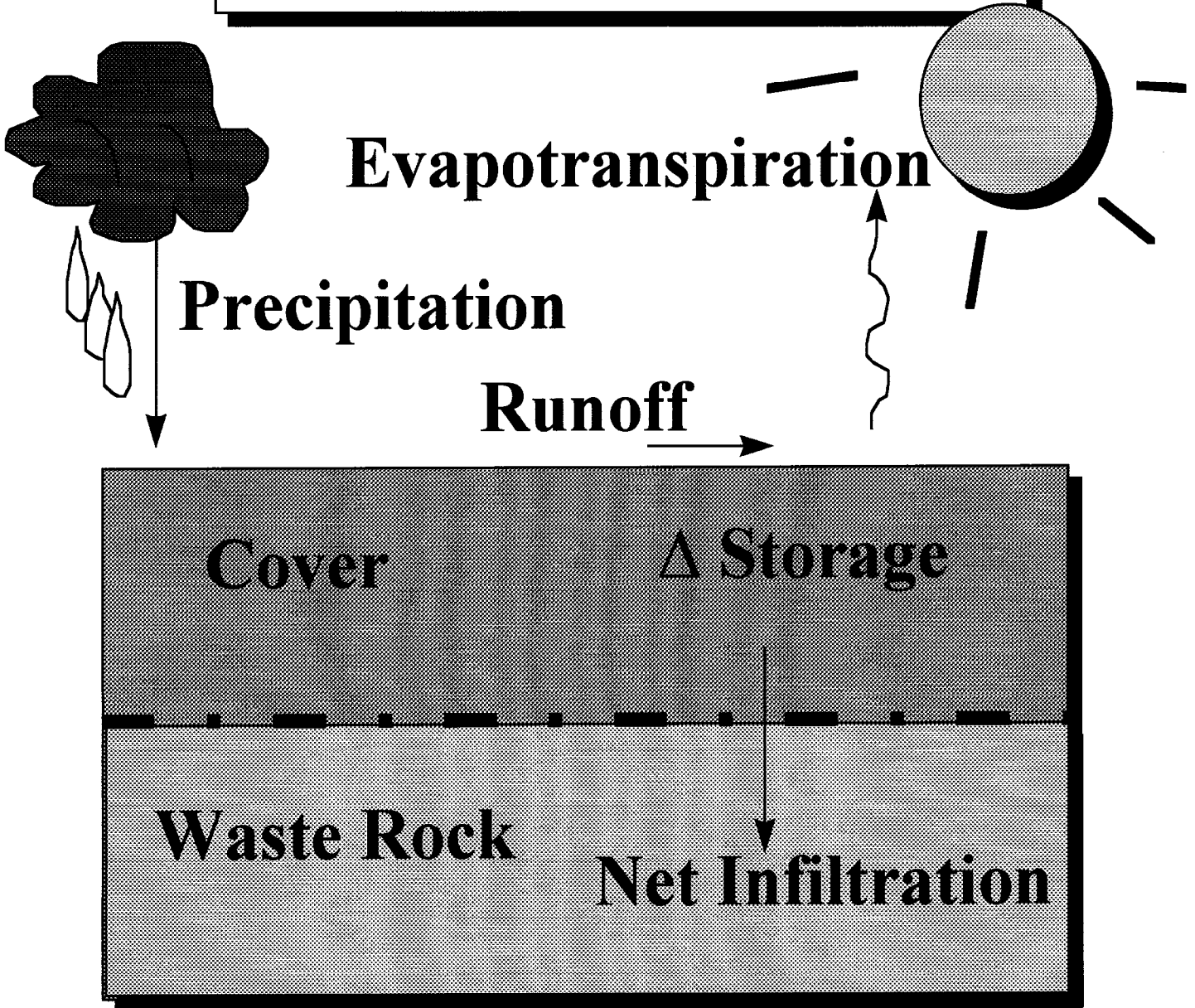
*The Design of Zero Water
Flux Covers Requires
Evaluation of the Heat
and Mass Balances at the
Ground Surface*

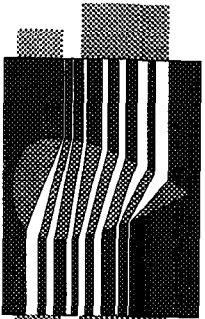
● **Energy Balance**

$$Q_{\text{Net Radiation}} + Q_{\text{Latent Heat}} + Q_{\text{Sensible Heat}} + Q_{\text{Ground Heat}} = 0$$

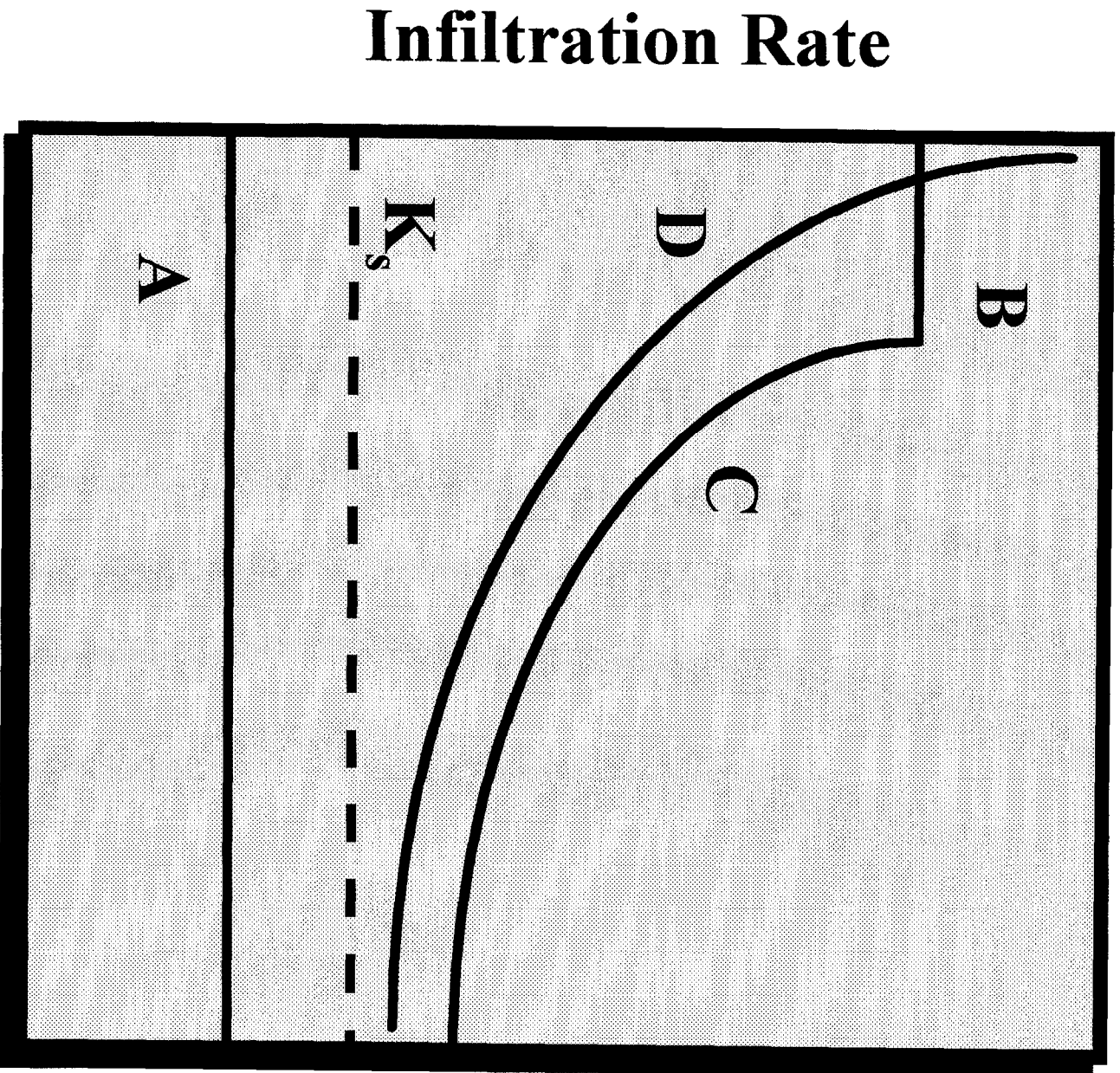



$$\text{Net Infiltration} = P - R - ET - \Delta S$$



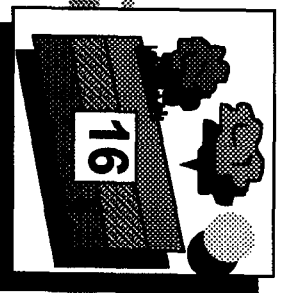


Infiltration versus Time

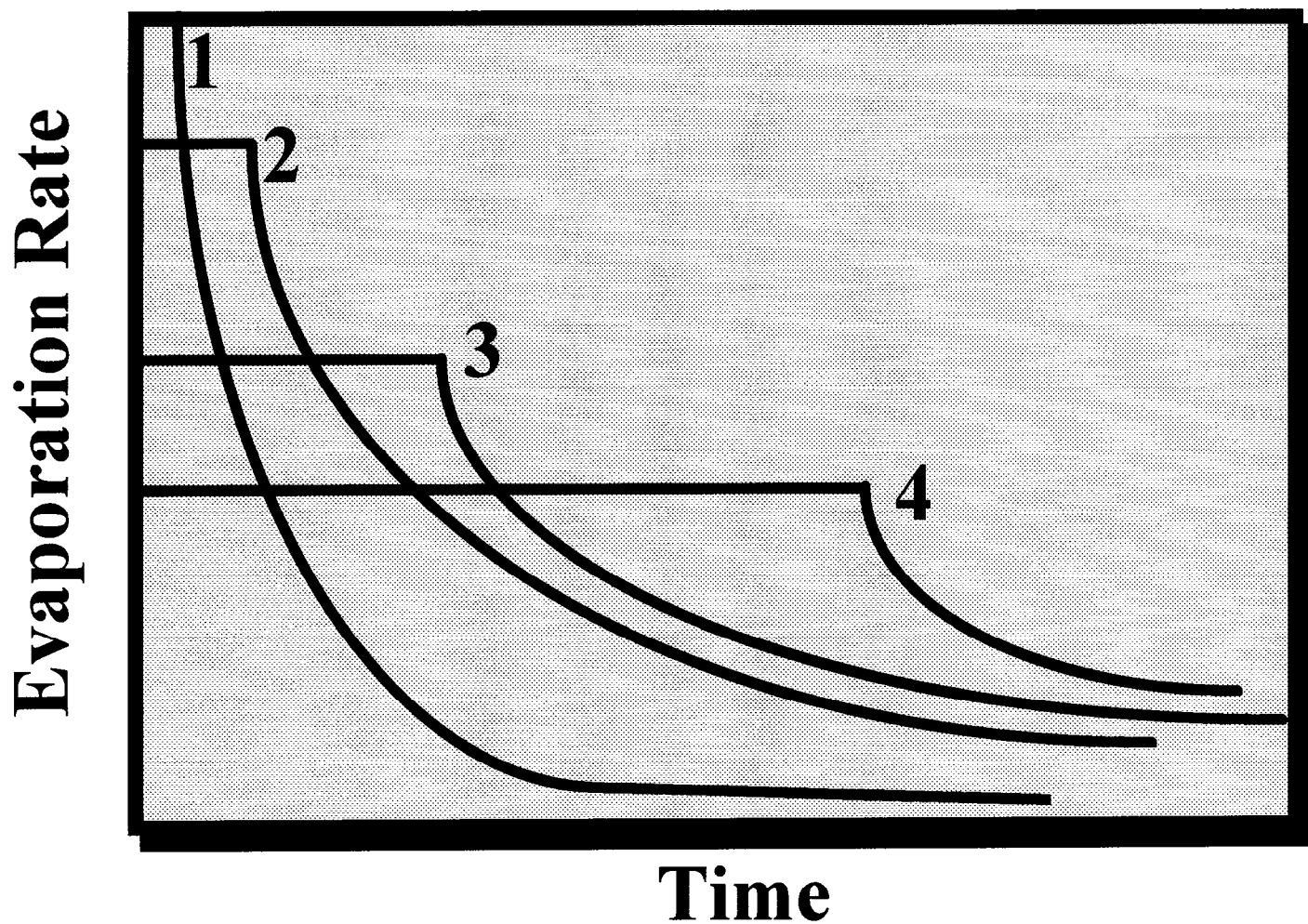


after Mein and
Larsen (1973)

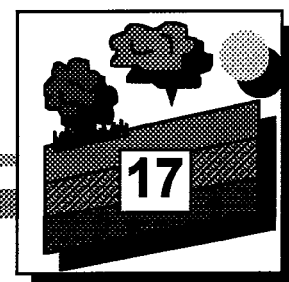
Time



Evaporation versus Time



after Hillel (1980)

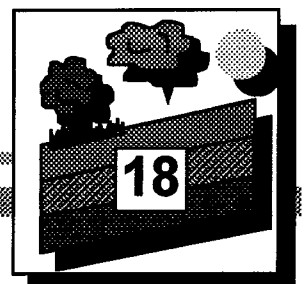




Conventional Methods Available for the Evaluation of Evaporation

- Thornthwaite Method
- Penman Method
- Priestley - Taylor Method
- Complimentary Relationship

**These methods are based on
climatic conditions only**

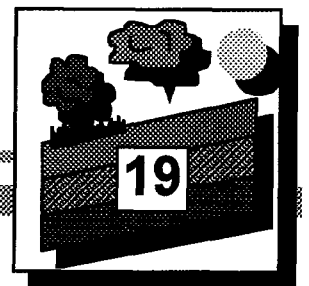




Soil Atmosphere Model

- Climatic
Conditions
- +
- Surface
Characteristics

Soil Properties
Groundwater Conditions
Vegetation





Soil / Atmosphere Model for Evaluating Evaporative Fluxes

■ Mass

Transfer

Equation:

- Darcy's Law for liquid flow
- Fick's Law for vapour flow
- Phase equilibrium assumed

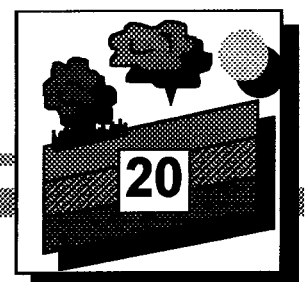
■ Heat Flow

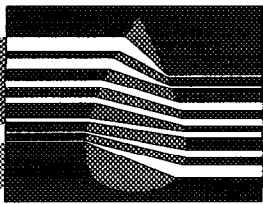
Equation:

- Conductive heat flux
- Latent heat flux

■ Evaporative Fluxes:

- Dalton's Law
- Modified Penman formulation





Proposed Soil- Atmosphere Model

For Moisture Flow:

$$\blacksquare \delta h_w / \delta \tau = C_w^1 \delta / \delta y [k_w \delta h_w / \delta y] + C_w^2 \delta / \delta y [D_v \delta P_v / \delta y]$$

Phase Coupling:

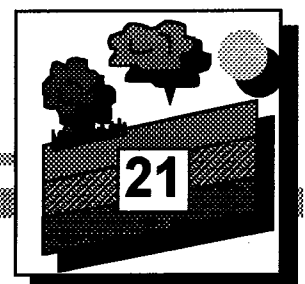
$$P_v / P_o = e [\psi M_w g / RT] \quad (\text{Relative Humidity})$$

For Heat Flow:

$$C_v \rho_s \delta T / \delta t = \delta / \delta y [\lambda \delta T / \delta y] - L_v [(P + P_v) / P] \delta / \delta y [D_v \delta P_v / \delta y]$$

Atmospheric Coupling:

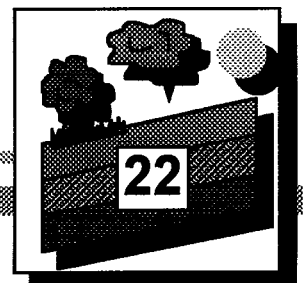
$$\bullet E = f(u) [P_v \text{ soil} - P_v \text{ air}]$$





Modified Penman Formulation

- The original Penman formulation assumes a fully saturated surface (i.e., Potential Evaporation)
- The combination approach used by Penman may be extended to unsaturated surfaces if the vapour pressure is known





Atmospheric Coupling

● The Penman Method

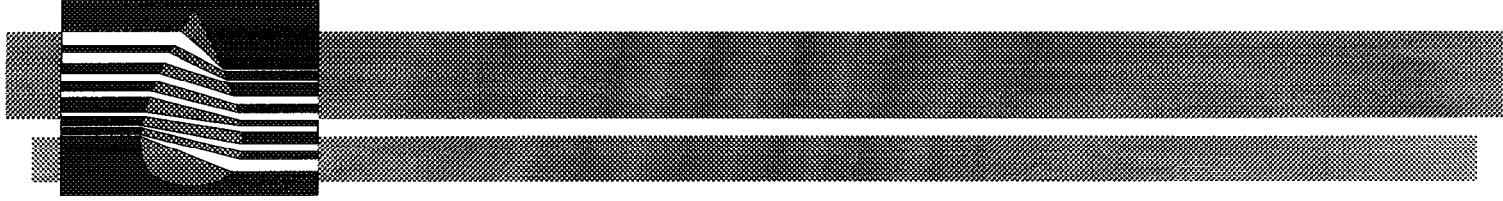
- Assumes a Fully Saturated Surface (i.e., Potential Evaporation)

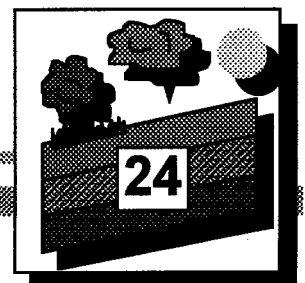
$$E = \frac{\Delta \Theta + \gamma E_a}{\Delta + \gamma}$$

● The Modified Penman Method

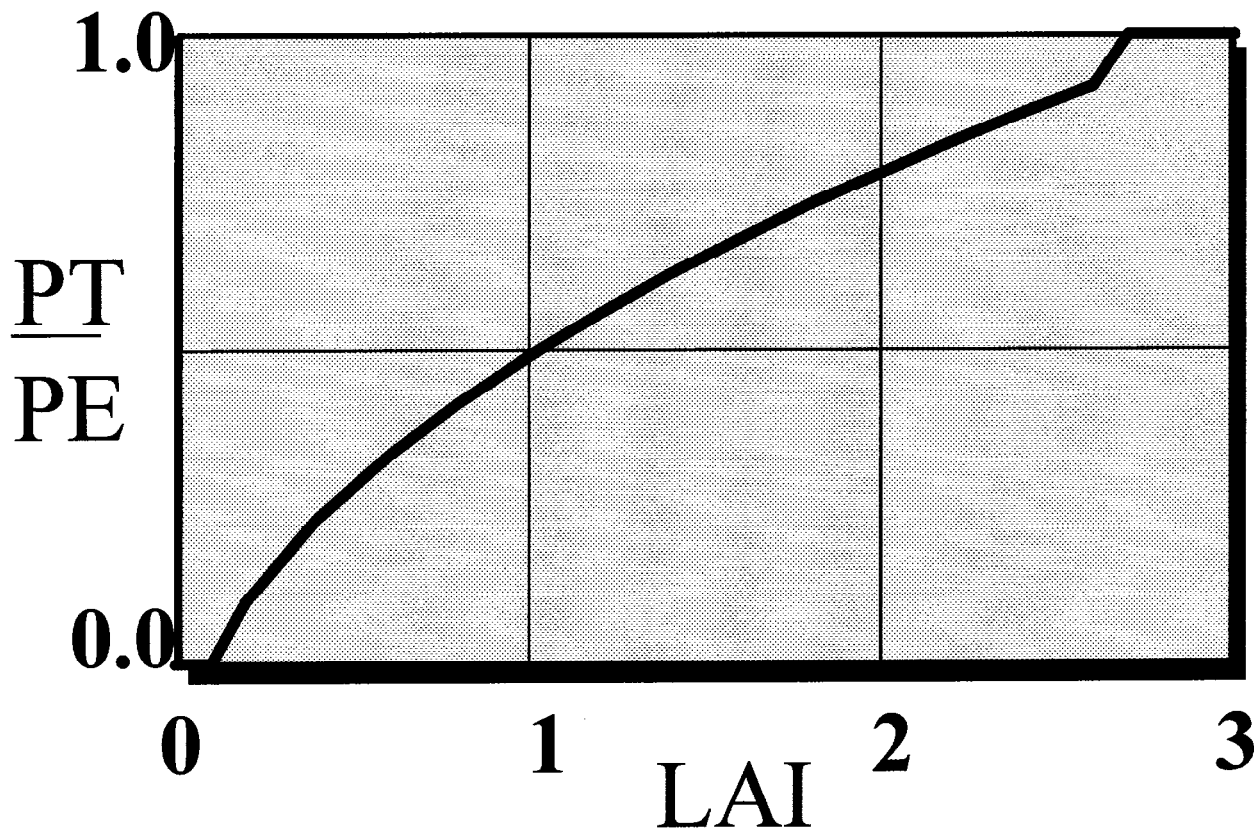
- Extending the Penman Formulation to Unsaturated Soil Surfaces

$$E = \frac{\Delta \Theta + \gamma E_a}{\Delta + A\gamma}$$

- 
- **The Modified Penman Method** is generally applied to bare surfaces to compute **actual evaporation** from the tailings or waste rock. **Transpiration** associated with root water uptake must also be considered if the surface is **vegetated**. The basic concepts for computing transpiration are outlined in the following laboratory experiment.

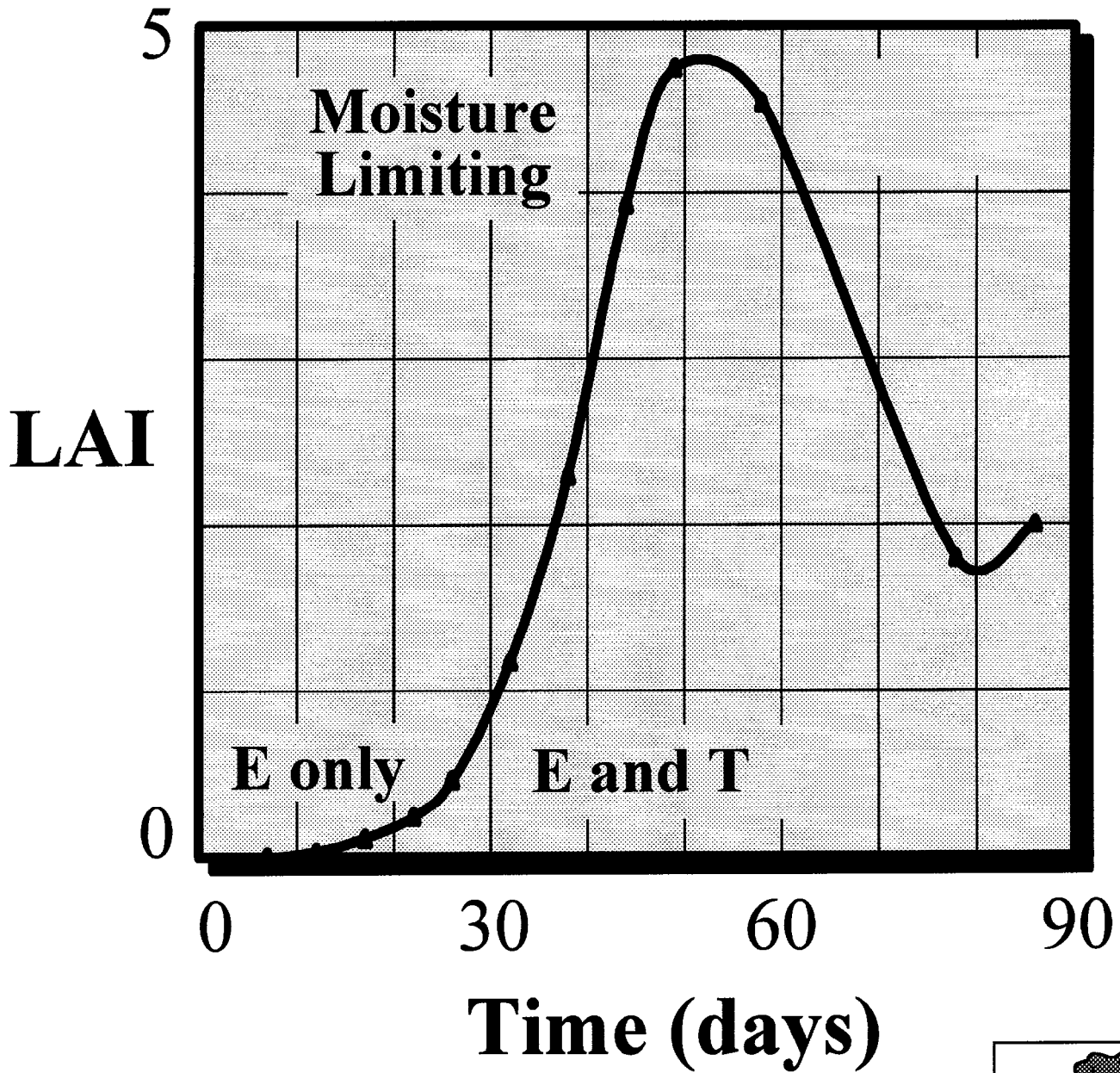


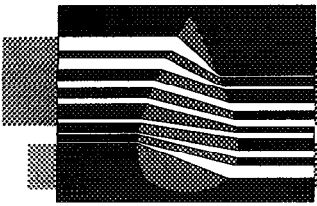
Modifying the PE by the Leaf Area Index



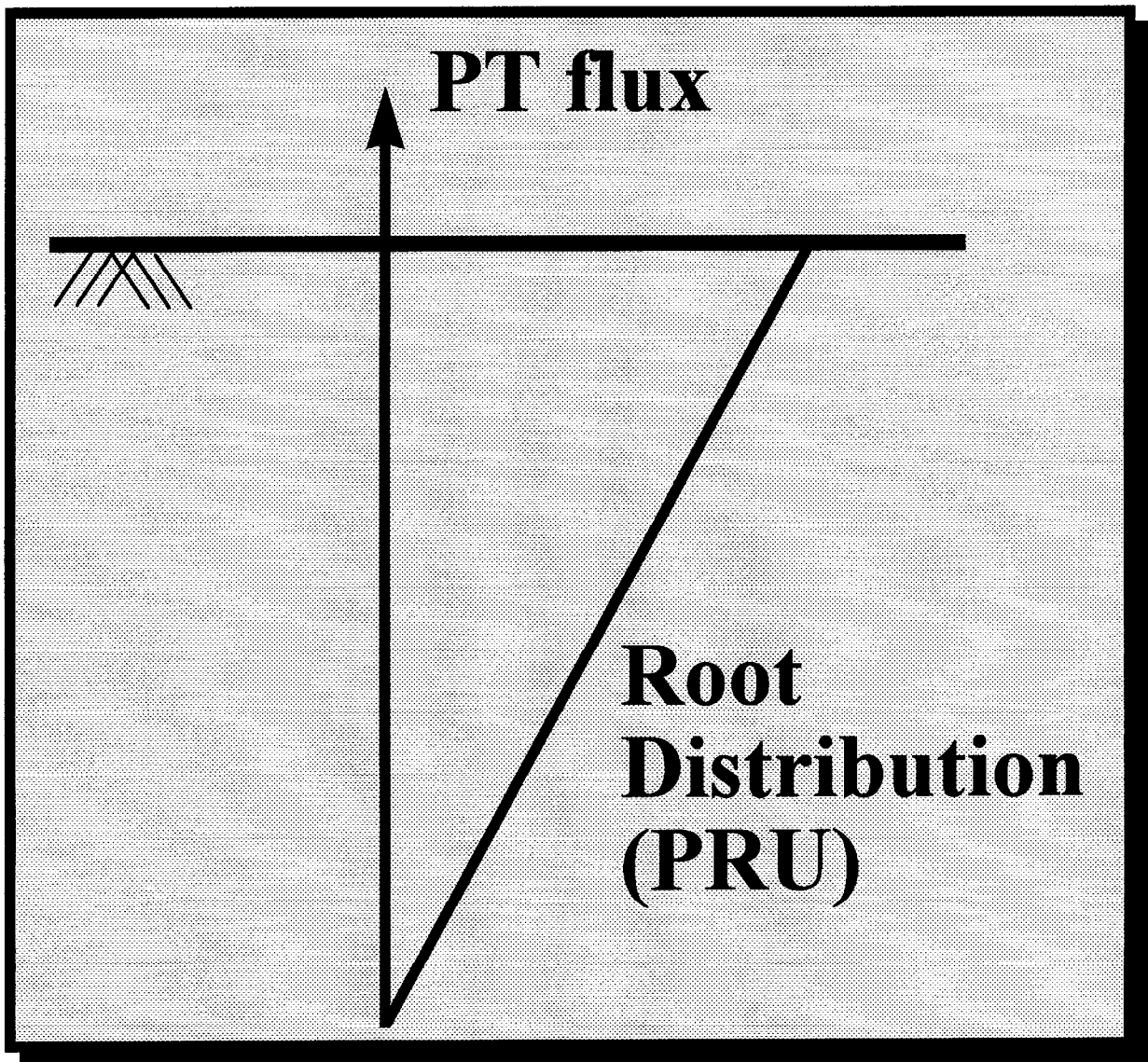
$$\text{LAI} = \frac{\text{Leaf Surface Area}}{\text{Soil Surface Area}}$$

Leaf Area Index



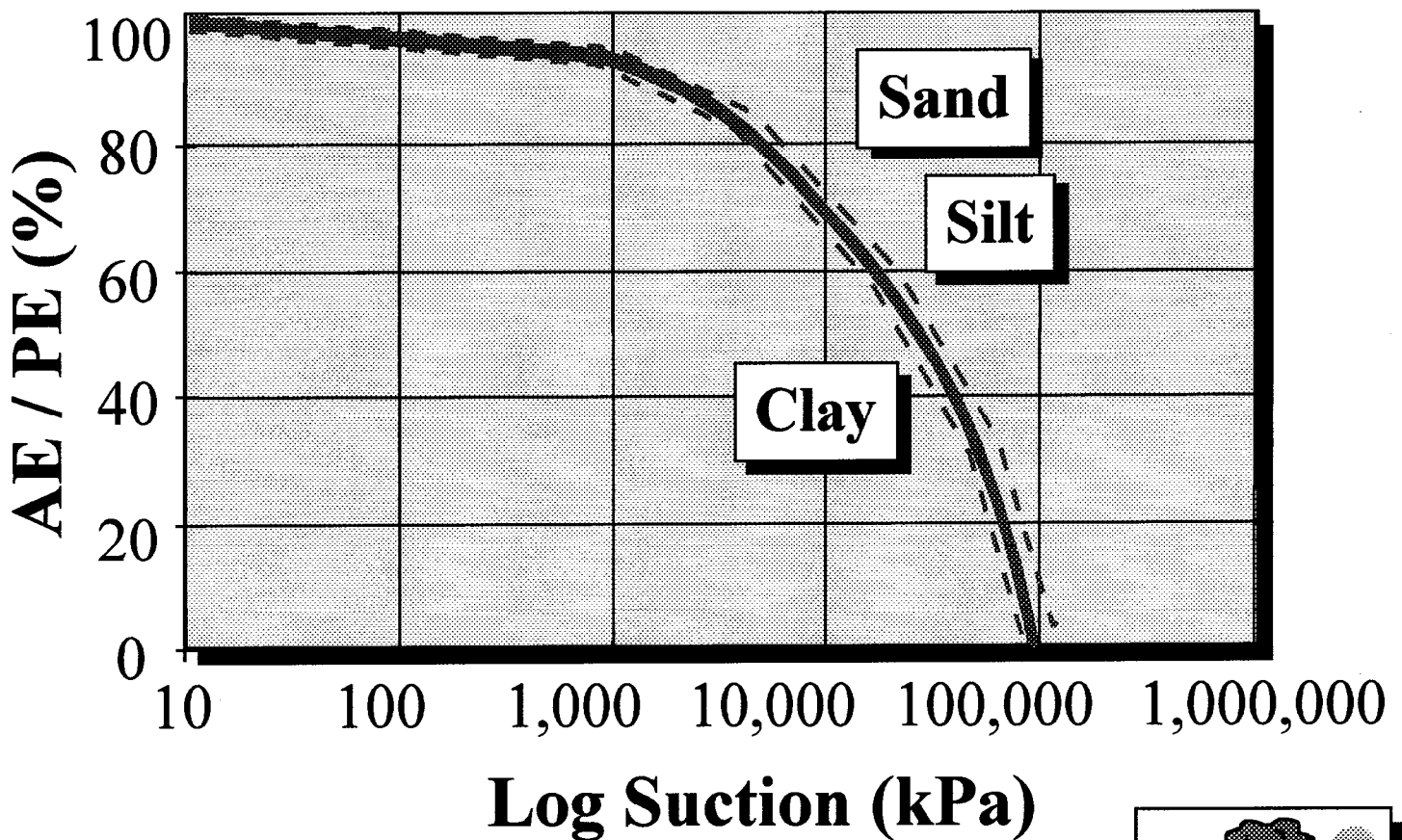


Distribution of PT Through Active Root Zone

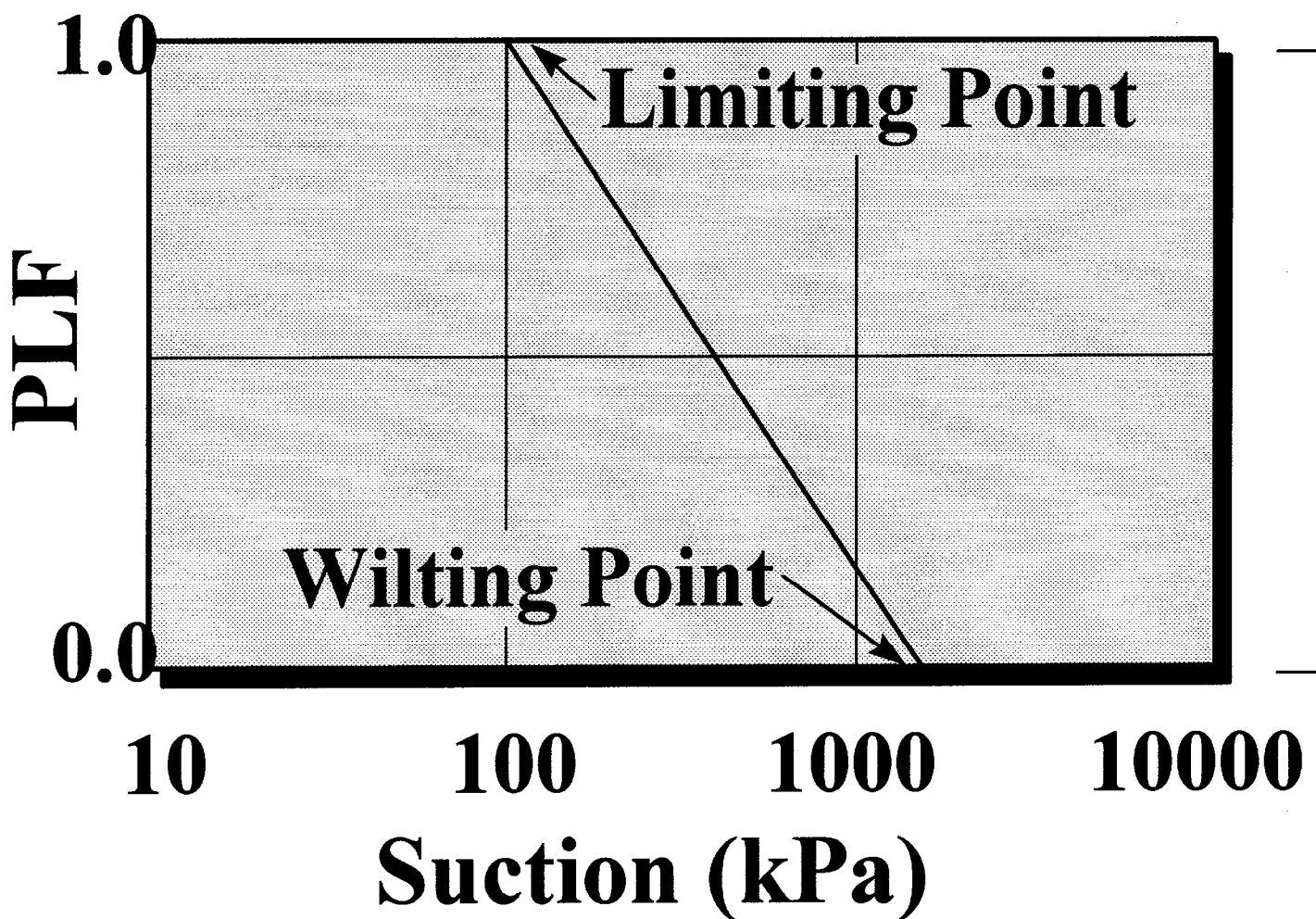


Computation of Upward Flux

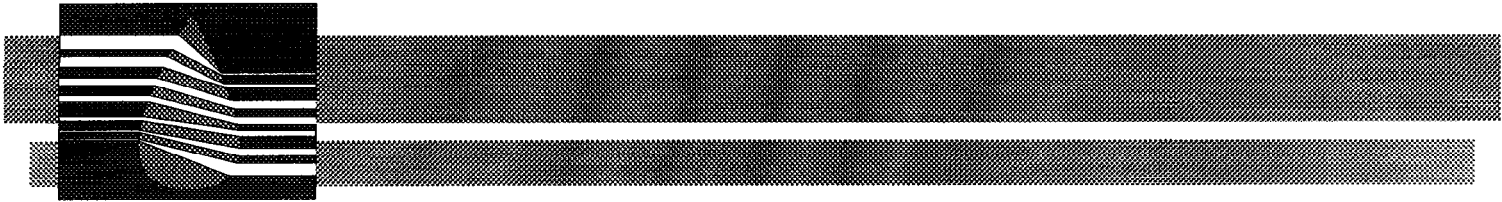
$$\frac{\text{Actual Evaporation, } AE}{\text{Potential Evaporation, } PE}$$



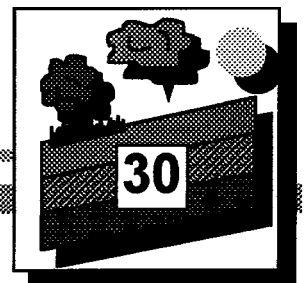
Reducing the PRU based on the PLF



$$AT = PT * PLF$$



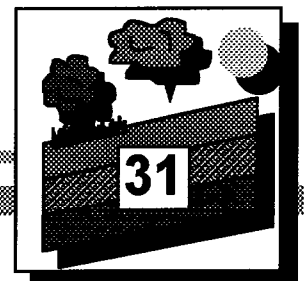
■ In general, the principle design objective for **Zero or Low Water Flux Covers** is to optimize storage and evapotranspiration. Runoff is also a major consideration.





Required Conditions for Zero Water Flux Covers

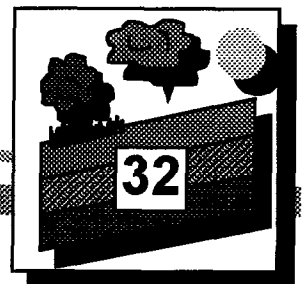
- ① Arid climates where potential evaporation greatly exceeds precipitation.
- ② SWCC which features a high storage capacity. Well graded silty soils tend to function best. Clay rich or compacted soils are undesirable. (continued...)





Required Condition for Zero Water Flux Covers (Con't)

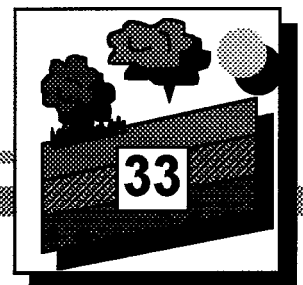
- ③ Moderately low hydraulic conductivity in the range of 10^{-4} cm/s to 10^{-6} cm/s.
- ④ Thick soil layers. Generally 1.0 m is an absolute minimum.
- ⑤ Deep rooted vegetation.
- ⑥ High, well-drained topographies.
- ⑦ Maximum runoff, provided erosion control permits.





Design Concepts for Oxygen Limiting Covers

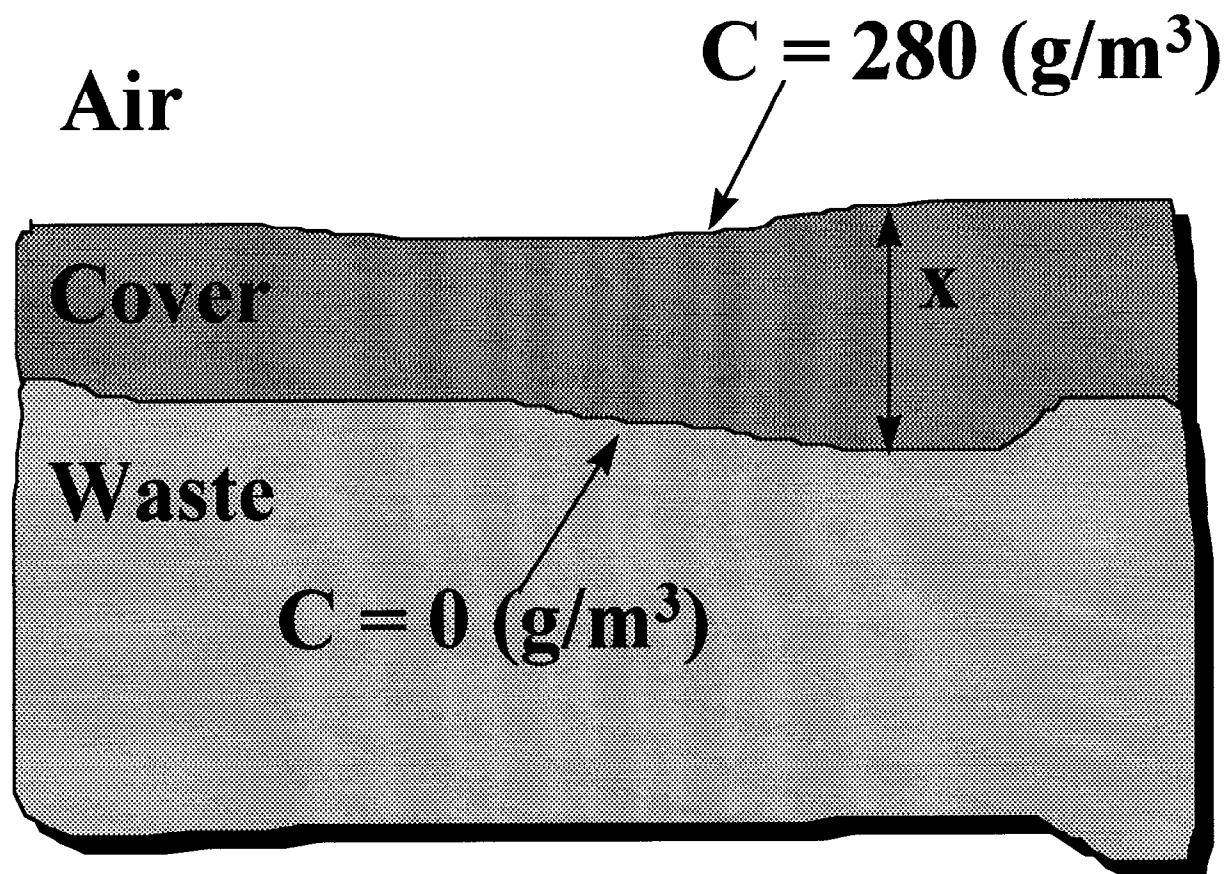
- The basic objective of the design is to maintain the highest degree of **saturation** within the cover profile.



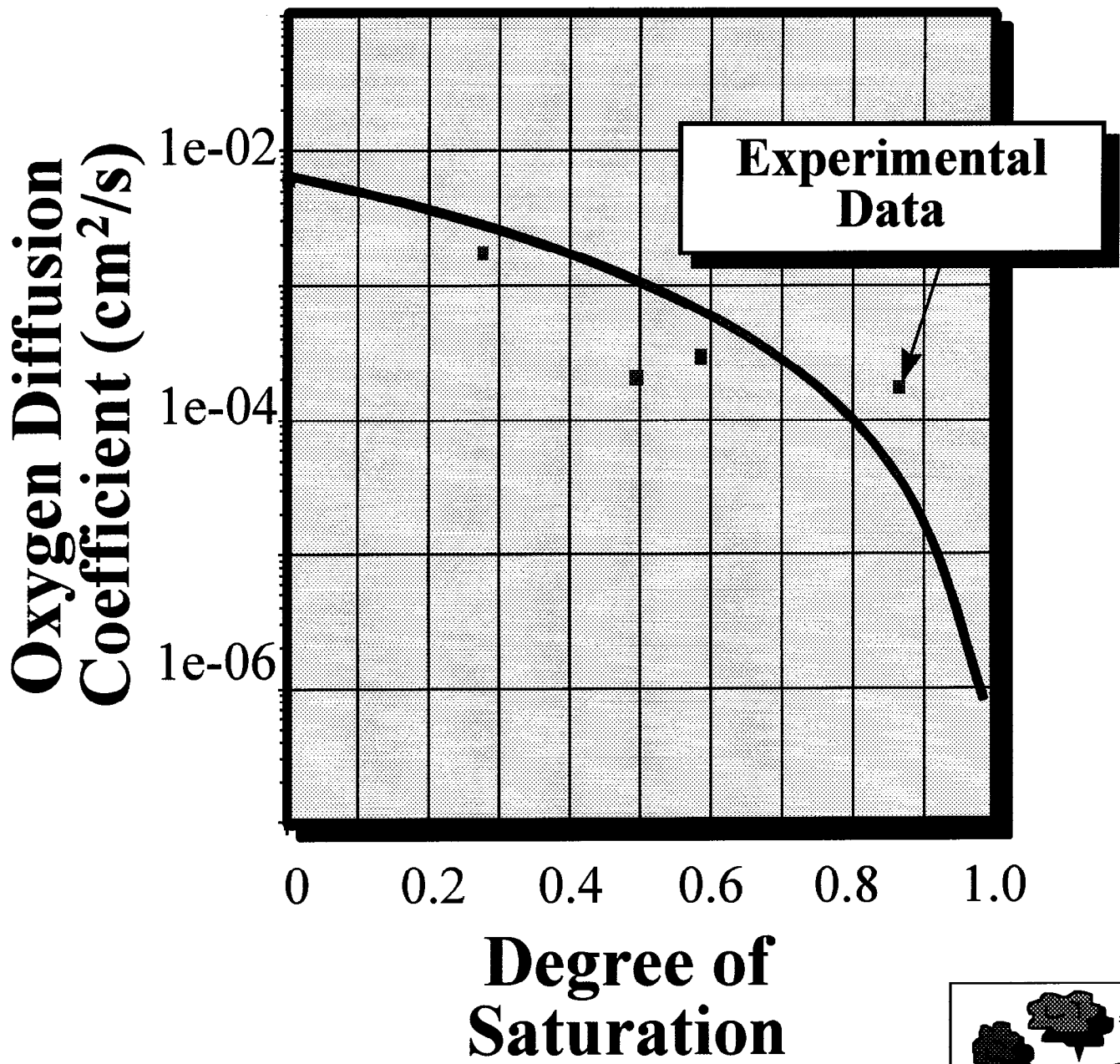
Oxygen Diffusion in a Cover

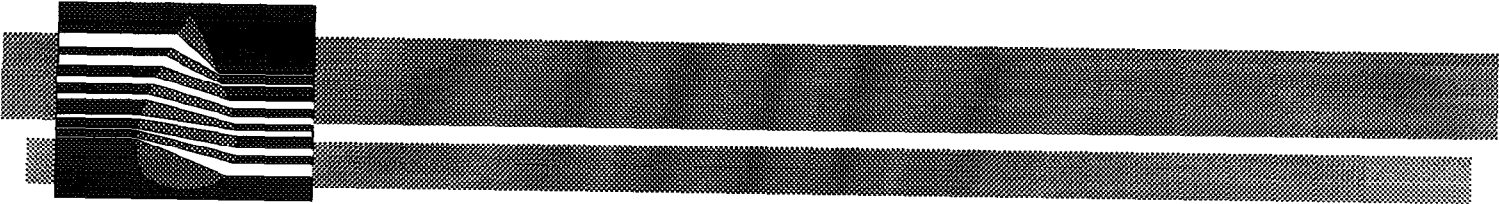
■ Based on Fick's Law:

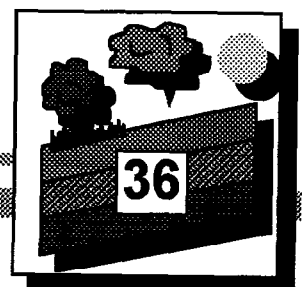
$$\text{Mass Flux, } J = D_c \Delta C / \Delta x$$

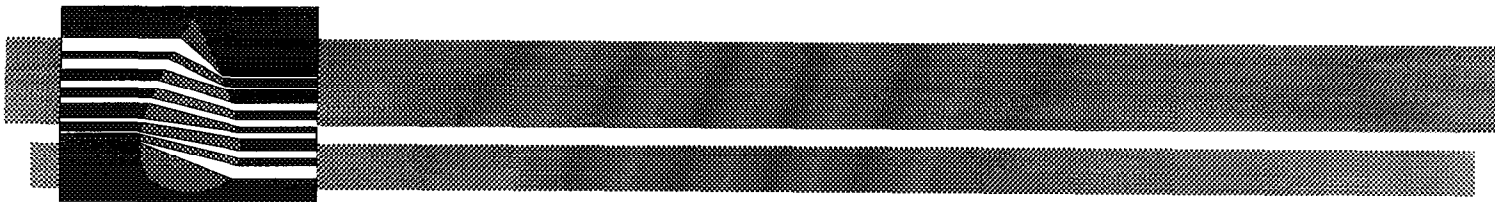


Oxygen Diffusion vs. Saturation



- 
- **Oxygen Limiting Covers** are Best Suited to Humid or Wet Climates. Some General Principles for Design are ...



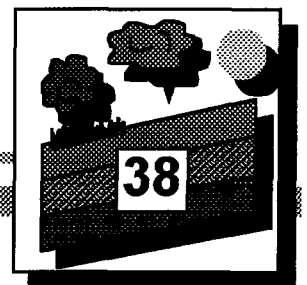
- 
- ① Precipitation exceeds potential evaporation.
 - ② Fine grained soils with a high air entry value are best. Typically, the AEV should exceed 50 kPa.
 - ③ Decreasing the saturated hydraulic conductivity improves performance.
 - ④ A loose protective cover is required to buffer against desiccation (i.e., high k_{sat} and high storage).
 - ⑤ Topographic highs and rapid runoff decrease the potential to maintain saturation.
 - ⑥ Deep rooted vegetation is undesirable.



Part III - Field Case Study

① Field case studies for covers in arid and humid climates

- Equity Silver Mine,
British Columbia, Canada
(Wet / Oxygen Limiting)
- Kidston Gold Mine,
Queensland, Australia
(Arid / Zero Flux)



REFERENCES

- Feddes, R.A., Kowalik, P.J., and Zaradny, H., 1978. *Simulation of Field Water Use and Crop Yield*. John Wiley and Sons, Toronto. 188 pp.
- Granger, R.J., 1989. An Examination of the Concept of Potential Evaporation. *Journal of Hydrology*, 111: 9-19.
- MEND, 1993. *SoilCover User's Manual for Evaporative Flux Model*. University of Saskatchewan, Saskatoon, Saskatchewan, Canada.
- Prasad, R., 1988. A Linear Root Uptake Model. *Journal of Hydrology*, 99: 297-306.
- Ritchie, J. T., 1972. Model for Predicting Evaporation from a Row Crop with Incomplete Cover. *Water Resources Research*, 8 (5): 1204-1213.
- Wilson, G.W., 1990. *Soil Evaporative Fluxes for Geotechnical Engineering Problems*. Ph.D. Thesis, Department of Civil Engineering, University of Saskatchewan, Saskatoon, Saskatchewan, Canada.
- Wilson, G.W., Fredlund, D.G. and Barbour, S.L., 1994. Coupled Soil-Atmosphere Modelling for Soil Evaporation. *Canadian Geotechnical Journal*, 31: 151-161.

**Instrumentation and modelling for
saturated/unsaturated performance
of soil covers for acid generating
waste rock**

G.W. WILSON ^{1*}
S.L. BARBOUR ^{1*}
D. SWANSON ^{2†}
M. O'KANE ^{2†}

*Mesure et modélisation des performances des couches de sol saturé et non saturé
installées sur des déchets rocheux (haldes) générant des acides*

Instrumentation and modelling for saturated/unsaturated performance of soil covers for acid generating waste rock

G.W. WILSON⁽¹⁾
S.L. BARBOUR⁽¹⁾
D. SWANSON⁽²⁾
M. O'KANE⁽²⁾

Mesure et modélisation des performances des couches de sol saturé et non saturé installées sur des déchets rocheux (haldes) générant des acides

Hydrogéologie, n° 4, 1995, pp. 99-108, 14 fig., 1 tabl.

Mots-clés : Modèle numérique, Sol, Etanchement, Haldes, Oxygène, Exhaure mine acide, Colombie britannique (couverture sol), Montana.

Key-words: Numerical models, Soils, Sealing, Tailings, Oxygen, Mine drainage, British Columbia (Soil covers), Montana.

Abstract

A research programme involving field instrumentation, laboratory testing and numerical modelling for the evaluation of soil covers installed on waste dumps at two mine sites in Canada and the United States, has been completed. One site is located in a humid environment, and the other site is situated in an arid climate. The objective of the research was to evaluate the performance of soil covers with respect to water and oxygen fluxes. A newly developed soil/atmosphere flux boundary model was used to predict mass transport rates. The analysis showed that the cover constructed at the humid site functions as an oxygen and infiltration barrier. The cover at the arid site reduces infiltration to values approaching zero.

Résumé étendu

L'objectif de cette recherche est d'évaluer la performance vis-à-vis des flux en eau et en oxygène, des couches (couvertures) de sol installées sur des haldes (décharges rocheuses). Ces couvertures sont réalisées sur les rejets rocheux de deux mines, l'une canadienne et l'autre américaine. Le premier site est situé dans un environnement humide et

le second dans un environnement aride. L'étude réalisée comporte une instrumentation in-situ, des essais en laboratoire et une modélisation numérique. Cet article décrit les principaux résultats obtenus jusqu'à présent permettant l'évaluation des performances des couches de sol.

La partie expérimentale comprend le contrôle de l'instrumentation in-situ, les mesures des propriétés hydrauliques et thermiques du matériau de couverture (argile de moraine) ainsi que celles des haldes. Le dispositif de mesure est constitué par : un capteur de conductivité thermique permettant de mesurer la température et la succion matricielle dans la couche de sol, une sonde à neutron mesurant la teneur en eau volumique et une station météorologique permettant d'enregistrer les conditions climatiques.

La couche de sol installée sur les haldes doit jouer le rôle d'une barrière d'infiltration afin de réduire le drainage de l'eau à travers ces déchets. L'autre fonction de ces couvertures est de réduire l'oxydation des sulfures afin d'empêcher le drainage acide (c'est-à-dire la barrière d'oxygène).

Un modèle de transfert couplé de masse tenant compte des conditions sol-atmosphère a été développé. La modélisation numérique du transfert de l'eau (précipitations et évaporation), de la chaleur et de l'oxygène à travers le sol est réalisé par le programme "Soil cover, version 1.0". Le logiciel permet de résoudre les équations du transport unidimensionnel concernant le transfert de masse couplé à la chaleur dépendant des conditions atmosphériques des couches de sol, la charge hydraulique et les conditions thermiques en fonction de la profondeur.

Les résultats des recherches obtenus sur les deux sites montrent que les couches de sol sur des sites de stockage des haldes peuvent être employés afin de réduire les flux de l'eau et/ou de l'oxygène vers ces déchets. Ainsi dans un environnement humide, une couverture réalisée avec des sols fins peut être utilisée avec succès. Pour la couverture du site I, en environnement humide, l'analyse montre que le transfert de l'eau est réduit à des valeurs comprises entre 1 et 5 % des précipitations pour une valeur initiale de 70 %. Par ailleurs, les simulations montrent que les flux d'oxygène pourraient être réduits par un facteur de 400. En revanche, la conception d'un système de couverture en sol

(1) Unsaturated Soils Research Group, Department of Civil Engineering, University of Saskatchewan, 57 Campus Drive, Saskatoon, Saskatchewan, Canada, S7N 5A9
(2) PTI Environmental Services, 4940 Pearl East Circle, Suite 300, Boulder, Colorado 80303, USA.

fonctionnant comme une barrière d'oxygène dans un site aride n'est pas une option satisfaisante. Cependant, cette couverture semble fonctionner efficacement comme une barrière d'infiltration. Les analyses indiquent que la couche de sol empêche toutes les infiltrations dans les années d'extrême humidité.

Introduction

Soil covers for waste rock are generally the last design option which can be implemented to reduce Acid Rock Drainage, ARD. These covers form the uppermost control surface or boundary which delivers water and oxygen to the underlying waste rock. The use of soil covers for waste rock dumps is gaining popularity in Canada and the United States, however the analytical techniques and design methodologies are still developing. Performance based experience is limited and the effectiveness of these cover systems in preventing or reducing ARD is still being evaluated. Issues which must be considered for the design of a soil cover system are climate, surface hydrology, hydraulic and thermal properties of the soil cover and waste rock, groundwater flow conditions, vegetation, slope and erosional integrity, and long term ecological stability.

This paper provides an assessment of the behaviour of soil covers at two waste rock sites. Site I is located in the province of British Columbia, Canada and Site II is located in the state of Montana, United States. A research programme to assess the performance of the soil covers installed at these sites has been completed. The research involves the installation and monitoring of field instrumentation, the measurement of the hydraulic and thermal properties of the cover materials and waste rock and numerical modelling. This paper summarizes the major findings of the research completed to date and provides an assessment of cover performance.

Background

The selection of the waste rock sites was not arbitrary. These sites were

chosen on the basis of climatic conditions. Site I is a humid environment (i.e., precipitation exceeding evaporation), while Site II is an arid environment (i.e., evaporation exceeding precipitation). These two environments impose different performance criteria for the soil cover systems. In general, soil covers are designed as infiltration barriers to reduce drainage from the waste rock. However, it may also be possible to design covers to function as oxygen barriers (Yanful *et al.*, 1993) which will reduce oxidation of the sulphide minerals.

The soil cover constructed in the humid environment of Site I was designed principally as an infiltration barrier. The designers also believed that it may be possible for the cover to maintain a high degree of saturation over time due to the high precipitation and relatively low evaporation, thus allowing the cover to function as an oxygen barrier. The cover installed at Site II was also designed as an infiltration barrier. However, due to the aridity of the site, the cover was not intended to serve as an oxygen barrier. The performance of the two cover systems with respect to net infiltration, moisture saturation and oxygen diffusion are the primary issues which will be discussed in this paper.

Site I

Site I is located in the humid alpine environment of central British Columbia. The mean annual precipitation is approximately 710 mm, 43 % of which occurs as rainfall while 57 % occurs as snow. The total annual potential evaporation varies between 300 mm to 500 mm per year, well below the total precipitation. The average monthly temperature is below zero November through March. Snowpack accumulation can exceed 350 mm (water equivalent), the majority of which melts in May. A maximum average temperature of 20.3°C occurs in June. Average wind speed varies between 6 and 8 km/hour throughout the year while average monthly relative humidity ranges between 43 % and 80 %.

Site I has three dumps located adjacent to each other which contain

approximately 85 Mt of waste rock. The waste rock is estimated to contain between 2 and 3 percent pyritic sulphide. Acidic drainage is currently being collected and treated with lime. Progressive construction of a 0.8 m thick glacial till cover began in 1990 and was completed in 1994. Seeding with clover and grasses has been completed and vegetative stands are developing well.

Site II

Site II is located in an arid environment in the Northwest United States. The mean annual precipitation is approximately 240 mm/year with about 80 % occurring as rainfall. Potential evaporation is approximately 750 mm per year, greatly exceeding precipitation. Mean monthly temperatures are below zero December through March with the highest average maximum of 29°C occurring in July. Mean monthly wind speed varies between 10 and 15 km/hr and the mean monthly relative humidity for the summer months is approximately 50 %.

Approximately 200 Mt of waste rock has been deposited in 2 large dumps over the past 12 years. The predominantly shale waste rock contains disseminated and massive sulphides which are highly reactive. The largest dump is approximately 100 m in height and was constructed by end dumping. High temperatures within the dumps (exceeding 65°C in some locations) indicate that oxidation is occurring. Numerous steam vents have been observed at the surface of the dumps. However, despite the evidence of sulphide oxidation, acidic drainage from the dump has not been observed and collection and treatment has not been required.

Reclamation of the dumps is underway. Regrading of the side slopes to a reduced slope of 2:1 was completed prior to the construction of a 1.2 m thick layered soil cover. The cover system includes 0.6 m of topsoil overlying 0.6 m of oxide cap material. The oxide cap is fully weathered waste rock and the topsoil layer consists of natural surface soils excavated and stockpiled for reclamation prior to dump placement. A number of test plots for the cover system were previously constructed and

instrumented. Seeding the reclaimed areas of the dumps and test plots with native grasses has been successful.

Theory and numerical modelling

Numerical modelling of water, heat and oxygen flow through the cover systems was carried out using software based on SoilCover Version 1.0 (MEND, 1993). The computer programme solves the equations for one-dimensional, transient, coupled heat and mass transfer through soil cover systems based on atmospheric forcing (i.e., precipitation and evaporation) and hydraulic head and temperature conditions at depth. Wilson *et al.* (1994) provide the equations for coupled heat and mass transport. Mass transfer includes liquid water and water vapour. The equation for the flow of liquid water and water vapour is given as follows:

$$\text{Eq. 1: } \frac{\delta h_w}{\delta t} = C_w^1 \frac{\delta}{\delta y} \left[K_w \frac{\delta h_w}{\delta y} \right] + C_w^2 \frac{\delta}{\delta y} \left[D_v \frac{\delta P_v}{\delta y} \right]$$

where h_w is total head, t is time, C_w^1 is the modulus of volume change with respect to the liquid water phase, y is position, K_w is hydraulic conductivity, C_w^2 is the modulus of volume change with respect to the water vapour phase, D_v is the coefficient of diffusion for water vapour through the soil, and P_v is the actual vapour pressure within the unsaturated soil voids. The vapour pressure within the soil is calculated on the basis of total suction, ψ , in the liquid phase as:

$$\text{Eq. 2: } P_v = P_{sv} e^{\frac{\psi g W_v}{RT}}$$

where g is acceleration due to gravity, W_v is the molecular weight of water, R is the universal gas constant, T is temperature, and P_{sv} is the saturation vapour pressure at temperature T . Heat flow is coupled with the mass transfer given by Eq. 1 and is represented by:

$$\text{Eq. 3: } C_h \frac{\delta T}{\delta t} = \frac{\delta}{\delta y} \left(\lambda \frac{\delta T}{\delta y} \right) - L_v \left(\frac{P + P_v}{P} \right) \frac{\delta}{\delta y} \left(D_v \frac{\delta P_v}{\delta y} \right)$$

where C_h is the volumetric specific heat of the soil as a function of water content, λ is the thermal conductivity of the soil as a function of water content, L_v is the latent heat of vaporization, and P is the total gas pressure in the air phase of the

soil. The finite element solution for the coupled system of equations is given by Joshi *et al.* (1993).

The upper boundary conditions for the heat and mass transfer equations are defined through coupling with climatic conditions. Precipitation events are specified as a positive flux boundary condition. Should this flux exceed infiltration capacity, the excess is set equal to runoff. Actual evaporation depends on both atmospheric forcing and the actual vapour pressure at the surface of the soil cover and is determined using the modified Penman formulation proposed by Wilson (1990) as follows:

$$\text{Eq. 4: } E = \frac{\Delta Q + \gamma E_a}{\Delta + A}$$

where E is evaporative flux, Δ is the slope of the saturation vapour pressure versus temperature curve at the temperature of the air, Q is net radiation, γ is the psychrometric constant, and E_a is equal to $f(u) e_a (B - A)$, where $f(u)$ is a function dependent on wind speed, surface roughness and eddy diffusion, e_a is the vapour pressure in the air above the soil surface, B is the inverse of the relative humidity of the air, and A is the inverse of the relative humidity at the soil surface. Temperature at the surface of the soil, T_s is defined using the relationship proposed by Wilson (1990):

$$\text{Eq. 5: } T_s = T_a + \frac{1}{\gamma f(u)} (Q - E)$$

where T_a is the temperature of the air above the soil surface.

Equation 4 which computes the rate of evaporation is used for the special case of a non-vegetated soil cover. Actual evapotranspiration is calculated by including a transpiration flux computed using a modified form of the method proposed by Ritchie (1972). Tratch (1995) modified the function given by Ritchie (1972) such that the potential transpiration is reduced by a plant limiting factor if the values of matric suction in the root zone exceed 100 kPa.

The potential oxygen flux through the soil cover is determined based on the degree of saturation in the soil cover profile. The flux of oxygen is computed assuming steady state conditions for

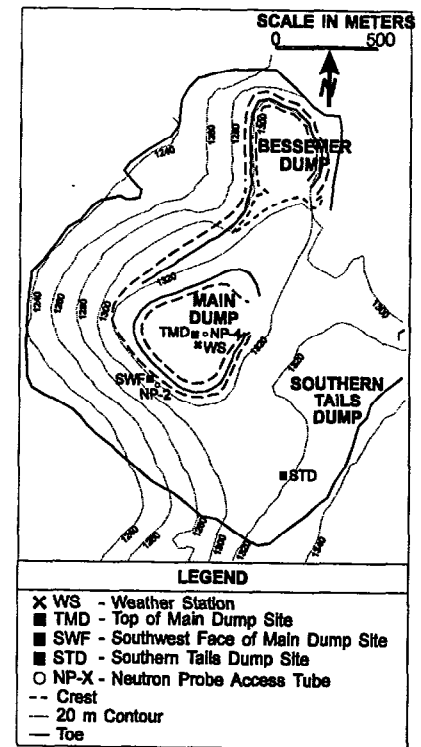


Fig. 1. - Site plan showing the location of field instrumentation at Site I (after O'Kane, 1995).

Fig. 1. - Plan du Site I montrant la localisation des appareils de mesure in-situ (d'après O'Kane, 1995).

each day with an oxygen concentration of 21 % at the surface of the cover and zero at the base. The mass potential flux of oxygen, J , is determined from Fick's First Law as follows :

$$\text{Eq. 6: } J = D_o \frac{\Delta C}{\Delta y}$$

where D_o is the coefficient of oxygen diffusion as a function of the degree of saturation, and $\frac{\Delta C}{\Delta y}$ is the vertical oxygen gradient. The coefficient of oxygen diffusion may be measured experimentally or calculated as a function of the degree of saturation using the empirical relationships developed by Millington and Shearer (1971) and Collin and Rasmussen (1988). Measured values were used for Site I and empirical estimates used for Site II.

Site I

An extensive field instrumentation programme for the soil cover system was initiated in August 1992. Instrumen-

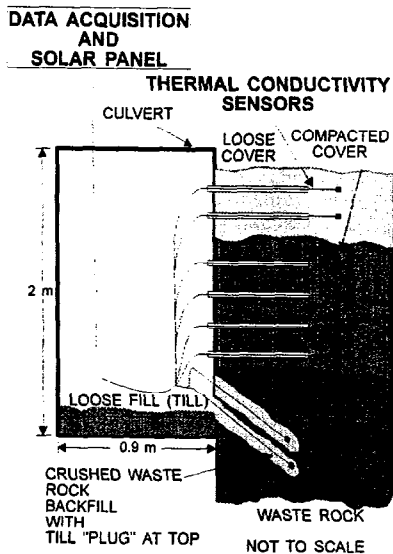


Fig. 2. – Cross-section of the instrumentation station and sensor installations for Site I (after O’Kane, 1995).

Fig. 2. – Coupe d’une station de mesure avec la disposition des capteurs dans le Site I (d’après O’Kane, 1995).

tation for the measurement of oxygen profiles and temperatures within the waste rock dump was installed prior to this research programme. A total of 7 oxygen probes, 10 temperature probes and 14 lysimeters were installed at various locations and depths. The lysimeters were installed at the surface of the waste rock prior to placement of the cover. Instrumentation installed in the cover itself are described below.

Field instrumentation and material properties

The instrumentation installed in the cover system consists of thermal conductivity sensors for the measurement of matric suction and temperature, neutron probe access tubes for the measurement of volumetric water content and a weather station for the measurement of climatic conditions. Figure 1 shows the location of the weather station on the top of the Main Dump (TMD) and three instrumentation stations on the Main Dump and Southern Tails Dump. The purpose of the instrumentation stations was to measure hydraulic head and temperature conditions in the profile of the soil cover.

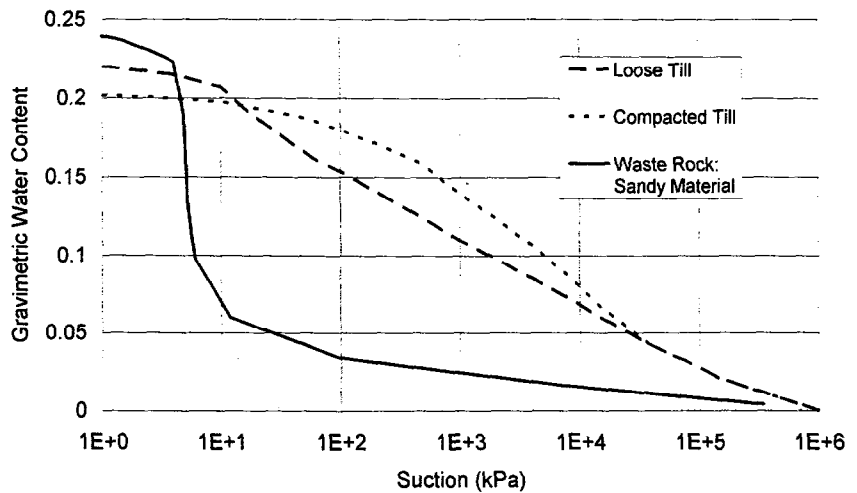


Fig. 3. – Soil water characteristic curves for the uncompacted till, compacted till and waste rock (after Swanson, 1995).

Fig. 3. – Courbes caractéristiques eau-sol (courbe de rétention d’eau) pour des matériaux fins compactés et non compactés (argile de moraine) utilisés dans la couverture et celles de déchets rocheux (haldes) (d’après Swanson, 1995).

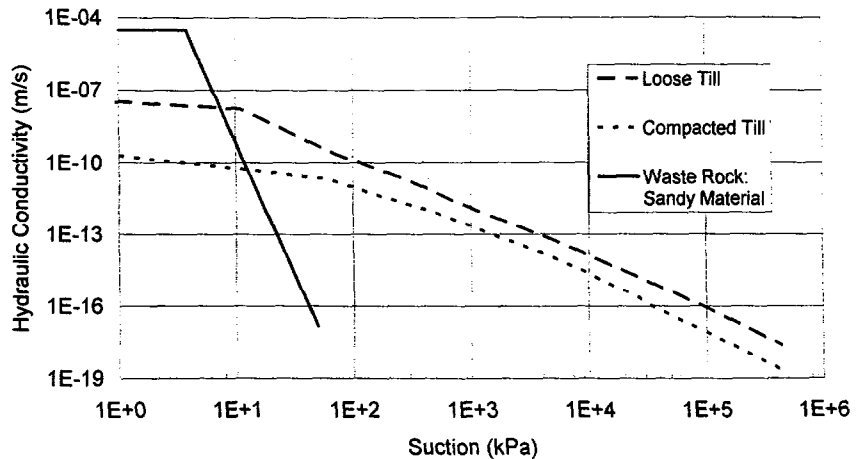


Fig. 4. – Unsaturated hydraulic conductivity versus matric suction for the cover materials and waste rock (after Swanson, 1995).

Fig. 4. – Conductivité hydraulique non saturée contre succion matricielle des matériaux de couverture (argile de moraine) et de déchets rocheux (haldes) (d’après Swanson, 1995).

The weather station on the Main Dump was fully automated to provide continuous measurement of precipitation, global and net radiation, air temperature, wind speed and relative humidity. Measurements were recorded each minute to give mean hourly values.

Figure 2 shows a cross-section for the instrumentation stations. A culvert measuring 0.9 m in diameter and 2.0 m in length was installed at each station. The culverts extend through the soil cover into the underlying waste rock. Eight thermal conductivity sensors were

installed in the cover and waste rock approximately 0.6 m from the edge of the culvert. The thermal conductivity sensors were connected to a data acquisition system and continuous readings of matric suction and soil temperature were obtained and stored for subsequent retrieval.

A total of 14 neutron probe access tubes were also installed at various locations to provide direct measurement of moisture content within the soil cover. These aluminum access tubes were pushed through the cover to the under-

lying waste rock. A neutron source was manually inserted down the tubes to give a continuous profile of water content. A calibration curve for each access tube was produced by retrieving small samples of the soil materials adjacent to the walls of the tubes for the direct determination of water content. Moisture profiles were obtained for the access tubes at various times and compared to the measurements obtained at the culvert station in order to assess spatial performance of the cover.

The till material used to construct the soil cover at Site I was classified as SC-CL using the Unified Soils Classification System with approximately 23 % cobble and gravel size, 28 % sand, 40 % silt and 9 % clay size particles. The till for the lower 0.5 m of the cover was compacted to a minimum of 95 % saturated proctor density (1.9 Mg/m^3) at an optimum gravimetric water content of approximately 14 %. The upper 0.3 m of the cover was not compacted. The soil water characteristic curves, SWCC, for the compacted and non-compacted tills are shown in Figure 3. The effect of compaction on the SWCC is indicated by an increase in the air entry value, AEV (i.e., approximately 100 kPa versus 10 kPa), and a reduction in the saturated water content (i.e., 0.20 versus 0.22) for the compacted till. The SWCC used to represent the waste rock underlying the cover is also shown in Figure 3. The relationship between hydraulic conductivity and matric suction for each of the materials (Fig. 4) was calculated using the commercially available software package called KCAL (Geo-Slope Int., 1993). Values for saturated hydraulic conductivity were based on data from SENES (1991) and O' Kane (1995). Relationships between thermal conductivity and specific heat capacity versus water content were determined for the uncompacted till, compacted till and waste rock using the commercially available computer programme, TheHyProS (Tarnawski and Wagner, 1992).

The hydraulic and thermal properties described above were required by SoilCover (MEND, 1993) to simulate flow through the layered system of uncompacted till, compacted till and waste rock. Climatic parameters obtained from

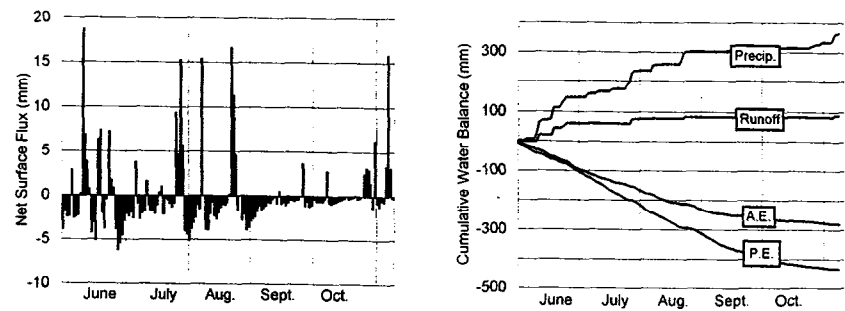


Fig. 5. – Surface Flux Boundary Condition for Site I (after Swanson, 1995).

Fig. 5. – Conditions limites des flux de surface dans le site I (d'après Swanson, 1995).

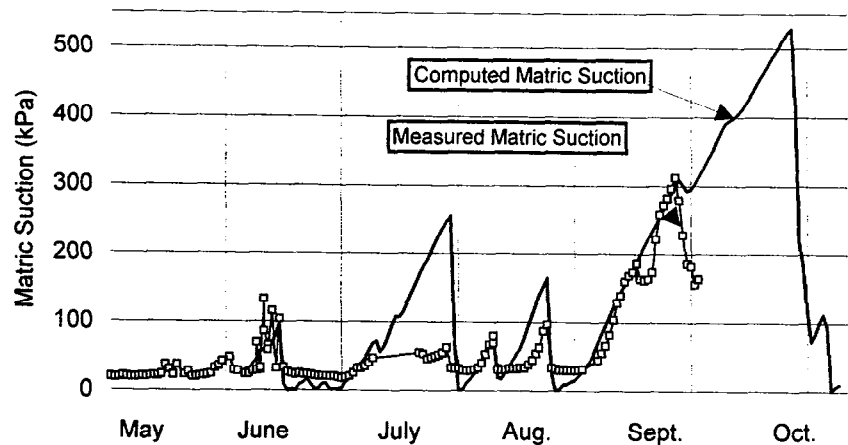


Fig. 6. – Measured and computed values of matric suction versus time at 13 cm depth in the soil cover at Site I (after Swanson, 1995).

Fig. 6. – Valeurs mesurées et calculées de la succion matricielle en fonction du temps à 13 cm de profondeur dans la couche de sol du site I (d'après Swanson, 1995).

the weather station were also used as input. The output from the model simulations were then compared to measured values obtained from the field instrumentation.

Modelling and assessment of cover performance

The TMD culvert site was selected for the model simulations since it was located next to the weather station. The area is gently sloping to flat and was sparsely vegetated at the time. A simulation period of approximately 150 days beginning June 1993 was selected. Initial water contents and temperature profiles through the cover were obtained from the culvert station and a nearby neutron access tube.

Figure 5 shows the calculated surface flux for the simulation period. The

positive fluxes represent precipitation events measured at the weather station, while negative fluxes are evaporation events. The values of evaporation were computed by SoilCover using the Modified Penman formulation given in Eq. 4. Figure 5 also shows the cumulative water balance for the simulation period. The total precipitation for the period was approximately 360 mm with runoff computed to be slightly less than 100 mm. The actual evaporation was computed to be 290 mm which exceeded the total precipitation less runoff.

It should be noted that the cumulative value of actual evaporation is less than the cumulative value of potential evaporation (400 mm). During the initial period in June, actual evaporation was approximately equal to potential evaporation since precipitation was adequate to keep soil moisture conditions wet. The actual evaporation fell below the poten-

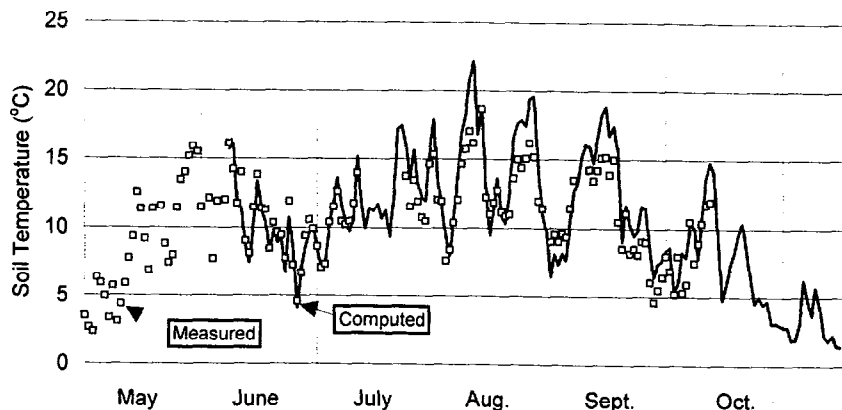


Fig. 7. - Measured and computed values of soil temperature at 13 cm depth within the cover system at Site I (after Swanson, 1995).

Fig. 7. - Valeurs mesurées et calculées de la succion matricielle en fonction du temps à 13 cm de profondeur dans la couche de sol du site I (d'après Swanson, 1995).

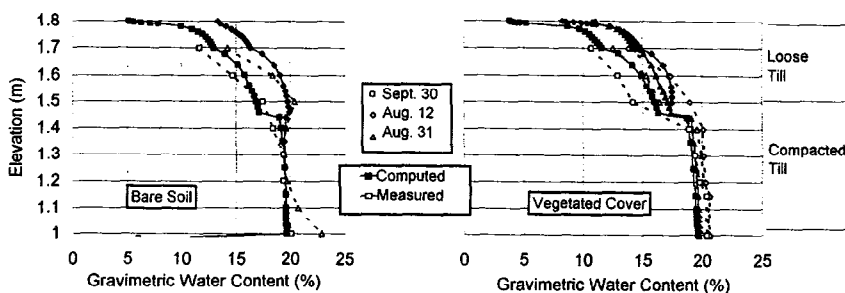


Fig. 8. - Measured and computed water content profiles for bare soil and areas with the protective vegetative cover at Site I (after Swanson, 1995).

Fig. 8. - Profils mesurés et calculés de la teneur en eau du sol dans une zone non protégée et une zone protégée par la végétation dans le site I (d'après Swanson, 1995).

tial evaporation as the simulation continued since precipitation was not sufficient to maintain the wet soil conditions and high evaporation. Had the values of potential evaporation instead of actual evaporation been used to define the upper flux boundary condition in the simulation, excessive soil moisture depletion would have been calculated.

Figure 6 shows the computed and measured values of matric suction at a depth of 13 cm in the loose till. This shallow depth was selected because it shows a more dynamic response in suction as compared to greater depths in the lower compacted till. It can be seen from Figure 6 that there is a good correlation between measured and computed values for matric suction. The response is most significant during the drying period in September and October where suctions increased to high values. Figure 7 shows the computed and

measured values of soil temperature at a depth of 13 cm. Good agreement between the measured and computed temperatures is apparent.

Figure 8 illustrates the effect of vegetation on the water content profile in the soil cover. The measured and computed water contents correspond to bare (NP 1) and vegetated (NP 2) soil surfaces at neutron access tube locations NP 1 and NP 2. It can be seen that the water content profile corresponding to the vegetated site is the driest, as might be expected. However, it is interesting to note that the water content profile in the lower compacted till layer remained high at approximately the saturated water content of 20%. The removal of water from the soil cover occurred in the upper loose layer leaving the lower compacted layer saturated. This is a positive result since maintaining saturated conditions in the lower section of the cover will help

minimize the diffusion of oxygen to the underlying waste rock.

Estimates of potential oxygen flux through the soil cover at Site I were made using SoilCover based on the computed water content profiles and Eq. 6. The relationship between the oxygen diffusion coefficient and the degree of saturation shown in Figure 9 was used for the analysis, based on measured values reported by SENES (1991). Simulations were performed for dry, mean and wet years determined on the basis of regional climatic data extending over a fifty year period beginning in 1943. The dry, mean and wet years corresponded to total annual precipitation of 343 mm, 549 mm and 760 mm respectively.

Simulations for Site I showed that the amount of water infiltrating through the cover to the waste rock was less than 3 mm per year for all three typical years (i.e., less than 1% of all precipitation entered the waste rock dump). This compares to 203 mm (60%), 371 mm (68%), and 593 mm (78%) for the dry, mean and wet years, respectively, for uncovered waste rock. This low value for infiltration through the cover is controlled largely by the low saturated hydraulic conductivity (2×10^{-10} m/sec) for the compacted till. Increasing this value by one order of magnitude increased the infiltration, but in general did not increase it to values exceeding 5% of the total annual precipitation. This maximum value corresponded to the bare soil condition.

Potential oxygen fluxes were computed to be low for each of the dry, mean and wet years. The maximum potential flux of oxygen through the soil cover occurred, as expected, in the dry year and with vegetation. This value was computed to be 0.02 kg/m² per year. Increasing the hydraulic conductivity by a factor of 10 resulted in a higher oxygen flux of 0.148 kg/m² per year. These numbers are considerably lower than those computed for the diffusion of oxygen into the uncovered waste rock found to vary between 7.695 and 9.232 kg/m² per year.

The analyses described above indicate that the installation of the soil

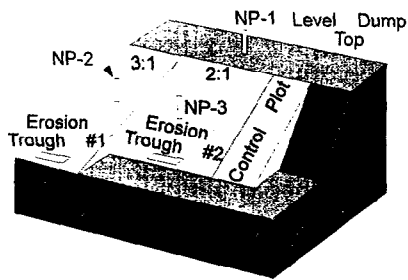


Fig. 10. - Instrumentation layout (neutron probes and erosion throughs only) for the High Grade Waste test plots (after Swanson, 1995).

Fig. 10. - Schéma de montage des instruments (sonde à neutron et dispositif d'érosion) pour les essais dans le site II (d'après Swanson, 1995).

cover at Site I will significantly reduce the flux of water and oxygen entering the waste dump. It is difficult to fully assess performance at this time since full closure with the cover has only recently been completed. However, early trends indicate that lime quantities for the treatment of the acidic drainage have decreased by up to 30 %. Furthermore, total discharge quantities have also decreased significantly.

Site II

The field instrumentation at Site II was installed by the mine operator prior to the initiation of this research programme. The neutron access tubes for the measurement of in-situ water content through the cover were installed on the level dump top and on the test slopes which were regraded to 2:1 and 3:1 slopes as shown in Figure 10. Erosion control is a potential concern therefore erosion troughs were installed to monitor soil losses. A weather station similar to that described for Site I was installed previously at a location near the test plots.

Material properties

The soil cover installed at the test area consists of 0.6 m of topsoil over 0.6 m of an oxidized waste rock (oxide cap). The top soil layer, is comprised of natural soil horizons which were excavated prior to dump placement and stockpiled for final reclamation. Figure 11 shows the SWCC for the topsoil,

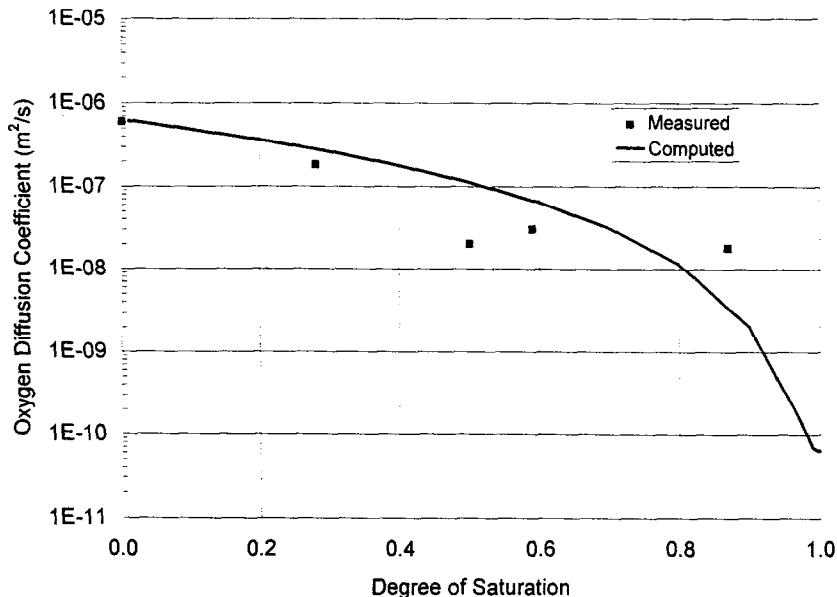


Fig. 9. - Oxygen diffusion coefficient versus degree of saturation for till cover at Site I (after Swanson, 1995).

Fig. 9. - Coefficient de diffusion de l'oxygène en fonction du degré de saturation du matériau de la couverture (argile de moraine) du site I (d'après Swanson, 1995).

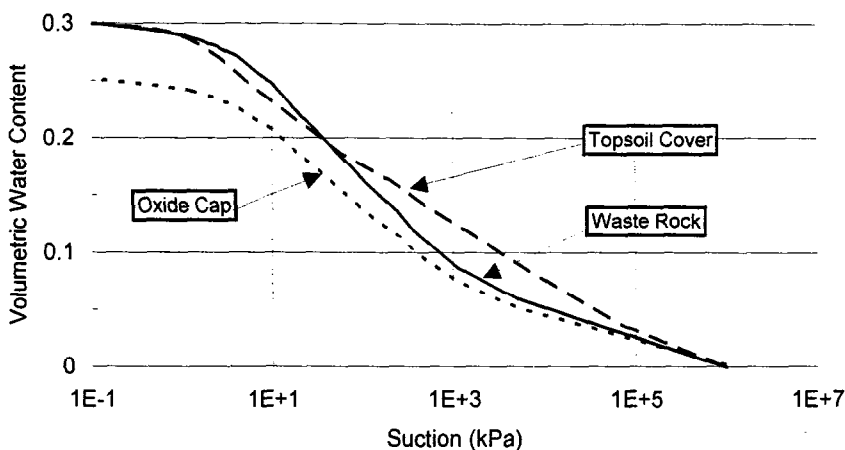


Fig. 11. - Soil water characteristic curves for the topsoil, oxide cap and waste rock materials used at Site II (after Swanson, 1995).

Fig. 11. - Courbes caractéristiques eau-sol (courbe de rétention d'eau) pour le sol de surface, la couche d'oxyde, et déchets rocheux (haldes) du site II (d'après Swanson, 1995).

oxide cap and underlying waste rock. The SWCC for each of the three materials are quite similar. The waste rock, oxide cap and topsoil all have a relatively low AEV ranging between approximately 1 kPa to 3 kPa. The most significant variation in the SWCC for each soil is the slope of the curves at values of matric suction exceeding the AEV. The SWCC for the waste rock drops more rapidly compared to the oxide cap and topsoil. This suggests that

the oxide cap and topsoil are less uniform. In general, the SWCC for the topsoil and oxide cap appear to be a slightly modified form of the curve for the waste rock. This is a logical result since all materials are basically derivatives of the same parent rock. Figure 12 shows the hydraulic conductivity versus matric suction relationship for each material calculated on the basis of the SWCC relationships using the programme KCAL (Geo-Slope Int.,

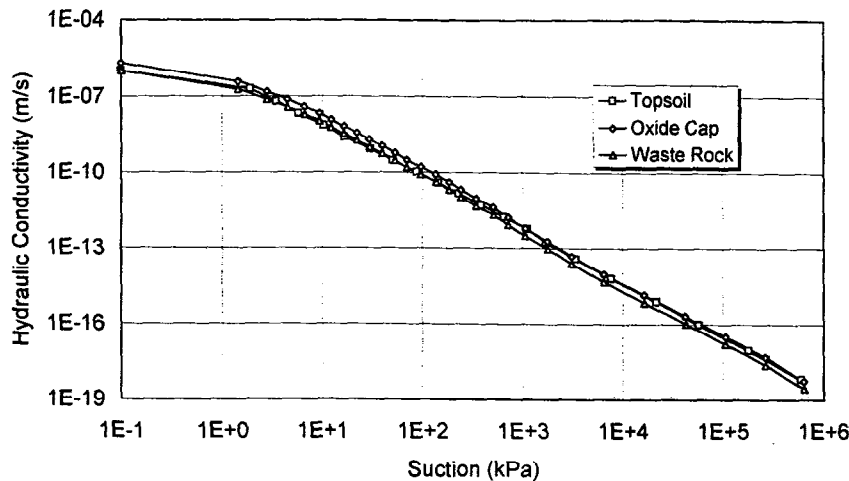


Fig. 12. - Unsaturated hydraulic conductivity functions for the topsoil, oxide cap and waste rock used at Site II (after Swanson, 1995).

Fig. 12. - Conductivité hydraulique non saturée en fonction de la succion matricielle pour le sol de surface, la couche d'oxyde et déchets rocheux (haldes) du site II (d'après Swanson, 1995).

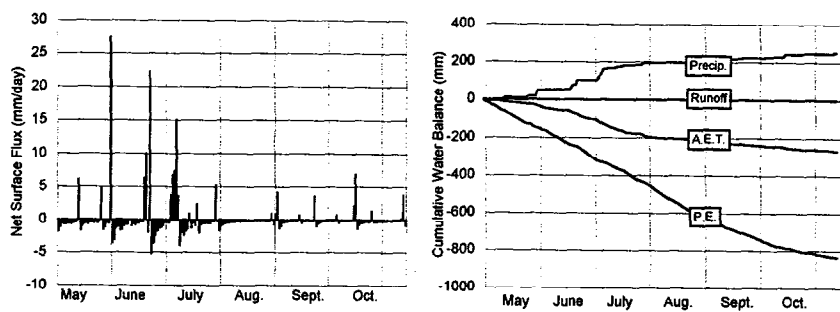


Fig. 13. - Calculated daily net surface flux and cumulative water balance components for Site II - 1992 (after Swanson, 1995).

Fig. 13. - Infiltrations journalières et bilan cumulé hydraulique dans le site II (d'après Swanson, 1995).

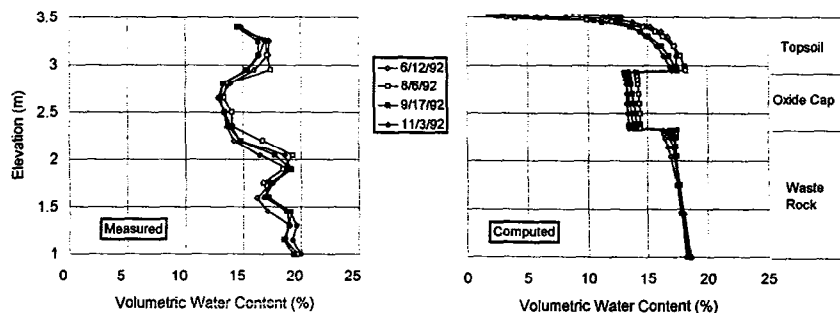


Fig. 14. - Measured and computed water content profiles for Site II (after Swanson, 1995).

Fig. 14. - Profils mesurés et calculés de la teneur en eau du sol dans le site II (d'après Swanson, 1995).

1993). Saturated hydraulic conductivities were estimated from particle size distribution and porosity. Thermal conductivity and heat capacity versus water content relationships were estimated on the basis of grain size distribution using TheHyProS (Tarnawski and Wagner, 1992).

Modelling and assessment of cover performance

Water balance and oxygen flux simulations were performed for the cover on the level dump top area for the period May 1 through mid November 1992. Figure 13 shows the computed

surface fluxes used for the period of May 1 through mid November of 1992. Total precipitation, most of which occurred before mid July, was approximately 225 mm. Actual evapotranspiration was slightly higher than precipitation at approximately 230 mm. Potential evaporation for the period greatly exceeded actual evapotranspiration (i.e., 820 mm versus 230 mm).

Reasonably good agreement can be seen between the measured and computed values of water content as shown in Figure 14. In both cases, the oxide cap shows lower water contents than the topsoil above and waste rock below. This can be attributed to the slight differences in the SWCC for each material which creates a somewhat layered system. Little change in the water content profile occurred over the simulation period. In general, the profiles show that progressive drying occurred during the period which is consistent with the surface fluxes shown in Figure 13.

The water content profiles show that conditions are unsaturated for the entire period of the simulation. Comparing measured and computed water contents for each material with the SWCC relationships shown in Figure 11 indicates degrees of saturation ranging between 50 % and 60 %. It is clear, based on this observation, that the soil cover will not function as an effective oxygen barrier. The primary focus for the subsequent analysis is therefore directed towards the evaluation of the net infiltrative fluxes which will enter the waste rock through the cover system.

Predictive modelling simulations to estimate net infiltrative fluxes were performed for the mean year and the extreme wet and dry years. Regional climatic records extending back to 1920 were used. The extreme dry year (1924) had a recorded precipitation of 159 mm, while the extreme wet year (1993), also the most recent year on record, had a total precipitation of 509 mm. The mean year (1973) precipitation was 263 mm.

In addition to varying climatic conditions, the level of vegetation and the hydraulic conductivity of the cover

layers were also varied. Table I summarizes the results of the analysis. The base case used the material properties previously described. The good vegetation case was the same as the base case except the root depth was extended to 80 cm from 60 cm and the leaf area indices were increased from 1 to 3 to represent a good grass stand (Schroeder *et al.*, 1984). Simulations were also performed with the hydraulic conductivity of all materials increased and decreased by one order of magnitude. Simulations were also performed for the case of uncovered waste rock.

Table I shows that the maximum infiltration into the waste rock occurred for the uncovered case with 12 mm, 20 mm and 80 mm of infiltration entering the waste rock for the dry, mean and wet years, respectively. These values correspond to between 7 % and 16 % of total precipitation. The quantity of infiltration through the cover was extremely small and even negative for the cases with dry and mean year precipitation. Infiltration through the covered systems occurred only for the wet year. Approximately 50 mm (10 % of the total precipitation) infiltrated through the cover for the base case simulation during the wet year. Increasing the vegetation cover reduced this quantity to 35 mm. In addition, decreasing the hydraulic conductivity decreased infiltration to 30 mm or 6 % of the total wet year precipitation. Simulations showed that increasing the hydraulic conductivity by one order of magnitude decreased the infiltration to zero. At first glance this appears erroneous. A higher hydraulic conductivity should allow infiltration to penetrate more rapidly. However, the increase in hydraulic conductivity also enhances upward flow or exfiltration due to evapotranspiration. Since the evaporation events extended over prolonged periods, the increased evaporation capacity of the cover material more than offset the

Scenario	Amount (mm per year)			Percent of Annual Precipitation		
	Dry Year 159 mm	Mean Year 263 mm	Wet Year 509 mm	Dry Year (%)	Mean Year (%)	Wet Year (%)
Covered-Base Case	upward net flux	0	50	0	0	10
Covered-Good Vegetation	upward net flux	upward net flux	35	0	0	7
Cover Layers High K	upward net flux	upward net flux	0	0	0	0
Cover Layers Low K	1	3	30	1	1	6
Uncovered Waste Rock	12	20	80	7	7	16

Table 1. – Annual infiltration rates to the waste rock for Site II.

Tabl. 1 – Taux d'infiltration annuelle dans les déchets rocheux pour le site II.

increase in infiltration rates which occurred during short precipitation events. Hence, overall net infiltration was reduced.

The numerical simulations suggest that very little infiltration will enter the waste rock with the soil cover installed. In addition, only a moderate amount of infiltration will enter the waste rock in an uncovered state (i.e., 20 mm or 7 % of mean year precipitation).

Summary and conclusions

Field instrumentation, monitoring and numerical modelling of soil cover systems constructed over waste rock at two sites have been completed. Covers may be used to restrict water and/or oxygen fluxes to the waste rock. Results of the research to date show that a fine grained cover material can be successfully used in a humid environment to significantly reduce both liquid water and oxygen fluxes to the underlying waste rock. The analysis showed that liquid water fluxes were reduced to between 1 % and 5 % from approximately 70 % using the soil cover installed at Site I. Furthermore, simulations revealed that oxygen fluxes would

be reduced by up to a factor of 400. Designing a cover system to function as an oxygen barrier at an arid site is not a feasible option. However, the soil cover system for Site II appears to be functioning effectively as a barrier to infiltration. The analysis indicates that the soil cover will prevent infiltration for all but the extreme wet years.

Acknowledgments

Some of the field and laboratory testing work for this research programme was performed by Mr Greg Herasymuk as part of his research towards a Master of Science Degree. Editing and preparation of the manuscript was carried out by Ms. Brenda Bews and Mr Andrew Durham. Financial support for the research programme was provided by Placer Dome Inc. and the Natural Sciences and Engineering Research Council of Canada. Mr. Mike Aziz and Mr. Troy Smith of Placer Dome gave valuable field support and access to historical data. Mr. Keith Ferguson initiated the research programme and provided technical and logistical support. The completion of this work would not have been possible without the contributions of these individuals and agencies and their assistance is gratefully acknowledged.

References

- COLLIN M., RASMUSON A. (1988). – Comparison of gas diffusivity models for unsaturated porous media. - *Soil Science Society of America Journal*, 52, pp. 1559-1565.
- GEO-SLOPE International Ltd. (1993). – SEEP/W User's Manual. Calgary, Alberta, Canada.

- JOSHI B., BARBOUR S.L., KRAUSE A.E. and WILSON G.W. (1993). – A finite element model for the coupled flow of heat and moisture in soils under atmospheric forcing. - Finite elements in analysis and design - The International Journal of Applied Finite Elements and Computer Aided Engineering, **15**, pp. 57-68.
- MEND (1993). – SoilCover User's Manual for Evaporative Flux Model. - University of Saskatchewan, Saskatoon, Saskatchewan, Canada.
- MILLINGTON R.J., SHEARER R.C. (1971). – Diffusion in aggregated porous media. *Soil Science*, **111-6**, pp. 372-378.
- O'KANE M. (1995). – Instrumentation and monitoring of engineered soil covers for acid generating mine waste. - M. Sc. Thesis, University of Saskatchewan, Saskatoon, Saskatchewan, Canada.
- RITCHIE J.T. (1972). – Model for predicting evaporation from a row crop with incomplete cover. *Water Resources Research*, **8-5**, pp. 1204-1213.
- SCHROEDER P.R., MORGAN J.M., WALSKI T.M., GIBSON A.C. (1984). – Hydrological Evaluation of Landfill Performance (HELP) Model, Volume I. - User's Guide for Version I, International Ground Water Modelling Center.
- SENES (1991). – Acid Generation Modelling: Equity Silver Waste Rock Dumps. - Report No 30938, December 1991.
- SWANSON D.A. (1995). – Predictive modelling of moisture movement in engineered soil covers for acid generating mine waste. - M. Sc. Thesis, University of Saskatchewan, Saskatoon, Saskatchewan, Canada.
- TARNAWSKI V.R., WAGNER B. (1992). – A new computerized approach to estimating the thermal properties of unfrozen soils. - *Canadian Geotechnical Journal*, **29**, pp. 714-720.
- TRATCH D. (1995). – Moisture uptake within the root zone. - M. Sc. Thesis, University of Saskatchewan, Saskatoon, Saskatchewan, Canada.
- WILSON G.W., FREDLUND D.G., BARBOUR S.L. (1994). – Coupled soil-atmosphere modelling for soil evaporation. - *Canadian Geotechnical Journal*, **31-2**, pp. 151-161.
- WILSON G.W. (1990). – Soil evaporative fluxes for geotechnical Engineering Problems. - Ph. D. Thesis, University of Saskatchewan, Saskatoon, Saskatchewan, Canada.
- YANFUL E.K., BELL A.V., WOYSHNER M.R. (1993). – Design of a composite soil cover for an experimental waste rock pile near Newcastle, New Brunswick, Canada. - *Canadian Geotechnical Journal*, **30**, pp. 578-587.

PRIX D'HYDROGÉOLOGIE GILBERT CASTANY

APPEL A CANDIDATURE

Le prix "Gilbert CASTANY" est décerné chaque année par un Jury constitué sous l'égide du Comité français de l'Association Internationale des Hydrogéologues (A.I.H.). Il est destiné à récompenser une contribution au progrès et à la promotion de l'hydrogéologie française.

Deux prix sont décernés conjointement :

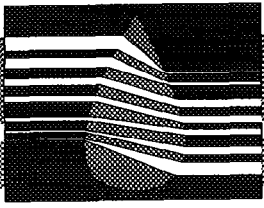
- un prix récompensant une œuvre initiale (thèse, résultats d'une première recherche ou d'une étude particulièrement importante ou originale),
- un prix récompensant l'ensemble d'une œuvre ou d'une carrière.

Peut faire acte de candidature tout chercheur, enseignant ou ingénieur d'étude, de nationalité française ou étrangère, diplômé d'un Etablissement d'enseignement français (Université ou école d'ingénieur) dont les travaux sont exprimés pour l'essentiel en langue française.

Les candidatures doivent être étayées par un dossier comprenant : un CV scientifique et professionnel, une liste des œuvres et des publications réalisées et d'un exemplaire des œuvres les plus remarquables.

La date limite des candidatures est fixée au 31 mai 1996.

Les dossiers doivent être adressés avant cette date à J.C. Roux secrétaire du Comité français de l'A.I.H. BRGM, BP 6009 - 45060 Orléans cedex 2.



ICARD SHORT COURSE:

MATERIAL CHARACTERIZATION AND HYDROGEOLOGICAL ANALYSIS

Dr. Michel Aubertin, Professor

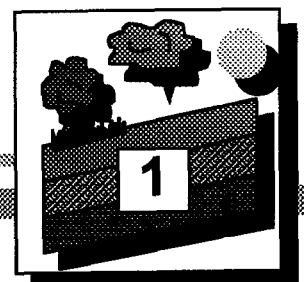
**École Polytechnique
de Montréal**

Tel.: 514-340-4046

Fax: 514-340-4477

E-mail: Michel.Aubertin@mail.polymtl.ca

Vancouver - June 1, 1997





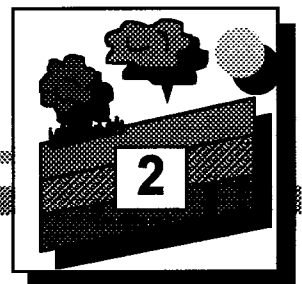
Short-Course Content:

III- MATERIAL CHARACTERIZATION AND HYDROGEOLOGICAL ANALYSIS

A- Introduction

B- Unsaturated flow in porous media

- 1- The water retention curve (WRC; SWCC)
- 2- Constitutive equations
- 3- Material characterization
- 4- Modeling





Short-Course Content:

MATERIAL CHARACTERIZATION AND HYDROGEOLOGICAL ANALYSIS

(continued)

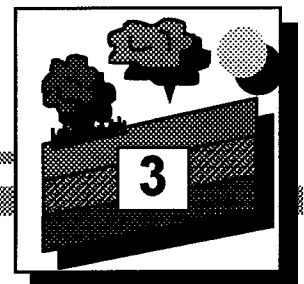
C- Capillary barrier effects

- 1- General principles
- 2- Vertical flow (1D)
- 3- Inclined systems (2D)

D- Applications

- 1- Laboratory tests for material selection
- 2- Laboratory validation
- 3- Intermediate scale experimentation
- 4- Large scale application

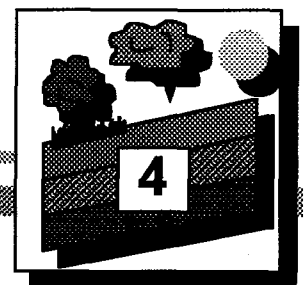
E- Final remarks

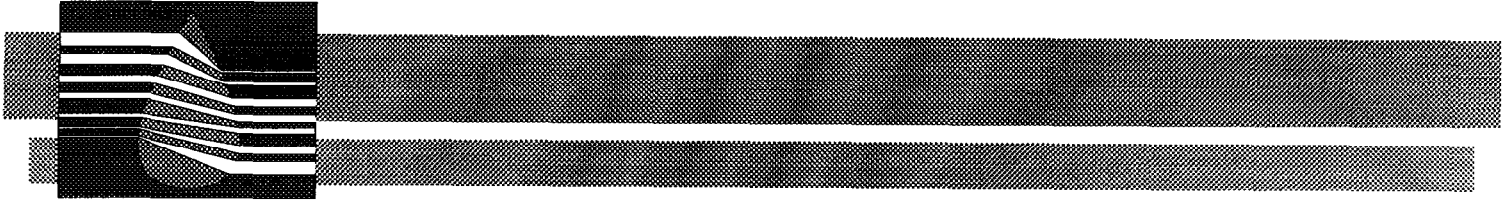




A- Introduction

- AMD produced by tailings and waste rocks is a source of environmental concerns.
- « Dry » covers (water retaining covers) constitute one of the few practical options to control AMD.
- Construction of covers may be expensive (50 to 300k US\$ /hectare).
- Must look for optimal cover efficiency (high efficiency/cost ratio).

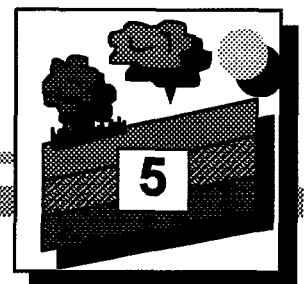




A- Introduction

(continued)

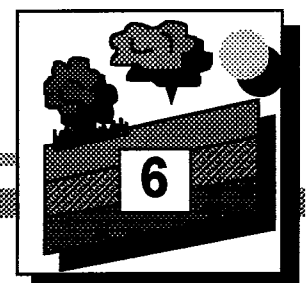
- Understanding of layered cover system behavior progressed over the last decade.
- Objective is to reduce water percolation and oxygen diffusion by using capillary barrier effects.
- Use different materials, with different textures and different hydrogeological properties.





B- Unsaturated flow in porous media

- Many geotechnical problems are related to unsaturated flow conditions.
- Applicable to conditions above the water table (e.g. Fredlund and Rahardjo, 1993).
- Important for cover analysis and design.
- Must evaluate moisture and pressure distribution; control flow of water and oxygen.

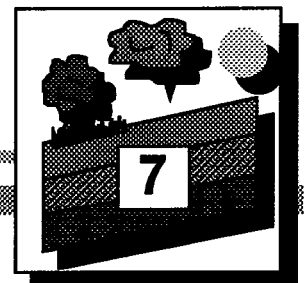




B- Unsaturated flow in porous media

1- The water retention curve (WRC)

- $\theta - \Psi$ relationship ; also known as SWCC
(and many other names).
- θ : volumetric water content
($\theta = V_w/V_t = nS_r$); adimensional.
- Ψ : matric suction ($\Psi = u_a - u_w$);
pressure units (kPa; $\Psi / \gamma_w = \text{height of water}$).
- Represents the capacity of the media to retain
water by capillarity and adhesion forces.
- WRC depends on grain size, porosity,
mineralogy, etc.
- Key parameters: Ψ_a (\equiv AEV), Ψ_r, θ_r .
- Hysteresis exists between wetting and drying.
- WRC can be used to estimate the $k_u - \Psi$
relationship.



B- Unsaturated flow in porous media

2- Constitutive equations

- Various models have been developed for descriptive and predictive purposes.
- van Genuchten (1980):

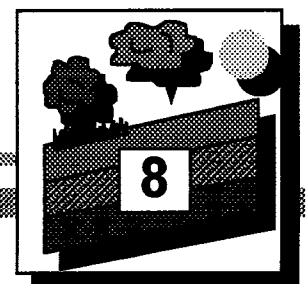
$$\Theta_e = \frac{\Theta - \Theta_r}{\Theta_s - \Theta_r} = \left[1 + |\alpha \Psi|^N \right]^{-M} \quad ; \alpha \equiv 1/\Psi_a$$

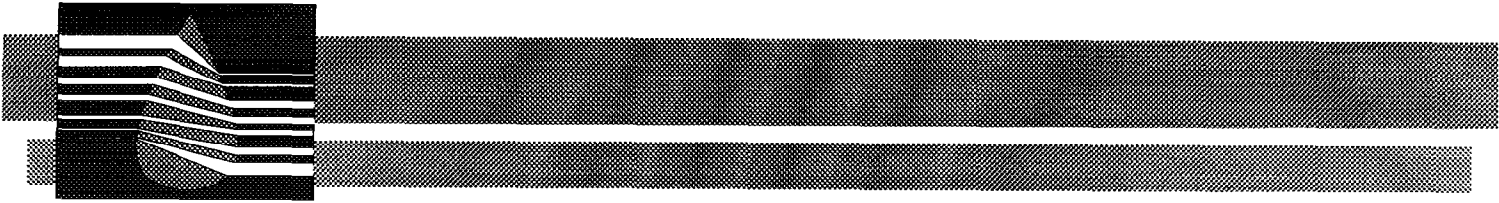
N, M: materials constants (M = 1-1/N suggested)

- Fredlund and Xing (1994):

$$\Theta = \Theta_s \left[\frac{1}{\ln \left(2.7 + \left(\frac{\Psi}{\Psi_a} \right) \right)^N} \right]^M C_\Psi$$

$$C_\Psi = 1 - \frac{\ln \left(1 + \frac{\Psi}{\Psi_r} \right)}{\ln \left(1 + \frac{\Psi_0}{\Psi_r} \right)} \quad ; \Psi_r \sim 1500 \text{ kPa} \text{ and } \Psi_0 \sim 10^6 \text{ kPa}$$





B- Unsaturated flow in porous media

2- *Constitutive equations (continued)*

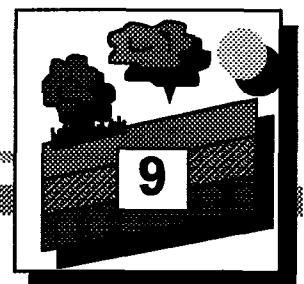
- Modified Kovacs (Aubertin et al., 1997):

$$\Theta = n(S_c + S_a(1 - S_c))$$

$$S_c = 1 - \left(\left(\frac{\Psi_{90}}{\Psi} \right) + 1 \right)^m \exp \left(-m \left(\frac{\Psi_{90}}{\Psi} \right)^2 \right) \quad ; m \sim 0.05$$

$$S_a = C_\Psi \frac{a \Psi_{90}^{2/3}}{e^{1/3} \Psi^{1/6}} \quad ; a \sim 0.006$$

$$\Psi_{90} = \frac{b}{eD_{10}} \quad ; b \sim 4 - 6 \text{ mm}^2$$



B- Unsaturated flow in porous media

2- Constitutive equations (continued)

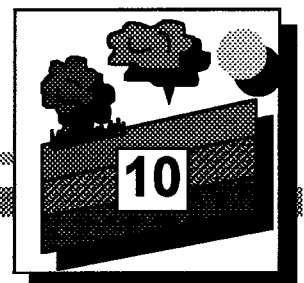
$$- k_u = k_{sat} \bullet \text{fct} (\Psi, \theta)$$

ex.: Mualem (1976), - Van Genuchten (1980)

$$k_u = \Theta_e^{1/2} \left[\frac{\int_0^{\Theta} \frac{d\Theta}{\Psi}}{\int_0^{\Theta_s} \frac{d\Theta}{\Psi}} \right]^2$$

$$k_u = k_{sat} \left\{ 1 - \left(1 - \Theta^{1/M} \right)^M \right\}^2 \Theta^{1/2}$$

- Need θ - Ψ and k_u - Ψ relationship for quantitative evaluations.

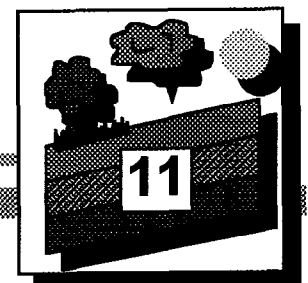




B- Unsaturated flow in porous media

3- Material characterization

- θ - Ψ is easily obtained in the lab.
- k_u - Ψ more difficult to obtain experimentally; often estimated from the $(\theta$ - $\Psi)$ relationship.
- Other properties:
 - mineralogy
 - grain size
 - relative density of solid grain
 - Atterberg limits
 - consolidation behavior
 - k sat ($\rightarrow k_w$)
 - D_e (fct S_r)
 - etc.



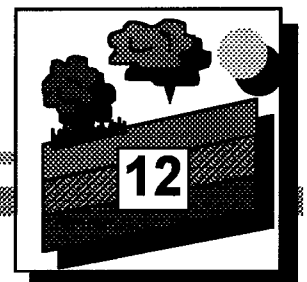


B- Unsaturated flow in porous media

3- Material characterization (continued)

Particular considerations:

- swelling and shrinkage
- freeze thaw effects on microstructure
- desiccation and cracking
- organic content
- solubility and durability
- etc.





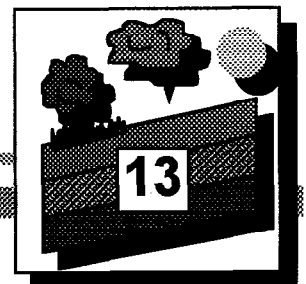
B- Unsaturated flow in porous media

4 - Modeling

- Physical models in the lab are often used to validate calculations (column tests).
- Numerical models:- unsaturated flow
 - transient and steady-state
 - HYDRUS, SEEP/W, etc.

$$\frac{\delta\Theta}{\delta t} = -\nabla \cdot \mathbf{q} = -\nabla \cdot (k_u \nabla H) = -\left(\frac{\delta q_x}{\delta x} + \frac{\delta q_y}{\delta y} + \frac{\delta q_z}{\delta z} \right)$$

- Equations solved numerically with FD, FEM.
- Also diffusion models (for O₂) and geochemical models

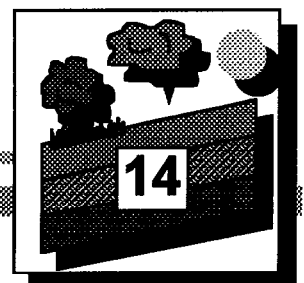




C- Capillary barrier effects

1- General principles

- Above the water table, Ψ (and θ) varies according to position and material properties.
- Finer grained material tend to retain more water
→ k_u/k_{sat} ratio drops less rapidly as Ψ increases.
- During water inflow, smaller pores saturate more quickly; also drain more slowly.
- A fine material layer on a coarse material layer will tend to increase S_r and keep a high S_r after infiltration episodes.
- Allows fine material layer to keep high S_r
→ reduces D_e and oxygen flux.





C- Capillary barrier effects

2 - Vertical flow (1D)

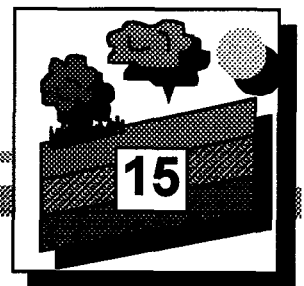
- 1D models have been used to establish basic design conditions (e.g. Nicholson et al., 1989, 1991; Collin and Rasmusen, 1990).

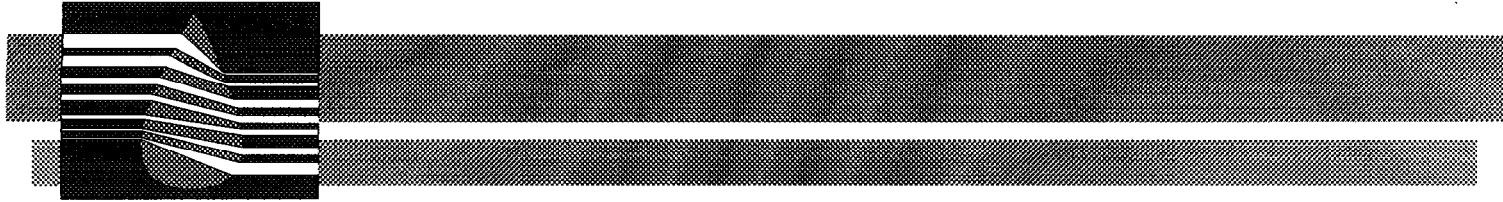
For deep water table $(L)_f \leq |\Psi_a|_f - |\Psi_r|_c$
(to maintain high S_r)

example:

$$(L)_f \leq 200 \text{ cm} - 80 \text{ cm} = 120 \text{ cm}$$

- There is a maximum thickness for maintaining nearly complete saturation.
- Useful for parametric calculations.
- Validated by column tests.

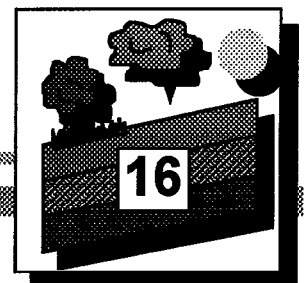




C- Capillary barrier effects

3 - *Inclined systems (2D)*

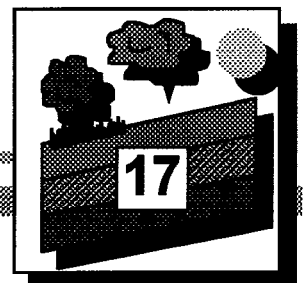
- More realistic.
- Slope angle and length affect moisture distribution (difference in elevation).
- Cover configuration becomes a key factor, with material properties and water budget components (e.g. Aubertin et al., 1997).





D- Applications

- General concepts for complex cover analysis are well understood.
- Few practical applications.
- Most available information comes from laboratory tests; also, field observations.





D- Applications

1 - Laboratory tests for material selection

- Characterize material properties
(θ - Ψ , k_u - Ψ , D_e - θ , etc.)

- Select material according to availability and characteristics
 - ♦ - fine materials: silt, clay, clean tailing, etc.
 - ♦ - coarse materials: sand, gravel, waste rock, etc.

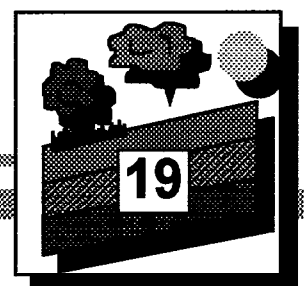
- Key factor is difference between $(\Psi_a)_f$ and $(\Psi_r)_c$; controls barrier efficiency and costs.



D- Capillary barrier effects

2 - *Laboratory validation*

- Can use column tests for validating calculation results on moisture distribution, and cover efficiency (geochemical models).
- Monitoring for θ , Ψ , evaporation, leachate chemistry
- Typical set ups have been proposed.

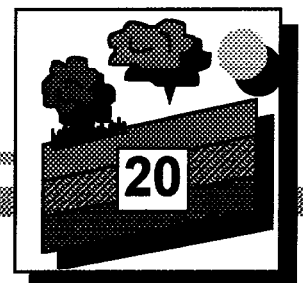




D- Applications

3 - Intermediate scale experimentation

- Useful to isolate site specific factors (ex. scale effects, climatic conditions, placement problems, etc.)
- Various experiments conducted in Canada
 - - Waite Amulet (NTC)
 - - Heath Steele (NTC)
 - - Equity Silver (USG - Sask.)
 - - Manitou-Barvue (Poly/URSTM)
- Must be properly instrumented and monitored (Aubertin et al., 1997).
- Can include oxygen flux measurements (Eberling and Nicholson, 1994).
- Can test different materials and configurations.
- Typical costs: 6 cells, 5 covers, instrumented, 20 m x 20 m. 115 k US \$ (vs. large scale cost).

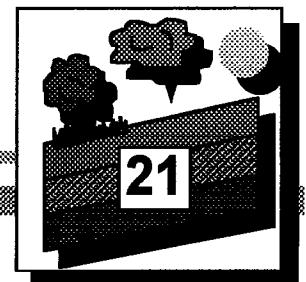




D- Applications

4 - Large scale application

- Few available (see this conference).
- LTA site (Ricard et al., 1997).
- Composite cover with tailings/till and sand.
- Instrumented for θ , Ψ , water budget, oxygen flux.
- Provides technical and practical information.
- Special construction technique.





E- Final Remarks

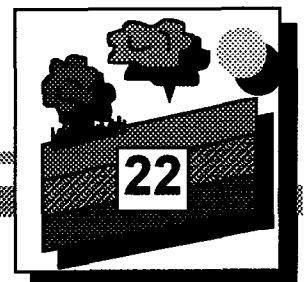
- Analysis uses various tools (experimental, numerical) to establish design parameters.
- Can compare cost and efficiency of various scenarios.

$$E = \frac{F_r}{F_c} = \frac{\left[k_r (D_e)_r \right] L}{(D_e)_c} + 1$$

(Nicholson et al., 1989)

(also obtained numerically)

- Can establish optimum \$/E (cost/efficiency) ratio as a function of cover thickness.



LABORATORY EVALUATION OF DRY COVERS BUILT FROM CLEAN TAILINGS

MEND Report 2.22.2a

M. Aubertin*, R.P. Chapuis, M. Aachib, B. Bussière,
J.F. Ricard, L. Tremblay,

École Polytechnique de Montréal

*PO Box 6079, Stat. Centre-ville, Montreal, QC, Canada, J4B 5S3

tel. (514) 340-4046 (4477 fax) ;

e-mail : michel.aubertin@mail.polymtl.ca

**ÉVALUATION EN LABORATOIRE
DE BARRIÈRES SÈCHES
CONSTRUITES À PARTIR DE
RÉSIDUS MINIERS**

Rapport NEDEM 2.22.2a

Ce programme de recherche a été réalisé dans le cadre du NEDEM avec la participation de Itec Minéral Inc., Barrick Gold Corporation, du Ministère des Ressources naturelles du Québec et du Centre Canadien de la technologie des minéraux et de l'énergie par le biais de l'entente Canada-Québec sur le développement minéral.

mars 1996

EXECUTIVE SUMMARY

Although the mining industry provides an essential contribution to the economy of several provinces across Canada, it is recognized that mining operations can also be the source of various detrimental effects for the environment. In that regard, probably the most serious problem associated with mining activities is acid mine drainage (AMD). Such AMD can be generated when sulphuric minerals (mainly iron sulphides such as pyrite and pyrrhotite) are oxidized in the presence of water. Acid waters may contain high levels of potentially toxic elements, such as lead, cadmium, mercury and arsenic, and this constitutes a serious hazard for the local ecosystems.

The control of acidic effluents during and after mining operations is often very costly. Although water treatment is an efficient process, used with success by mines for decades, it can become a heavy financial burden on any mining company faced with the prospect of having to control water quality for tens if not hundreds of years.

One possible alternative is to control the production of AMD. This approach is often considered when one wishes to reclaim the land and return it to a productive state. Among the few techniques available for that purpose is the use of covers (or caps) installed over existing tailings ponds. It is also one of the most practical options. However, building such covers is very expensive, with most estimates above 200 000 dollars/hectare. In order to reduce these costs, the authors have proposed the use of tailings, free of acid generating minerals, to built such covers. This option would be advantageous for various reasons, including the fact that such materials are often available close to the site being rehabilitated. It is also an interesting option for mills that treat ores free of sulphides, since the resulting non-acid generating tailings could be used as a cover for the acid generating tailings. Another application is related to recent projects where mining companies have used a separation technique to produce sulphide-free tailings, as these could also be used in a cover system.

If a tailings pond is to be reclaimed, it is advisable to stop production of AMD. It is often considered that a cover that limits the flow of oxygen and/or water is one of the most practical approaches for that purpose. A cover is called «wet» when water is used to submerge the tailings, thus reducing oxygen flux to negligible levels. However, such water covers may be

difficult to build and maintain over time, as topography and long term stability of the dams become key factors to the success of the project.

One could also make use of geosynthetics (geomembranes) as an impervious layer in a cover, but costs and durability are major concerns.

Because there is a great deal of experience available from the use of so-called «dry» covers built from geological materials, mostly for industrial and municipal wastes, these are often considered for reclamation projects of acid generating milling wastes. Such covers are not free of potential problems either, but they can represent the most practical solution available to mining companies who are reclaiming their tailings impoundments.

To efficiently control the generation of AMD, it is now generally accepted that a multilayer barrier system, with each layer having its own specific function, should be used. A schematic representation of a multilayer cover is presented on Figure 1.1. The cover layers encountered, starting with the uppermost, are as follows : a humid layer to support vegetation (layer A, thickness $t \geq 15$ cm); a coarse material layer containing a large portion of cobbles to prevent biological intrusions from roots and animals (layer B, $t \geq 30$ cm); a sandy material acting as a drainage layer (layer C, $t \geq 30$ cm); a fine grain material acting here as a moisture retention zone (layer D, $t = 50$ to 150 cm); and a non-capillary layer (layer E, $t \geq 30$ cm) to stop capillary rise from the underlying reactive tailings (layer F) and to prevent significant moisture drainage from the fine material layer above (layer D). Each adjacent layer of the cover should satisfy filter criteria to prevent particles migration that could affect the integrity of the barrier. In this multilayer structure, the two coarse grain material layers (layer C and E) placed adjacent to the capillary layer (D) play a double role. First, these materials (typically sands) provide a flow path for the water to the drainage zones built around the site. Second, the grain size contrast with the fine grained material produces a large difference in suction properties which minimizes moisture drainage and maintains the middle layer close to saturation. It is essential that a saturation ratio of close to 100 % be maintained in this capillary layer to provide an efficient barrier to oxygen transport into the underlying reactive tailings.

In this composite cover, the possibility exists of using various mining wastes for the construction of the different layers. For example, the tailings fine fraction (slimes), obtained by natural segregation or by hydrocyclones, could be used to build the capillary layer (layer D on Figure

1.1). The coarse tailings fractions (sands) could then be used in layers C and E, depending on their availability and hydrogeological properties. Layer B could include cobbles found in the overburden or waste rock from the mine. Finally, humid layer A could be made with the excavated overburden soil, with the original topsoil (stacked and protected) used as the final vegetative layer.

Because the efficiency of such a cover system depends on its effectiveness to reduce water infiltration and/or oxygen flux, the most critical component is the material used for layer D. This experimental study concentrated on finding lower cost materials for this moisture retention layer. Tailings with the correct hydro-geotechnical properties may be used. Samples recovered from various sites located in the province of Québec have been studied as possible candidate materials.

This report contains six (6) Chapters. Chapter 1 summarized above, presents an introduction on the overall problem of AMD and the general principals behind the use of covers. Chapter 2 is a state-of-the-art review on cover technology that considered not only mining related projects but also other types of waste where covers have been installed, including landfills, industrial refuse piles or contaminated soils. Chapter 3 reviews the capillary barrier effects created in layered covers. Material properties, including mineralogical composition, grain size, compaction curves, consolidation characteristics, hydraulic conductivity, moisture retention curves and the effective diffusion coefficient of oxygen, are presented in Chapter 4. Chapter 5 presents the physical and numerical modeling work, and the conclusions follow in Chapter 6.

The reader is reminded that this report summarizes nine interim reports containing more than 600 pages already submitted to MEND, which include all the details of the testing program. These reports are available from the MEND Secretariat in Ottawa. Also, some of the more fundamental portions of this research were the subject of several graduate thesis and internal reports.

Cover systems are used in various waste site remediation projects, and may serve different functions. They form an essential component in the overall management of liquid and gas in and out of the disposal site. One major reason for building covers is to separate the wastes (industrial, municipal, mining, etc.) from the surface environment, to limit water infiltration and/or to control gaz flow from/to the wastes. Site specific characteristics must be considered

for cover design to meet the requirements of a project. However, there are some basic principles that must be understood before undertaking any cover design. In that regard, one should be up to date on the enormous amount of experience and practical information on cover applications disseminated in the literature, and summarized in Chapter 2. After presenting the basic concepts in the use of cover systems, the authors describe different configurations, including materials, thicknesses and functions, of cover systems. Advantages and limitations of the different cover systems are also given.

In composite cover systems, capillary barrier effects are created when a coarse grain material is placed below a fine grain material. The difference in moisture retention curves and hydraulic conductivity functions between these materials creates conditions that allow the fine material to remain practically saturated at all time. In Chapter 3, this phenomena is explained using continuity conditions for pressure and flux at the interface between two materials. The analysis shows that capillary barrier effects are favoured by large contrasts in grain size between two adjacent materials.

Early in the experimental program, a general testing protocol was developed to evaluate the efficiency of different materials and configurations used in cover systems. It includes the evaluation of hydro-geotechnical properties, physical modeling and numerical calculations. These components are presented in Chapters 4 and 5. Results are summarized below.

At the beginning of the project, more than 30 different tailings sites in Québec (most of which being located in the Abitibi region) were sampled. After completing a series of preliminary tests, including mineralogical analysis, grain size and Atterberg limits, five sites were selected and further sampled for more detailed studies. The grain size curve of these tailings are shown in Figure 4.1. These are representative of average grain size curves for hard rock mine tailings. Using the Unified Soil Classification System, these materials are classified as sandy silts or silty sands with low plasticity.

Tailings sampled in bulk were homogenized and submitted to various laboratory tests. Tables 4.1 to 4.3 presents some basic properties of the tailings. Consolidation characteristics were obtained using a conventional oedometer apparatus. For these tests, the densification energy for placement of the material was controlled to obtain an initial void ratio e that could be varied from 0.5 to 1.1. The required densification energy was determined from compaction tests.

Figure 4.3a shows some typical results. For the different tailings, the observed compression index C_c varied from about 0.05 to 0.15 and the coefficient of consolidation c_v was found to be between 10^{-3} and 10^{-1} cm²/s (see Table 4.4). The consolidation properties of the homogenized tailings are well within the range of what is usually found for similar materials (i.e. sandy silts or silty sands).

The hydraulic conductivity k is one of the most important properties of any material used in a cover system. To evaluate k , three different tests were carried out on the homogenized tailings. They are : rigid wall permeameter tests with constant head and falling head conditions; permeability tests in the oedometer cells with constant total stress and varying water pressure; and flexible wall permeability tests. These tests were carried out on tailings for different void ratios. This allowed an evaluation of the effect of different factors on the k value. Among the existing relationships established to quantify the influence of these factors, it was found that the Kozeny-Carman equation (Eq. 4.1) described the observed behavior fairly well. Figure 4.4a shows a correlation between the measured and calculated values for one of the studied tailings. Other relationships have also been used. The practicality of such type of relationship is that it allows an approximate evaluation of the hydraulic conductivity of homogenized tailings, and its evolution as a function of the void ratio and for other parameters as shown in Eq.4.1. The measured and calculated k values are given for total saturation ($S_r = 100\%$). The k values are corrected for unsaturated conditions, using the moisture characteristic curve.

The moisture characteristic curve of the homogenized tailings, which gives the relationship between the volumetric moisture content Θ and the negative pore pressure (or suction) ψ was measured using a pressure plate apparatus and a modified Tempe cell. Typical results are shown on Figure 4.6a. The results indicate that typical Air Entry Values (AEV) range from 1.5 to 3.5 m (about 15 to 35 kPa). The results are well described by the van Genuchten model (Eq. 4.5).

The ability to control oxygen transport is among the most critical cover characteristics that play an important role in the efficiency of the system. It is considered that oxygen flux is usually controlled by Fickian type diffusion (Eq. 4.6 to 4.8) and that pressure and temperature gradient effects are negligible. In a Fickian flow, the oxygen flux is largely dependent upon the effective diffusion coefficient of oxygen D_e which in turn is related to grain size, porosity, tortuosity and volumetric water content. This latter factor is very important, as the diffusion coefficient in water is about 10 000 times lower than in air. Unfortunately, the precise measurement of D_e ,

as a function of the above noted parameters, is not simple. A special setup shown on Figure 4.7 was created with the help of the Noranda Technology Center (NTC). The values of D_e , obtained by comparing the evolution of oxygen concentration measured and calculated with the POLLUTE program, are shown on Figure 4.8a with predictive models (Eq. 4.9 to 4.11). The results are in fair agreement with the theoretical estimates.

The behavior of the homogenized tailings materials in cover systems has also been investigated by using physical and numerical models. The hydraulic conditions in layered systems was first studied using a plexiglass drainage column with an internal diameter of 15.5 cm and a height of 110 cm (Figure 5.1). The column is instrumented with tensiometer and TDR ("time domain reflectometry") probes to measure suction and volumetric water content, respectively, along its length. The column design was based on the ones used at NTC and University of Waterloo for other cover projects. Results of the drainage column tests are compared to results obtained on individual materials in capillary tests and to numerical calculations (Figure 5.3b). The results are in accordance with the project assumptions, and show that the fine layer will remain close to saturation even after long periods of drought.

The efficiency of different cover systems placed over sulphide tailings was also evaluated using plexiglass columns of 1.7m in height. Duplicate columns were prepared for each system, the first instrumented with TDR probes and thermocouples (Figure 5.2) and the second free of any instruments. The cover layers placed over a layer of sulphide containing tailings (about 20 % of iron sulphide) include a sand layer (30 cm in thickness), a fine tailings layer (60 cm in thickness) and a top layer of sand (10 to 20 cm in thickness). Concrete sand was used in the covers. The capillary layers consisted of three different sulphide free tailings. The last two columns had tailings with a small amount of pyrite in the capillary layer. Two smaller columns (called reference columns) were also built with reactive tailings without a cover and are used as controls to evaluate the relative effectiveness of the covers. In all the columns, water is added from the top periodically, and the percolating water sampled at the bottom is analyzed for electric conductivity, pH, sulphate and metal contents. These results provide indications of the possible reactions happening in the system. Temperature measurements in the columns also serve as indirect evidence of chemical reactions. The effectiveness of the cover systems is illustrated by comparing the parameters for the different columns (e.g. Figures 5.4a and 5.4b for pH, and Figures 5.5a and 5.5b for sulphates). Although some columns have shown some abnormal behavior, usually as a result of experimental problems (leaks, preoxydation, etc.), it is clearly

shown that the covers can effectively prevent acid generation and the oxidation of sulphidic minerals. While looking at the column tests results, the reader should also keep in mind that the cover configurations used in the control columns were not selected for optimizing the efficiency, but rather to verify the predictive capabilities of the experimental and numerical tools developed.

Using the available information, the efficiency of various covers was finally calculated by comparing the reduction in oxygen flux, and the results are shown in Figure 5.11. This shows that if high saturation ($S_r \geq 90\%$) can be maintained in the cover through capillary barrier effects, then a one meter layer of fine material sandwiched between two sand layers will effectively reduce the oxygen flux to the reactive tailings material by a factor of about 1000 or more. The results are in accordance with calculations made by other authors for natural soils, thus showing that tailings can be used effectively as the fine material layer in cover systems.

The results presented in this report are very encouraging and warrant the continuation of the research program using more representative conditions. For that purpose, field test plots have been constructed during the summer of 1995 and new column tests were started to further analyze the practical use of non reactive tailings in layered cover systems to control AMD.

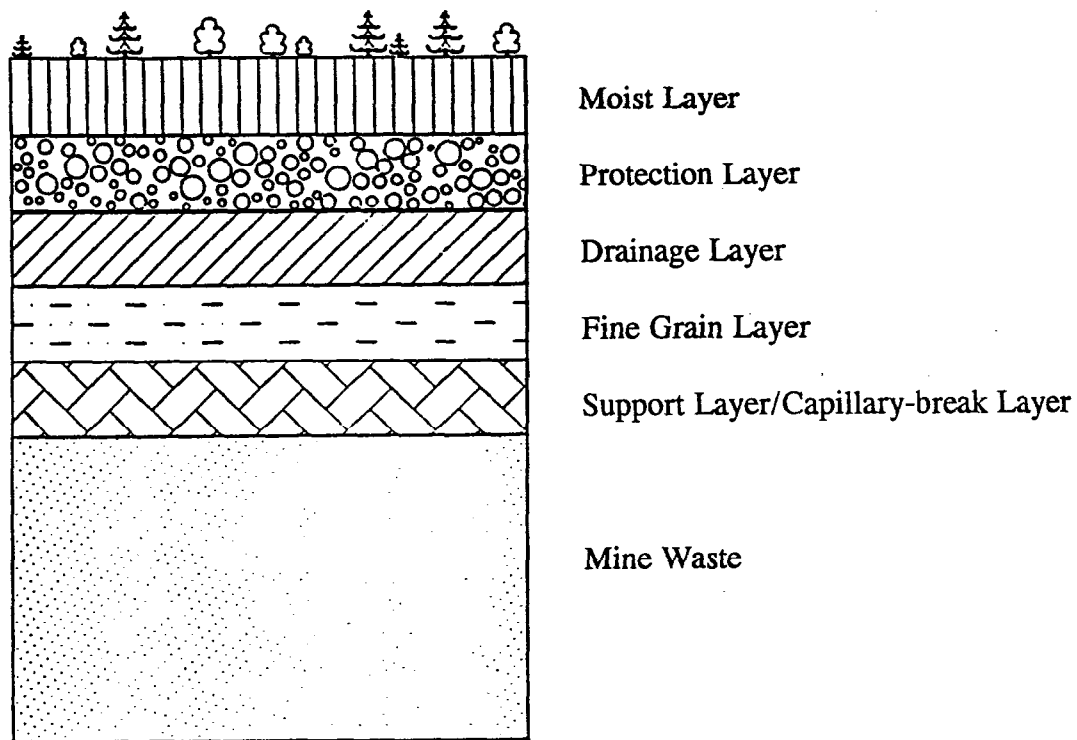


Figure 1.1 Typical section of a multilayer cover system (after Aubertin et Chapuis, 1991)

Table 4.1 Mineralogy Analyses and Average Relative Density (D_r) for the Studied Sites

Mineral	Sigma	Bevcon	Senator - Fine	Senator - Coarse	Manitou- Barvue	Solbec-Cupra
Calcite	10%	8%	—	5%	—	—
Chlorite	25%	5%	15%	10%	14%	8%
Dolomite	—	15%	15%	25%	—	—
Mica	5%	—	10%	10%	15%	—
Plagioclase	30%	27%	20%	20%	5%	30%
Pyrite	—	—	—	—	3%	27%
Quartz	25%	45%	40%	30%	63%	35%
Tourmaline	5%	—	—	—	—	—
D_r	2.793	2.784	2.841	2.865	2.873	3.393

Table 4.2 Typical Values of Grain-sizes and Atterberg Limits

Location	D_{10} (mm)	D_{50} (mm)	D_{90} (mm)	C_u	Passing # 200	$<2\mu\text{m}$	w_L^* (%)	w_p (%)
Sigma	0.0034	0.050	0.011	14.7	66%	6%	18	N.P.
Senator - Coarse	0.0080	0.095	0.034	11.9	50%	3%	17	N.P.
Senator - Fine	0.0050	0.060	0.016	12.0	68%	4.5%	18	N.P.
Bevcon	0.0038	0.042	0.012	11.1	77%	5.5%	17	N.P.
Manitou Barvue	0.0023	0.040	0.008	17.4	80%	8.5%	25	0.25
Solbec-Cupra	0.0095	0.080	0.040	8.4	58%	2%	13	N.P.

* = Upper boundary of w_L (see report)

C_u = Uniformity coefficient (D_{90}/D_{10})

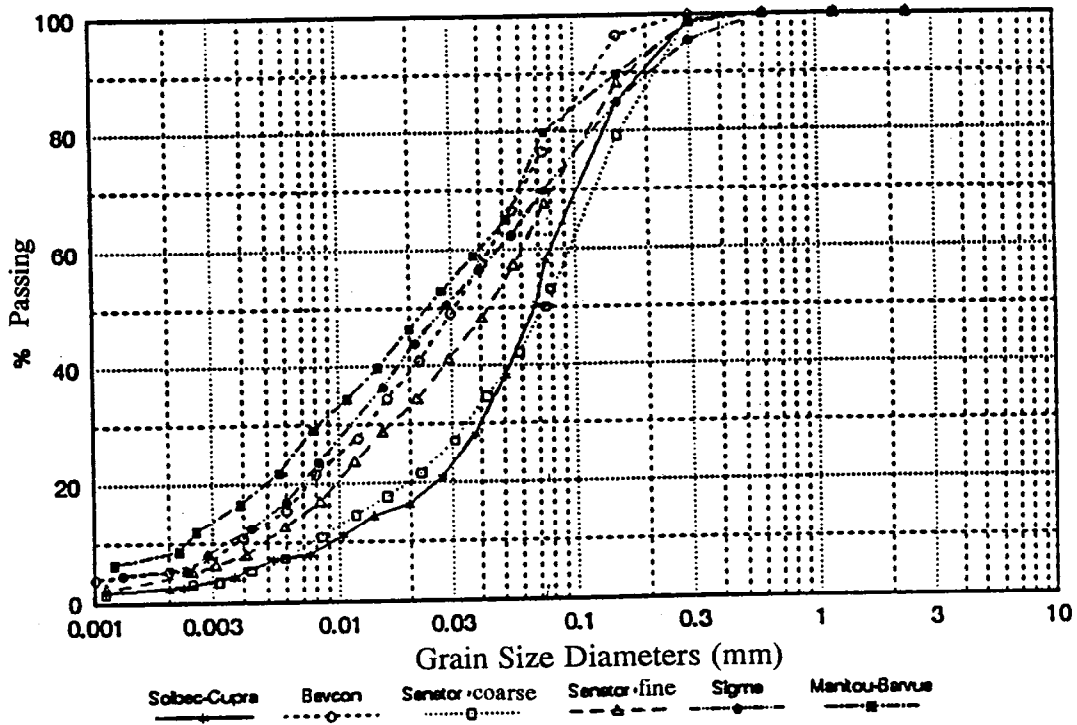
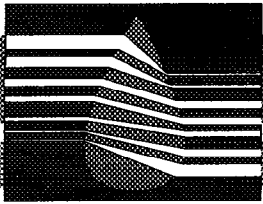


Figure 4.1 Grain Size Curves for the Selected Sites

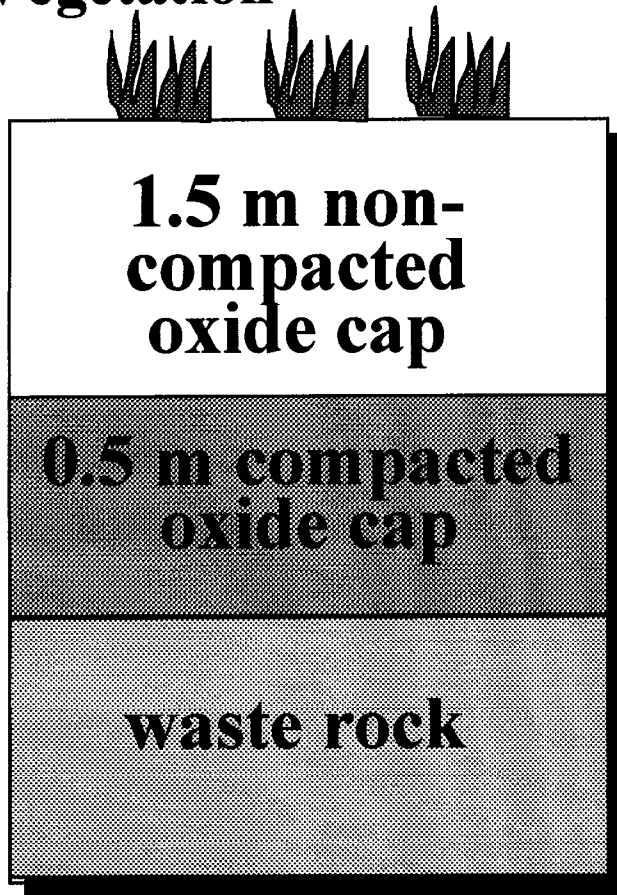


Zero Flux Cover Design Alternatives Considered for Kidston

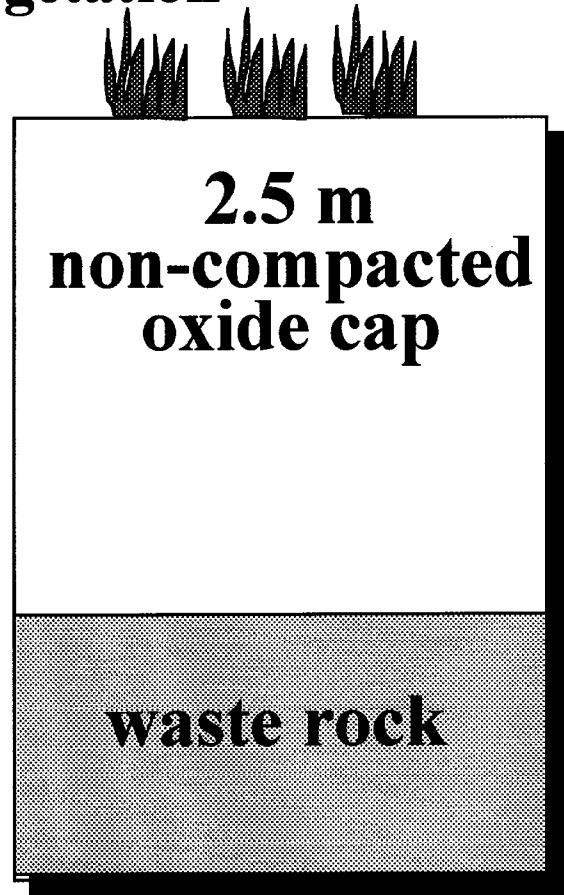
■ **Barrier/Storage
System**

● **Storage
System**

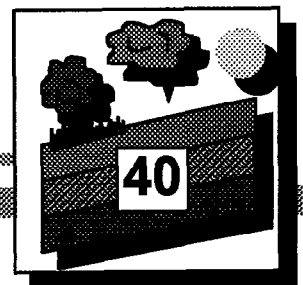
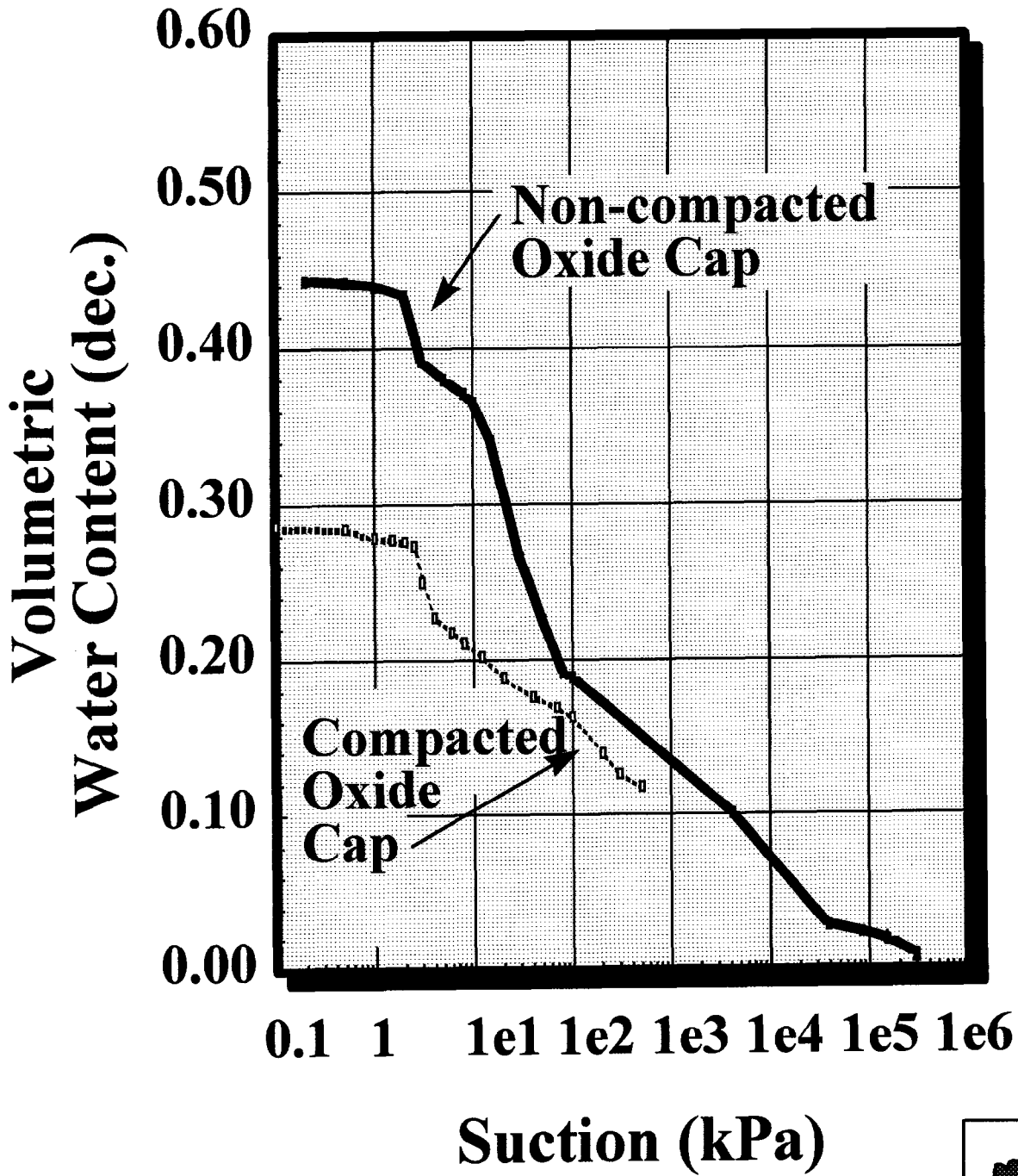
Vegetation



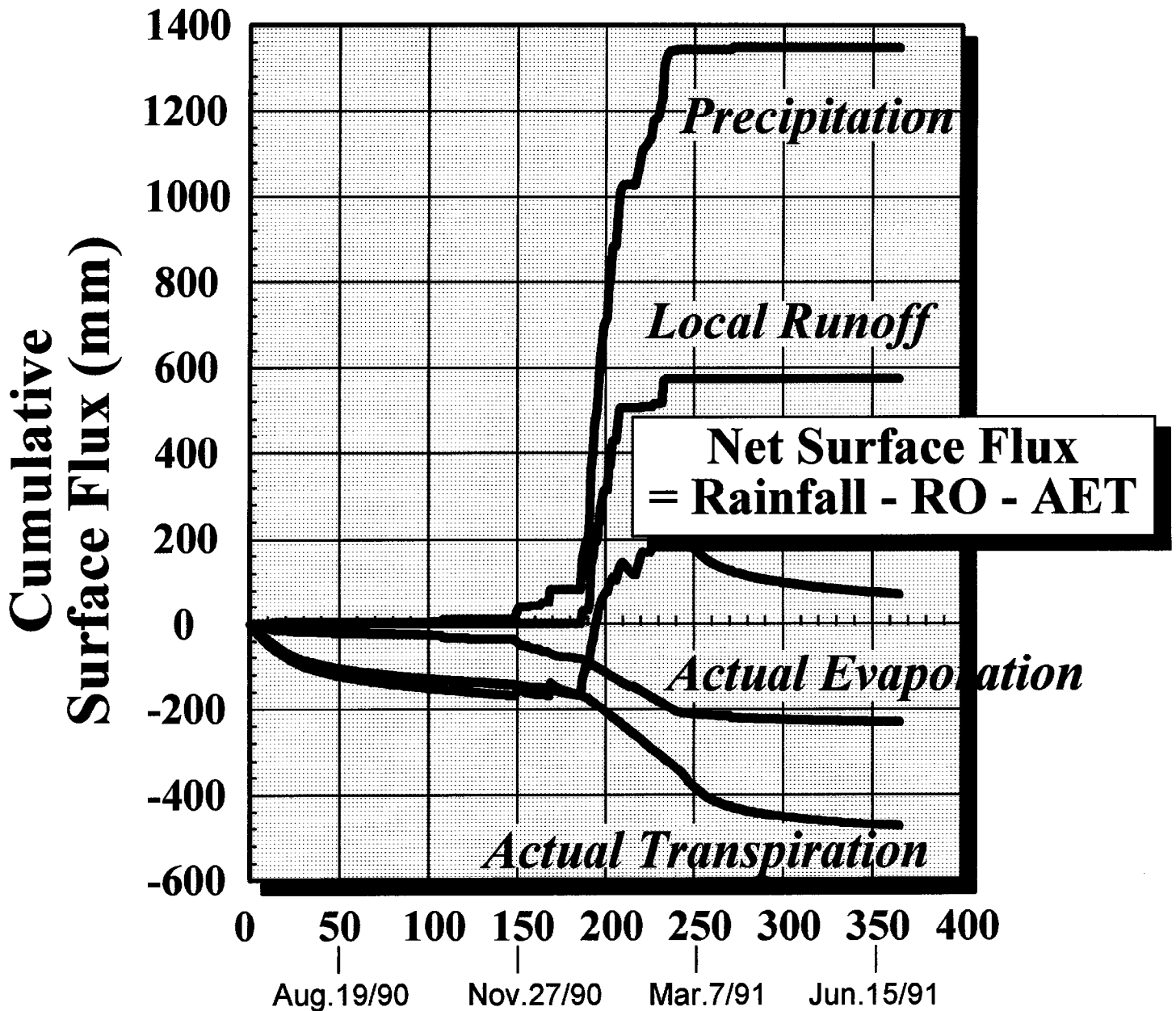
Vegetation



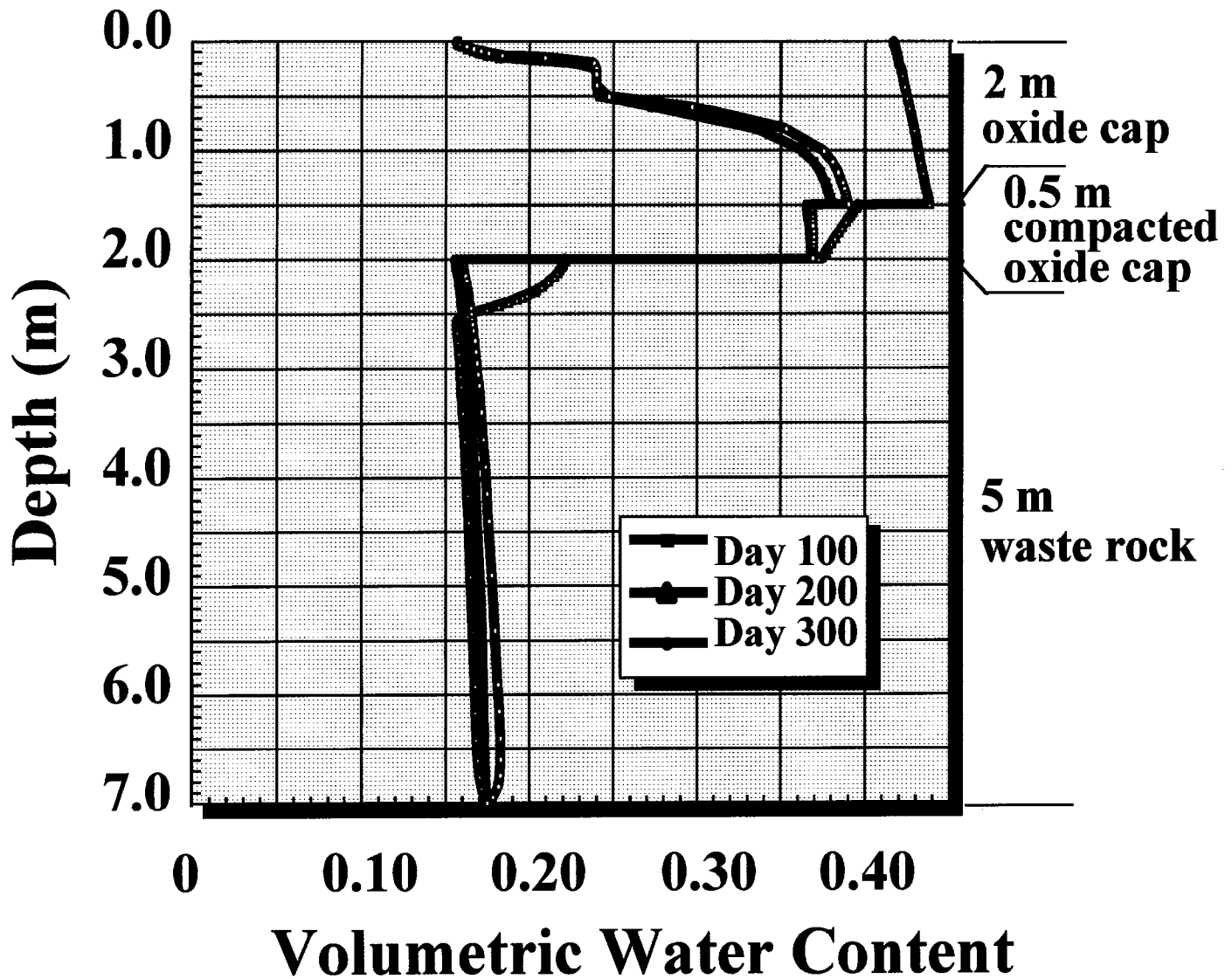
SWCC



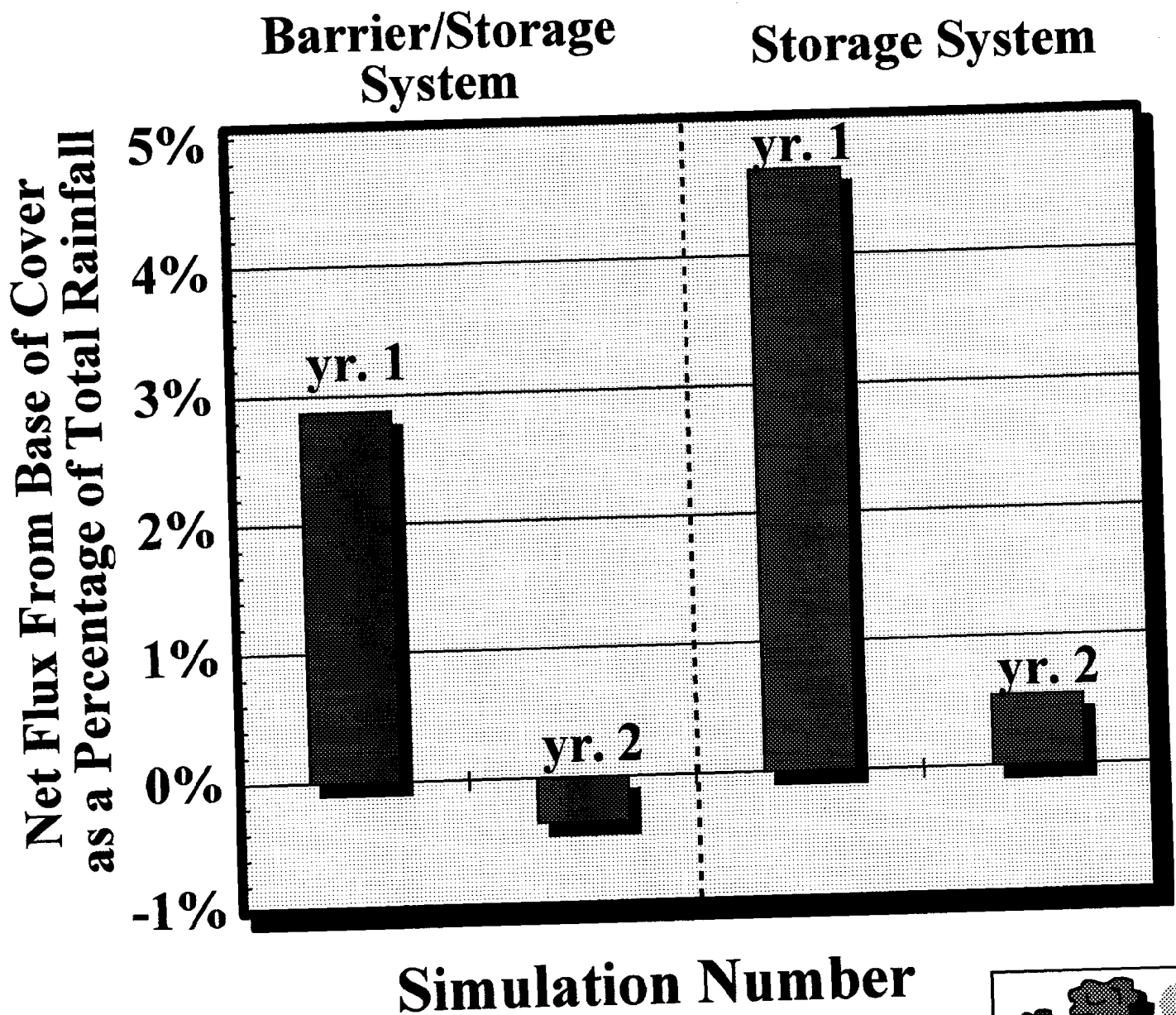
Cumulative Fluxes



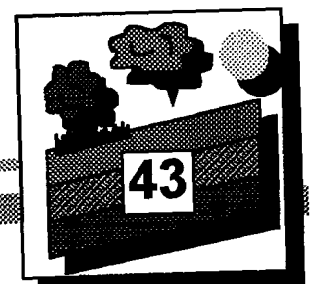
Vol. w/c versus Depth



Net Infiltrative Flux as a % of Rainfall



Simulation Number



The effect of soil suction on evaporative fluxes from soil surfaces

G.W. Wilson, D.G. Fredlund, and S.L. Barbour

Abstract: This paper presents a theoretical approach in which a Dalton-type mass transfer equation is used to predict the evaporative fluxes from nonvegetated soil surfaces. Soil evaporation tests were conducted in the laboratory on three different soil samples of Beaver Creek sand, Custom silt, and Regina clay. The soil surfaces were saturated and allowed to evaporate to a completely air-dried state. The actual evaporation rate for each soil surface was measured along with the potential evaporation rate for an adjacent water surface. The ratio of actual evaporation to potential evaporation or normalized soil evaporation was then evaluated with respect to drying time, soil-water content, and soil suction. The value of the normalized soil evaporation was found to be approximately equal to unity for all soils until the total suction in the soil surfaces reached approximately 3000 kPa. The rate of actual soil evaporation was observed to decline when the total suction exceeded 3000 kPa. A relationship between the actual evaporation rate and total suction was found to exist for all three soil types which appears to be unique and independent of soil texture, drying time, and water content.

Key words: actual evaporation, potential evaporation, soil suction.

Résumé : Cet article présente une approche théorique dans laquelle une équation de transfert de masse de type Dalton a été utilisée pour prédire les flux d'évaporation des surfaces de sol non couvertes de végétation. Des essais d'évaporation des sols ont été faits en laboratoire sur trois échantillons de sols différents, soit un sable de Beaver Creek, un silt Custom, et une argile de Regina. Les surfaces du sol ont été saturées et soumises à une évaporation jusqu'à un état de sécheresse complète à l'air. La vitesse réelle d'évaporation pour chaque surface de sol a été mesurée en même temps que la vitesse d'évaporation potentielle d'une surface d'eau adjacente. Le rapport de l'évaporation réelle sur l'évaporation potentielle, ou l'évaporation normalisée du sol, était alors évalué par rapport au temps de séchage, de la teneur en eau et de la succion du sol. L'on a trouvé que la valeur de l'évaporation normalisée du sol était approximativement égale à l'unité pour tous les sols jusqu'à ce que la succion totale dans les surfaces de sol atteignent approximativement 3000 kPa. L'on a observé que la vitesse de l'évaporation réelle du sol diminue lorsque la succion totale dépasse 3000 kPa. Il existe une relation entre la vitesse d'évaporation réelle et la succion totale pour les trois types de sol qui semble être unique et indépendante de la texture du sol, du temps de séchage, et de la teneur en eau.

Mots clés: évaporation réelle, évaporation potentielle, succion du sol.

[Traduit par la rédaction]

Introduction

Engineered soil covers cannot be designed without evaluating the evaporative fluxes at the soil surface. The purpose of any soil cover system is to control the mass flux of water entering the underlying waste materials. Net water fluxes are a function of the infiltration entering the soil cover due to precipitation and exfiltration leaving the soil cover due to atmospheric evaporation. A clear rationale for predicting infiltration is available. However, a suitable methodology for evaluating soil evaporation has yet to be demonstrated. The need for the development of an appropriate technique is great, since geotechnical engineers in many regions of the world find that the frequency and duration of evaporative events greatly exceed that for infiltration events.

Recent studies have illustrated the need for predictive techniques to evaluate evaporation rates from soil surfaces. Yanful

et al. (1993) provides design criteria and performance modeling for a composite soil cover system constructed on an acid-generating waste rock dump in New Brunswick. The cover was designed to minimize water and oxygen fluxes to the underlying waste rock. Cover efficiency with respect to oxygen fluxes depended on maintaining high saturation, since moisture losses due to evaporation may have led to failure. Laboratory tests were required in order to estimate the appropriate evaporation function for the cover.

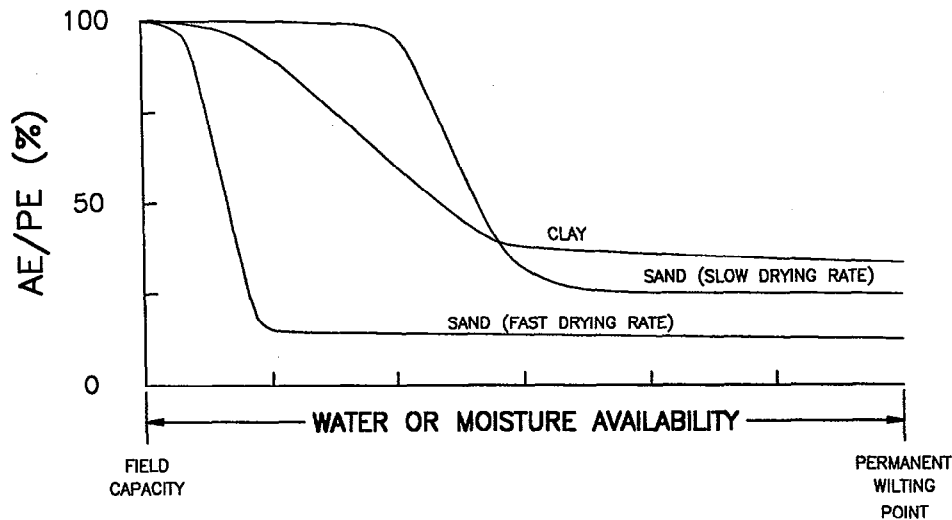
Barbour et al. (1993) evaluated the saturated-unsaturated groundwater conditions of a sulphide-rich thickened tailings deposit in Ontario. Oxidation of the tailings at the surface is known to increase as the degree of saturation decreases. The analysis showed that increased evaporative fluxes during the summer months decreased the thickness of the tension-saturated zone above the water table resulting in the increased potential for desaturation of the tailings surface. The evaporative fluxes used for the analysis were assumed on the basis of observed pan evaporation rates. Since actual evaporative fluxes were not evaluated, the accuracy of the analysis can be questioned.

Other applications exist for which geotechnical engineers must evaluate evaporative fluxes at the soil surface. Silvestri et al. (1990) showed settlement problems in lightweight structures

Received November 20, 1995. Accepted September 4, 1996.

G.W. Wilson, D.G. Fredlund, and S.L. Barbour.
Unsaturated Soils Group, Department of Civil Engineering,
University of Saskatchewan, Saskatoon, SK S7N 5A9,
Canada.

Fig. 1. Typical drying curves for sand and clay showing actual evaporation, AE, as a percentage of potential evaporation, PE, versus water availability (after Holmes 1961).



founded on Champlain clays in Montréal to be strongly controlled by potential evapotranspiration and associated rainfall deficits. Sattler and Fredlund (1989) demonstrated how heave and settlement for expansive clay soils are influenced by evaporation.

Most of the previous work describing evaporation is found outside the traditional area of geotechnical engineering in disciplines such as hydrology and soil science. In response to the need to develop a clear rationale for geotechnical applications, this paper reviews the necessary background for evaluating evaporation found in these other disciplines. Laboratory data are presented where actual evaporation rates from initially saturated soil surfaces of sand, silt, and clay were measured. A simple theoretical approach for the prediction of evaporation from soils is presented and comparisons are made with measured values.

Definitions

The concept of potential evaporation (PE) has been used in engineering practice for nearly 50 years (Thornthwaite 1948). In the most simple terms, PE is considered to be an upper limit or maximum rate of evaporation. The International Glossary of Hydrology (World Meteorological Organization 1974) defines potential evaporation as "The quantity of water vapour which could be emitted by a surface of pure water per unit surface area and unit time under the existing atmospheric conditions."

Evaporation from a water surface may be computed by the simple and well-known equation for mass transfer first given by Dalton in 1802 (Gray 1970):

$$[1] \quad E = f(u) (e_s - e_a)$$

where E is the rate of evaporation (mm/day), e_s is the saturation vapour pressure at the temperature of the water surface (kPa), e_a is the vapour pressure of the air in the atmosphere above the water surface (kPa), and $f(u)$ is a transmission function that depends on the mixing characteristics of the air above the evaporating surface. The transmission function $f(u)$ may be established empirically (Gray 1970).

Many contemporary mass transfer equations in use take the same basic form as Dalton's equation with the function $f(u)$

evaluated on the basis of the aerodynamic profile and eddy diffusion similarity theory.

In simple terms, the mass transfer equation given in [1] describes evaporation as a function of the difference in vapour pressure between the water surface and overlying air. The vapour pressure of the evaporating water surface, e_s , is the saturation vapour pressure of the water given by the Clausius-Clapeyron equation, which is a function of temperature (Brutsaert 1982). The vapour pressure in the air above the water, e_a , is determined on the basis of the saturated vapour pressure at the measured air temperature and relative humidity. Determining the surface temperature of the water can be extremely difficult (Gray 1970), and as a result, [1] often becomes indeterminate. Penman (1948) rendered the problem determinant by incorporating the energy balance and net radiation available to the evaporating water surface.

The actual rate of evaporation from vegetated and bare soil surfaces is stated to be approximately equal to the rate of evaporation from an open or free water surface (i.e., PE), provided that the supply or availability of water to the surface is unlimited (Penman 1948). This suggests that the rate of evaporation from a wet soil surface can be evaluated using the same techniques as used for free water surfaces. However, the approach becomes inaccurate once the soil surface begins to dry and becomes unsaturated. As a result, traditional methods for predicting potential evaporation from saturated surfaces, such as the Penman method, provide overestimates of evaporation for unsaturated soil surfaces (Morton 1985; Granger 1989a).

Literature review

Hydrologists, soil scientists, and engineers have been attempting to evaluate evaporation from unsaturated soils for a number of decades. Figure 1, after Holmes (1961) and Gray (1970), shows the relationship between potential evaporation, PE, from a free water surface and actual evaporation, AE, for typical sand and clay soil surfaces that are allowed to evaporate from initially wet or nearly saturated states. Holmes (1961) showed that the AE is equal to the PE (i.e., AE/PE equals unity) for both the sand and clay soils when the water content

Table 1. Summary of material properties used for each soil type in the evaporation tests.

Item	Beaver Creek sand	Custom silt	Regina clay
Description	Fine, uniform clean sand; aeolian	Coarse to medium clean silt; laboratory produced	Highly plastic clay; lacustrine
Texture	98.0% sand 2.0% silt and clay	7.0% sand 84.0% silt 9.0% clay	8.0% sand 41.0% silt 51.0% clay
Atterberg limits	Nonplastic	Plastic	Plastic
Liquid limit	—	26.8%	75.5%
Plastic limit	—	25.4%	24.9%
Plasticity index	—	1.4%	50.6%
USCS ^a	SP	ML	CH
Specific gravity	2.67	Not measured – 2.72 estimated	2.83
Void ratio at 100 kPa suction	0.63	0.85	1.34

^aUnified Soil Classification System.

is high or near the field capacity. The ratio of AE/PE for each soil type begins to decline as the availability of water decreases to the permanent wilting point for plants. Holmes (1961) and Gray (1970) do not explicitly state the units of water or moisture availability, but the limit of the permanent wilting point (i.e., approximately equal to 15 atmospheres of suction) implies that the soil has large negative pore-water pressures or suction.

Figure 1 shows that as water becomes less available, the decline in the ratio AE/PE varies significantly depending on the soil texture and drying rate. For example, the ratio AE/PE for the sand undergoing rapid drying is significantly less than that for the slow drying sand when the water availability is at the mid-point between the field capacity and the permanent wilt point. The curve for the clay indicates a higher rate of actual evaporation than either the fast or slow drying sand as the water availability approaches the permanent wilt point. In summary, Fig. 1 indicates that the actual evaporation rate from soil surfaces relative to the potential evaporation rate is a function of water availability, soil texture, and drying rate. No single variable or soil property appears to control the evaporation rate from the soils.

The difficulty with respect to defining the soil properties that control evaporation from unsaturated soil surfaces has resulted in the development of empirical methods. For example, Hillel (1980) suggests the drying of a soil surface may be simulated using square-root time relations. The function is purely empirical, and the actual mechanisms that control soil evaporation are not identified. Yanful et al. (1993) essentially adopted an empirical approach for evaluating the performance of a soil cover system for acid-generating waste rock.

A few attempts have been made to define the dependent variables that control evaporation from unsaturated soil. Barton (1979) suggested soil evaporation may be estimated on the basis of the humidity and water content of the near surface soil. Hammel et al. (1981) also described actual evaporation from soil as a function of soil-water content and included water flow processes in the soil with combined moisture and temperature

gradients. Granger (1989b) stated that evaporation from unsaturated soil surfaces is a function of the actual vapour pressure at the soil surface. This behavior is in agreement with [1]. The actual vapour pressure for unsaturated soil surfaces is less than the vapour pressure that would occur at full saturation of the soil, hence, evaporation is suppressed. However, Granger (1989b) did not provide a means for evaluating the actual vapour pressure at the unsaturated soil surface.

Wilson et al. (1994) developed a coupled soil-atmosphere model for soil evaporation. The model solved for evaporation using [1] with the vapour pressure at the soil surface determined on the basis of solving coupled heat and mass transfer equations for the soil profile below the surface. Model predictions for a sand profile were compared to laboratory measurements with good correlations. However, the laboratory tests were conducted using a column of ideal cohesionless uniform sand. The suitability of the theoretical model for other soils such as a fine-grained silt or cohesive clay was not demonstrated.

In general, the work described above shows that for given climatic conditions, the evaporation rate from unsaturated soils is less than the evaporation rate from saturated soils or water. The mass transfer equation, [1], which defines evaporation, indicates that a reduction in the evaporation rate from a soil surface that is drying from an initial state of saturation under constant climate conditions will occur only if the vapour pressure at the soil surface, e_s , decreases during drying. However, this basic principle has not been clearly demonstrated. Instead, the decline in evaporation rates for unsaturated soil surfaces has been explained on the basis of a variety of other factors such as soil water availability or water content, soil texture, drying rate, and drying time.

The present work evaluates the process of evaporation from soil surfaces composed of various soil types that were allowed to evaporate under controlled laboratory conditions. The laboratory testing program carried out used two identical evaporation pans. One pan contained water to measure the potential evaporation rate and the second pan contained soil to measure

Fig. 2. Water-content characteristic curves for Beaver Creek sand at 20°C.

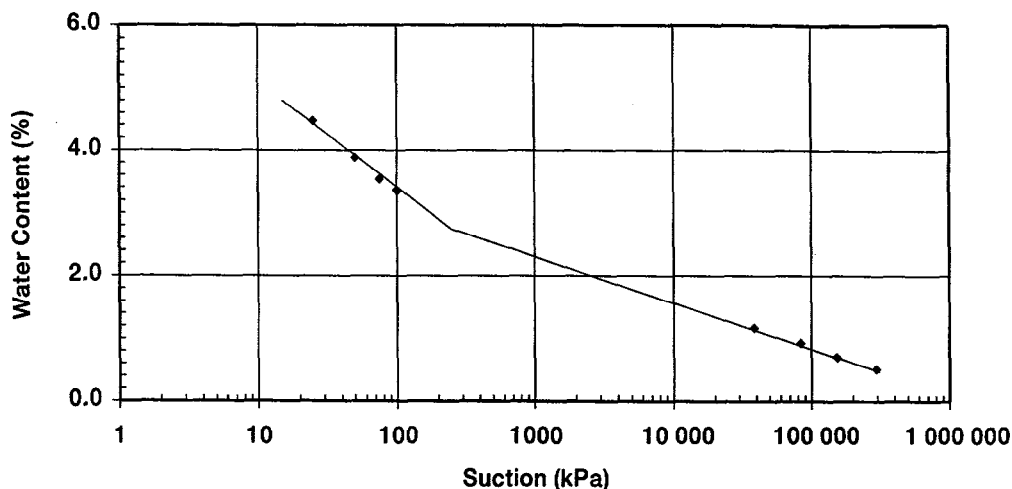


Table 2. Summary of saturated salt solutions, activity coefficients, and osmotic suctions used for the vacuum desiccators at 20°C.

Salt solution	Activity coefficient	Osmotic suction (kPa × 10 ³)
Lithium chloride [LiCl H ₂ O] and [LiCl 2H ₂ O]	0.115	292.4
Magnesium chloride [MgCl ₂ 6H ₂ O]	0.330	152.4
Magnesium nitrate [Mg(NO ₃) ₂ 6H ₂ O]	0.543	84.0
Sodium chloride [NaCl]	0.755	38.6
Potassium sulphate [K ₂ SO ₄]	0.970	4.19

the actual soil evaporation rate. The simultaneously measured actual and potential evaporation rates were compared as the soil surfaces desiccated from wet to dry. The influence of soil parameters such as texture, drying time, water content, and soil suction were also evaluated.

Laboratory test program

Evaporation tests were carried out using three texturally distinct soil types selected to represent the clay, silt, and sand soil groups. They were as follows: (1) Beaver Creek sand; (2) Custom silt; and (3) Regina clay.

The Beaver Creek sand was a fine, uniform, natural aeoline soil consisting of 98% sand and 2% silt and clay. This material was selected to represent granular, cohesionless soils. Regina clay, which is a highly plastic lacustrine deposit, was the natural soil selected to represent fine-grained, cohesive soils. A silt material was also included to represent a fine-grained cohesionless soil intermediate to the extremes of a clean sand and a highly plastic clay. The silt was a custom material containing 84% silt produced in the laboratory. A summary of the soil properties for each soil type are presented in Table 1.

Water-retention characteristics

The soil-water characteristic curves were determined for each of the selected soil types. The soil-water characteristic curve of a soil is a measure of the availability of water since it provides a relationship between water content and suction. The soil-water characteristic curves for the Beaver Creek sand, Custom silt, and Regina clay were evaluated using pressure plates and glass desiccators containing electrolyte solutions.

Pressure plates were used to determine soil-water contents at various values of matric suction between 0 and 100 kPa. Soil-water contents for high values of suction were determined using osmotic pressures induced by electrolyte solutions. The osmotic pressure of the electrolyte solutions in the glass desiccators was calculated using the well-known expression for thermodynamic equilibria of solvents given by Robinson and Stokes (1955) as follows:

$$[2] \quad \pi = \frac{RT}{V_A} \ln a_w$$

where π is osmotic pressure or suction (kPa), R is the universal gas constant (8.314 J/(mol·K)), T is absolute temperature (K), V_A is molar volume, and a_w is the activity of water for the aqueous solution.

Five aqueous solutions were selected to give a suitable range of osmotic suction. Table 2 provides a summary of the salt solutions used and the corresponding values of osmotic suction.

Each soil type was slurried with distilled water and placed into the pressure plate in a saturated state. The air pressure in the pressure plate was increased by increments of 25 kPa allowing the samples to reach an equilibrium water content for each increment of matric suction to a maximum of 100 kPa. Small soil samples were then removed from the pressure plate at the end of the procedure, as described by Wilson (1990). These samples were placed directly into each of the five glass desiccators, and the soil-water contents were allowed to come to equilibrium with the osmotic suction established in the desiccators. The samples were separated from the electrolyte solutions in the reservoirs of the glass desiccators by an air space that functioned as a semi-permeable membrane. The temperature was maintained at 20°C for the samples in the pressure plate and glass desiccators. Figures 2, 3, and 4 show the measured

Fig. 3. Water-content characteristic curves for Custom silt at 20°C.

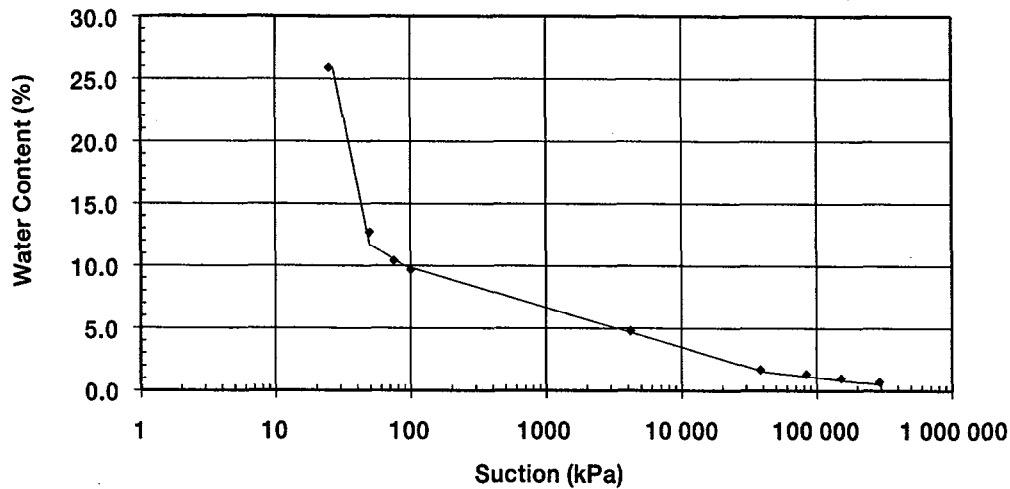
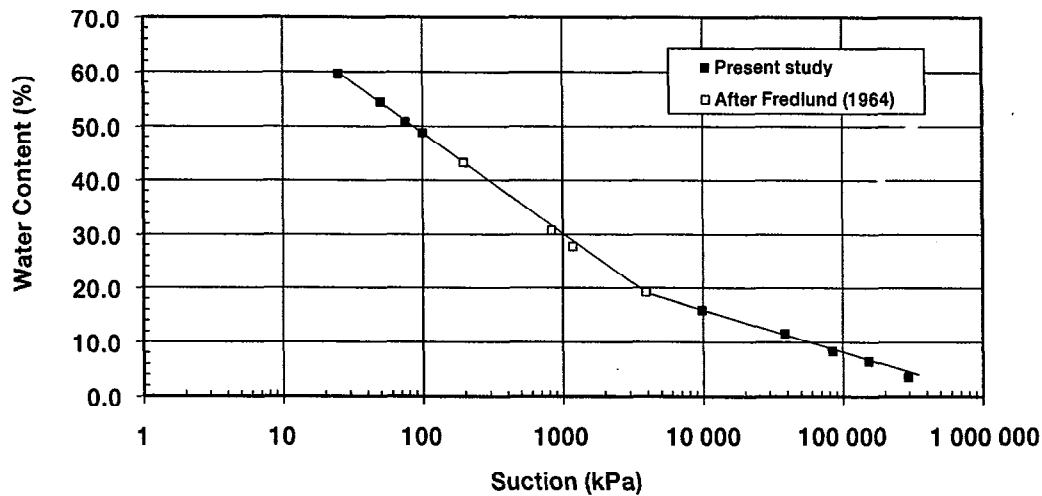


Fig. 4. Water-content characteristic curves for Regina clay at 20°C.



soil-water characteristic curves for the Beaver Creek sand, Custom silt, and Regina clay, respectively, for suctions ranging from 25 kPa to approximately 300 000 kPa.

The soil-water characteristic curve for the Regina clay at 20°C (Fig. 4) was established using several additional values of water content and corresponding values of suction obtained from Fredlund (1964). Fredlund determined these points by the pressure plate and glass desiccator methods as described above. The properties of the Regina clay samples used by Fredlund (1964) with respect to texture and plasticity are similar to those reported in Table 1.

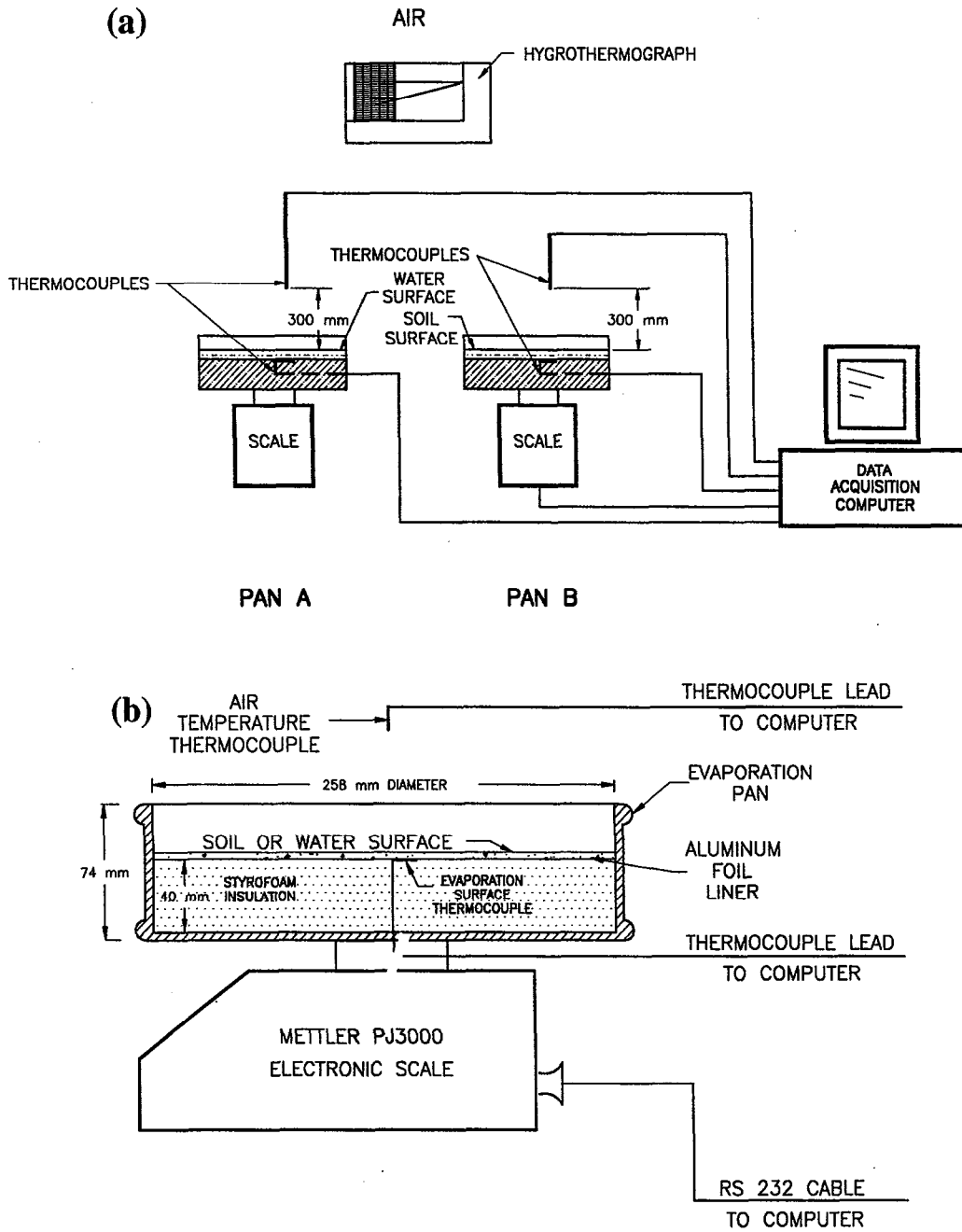
Evaporation tests

The second stage of the testing program was to conduct evaporation tests using specimens of each soil type. Thin soil sections were selected in order to minimize the influence of soil water below the evaporating soil surface. Hillel (1980) states: "the actual evaporation rate is determined either by external evaporativity or by the soil's own ability to deliver water, whichever is the lesser (and hence the limiting factor)." The objective of the test procedure described here was to determine

the soil properties at the soil surface or the soil boundary layer that control evaporation. The soil sections were therefore made as thin as possible to minimize potential flow processes in the soil below the surface from influencing the rate of evaporation from the surface of the soil.

The thin soil section evaporation tests were conducted such that the AE from the soil surfaces was continually measured as drying took place from an initially saturated state to a completely air-dried state. The thin soil sections were artificially formed on a circular, 258 mm diameter, evaporation pan, as shown in Figs. 5a and 5b. Each evaporation test was carried out using two identical evaporation pans. One pan contained the thin section of soil surface to determine the AE, while the second identical pan contained distilled water which provided the reference for the PE. The mass and change in mass of each pan was continually monitored to determine the rate of evaporation from the pans. The water contents of the soil specimens at various times during each test were determined using the final mass of dry soil and water at the end of the test plus the instantaneous masses measured during the test. The temperature of the soil surfaces, the water surface, and the air was also monitored continuously along with the relative humidity of the

Fig. 5. (a) Thin soil section drying test apparatus. (b) Detailed section of the evaporation pan used for the thin soil section evaporation test.



air above the evaporating surfaces. All tests were conducted at room temperature in the geotechnical laboratory at the University of Saskatchewan.

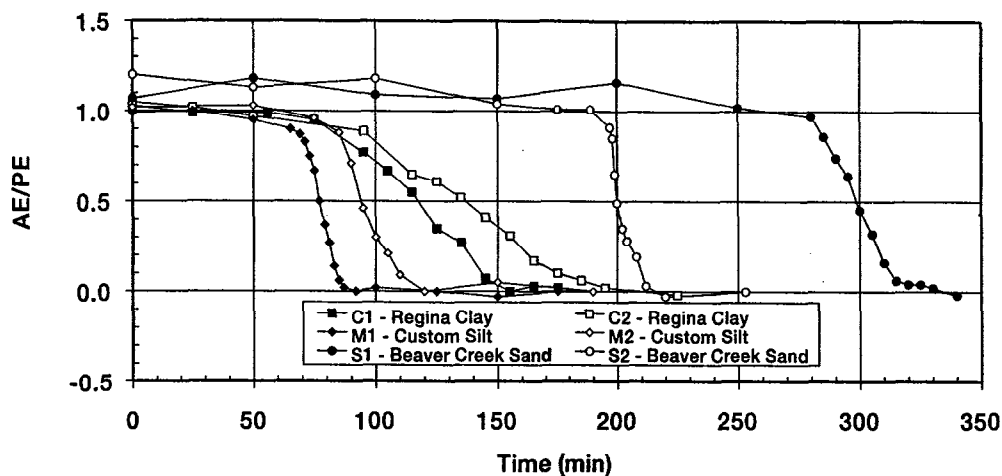
Two thin section drying tests were completed for each soil type (i.e., sand, silt and clay). Numerous attempts were required in order to develop a procedure that provided a thin layer of soil with a uniform thickness and an initial target water content. The thin soil sections were prepared by gently dusting a layer of soil onto the pan using a hand-held sieve filled with powdered dry soil. An 850 μm sieve was used to apply the Beaver Creek sand, while a 425 μm sieve was used to apply the Custom silt and Regina clay. The dusted soil layers were applied uniformly until a thickness just adequate to visually cover the aluminum surface of the pan was achieved. The final layer thickness for the two Beaver Creek sand specimens were

0.5 mm and 0.7 mm, while the final layer thicknesses for the two Custom silt and one of the Regina clay surfaces was 0.3 mm. A layer thickness of 0.2 mm was used for the second Regina clay sample.

The dry soil layers were wetted to saturation using a fine uniform mist of distilled water. The mass of the soil specimens were then monitored while evaporating to an air-dry state. Table 3 provides a summary of the six thin soil section drying tests. Figure 6 shows the normalized evaporation, AE/PE , obtained for the soil and water surfaces measured with respect to time for the Beaver Creek sand, Custom silt, and Regina clay. The normalized evaporation parameter is selected for convenience, since the term PE is controlled primarily by atmospheric conditions and surface temperature, which are the same for both the water and soil surfaces during each evaporation test.

Table 3. Summary of thin soil section evaporation tests.

Specimen No.	Soil type	Sample thickness (mm)	Initial water content (%)	Test duration (min)	Mean room air temperature (°C)	Mean relative humidity of air (%)	Mean water pan evaporation (mm/day)
S1	Beaver Creek sand	0.7	25.0	330	23.1	53	1.31
S2	Beaver Creek sand	0.5	25.5	250	22.7	44	1.40
M1	Custom silt	0.3	30.0	125	22.5	39	1.71
M2	Custom silt	0.3	28.8	190	23.0	62	1.16
C1	Regina clay	0.3	63.5	195	22.8	35	1.54
C2	Regina clay	0.2	61.2	225	25.5	50	1.29

Fig. 6. The ratio of actual evaporation and potential evaporation, AE/PE, versus drying time for the Beaver Creek sand, Custom silt, and Regina clay.

Discussion and analysis

The soil-water characteristic curves for each soil are shown in Figs. 2, 3, and 4. These drying curves are important in geotechnical engineering because they show the amount of water retained in the soil over the total range of soil suction. Wetting the soils from a dry state to a wet state (i.e., high suction to low suction) would result in slightly different curves due to the effects of hysteresis. The drying curves shown are most applicable to the thin soil section evaporation test.

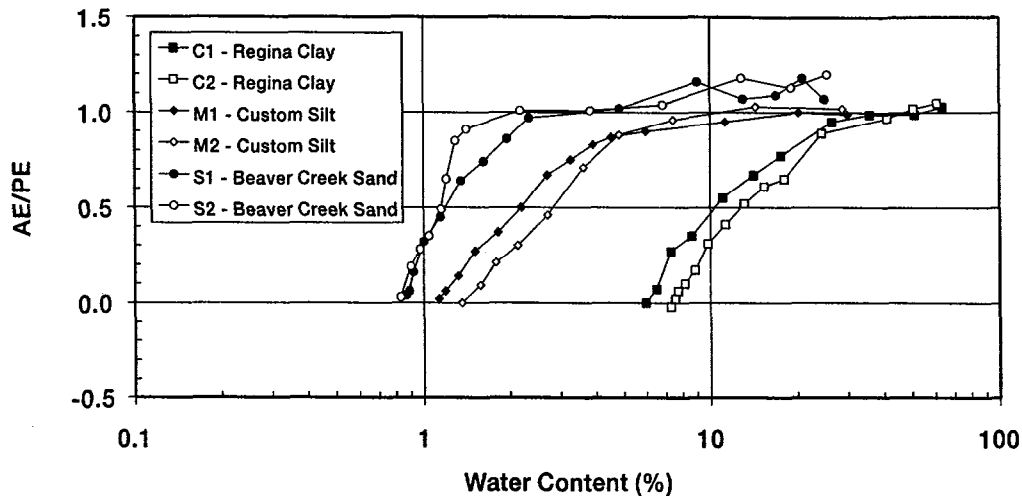
Geotechnical engineers are most familiar with soil suctions that are relatively low when compared with those shown in Figs. 2, 3, and 4. The unsaturated soils dealt with usually have values of matric suction that do not exceed 500 kPa. In nature, however, soils at the ground surface commonly have extremely high values of suction. The permanent wilting point of plants found in semi-arid climates is commonly reported to be 15 bar (Hillel 1980) or approximately 1500 kPa. Even at large values of suction, considerable water may still be present in the soil. For example, in Fig. 4, Regina clay has a water content of approximately 25% at 1500 kPa of suction. This corresponds approximately to the water content at the plastic limit. Natural soils commonly reach a completely air-dried state at the ground surface. This would be the case for the exposed soil surface of a cover for a municipal landfill after several days of continuous drying without precipitation. The water content for Regina clay, for example, may be as low as 6% at the ground surface. Figure 4 shows that this water content

would correspond to a value of total suction of approximately 200 000 kPa. Oven drying at a temperature of 105°C results in a suction approaching 1 000 000 kPa. Although the physical properties of soil water at extremely high values of suction are not yet fully explained (Fredlund 1991), it can be argued that understanding the behaviour of natural soils at and near the ground surface requires the acceptance of soil suctions far in excess of 500 kPa.

It should be noted that a distinction has been made between matric suction and total suction in Figs. 2, 3, and 4. The suctions established using the pressure plate method correspond to values of matric suctions (i.e., $u_a - u_w$). Osmotic suction due to the presence of dissolved solids is not included. Distilled water was used for all test procedures, therefore, the value of osmotic suction for the Beaver Creek sand and Custom silt may be assumed to be relatively small. This assumption may not, however, be true for the Regina clay because of its geochemical nature. Krahn (1970) showed osmotic suction to be approximately 200 kPa for Regina clay having a water content of 30%. This indicated that a high level of dissolved solids was present in the clay. The use of distilled water during sample preparation dilutes but does not remove the salts. In summary, the values of matric suction established by the pressure plate method for the Regina clay may underestimate total suction.

The soil-water contents shown in Figs. 2, 3, and 4 that correspond to high values of suction (i.e., greater than 1500 kPa) were established in the desiccators through vapour equilibrium

Fig. 7. The ratio of actual evaporation and potential evaporation, AE/PE, versus water content for the Beaver Creek sand, Custom silt, and Regina clay.



with the osmotic suction of the electrolyte solutions. The soil-water contents actually correspond to total suction, which includes both matric and osmotic suction. It is difficult to establish the relative components of matric and osmotic suction at such high values of total suction, but it is reasonable to assume that the magnitude of osmotic suction will increase at lower water contents, since the mass of dissolved solids remains constant.

Figure 6 shows the ratio of AE/PE versus time for each sample of Beaver Creek sand, Custom silt, and Regina clay. The curves are similar to those given by Holmes (1961) in Fig. 1, except that the AE/PE ratio is plotted as a function of time rather than water availability. Time zero in Fig. 6 corresponds to a nearly saturated state (or a high water availability), which is similar to the field capacity in Fig. 1. The normalized evaporation, AE/PE, is approximately unity for all specimens at the start of the evaporation test. It can be seen that the ratio is slightly greater than 1.0 for the Beaver Creek sand specimens S1 and S2. This deviation can be attributed to slight variations in the aerodynamic resistance in the air spaces above the water and soil evaporation pans, as well as the surface temperatures at the time of the tests. All specimens continue to evaporate at a near potential rate and then begin to decline after a period of time. The rate of evaporation decreases first for the silt, followed by the clay, and finally the sand. The evaporation rate for all soils falls to zero after each soil specimen reaches an air-dry state. It is difficult to understand and compare all of the controlling variables for Fig. 6, since each soil type has a different initial water content, sample thickness, and volume of water available for evaporation.

Figure 7 shows a plot of the AE/PE ratio versus water content for each specimen. The break or decline in evaporation rate occurs at a specific water content for each soil type. For example, the decline in evaporation for Regina clay specimens C1 and C2 occurs at a water content of approximately 20%. The Custom silt and Beaver Creek sand have a break in the evaporation rate at water contents of 5 and 2%, respectively. When the plots for the clay specimens C1 and C2, and for the silt specimens M1 and M2, are compared, they show slight variations. Specimens C1 and M1 reach zero evaporation at slightly lower water contents than specimens C2 and M2. This

slight variation can be attributed to a difference in the relative humidity of the air at the time of each test, since relative humidity control in the test area was not available. Table 3 shows the relative humidity in the air at the time of each test, and it can be seen that tests C1 and M1 were performed at significantly lower relative humidities than tests C2 and M2. Hence, the air-dried soils for tests C1 and M1 have less hygroscopic moisture. Tests S1 and S2 were performed with similar humidities and therefore show closer agreement for the final water content corresponding to zero evaporation (or an AE/PE ratio equal to zero).

The data shown in Fig. 7 suggest that the water content of the soil influences the rate of evaporation for each soil type. However, water content alone cannot be identified as the unique independent variable controlling the actual rate of evaporation for all soil types. Soil texture must also be taken into consideration. Water content may, however, be used to determine the value of total suction in the soil. The soil-water characteristic curves shown in Figs. 2, 3, and 4 were used to determine corresponding values of total suction at each measured water content during the evaporation tests. Figure 8 shows a plot of the AE/PE ratio versus total suction for the Beaver Creek sand specimen S1, Custom silt specimen M1, and Regina clay specimen C2. The tests for specimens S1 and C2 were conducted at a relative air humidity of approximately 50% while the test for specimen M1 was performed at a lower relative air humidity of approximately 40%.

Figure 8 shows a reasonably good correlation between the ratio of AE/PE and total suction. This correlation is independent of time, water content, and soil texture. The ratio of AE/PE is approximately constant and equal to unity for values of total suction less than approximately 3000 kPa. The actual rate of evaporation begins to decline once the value of the total suction exceeds approximately 3000 kPa. The rate of actual evaporation continues to decrease as the value of total suction increases. The AE/PE ratio then falls to zero for the three soil types at values of total suctions slightly larger than 100 000 kPa.

The relationship between total suction and AE/PE can be explained by considering the relationship between relative humidity and total suction given by Edlefsen and Anderson (1943):

Fig. 8. The ratio of actual evaporation and potential evaporation, AE/PE, versus total suction for the Beaver Creek sand, Custom silt, and Regina clay.

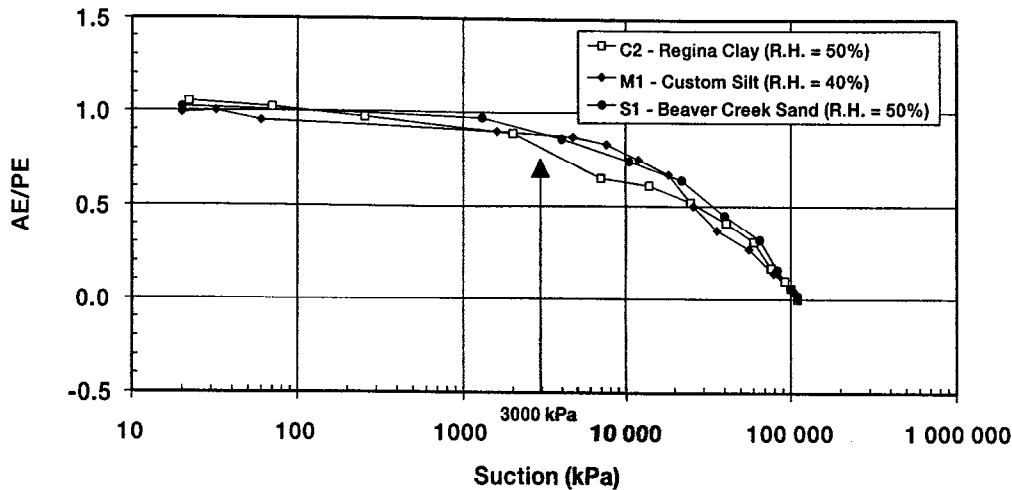
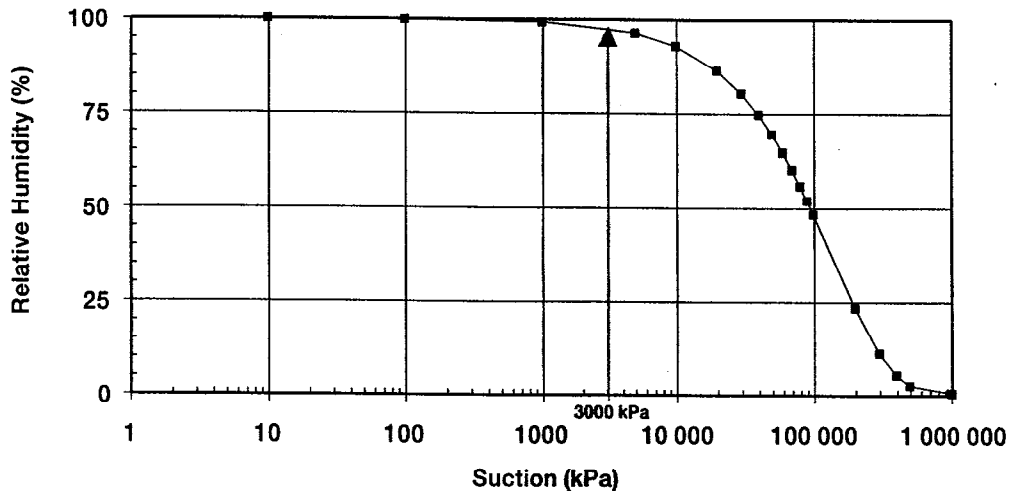


Fig. 9. Relative humidity versus total suction calculated on the basis of eq. [3] (20°C).



$$[3] \quad h_r = \exp\left(\frac{\Psi g W_v}{RT}\right)$$

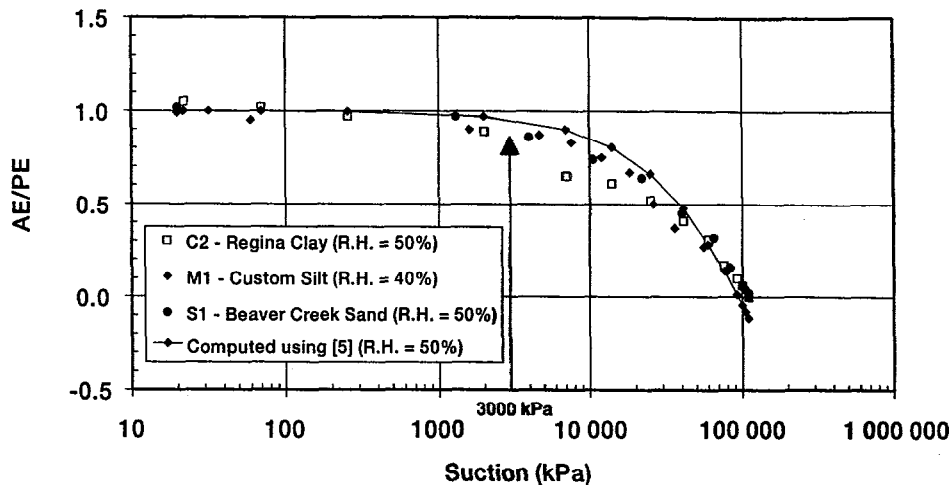
where h_r is relative humidity in the unsaturated soil voids (i.e., actual vapour pressure divided by saturation vapour pressure), Ψ is the total suction in the liquid water phase expressed as equivalent matric suction and as a negative value (m), W_v is the molecular weight of water (0.018 kg/mol) and g is acceleration (m/s^2).

Figure 9 shows this relationship graphically on a log–arithmetic plot. Relative humidity is an exponential function of total suction, and the decline in relative humidity with increasing suction is initially small. A substantial decrease in the relative humidity occurs only after the value of total suction exceeds 2000 to 3000 kPa (i.e., 3000 kPa of total suction corresponds to a relative humidity of approximately 98%). The suppression of relative humidity results in an equivalent decline in the absolute vapour pressure at the soil surface. Since [1] shows the rate of evaporation to be a function of the vapour pressure at the evaporating surface, the rationale which suggests that the actual rate of evaporation depends on the total suction at the soil surface appears valid.

Figure 8 has illustrated that the AE/PE ratio is equal to zero for a value of total suction slightly greater than 100 000 kPa. This point of zero evaporation is controlled by the relative humidity in the air. The evaporating soil surface dries to a point that is in equilibrium with the air. For example, test C2 was performed with a room air relative humidity of 50%. As shown in Fig. 9, this corresponds to a total suction of approximately 100 000 kPa. Soil evaporation should cease when the relative humidity in the soil reaches equilibrium with the relative humidity of the air above the soil. Hence, zero evaporation should correspond to a suction of 100 000 kPa, as shown in Fig. 8. Alternately, evaporation would have continued to a higher value of total suction if the humidity in the air were less. A room air relative humidity of 20% would have resulted in a total suction of approximately 200 000 kPa for the soil surface to reach air–dry equilibrium.

The relationship between actual soil evaporative fluxes and total suction in the soil is important to geotechnical engineers, since it forms the basis for the prediction of actual evaporative fluxes. Predicting the values of AE/PE as a function of total suction shown in Fig. 8 can be achieved by combining [1] and

Fig. 10. Comparison of the measured AE/PE versus total suction for the Beaver Creek sand, Custom silt, and Regina clay to the curve computed using eq. [5].



[3]. Using [1] and assuming $f(u)$ is the same for both the soil surface and the water surface gives

$$[4] \quad \frac{AE}{PE} = \frac{(e_o - e_a)}{(e_s - e_a)}$$

where e_o is the actual vapour pressure of the soil surface equal to the product of h_s and e_s (kPa); e_s is defined by the temperature of the soil, water, and air; and e_a is equal to the product of the relative humidity measured in the air (i.e., Table 3) and e_s .

Assuming the air, water, and soil are at approximately the same temperature so that e_s cancels out and substituting [3] into [4] gives

$$[5] \quad \frac{AE}{PE} = \left[\frac{\exp\left(\frac{\Psi_g W_v}{RT}\right) - h_a}{1 - h_a} \right]$$

where h_a is the relative humidity of the air above the evaporating soil and water surfaces.

It is important to note that should the soil, water, and air temperatures not be equal, [3] and [4] must be solved using the saturated vapour pressure corresponding to each temperature.

Equation [5] provides the value of AE/PE as a function of total suction at the soil surface. The accuracy of the functional relationship can be tested through comparison with the experimental data. Figure 10 shows the curve for AE/PE as a function of total suction computed using [5], along with the values measured for the sand, silt, and clay surface. It can be seen that the predicted curve compares reasonably well to the measured values. The predicted curve is least reliable for the Regina clay. This may be attributed to a nonuniform water content across the thickness of the soil specimen during the evaporation test, since the particle size of the clay is much smaller than the thickness of the thin soil section (i.e., 0.2 to 0.3 mm). In general, however, the principle that soil suction controls the normalized evaporation for a soil surface appears valid. Furthermore, this principle is independent of other soil properties such as moisture content, texture, and mineralogy.

It should be noted that this discussion has addressed only the properties of soil surfaces that control evaporative fluxes into the atmosphere. The soil evaporation tests considered only thin soil sections in the absence of the influence due to soil

water below the surface. Increasing the thickness of the soil layers would greatly influence evaporative fluxes, as deeper soil water would be available as recharge to the desiccating soil surfaces. The analysis of this more complex problem would require a theoretical approach that includes the influence of flow processes below the soil surface.

Summary and conclusions

Many problems in geotechnical engineering require that the exchange of water between the atmosphere and ground surface be known. The process of evaporation from soil surfaces in particular has not been clearly defined in the past. This study has found that a relationship between the actual or normalized evaporation rate and total suction does exist for three different soil types.

Evaporation from a soil surface is a function of the vapour pressure gradient between the soil surface and the ambient atmosphere. The mass transfer equation, [1], initially proposed by Dalton for evaluating evaporation from water surfaces, can be modified and applied to soil surfaces. Saturated and nearly saturated soil surfaces evaporate at a potential rate approximately equal to the evaporation rate from free water surfaces. It has been found that the actual rate of evaporation from a soil surface falls below this potential rate of evaporation once the soil becomes unsaturated and the value of total suction exceeds a value of approximately 3000 kPa. This relationship occurs independently of water content. The rate of evaporation continues to decline as the total suction increases. In general, total suction (i.e., matric suction plus osmotic suction) appears to be a suitable state variable for describing soil atmosphere evaporative fluxes. This is consistent with the stress-state variables generally used in unsaturated soil mechanics.

In summary, evaporative fluxes from soil surfaces can be evaluated on the basis of easily measured soil properties. The measured water content can be used in conjunction with the soil-water characteristic curve for total suction to calculate the vapour pressure at the soil surface. Evaporative fluxes from unsaturated soil surfaces at high values of suction are less than those from saturated surfaces under identical climatic conditions. This is an important consideration with respect to the design, for example, of soil cover systems for the control of

water fluxes into underlying waste materials. In such an application, the geotechnical engineer could use a conventional method for evaluating the potential rate of evaporation (i.e., the Penman method) and modify it to obtain the actual evaporation for unsaturated conditions using [5].

References

- Barbour, S.L., Wilson, G.W., and St-Arnaud, L.C. 1993. Evaluation of the saturated-unsaturated groundwater conditions of a thickened tailings deposit. *Canadian Geotechnical Journal*, **30**: 935-946.
- Barton, I.J. 1979. A parameterization of the evaporation from non-saturated surfaces. *Journal of Applied Meteorology*, **18**: 43-47.
- Brutsaert, W.H. 1982. *Evaporation into the atmosphere*. P. Reidel Publishing Company, Dordrecht, Holland.
- Edlefsen, N.E., and Anderson, A.B.C. 1943. Thermodynamics of soil moisture. *Hilgardia*, **15**(2): 31-298.
- Fredlund, D.G. 1964. Comparison of soil suction and one-dimensional consolidation characteristics of a highly plastic clay. M.Sc. thesis, University of Alberta, Edmonton.
- Fredlund, D.G. 1991. How negative can pore-water pressures get? *Geotechnical News*, **9**(3).
- Granger, R.J. 1989a. An examination of the concept of potential evaporation. *Journal of Hydrology*, **111**: 9-19.
- Granger, R.J. 1989b. Evaporation from natural non-saturated surfaces. *Journal of Hydrology*, **111**: 21-29.
- Gray, D.M. 1970. *Handbook on the principals of hydrology*. Canadian National Committee for the International Hydrological Decade, National Research Council of Canada, Ottawa.
- Hammel, J.E., Papendick, R.I., and Campbell, G.S. 1981. Fallow tillage effects on evaporation and seedzone water content in a dry summer climate. *Soil Science Society of America Journal*, **45**: 1016-1022.
- Hillel, D. 1980. *Applications of soil physics*. Academic Press, New York.
- Holmes, R.M. 1961. Estimation of soil moisture content using evaporation data. *Proceedings of Hydrology Symposium, No. 2 Evaporation*. Queen's Printer, Ottawa, pp. 184-196.
- Krahn, J. 1970. Comparison of soil pore water potential components. M.Sc. thesis, University of Saskatchewan, Saskatoon.
- Morton, F. I., 1985. The complementary relationship areal evapotranspiration model: How it works. *Proceedings of the National Conference on Advances in Evapotranspiration*, American Society of Agricultural Engineers, Chicago, Ill., pp. 377-384.
- Penman, H.L. 1948. Natural evapotranspiration from open water, bare soil and grass. *Proceedings of the Royal Society of London, Series A*, **193**: 120-145.
- Robinson, R.A., and Stokes, R.H. 1955. *Electrolyte solutions: The measurement and interpretation of conductance, chemical potential and diffusion in solutions of simple electrolytes*. Academic Press, New York.
- Sattler, P., and Fredlund, D.G. 1989. Use of thermal conductivity sensors to measure matric suction in the laboratory. *Canadian Geotechnical Journal*, **26**: 491-498.
- Silvestri, V., Soulie, M., Lafleur, J., Sarkis, G., and Bekkouche, N. 1990. Foundation problems in Champlain clays during droughts. 1: Rainfall deficits in Montréal (1930-1988). *Canadian Geotechnical Journal*, **27**: 285-293.
- Thornthwaite, C.W. 1948. An approach toward a rational classification of climate. *Geographical Review*, **38**: 55-94.
- Wilson, G.W. 1990. The evaluation of evaporative fluxes from unsaturated soil surfaces. Ph.D. thesis, University of Saskatchewan, Saskatoon.
- Wilson, G.W., Fredlund, D.G., and Barbour, S.L. 1994. Coupled soil-atmosphere modeling for soil evaporation. *Canadian Geotechnical Journal*, **31**: 151-161.
- World Meteorological Organization. 1974. *International glossary of hydrology*. WMO Report No. 385.
- Yanful, E.K., Bell, A.V., and Woysner, M.R. 1993. Design of a composite soil cover for an experimental waste rock pile near Newcastle, New Brunswick, Canada. *Canadian Geotechnical Journal*, **30**: 578-587.



NRC · CNRC

Reprinted from
**Canadian
Geotechnical
Journal**

Réimpression de la
**Revue
canadienne
de géotechnique**

Coupled soil-atmosphere modelling for soil evaporation

G. WARD WILSON, D.G. FREDLUND, AND S.L. BARBOUR

Volume 31 • Number 2 • 1994

Pages 151 – 161

Coupled soil-atmosphere modelling for soil evaporation

G. WARD WILSON, D.G. FREDLUND, AND S.L. BARBOUR

Department of Civil Engineering, University of Saskatchewan, Saskatoon, SK S7N 0W0, Canada

Received August 11, 1992

Accepted September 9, 1993

Traditional methods of evaluating evaporation provide an estimate of the maximum or potential rate of evaporation determined on the basis of climatic conditions. Methods such as these are appropriate for open water or fully saturated soil surfaces. Actual rates of evaporation from unsaturated soil surfaces are generally greatly reduced relative to the potential rate of evaporation. A theoretical model for predicting the rate of evaporation from soil surfaces is presented in this paper. The model is based on a system of equations for coupled heat and mass transfer in soil. Darcy's Law and Fick's Law are used to describe the flow of liquid water and water vapour, respectively. Heat flow is evaluated on the basis of conductive and latent heat fluxes. Dalton's Law is used to calculate the rate of soil evaporation to the atmosphere based on the suction at the soil surface. The soil-atmosphere model was used to predict soil evaporation rates, water-content profiles, and temperature profiles for a controlled column evaporation test over a 42 day period. The values computed by the soil-atmosphere model agreed well with the values measured for two columns of Beaver Creek sand in the evaporation test.

Key words: modelling, evaporation, unsaturated, soil surfaces.

Les méthodes traditionnelles pour évaluer l'évaporation fournit une évaluation du taux d'évaporation potentiel ou maximum déterminé sur la base des conditions climatiques. De telles méthodes appropriées pour les surfaces d'eau libres ou de sol complètement saturé. Les taux réels d'évaporation à la surface des sols partiellement saturés sont en général grandement réduites par rapport au taux potentiel d'évaporation. Un modèle théorique pour prédire le taux d'évaporation à la surface des sols saturés est présenté dans cet article. Le modèle est basé sur un système d'équations pour le transfert couplé de chaleur et de masse dans le sol. Les lois de Darcy et de Fick sont utilisées pour décrire respectivement l'écoulement du liquide et de la vapeur d'eau. L'écoulement de chaleur est évalué sur la base des flux de chaleur latente et conductrice. La loi de Dalton est utilisée pour calculer le taux d'évaporation du sol vers l'atmosphère sur la base de la succion à la surface du sol. Le modèle sol-atmosphère a été utilisé pour prédire les taux d'évaporation, les profils de teneur en eau, et les profils de température pour un essai contrôlé d'évaporation dans une colonne durant une période de 42 jours. Les valeurs calculées par le modèle sol-atmosphère concordent bien avec les valeurs mesurées pour deux colonnes de sable de Beaver Creek dans l'essai d'évaporation.

Mots clés : modélisation, évaporation, non saturé, surfaces de sol.

[Traduit par la rédaction]

Can. Geotech. J. 31, 151-161 (1994)

Introduction

Prediction of the flux boundary condition with respect to water flow across the soil-atmosphere boundary is essential for many problems in geotechnical engineering. Examples include the design of soil cover systems for the long-term closure of hazardous-waste sites, saturated-unsaturated groundwater-flow modelling, and the prediction of heave for shallow foundations on expansive soils.

Two principal processes govern the exchange of water between the soil surface and the atmosphere. Water enters the soil surface as liquid through the process of infiltration. Alternately, water exfiltrates from the soil surface as vapour through the process of evaporation. The process of infiltration depends primarily on soil properties such as hydraulic conductivity and is reasonably well understood. The evaluation of the evaporative fluxes from a soil surface is more difficult, since the rate of evaporation depends on both soil properties and climatic conditions. Accurate prediction of evaporative fluxes is critical, for example, in the design of soil cover systems which are to function as oxygen barriers for mine tailings that produce acid drainage.

This paper presents a theoretical approach for the evaluation of evaporative fluxes based on measured soil properties and climatic conditions. The theoretical model is used to simulate evaporative fluxes for comparison with the measured results from a sand column evaporation test conducted under controlled climatic conditions. The theoretical approach

presented considers nonvegetated or bare soil surfaces. This work forms the basis of a more general formulation which could incorporate the effects of a vegetative cover on evaporation rates from soil surfaces.

Background

Engineers have traditionally used a term defined as potential evaporation (PE) to estimate evaporation or evapotranspiration rates. The term, which has been in use for at least 40 years, was first introduced by Thornthwaite (1948). Potential evaporation may be defined as the upper limit or maximum rate of evaporation from a pure water surface under given climatic conditions. The potential rate of evaporation may be computed using the Dalton-type equation (Gray 1970):

$$[1] \quad E = f(u) (e_s - e_a)$$

where E is rate of evaporation (mm/day), e_s is the saturation vapour pressure of water at the temperature of the surface (mm Hg or kPa), e_a is vapour pressure of the air in the atmosphere above the water surface (mm Hg or kPa), and $f(u)$ is a turbulent exchange function which depends on the mixing characteristics of the air above the evaporating surface.

The use of the apparently simple expression given in [1] is considered a direct approach (van Bavel 1967; Granger 1989). However, the application of [1] to field problems can be difficult. Accurate evaluation of the turbulent exchange

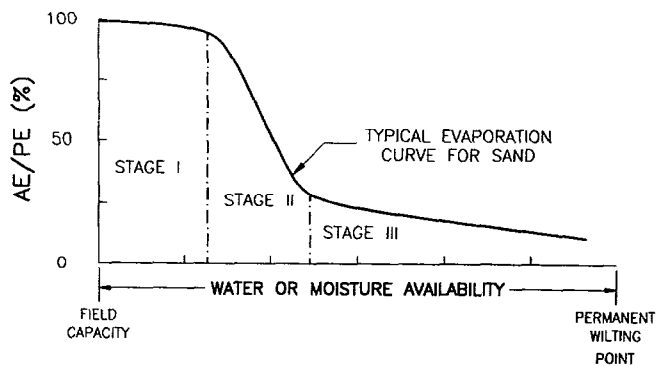


FIG. 1. The relationship between the rate of actual evaporation and potential evaporation (AE/PE) and water availability.

function requires either an empirical approach or the application of rigorous aerodynamic profile methods. Furthermore, [1] is often indeterminate when applied to field studies because of difficulties associated with the evaluation of surface temperatures and vapour pressure (Granger 1989). The Dalton equation is generally not applied in the elementary form stated in [1]. However, [1] forms the basis for the widely used Penman method. Penman (1948) resolved the difficulty associated with surface temperature in [1] by combining it with a second simultaneous equation for the sensible heat flux at the surface. Penman (1948) also provides a relatively simple method for determining the turbulent exchange function on the basis of mean wind speed. The Penman method assumes the surface to be saturated at all times and therefore provides an estimate of the potential rate of evaporation.

Numerous other methods are available for calculating the rate of potential evaporation. These include the temperature-based method proposed by Thornthwaite (1948) and the energy-based method developed by Priestley and Taylor (1972). Although all of the various methods for potential evaporation may predict different rates of evaporation when applied to a specific site (Granger 1989), they all attempt to predict a maximum or potential rate of evaporation. The fundamental assumption used by the methods outlined above is that water is freely available at the surface for evaporation. In other words, the surface is an open water surface or a saturated soil surface.

The actual rate of evaporation (AE) begins to decline as the surface becomes unsaturated and the supply of water to the surface becomes limited (Gray 1970; Morton 1975; Brutseart 1982). Figure 1 shows a typical relationship for the ratio of actual evaporation and potential evaporation (AE/PE) versus water availability for a sand surface. Gray (1970) presents similar curves for sand and clay surfaces. The rate of actual evaporation is approximately equal to the potential rate (i.e., AE/PE = 100%) when the sand is saturated or nearly saturated (i.e., water content at or above the field capacity). The rate of AE/PE decreases as the sand surface becomes drier and eventually falls to a low, relatively constant residual value as the sand surface desiccates to the permanent wilting point for plants.

The shape of the drying curve shown in Fig. 1 is well known and has been described by others including Hillel (1980). In general, the curve is described as having three stages of drying. Stage I drying is the maximum or potential rate of drying that occurs when the soil surface is at or near

saturation and is determined by climatic conditions. Stage II drying begins when the conductive properties of the soil no longer permit a sufficient flow of water to the surface to maintain the maximum potential rate of evaporation. The rate of evaporation continues to decline during stage II drying as the surface continues to desiccate and reaches a slow residual value defined as stage III drying. Hillel (1980) states that the slow rate of evaporation during stage III drying occurs after the soil surface becomes sufficiently desiccated to cause the liquid-water phase to become discontinuous. The flow of liquid water to the surface ceases and water molecules may only migrate to the surface through the process of vapour diffusion. In summary, it can be seen that the rate of actual evaporation from a soil surface is controlled by both climatic conditions, which define the potential rate of evaporation, and soil properties such as hydraulic conductivity and vapour diffusivity.

Since the actual rate of evaporation is controlled by both climatic conditions and soil properties, accurate prediction of the actual rate of evaporation from soil surfaces requires a method of analysis that includes both factors. The methods previously outlined (i.e., the use of [1] or the Penman method) are based on climatic conditions such as temperature, relative humidity, wind speed, and net radiation. These methods are reliable only for special conditions where the rate of evaporation is controlled solely by climatic conditions (i.e., stage I drying). The climate-based methods of analysis for potential evaporation often over-estimate actual evaporation rates, since the actual rate of evaporation is soil limited. This is frequently the case for unsaturated soil surfaces in arid and semiarid environments (Wilson 1990). Geotechnical engineers are often required to predict evaporative fluxes under these conditions. A method that includes both atmospheric conditions and soil properties is required.

The method given by Penman (1948) for predicting the potential rate of evaporation has been modified a number of times for application to nonpotential conditions (Monteith 1965; Shuttleworth and Wallace 1985; Choudhury and Monteith 1988). These extended forms of the Penman equation incorporate a number of soil and canopy resistance terms to reduce the computed rate of evaporation and evapotranspiration (Stannard 1993). In general, the resistance terms for the soil surface are determined using either empirical methods or simplified assumptions for vapour diffusion in the drying soil at the surface. Properties of the soil profile below the surface such as hydraulic conductivity are not considered. Since geotechnical engineers are interested in predicting the movement of groundwater in the soil below the surface, they require a soil-atmosphere model based on the explicit hydraulic properties of the soil.

A variety of soil-atmosphere-based models for the evaluation of soil evaporative fluxes have been proposed (Passerat De Silans et al. 1989). Most of the methods proposed calculate actual evaporative fluxes from bare soil surfaces using a system of coupled heat and water transport equations. The actual rates of evaporation are predicted using equations similar to [1]. The actual vapour pressure of the soil surface replaces the saturated vapour pressure. In most cases the vapour pressure at the soil surface is calculated using the well-known Philip and de Vries (1957) formulation for the transport of heat and moisture in soil.

The soil-atmosphere models proposed by Schieldge et al. (1982), Camillo et al. (1983), Witonon and Bruckler (1989),

and Passerat De Silans et al. (1989) use the Philip and de Vries (1957) formulation. In general, the models appear to provide good estimates of evaporative fluxes, water-content profiles, and temperature profiles for drying events ranging between 2 and 7 days. Few difficulties have been reported when the models are applied to relatively short periods of evaporation. However, the accuracy of the models with respect to extended periods of evaporation has not been demonstrated. The results of field tests and model simulations do not show the development of stage III drying previously described. Periods of continuous evaporation in arid and semiarid regions of the world commonly extend over several weeks. The application of these soil-atmosphere models to the prolonged evaporative events can be questioned.

In addition to the lack of experimental verification, the soil-atmosphere models based on the Philip and de Vries (1957) formulation have other shortcomings with respect to application to geotechnical problems. The most important difficulty relates to the Philip and de Vries (1957) formulation that assumes flow in response to a volumetric water content gradient. This is fundamentally incorrect, since the flow of liquid water occurs in response to a hydraulic-head gradient. Because of this limitation, the formulation is applicable only to the analysis of homogeneous and isotropic systems. Geotechnical engineers are commonly required to analyze multilayered, anisotropic systems. In fact, the design of covers is by definition a multilayer system. For these reasons the Philip and de Vries (1957) formulation is not acceptable for application to problems in geotechnical engineering.

Attempts have been made to modify the volumetric water content based Philip and de Vries (1957) formulation. Sophocleous (1979) and Milly (1982, 1984a, 1984b) use a matric head based formulation. Sophocleous (1979) conducted model simulations to study the effects of coupled and uncoupled heat and moisture flow on evaporative fluxes. Milly (1984a, 1984b) provided model simulations of evaporative fluxes under atmospheric forcing. Sophocleous (1979) and Milly (1984a, 1984b) did not compare field and (or) laboratory observations with the theory and as such it is difficult to determine the accuracy of these models.

The objective of this paper is to provide a basis for the development of a soil-atmosphere model to predict evaporative fluxes from soil surfaces. The model should be formulated in a manner suitable for application in geotechnical engineering. In this paper, a model is formulated using stress-state variables and conventions suitable for application to problems in geotechnical engineering. The accuracy of the assumptions used in the proposed model are tested using a controlled column drying test. The surfaces of two identical columns of fine uniform sand are allowed to desiccate in an arid laboratory chamber. The rates of actual evaporation from the sand surfaces are measured directly along with water-content changes in the soil profile of the columns. The drying test was conducted over a prolonged time such that the third stage of drying was fully developed. The measured results from the column drying tests are compared with theoretical simulations obtained from the proposed soil-atmosphere model.

Soil-atmosphere model formulation

The development of a soil-atmosphere model for the evaluation of evaporative fluxes requires a system of equations

which describe the flux of water vapour into the atmosphere and the flow of liquid water and water vapour below the soil surface.

Wilson (1990) provides a modification to the Penman method for the calculation of nonpotential evaporation from unsaturated soil surfaces:

$$[2] \quad E = \frac{\Gamma Q_n + \eta E_a}{\Gamma + \eta A}$$

where E is evaporative flux (mm/day), Γ is slope of the saturation vapour pressure versus temperature curve at the mean temperature of the air (mm Hg/°C), Q_n is all net radiation at the soil surface (mm/day of water), η is psychrometric constant, and E_a is $f(u) e_a (B - A)$, where $f(u) = 0.35 (1 + 0.146 Wa)$, Wa is wind speed (km/h), e_a is water vapour pressure of the air above the soil surface (mm Hg), B is inverse of the relative humidity in the air, and A is inverse of the relative humidity at the soil surface. The fundamental assumption made in the formulation of [2] is that the term e_s for the saturated vapour pressure of water at the soil surface in [1] can be replaced using the actual vapour pressure at the soil surface. It may be noted that [2] transforms to the original Penman equation if the soil surface is saturated (i.e., $A = \text{unity}$ for a relative humidity of 100%). The actual vapour pressure at the soil surface is in turn calculated on the basis of the flow of liquid water and water vapour below the soil surface.

Application of the extended form of the Penman equation given in [2] is not suited to the laboratory column drying test described in this paper. However, the Dalton-type equation shown in [1] can readily be applied to the column drying test. In general, [1] is the most fundamental expression which describes soil evaporation. Since [1] provides the basis for the modified form of the Penman equation in [2], it will be used for the formulation of the soil-atmosphere model presented in this paper.

Examination of [1] which is used to calculate the rate of evaporation, shows evaporation to be a function of the vapour-pressure gradient between the soil surface and the overlying air. The vapour pressure in the air is computed as the product of the saturation vapour pressure of water at the measured air temperature and the measured relative humidity of the air. The vapour pressure at the soil surface, which may be saturated or unsaturated, is calculated as the product of the saturation vapour pressure of water at the temperature of the soil and the relative humidity of the pore air. The relative humidity of the soil surface is evaluated on the basis of the total suction of the soil (Wilson 1990). The turbulent exchange function $f(u)$ may be evaluated either empirically or through the use of aerodynamic profile methods (Gray 1970). An empirical method was adopted for the present work, since it is the most direct.

The total suction at the soil surface depends on the evaporative flux to the atmosphere (i.e., as specified by [1]) and the flow of groundwater to the soil surface. In most cases, the process is transient. Water may flow to the ground surface as liquid water or water vapour. The vapour pressure in the soil is a function of both the soil temperature and soil suction. In general, a system of equations is required to describe the coupled flow of liquid water, water vapour, and heat in the soil under transient conditions.

The flow of liquid water in saturated or unsaturated soil occurs in response to a hydraulic gradient and can be

described using Darcy's Law (Childs and Collis-George 1950):

$$[3] \quad q_1 = -k_w \frac{\partial h_w}{\partial y}$$

where q_1 is volumetric liquid water flux (m/s), k_w is coefficient of hydraulic conductivity (m/s), h_w is hydraulic head in the water phase (m) (i.e., $\frac{u_w}{\rho_w g} + y$), u_w is pore-water pressure (kPa), y is position (m), g is acceleration due to gravity (m/s²), and ρ_w is density of liquid water (kg/m³).

The flow of water vapour in an unsaturated soil can be described using Fick's Law (Philip and de Vries 1957; de Vries, 1975; Fredlund and Dakshanamurthy 1982):

$$[4] \quad q_v = -D_v \frac{\partial P_v}{\partial y}$$

where q_v is water vapour flux (kg/(m²·s)), P_v is partial pressure due to water vapour (kPa), and D_v is the diffusion coefficient of the water vapour through soil (kg·m/(kN·s))

= $(\alpha)(\beta) \left(D_{\text{vap}} \frac{W_v}{RT} \right)$ (Wilson, 1990), where α is tortuosity

factor of soil = $\beta^{2/3}$ (Lai et al. 1976), β is cross sectional area of soil available for vapour flow (i.e., $(1 - S)n$), D_{vap} is molecular diffusivity of water vapour in air (m²/s)

= $0.229 \times 10^{-4} \left(1 + \frac{T}{273} \right)^{1.75}$ (Kimball et al. 1976), W_v is

molecular weight of water (0.018 kg/mol), R is universal gas constant (8.314 J/(mol·K)), T is temperature (K), n is porosity, and S is degree of saturation.

The combined transient flow of liquid water and water vapour in unsaturated soil results in a change in the volume of the soil structure, the water phase, and (or) the air phase. In the case of a uniform sand, volume change in the soil structure is small and a decrease in the volume of the water phase is approximately equal to the increase in volume of the air phase and vice versa. Fredlund and Morgenstern (1976) provide a constitutive relationship for the change in volume of water in an element:

$$[5] \quad \frac{\Delta V_w}{V} = [m_1^w d(\sigma_y - u_a) + m_2^w d(u_a - u_w)]$$

where $\frac{\Delta V_w}{V}$ is change in volumetric water content, σ_y is vertical stress (kPa), u_a is pressure in the air phase (kPa), u_w is pressure in the water phase (kPa), m_1^w is slope of the $d(\sigma_y - u_a)$ versus volumetric water content plot for $d(u_a - u_w)$ equal to zero (m²/kN), and m_2^w is slope of the $d(u_a - u_w)$ versus volumetric water content plot for $d(\sigma_y - u_a)$ equal to zero (m²/kN).

Combining [3] and [4] and differentiating with respect to vertical position y describes the divergence of flux (i.e., change in volumetric water content with respect to time) in one-dimensional space due to imposed hydraulic and vapour pressure gradients in the soil. This relationship may be equated to the time differential of the constitutive relationship given in [5]. Assuming the change in vertical stress σ_y and air pressure u_a equal to zero and setting pore-water pressure u_w equal to $\rho_w g(h - y)$, rearranging and simplify-

ing, leads to a transient equation for the one-dimensional flow of liquid water and water vapour as follows:

$$[6] \quad \frac{\partial h}{\partial t} = C_w \frac{\partial}{\partial y} \left(k_w \frac{\partial h_w}{\partial y} \right) + C_v \frac{\partial}{\partial y} \left(D_v \frac{\partial P_v}{\partial y} \right)$$

where the modulus of volume change with respect to the liquid phase is defined as

$$C_w = \frac{1}{\rho_w g m_2^w}$$

and the modulus of volume change with respect to the vapour phase is defined as

$$C_v = \frac{1}{(\rho_w)^2 g m_2^w} \left(\frac{P + P_v}{P} \right)$$

where $(P + P_v)P$ is a correction factor for vapour diffusion, and P is the total atmospheric pressure (kPa), and P_v is partial pressure in the soil due to water vapour (kPa).

Equation [6] has two variables (i.e., hydraulic head and vapour pressure). These variables are not independent. The vapour pressure P_v may be related to the pressure head in the water phase (i.e., $u_w = \rho_w g(h - y)$) by using the widely accepted thermodynamic relationship given by Edlefsen and Anderson (1943) as follows:

$$[7] \quad P_v = P_{vs} h_r$$

where P_v is partial pressure due to water vapour within the voids of the unsaturated soil (kPa), P_{vs} is saturation vapour pressure (kPa) of the soil water at the soil temperature T , and relative humidity is defined as $h_r = e^{\Psi g W_v / RT}$ where Ψ is total potential in the liquid water phase expressed as equivalent matric potential (m).

The calculation of the vapour pressure in [7] depends on the saturation vapour pressure and the temperature of the soil. Hence, the temperature profile of the soil must be evaluated simultaneously with [6] and [7]. Wilson (1990) used the following equation for heat flow:

$$[8] \quad C_h \frac{\partial T}{\partial t} = \frac{\partial}{\partial y} \left(\lambda \frac{\partial T}{\partial t} \right) - L_v \left(\frac{P + P_v}{P} \right) \frac{\partial}{\partial y} \left(D_v \frac{\partial P_v}{\partial y} \right)$$

where C_h is volumetric specific heat (J/(m³·°C)), λ is thermal conductivity (W/(m·°C)), and L_v is latent heat of vaporization for water (J/kg).

Equation [8] describes heat flow due to conductive and latent heat transfer. Convective heat flow is not included. Andersland and Anderson (1978), Jame and Norum (1980), Milly (1984a), and others point out that this term is negligible for most applications. Philip and de Vries (1957) and de Vries (1987) used an equation for heat flow similar to [8].

Equations [6], [7], and [8] describe the transfer of liquid water, water vapour, and heat, respectively, in a porous medium. These equations assume the soil structure to be rigid and neglect secondary effects due to flow in the air phase and storage changes in the air and liquid phases. These assumptions are reasonable for the application in this paper as the theory is used to simulate heat and mass transfer processes in a fine to medium, uniform sand that shows little volume change during the evaporation process. Wilson (1990) provides a more rigorous system of equations to account for the effects of volume change in the soil structure and secondary fluxes.

ENVIRONMENTAL CHAMBER

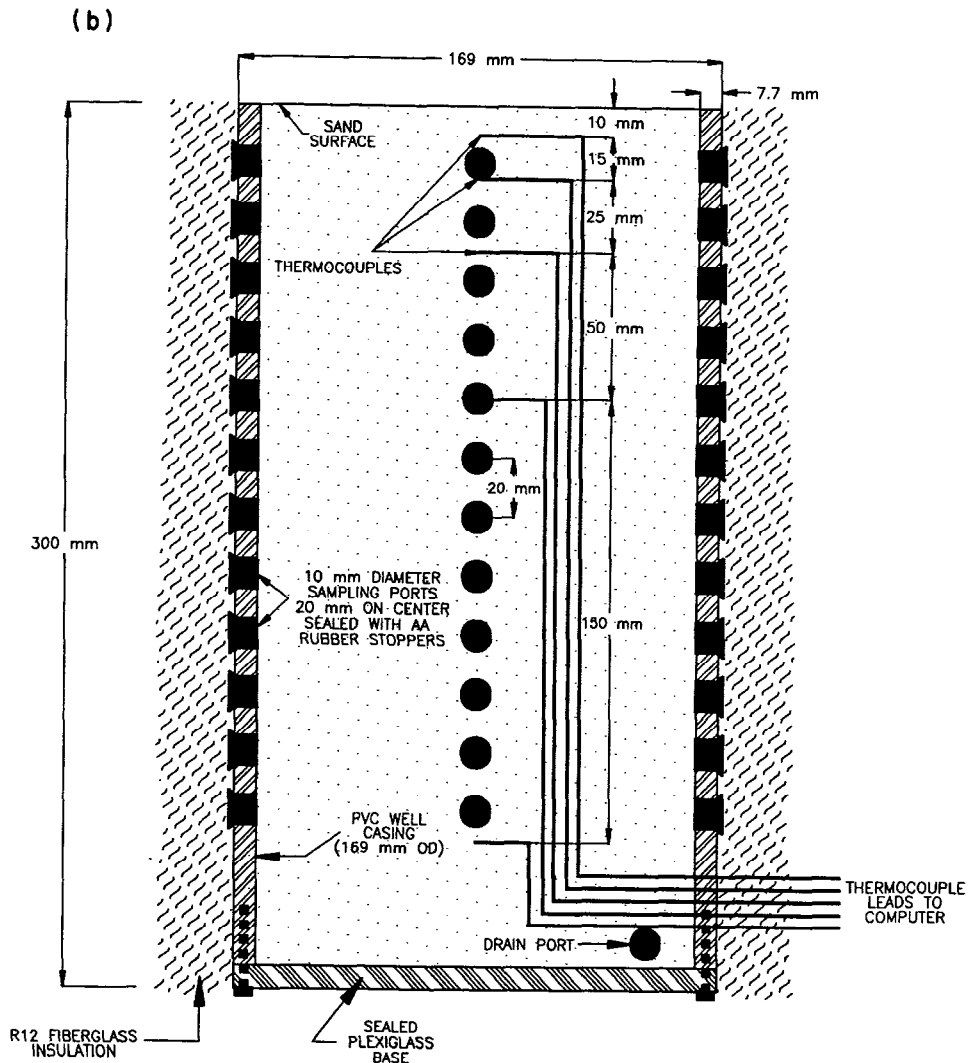
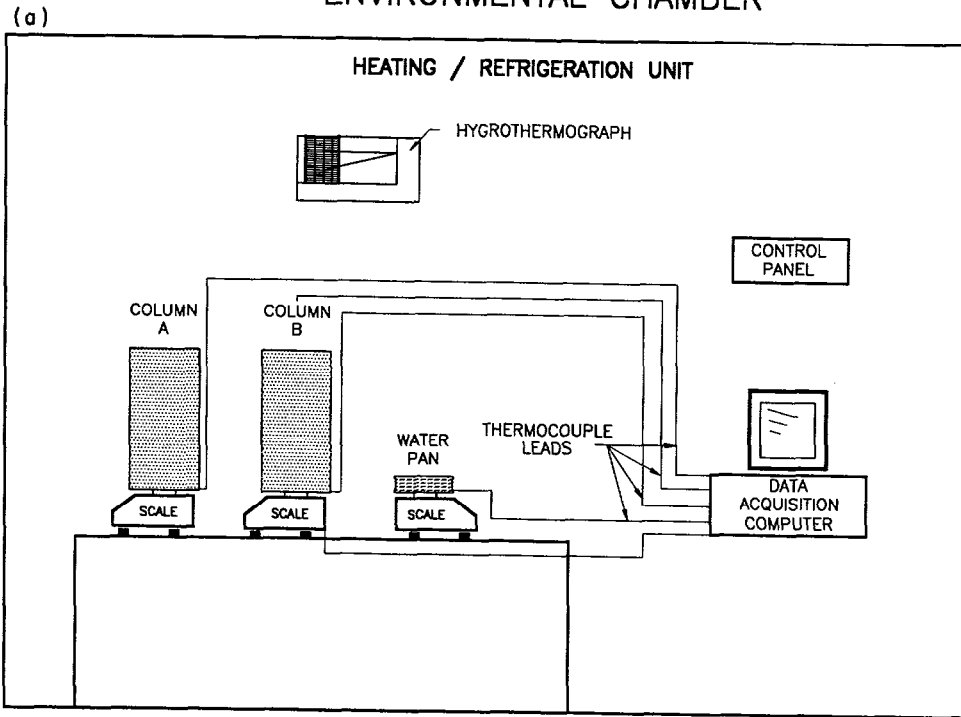


FIG. 2. (a) Apparatus used for the column drying test. (b) Details of the sand-filled column A and associated instrumentation.

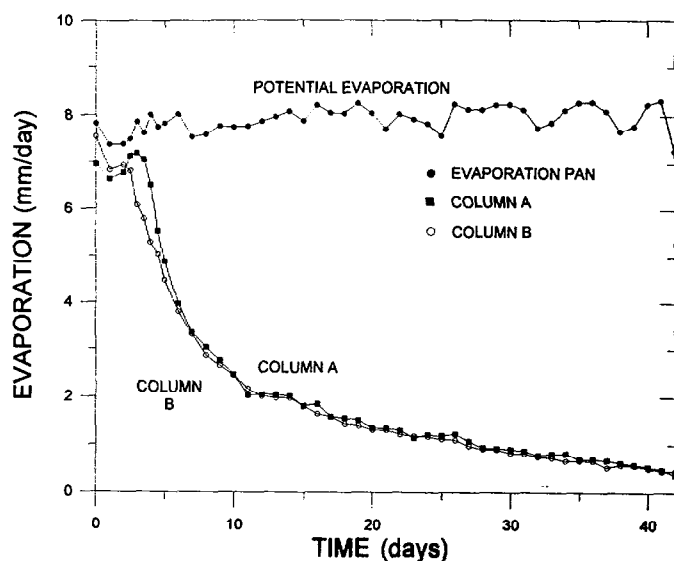


FIG. 3. Measured rates of evaporation from the evaporation pan and columns A and B vs. time.

The term $(P + P_v)/P$ used in [6] and [8] is a correction factor used by Wilson (1990) to account for combined flow due to vapour diffusion and bulk air advection. Philip and de Vries (1957) used a similar mass-flow factor equal to $P/(P - P_v)$. In most applications, the correction factor is approximately equal to unity and has little effect on the solution.

The soil-atmosphere model computes the evaporation rate from soil by solving [1], [6], [7], and [8] simultaneously. The vapour pressure at the soil surface in [1] (i.e., e_s) is set equal to the vapour pressure at the soil surface (i.e., P_v) computed by solving [6], [7], and [8]. The numerical results subsequently presented were obtained using an explicit finite difference technique.

Column drying test

The objective of the column drying test was to measure the actual rates of evaporation from a soil profile and to compare these with the predicted values of evaporation obtained from the proposed soil-atmosphere model. The exposed surfaces of two identical columns of a fine to medium aeoline sand (Beaver Creek sand) were allowed to evaporate under controlled laboratory conditions. The columns were filled with saturated sand and were allowed to drain to a hydrostatic condition. The columns were then sealed at the base and the upper surfaces were allowed to desiccate for a period of 42 days.

Figure 2 illustrates the apparatus used to conduct the column drying test. Two columns were constructed using 169 mm outside diameter PVC casing. The columns were 300 mm in height and sealed at the base. Sampling ports in the sidewall of the PVC casing were installed vertically down the columns to allow for sample extraction and the measurement of water content. Conventional thermocouples were also installed along a vertical profile in the centre of the columns as shown in Fig. 2b. A modified PC computer with a data-acquisition board was used to automatically record the temperatures at 15 min intervals. The sand columns were wrapped with insulation to minimize the effects of lateral heat flow.

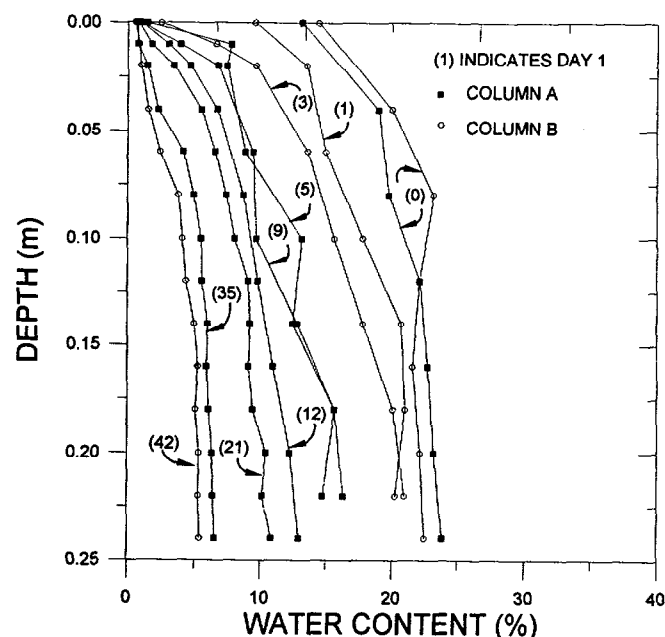


FIG. 4. Measured water-content profiles in columns A and B at various times during the column drying test.

The sand columns were supported on scales to give a continuous measurement of their mass and, therefore, their change in mass. The actual rate of soil evaporation was determined on the basis of change in mass for each column which was automatically recorded at 15 min intervals. An evaporation pan filled with water and having an identical surface area and geometry to that of the columns was installed adjacent to the columns to determine the potential rate of evaporation. The entire test apparatus was installed within a climatically controlled environmental chamber with a constant temperature of 38°C and a relative humidity of approximately 10%. The resulting potential rate of evaporation in the environmental chamber was approximately 8 mm/day. The temperatures of the water surface and chamber air were monitored continuously along with the relative humidity of the ambient air. Soil samples were taken through the sampling ports at various times to obtain a direct measurement of water content along the column profiles.

Figure 3 shows the measured rates of evaporation from the evaporation pan, column A, and column B with respect to time. The measured rate of evaporation from the water pan is shown as the potential rate of evaporation. Figure 4 shows the measured water contents in columns A and B at the start of the tests and at various times throughout the duration of the test.

The actual rate of evaporation from both sand columns was approximately equal to the potential rate of evaporation for the first 3 or 4 days. This corresponds to the stage I drying phase as previously defined. During this period, the water contents of the sand surfaces were observed to decline continuously from the initial values of 13–14% but remained wet in visual appearance. It can be seen that the initial high rate of actual soil evaporation was slightly below the potential rate defined by the water-filled evaporation pan. In general, saturated and nearly saturated soils evaporate at the potential rate (Wilson 1990). However, both sand surfaces were observed to be approximately 1°C cooler than the surface of the water-filled evaporation pan. This resulted in a slightly lower saturation vapour pressure at the surfaces of

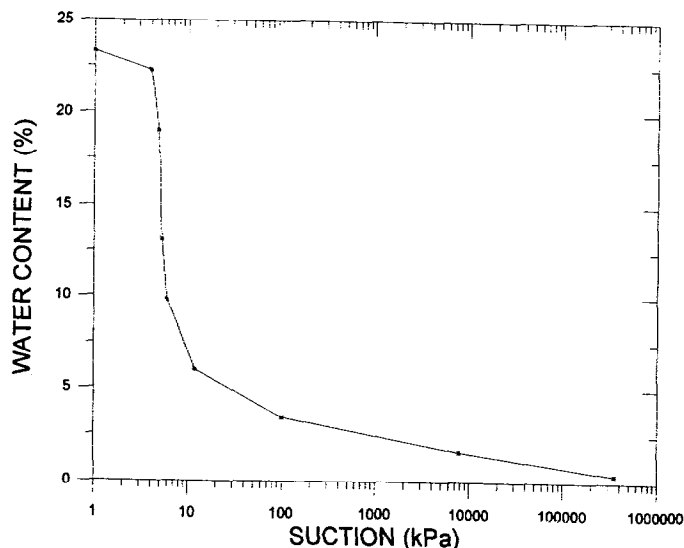


FIG. 5. Water content characteristic curve for the Beaver Creek sand.

the sand columns compared with the water and hence a slightly lower rate of evaporation (i.e., as defined by [1]).

The actual rate of evaporation for columns A and B declined rapidly after the initial high rate stage I phase. The rapid decline in the rate of evaporation continued for approximately 11 days. The drying period between 3 and 11 days corresponds to stage II drying as previously discussed. The onset of stage II drying was observed to begin at the same time that the surface of the sand became visually dry. This corresponded to a water content at the sand surface slightly less than 2%. The drying surface was initially very thin. The water content of the sand immediately below the dry surface remained relatively high, as can be seen in Fig. 4 (i.e., after 5 and 9 days). The dry surface layer was observed to gradually increase in thickness as the rate of evaporation continued to decline.

The decline in the actual rates of evaporation slowed after approximately 11 days for columns A and B. This may be defined as the onset of stage III drying, which is defined as the slow residual rate of evaporation. The water content of the sand at both surfaces was measured to be approximately 1% after 12 days of drying. Distinct drying fronts developed which extended to a depth of approximately 1 cm after 21 days and advanced to a depth of approximately 8 cm after 42 days of continuous evaporation. The sand within the drying fronts was extremely dry, and the liquid phase appeared to be absent. The final rate of actual evaporation was approximately 0.4 mm/day compared with the potential evaporation rate equal to approximately 8 mm/day.

Analysis and discussion

The proposed soil-atmosphere model was used to calculate the evaporative fluxes measured in the column drying test. The coefficients for the solution of [1], [6], and [8] include the turbulent exchange function $f(u)$, hydraulic conductivity k_w , the modulus of volume change with respect to the liquid and vapour phases C_w and C_v , specific heat capacity C_h , and thermal conductivity λ . The turbulent exchange function was calculated directly on the basis of the measured evaporative flux from the water-filled evaporation pan (i.e., $f(u) = E/(e_s - e_a)$), given that the vapour pressures at the water surface and in the air were known.

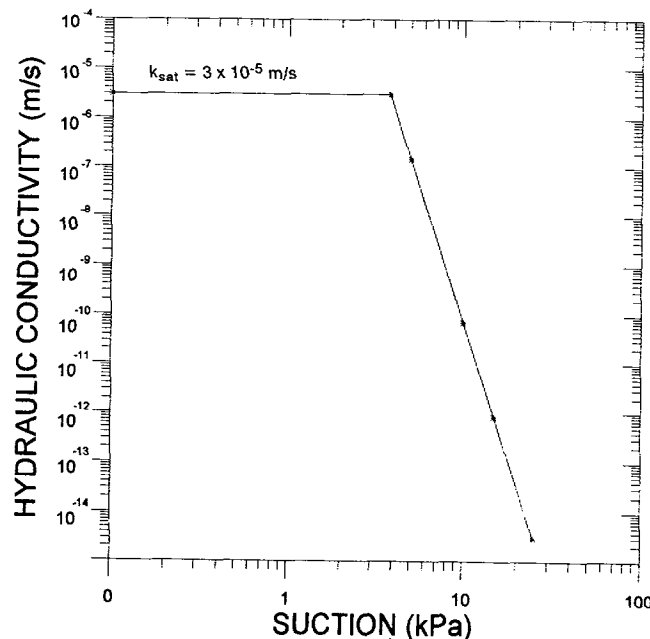


FIG. 6. Hydraulic conductivity vs. matric suction for the Beaver Creek sand. k_{sat} is the hydraulic conductivity of saturated soil.

The remaining coefficients were calculated on the basis of measured soil properties.

The modulus of volume change with respect to the liquid and vapour phases were calculated on the basis of the slope m_2^w of the water content characteristic curve. Figure 5 shows the water content characteristic curve for the Beaver Creek sand determined in the laboratory. The Tempe cell method was used to establish the water content characteristic curve between 0 and 100 kPa suction. Vapour-equilibrium desiccators were used for the higher values of suction to a maximum of approximately 300 000 kPa. It should be noted that the soil water characteristic curve shown in Fig. 5 corresponds to drying or drainage of the sand. In addition to calculating the coefficient of consolidation, the water content characteristic curve was also used to determine the values of suction based on water contents measured in the profile of the sand columns.

The hydraulic conductivity k_w , for the Beaver Creek sand depends on the water content and therefore, in turn, on matric suction. The relationship between the coefficient of hydraulic conductivity and matric suction was evaluated using the method described by Laliberte et al. (1968) and is shown in Fig. 6. The functional relationship shown in Fig. 6 is determined on the basis of the measured saturated hydraulic conductivity and the water content characteristic curve shown in Fig. 5. The effect of hysteresis associated with wetting and drying of the sand was not evaluated, since the sand columns were subjected only to continuous drying due to evaporation. The diffusion coefficient D_v for water vapour in the soil was calculated directly as shown in [4] on the basis of porosity and degree of saturation.

The thermal conductivity λ and the volumetric specific heat of the Beaver Creek sand were determined using the method described by de Vries (1963), who provides the following equation for the calculation of the specific heat capacity of a soil:

$$[9] \quad C_h = C_s \theta_s + C_w \theta_w + C_a \theta_a$$

where C_s is volumetric specific heat capacity of the soil

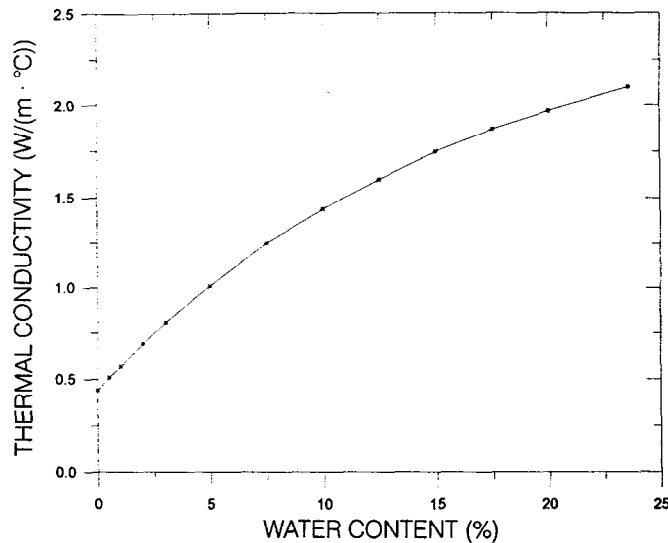


FIG. 7. Thermal conductivity vs. water content for the Beaver Creek sand.

solids ($2.24 \times 10^6 \text{ J/(m}^3 \cdot \text{°C)}$); C_w is volumetric specific heat capacity of the liquid water phase ($4.15 \times 10^6 \text{ J/(m}^3 \cdot \text{°C)}$); C_a is volumetric specific heat capacity of the air phase, which can be assumed to be negligible (de Vries 1963); and θ_s , θ_w , and θ_a are volumetric fractions of the soil solids, water, and air, respectively.

The thermal conductivity λ of the Beaver Creek sand is also a function of the water content of the soil. The method used for calculating thermal conductivity was more rigorous than that given in [9] and the reader is referred to de Vries (1963). Figure 7 shows the computed relationship between thermal conductivity and water content on the basis of de Vries (1963). The methods for calculating volumetric specific heat capacity and thermal conductivity provided by de Vries (1963) are theoretical. Jame (1977), however, found that the theoretical model given by de Vries (1963) provided good agreement with measured values.

The soil-atmosphere model was applied using the coefficients evaluated as described above. Equations [6] and [8] are nonlinear. All of the functional relationships for the soil coefficients depend on either matric suction or water content. Furthermore, the analysis of the column drying test was for transient conditions. Soil evaporative fluxes, water content, soil suction, and soil temperature are all nonsteady. Extremely small time steps of approximately 0.1 s were selected for the explicit finite difference solutions, and soil coefficients were evaluated at each time step.

Figure 8 shows the computed rate of soil evaporation and the measured rates of soil evaporation for the 42 day column drying test. A good correlation between the computed rate of evaporation and the measured rate of evaporation was observed when using the measured soil properties. Figures 9a and 9b show the computed and measured water-content and temperature profiles, respectively, at various times during the test. Again, the correlation between the values computed by the soil-atmosphere model appears to be good. The proposed soil-atmosphere model appears capable of predicting soil evaporation rates, water-content profiles, and temperature profiles on the basis of measured atmospheric conditions and soil properties with reasonable accuracy. This indicates that the theoretical model based on the Dalton-type equation for evaporation, Darcy's Law for liquid trans-

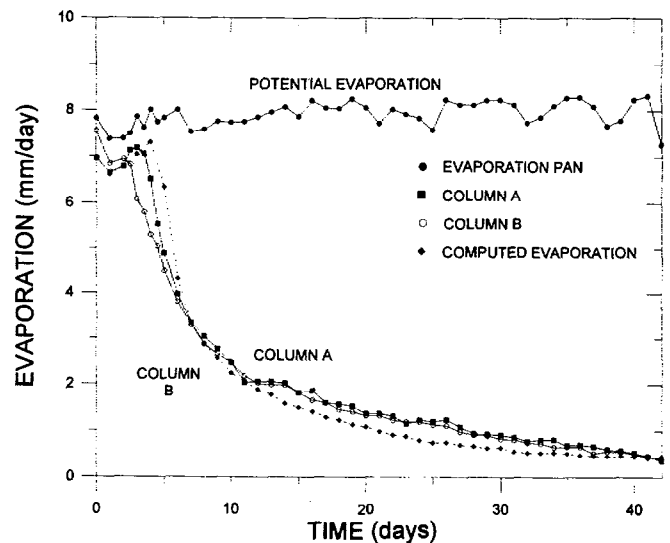


FIG. 8. Measured and computed rates of evaporation vs. time for the column drying test.

fer in soil, and Fick's Law for vapour diffusion in soil was appropriate.

The mechanisms for water transport to the soil surface should be considered because water may flow upward to the soil surface as liquid water and (or) water vapour. During stage I evaporation over the first 3–4 days, the surface of the sand and underlying soil were very moist or nearly saturated. Suctions were relatively low and the corresponding hydraulic conductivity was at or near the saturated hydraulic conductivity. As can be seen in Fig. 6, the hydraulic conductivity of the Beaver Creek sand remains equal to the saturated value until matric suction exceeds the air entry value (AEV) of 3.8 kPa. In other words, the flow of water in the liquid phase was not restricted. The values of suction increased as stage I evaporation continued, and the hydraulic conductivity decreased rapidly once the value of matric suction exceeded the AEV. This caused the flow of liquid water to become increasingly restricted as evaporation continued. The development of this restriction in the flow of liquid water to the soil surfaces most likely corresponds to the transition from the high-rate stage I drying to the falling-rate stage II drying.

Stage II drying or the falling-rate stage was observed to begin once a dry zone of sand appeared on the surface of the columns after approximately 4 days of drying. The soil surfaces were sufficiently dry such that the liquid water phase was absent. The continuation of the evaporation can be explained by the process of water molecules diffusing to the surface of the sand through the vapour phase in the dry sand. The actual rate of evaporation declined rapidly after 5 days as the thickness of the dry zone increased. The formation of a dry soil surface was important, as it signaled the rapid decline in evaporative flux and the transition to vapour diffusion.

The transition from stage II drying to stage III is somewhat arbitrary. However, Hillel (1980) describes stage III as a vapour-diffusion process. The thickness of the dry surface zone increased to form a distinct drying front approximately 0.5 cm thick after 11 or 12 days of drying. The rate of decline in the evaporation rate appears to decrease after this point in time and can be defined as the onset of stage III drying. The drying front or zone of vapour diffusion slowly

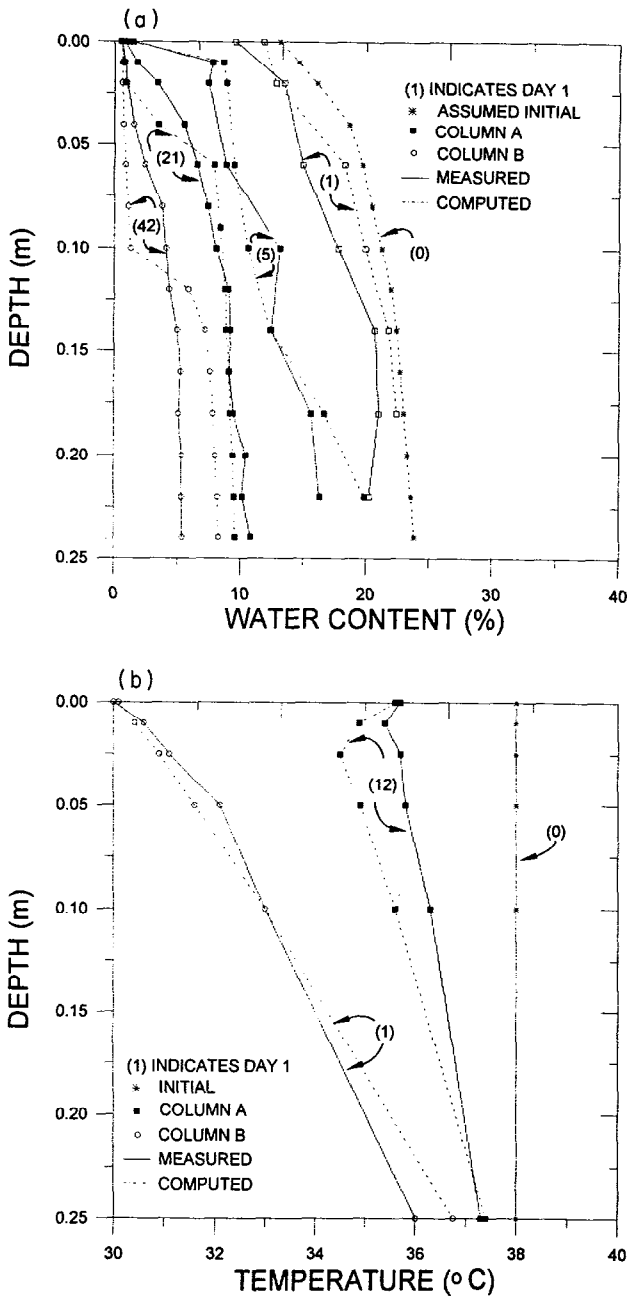


FIG. 9. (a) Measured and computed water-content profiles after 1, 5, 21, and 42 days of evaporation. (b) Measured and computed temperature profiles after 1 day and 12 days of evaporation.

increased in thickness with time to approximately 1 cm after 21 days and 6–8 cm after 42 days. The evaporative flux decreased from approximately 2 mm/day to 0.4 mm per/day during the same period of time.

Figure 10 helps illustrate the transition from liquid flow to vapour flow across the drying front after 29 days of evaporation. Figure 10a shows the suctions based on measured water contents (i.e., using Fig. 5) and the suctions computed by the soil-atmosphere model. Both computed and measured suctions within the top 2 cm compare very well. Suctions in the drying front exceed 100 000 kPa. The corresponding hydraulic conductivity (i.e., Fig. 7) and liquid flow at these values of suction are virtually zero. The flow of water to the surface must be predominantly by vapour diffusion.

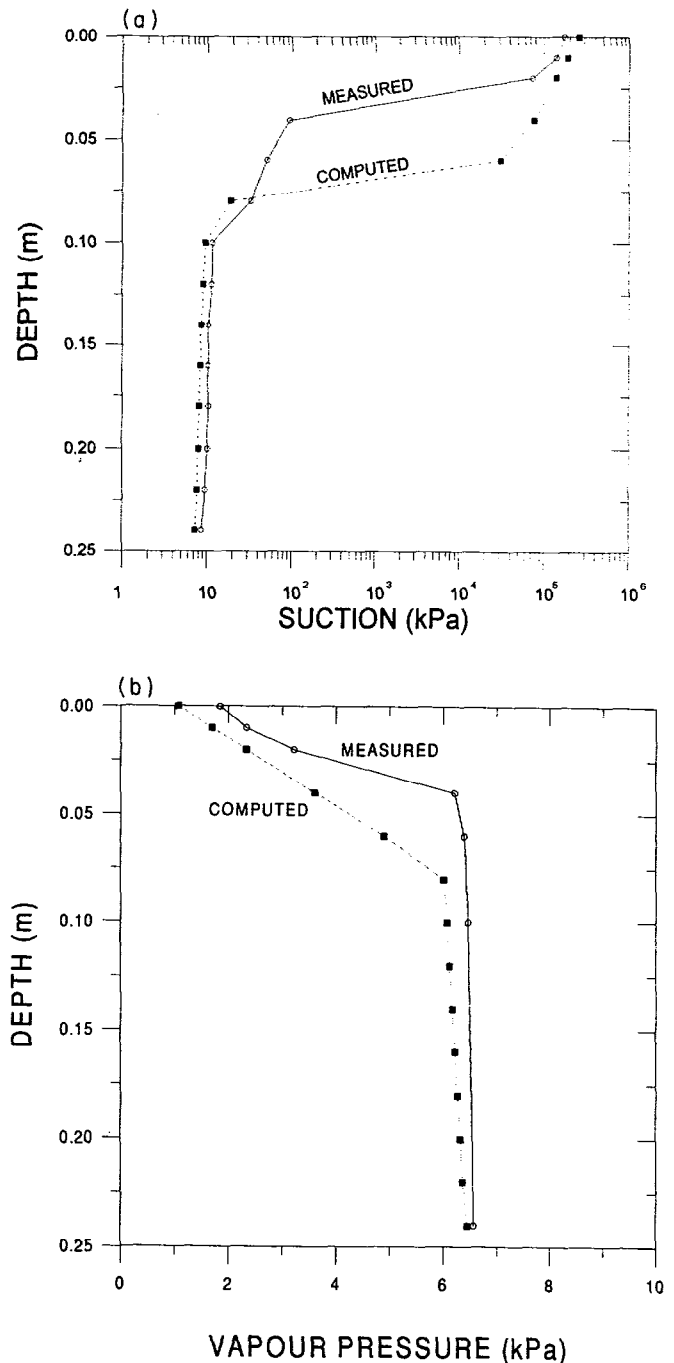


FIG. 10. (a) Measured and computed suctions in the sand columns after 29 days of evaporation. (b) Measured and computed vapour pressures in the sand columns after 29 days of evaporation.

Both computed and measured suctions in Fig. 10a decreased from approximately 100 000 to 20 kPa between 2 and 8 cm in depth. This zone may be noted as the transition zone from predominant vapour flow to predominant liquid flow. The correlation between the measured and computed suctions is not as good within this zone. This may be attributed to the limitation of the function used to define the relationship between hydraulic conductivity and matric suction.

Laliberte et al (1968) stated the proposed function for hydraulic conductivity is accurate only for water contents above the residual water content. The residual water content for the Beaver Creek sand based on the method described

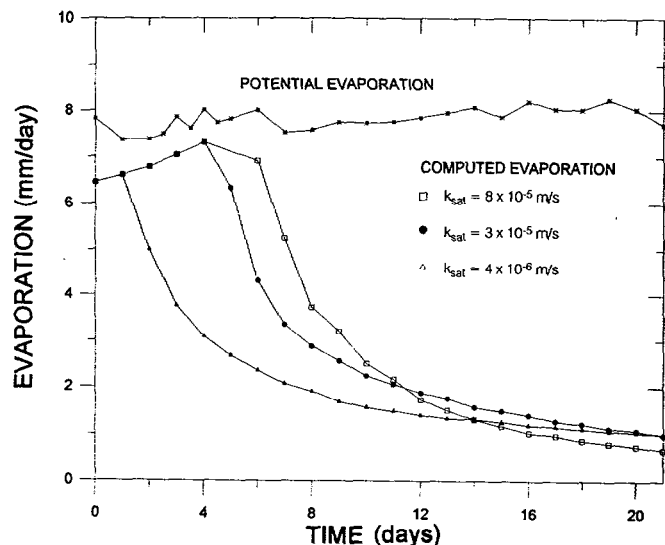


FIG. 11. Computed rates of soil evaporation vs. time for various values of saturated hydraulic conductivity.

by Laliberte et al. (1968) is approximately 5.7% at 20 kPa suction. This corresponds approximately to the suctions where the inaccuracy becomes apparent in Fig. 10a. The correlations between the measured and the computed suctions are good below the transition zone when the values of suction are less than 20–30 kPa. A similar inaccuracy may be noted in Fig. 9a for the measured and predicted water contents for the sand profile after 42 days of drying as the entire sand profile approaches the residual water content.

Figure 10b shows the mechanism that drives vapour flow across the transition and vapour-flow zones (i.e., drying front). The measured vapour pressures shown in Fig. 10b were determined on the basis of the measured suction shown in Fig. 10a (i.e., which gives relative humidity using eq. [7]) and the measured soil temperature. The curve showing computed vapour pressure was computed by the soil-atmosphere model. A distinct pressure difference of approximately 4 kPa may be noted for both curves between the surface of the sand and the top 4–8 cm. This pressure gradient is the mechanism that drives vapour diffusion as described by Fick's Law in [4]. The gradient decreases to a small value below approximately 8 cm and hence vapour diffusion decreases to a small value in the zone where liquid flow predominates.

The transition zone at the drying front is the location where evaporation occurs and water molecules move from the liquid water phase to the vapour phase. At the start of the test, evaporation initially occurs at the surface of the sand. It may be noted in Fig. 9b that this is the coldest point in the sand column profile after 1 day of evaporation. Evaporation provides a heat sink where energy is required for latent heat of vaporization. The location of the evaporation surface advanced into the column with the drying front. It can be seen in Fig. 9b, for example, that the coldest points in the temperature profile after 12 days of evaporation for the measured and computed temperatures occurred at approximately 1.0 and 2.5 cm, respectively, below the sand surface. The temperatures were coldest at these points because of the latent heat required to transfer water from the liquid phase to the vapour phase. The location of the measured and computed cold front varies somewhat. This may be attributed to the difficulty previously described with respect to the accuracy of determining hydraulic conductivity in the transition zone.

The soil-atmosphere model appears to predict the actual evaporative fluxes with accuracy when compared with the measured values. All simulations were conducted using the measured soil properties for the Beaver Creek sand. Questions may be asked regarding the importance or significance of the various material properties. Laboratory tests were not conducted with other soil types, however, model simulations were conducted with different soil properties. The coefficient of hydraulic conductivity is one of the most important soil properties, as it controls the flow of liquid water. The value of the saturated hydraulic conductivity for determining the functional relationship between hydraulic conductivity and matric suction for the Beaver Creek sand (i.e., Fig. 6) was set equal to a low value of 4×10^{-6} m/s and a high value of 8×10^{-5} m/s. All other soil properties were set equal to values previously used.

Figure 11 shows the rate of soil evaporation versus time computed for the different values of saturated hydraulic conductivity. It can be seen that varying the saturated hydraulic conductivity has a significant impact on the computed rates of soil evaporation. Decreasing the saturated hydraulic conductivity to 4×10^{-6} m/s reduces the time for high-rate stage I drying previously established for the column drying test from approximately 4 days to 1 day. Alternately, increasing the saturated hydraulic conductivity to 8×10^{-5} m/s extends stage I drying to approximately 6 days. It may be noted that in all cases the magnitude of the slow residual rate of evaporation in stage III drying is not significantly effected. This is considered reasonable, as this stage of drying is controlled by vapour diffusion through the drying front.

Summary and conclusions

A soil-atmosphere model for the evaluation of soil evaporative flux has been developed. The theoretical formulation of the model is based on the Dalton-type equation for evaporation from a surface into the atmosphere. Darcy's Law for the flow of liquid water and Fick's Law for the flow of water vapour in the soil below the surface were also used. The values for actual evaporation rates, water-content profiles, and temperature profiles predicted by the soil-atmosphere model were compared with the values measured in a controlled column evaporation test over a 42-day period. The results of the model simulations agree well with the measured values of the column drying test for the Beaver Creek sand.

Both the soil-atmosphere model and the laboratory test showed the development of the three stages of drying described by Hillel (1980). The high rate of evaporation for saturated or nearly saturated soil during stage I is approximately equal to the potential rate of evaporation for a free water surface. This high rate of evaporation is controlled primarily by atmospheric conditions. Stage I drying was found to continue until a dry surface zone developed. The development of the dry surface zone greatly reduced the rate of evaporation during the falling-rate phase of stage II drying. Simulations conducted with the soil-atmosphere model showed the length of time for stage I drying is strongly controlled by the hydraulic conductivity of the soil. The column drying test and the soil-atmosphere model also showed the long-term development of stage III drying. The rate of evaporation from the sand surface during stage III drying was reduced by a factor of approximately 20 when

compared with the initial high rate of evaporation (i.e., 8 mm/day versus 0.4 mm/day after 42 days).

The ability to predict evaporative fluxes is useful to geotechnical engineers, for example, in the design of soil covers for mine tailings. Conventional methods of evaluating evaporation such as the Penman method (1948) provide only estimates of the potential rate of evaporation (i.e., stage I). This could result in considerable error if applied to a soil surface over extended periods of drying between rainfall events. However, comparison of the evaporative fluxes computed using the Dalton-based soil-atmosphere model with the results measured in the column drying test indicates using the actual vapour pressure corrects the difficulties associated with predicting evaporation from unsaturated soil surface. Furthermore, it suggests the Penman equation may be extended as shown in [2] for field problems where the rate of evaporation is less than the potential rate of evaporation. This could be achieved by computing the actual vapour pressure at the soil surface using [6]–[8]. However, field tests will be required to demonstrate this application.

- Andersland, O.B., and Anderson, D.M. 1978. Geotechnical engineering for cold regions. McGraw-Hill Inc., New York.
- Brutsaert, W.H. 1982. Evaporation into the atmosphere: theory, history and applications. P. Reidel Publishing Company, Dordrecht, The Netherlands.
- Camillo, P.J., Gurney, R.J., and Schmügge, T.J. 1983. A soil and atmospheric boundary layer model for evapotranspiration and soil moisture studies. *Water Resources Research*, **19**(2): 371–380.
- Childs, E.C., and Collis-George, N. 1950. The permeability of porous materials. *Proceedings of the Royal Society of London*, **201**: 392–405.
- Choudhury, B.J., and Monteith, J.L. 1988. A four-layer model for the heat budget of homogeneous land surfaces. *Quarterly Journal of the Royal Meteorology Society*, **114**: 373–398.
- de Vries, D.A. 1963. Thermal properties of soils. In *Physics of plant environment*. Edited by W.R. Van Wijk, North Holland Publishing Company, Amsterdam, The Netherlands, pp. 210–235.
- de Vries, D.A. 1975. Heat transfer in soil. In *Heat and mass transfer in the biosphere*. 1. Transfer processes in plant environment. Edited by D.A. deVries and N.H. Afgan. Scripta Book Company, Washington, D.C., pp. 5–28.
- de Vries, D.A. 1987. The theory of heat and moisture transfer in porous media revisited. *International Journal of Heat and Mass Transfer*, **30**(7): 1343–1350.
- Edlefsen, N.E., and Anderson, A.B.C. 1943. Thermodynamics of soil moisture. *Hilgardia*, **15**(2): 31–298.
- Fredlund, D.G., and Dakshanamurthy, V. 1982. Prediction of moisture flow and related swelling or shrinking in unsaturated soils. *Geotechnical Engineering*, **13**: 15–49.
- Fredlund, D.G., and Morgenstern, N.R. 1976. Constitutive relations for volume change in unsaturated soils. *Canadian Geotechnical Journal*, **13**: 261–276.
- Granger, R.J. 1989. An examination of the concept of potential evaporation. *Journal of Hydrology*, **111**: 9–19.
- Gray, D.M. 1970. Handbook on the principals of hydrology. Canadian National Committee for the International Hydrological Decade, National Research Council of Canada, Ottawa.
- Hillel, D. 1980. Applications to soil physics. Academic Press, New York.
- Jame, Y.W. 1977. Heat and mass transfer in freezing unsaturated soil. Ph.D. dissertation, University of Saskatchewan, Saskatoon.
- Jame, Y.W., and Norum, D.I. 1980. Heat and mass transfer in a freezing unsaturated porous medium. *Water Resources Research*, **16**(4): 811–819.
- Kimball, B.A., Jackson, R.D., Reginato, R.J., Nakayama, F.S., and Idso, S.B. 1976. Comparison of field-measured and calculated soil-heat fluxes. *Soil Science Society of America Proceedings*, **40**(1): 18–25.
- Lai, S., Tiedje, J.M., and Erickson, A.E. 1976. In situ measurement of gas diffusion coefficient in soils. *Soil Science Society of America Proceedings*, **40**(1): 3–6.
- Laliberte, A.M., Brooks, R.H., and Corey, A.T. 1968. Permeability calculated from desaturation data. *ASCE Journal of the Irrigation and Drainage Division*, **94**: 57–71.
- Milly, P.C.D. 1982. Moisture and heat transport in hysteretic, inhomogeneous porous media: A matric head-based formulation and a numerical model. *Water Resources Research*, **18**(3): 489–498.
- Milly, P.C.D. 1984a. A linear analysis of thermal effects on evaporation from soil. *Water Resources Research*, **20**(8): 1075–1085.
- Milly, P.C.D. 1984b. A simulation analysis of thermal effects on evaporation from soil. *Water Resources Research*, **20**(8): 1087–1098.
- Monteith, J.L. 1965. Evaporation and environment. In *The State and Movement of Water in Living Organisms*, Symposium: Society of Experimental Biology. Vol. 19. Edited by G.E. Fogg. Academic Press, San Diego, Calif. pp. 205–234.
- Morton, F.I. 1975. Estimating evaporation and transpiration from climatological observations. *Journal of Applied Meteorology*, **14**(4): 488–497.
- Passerat De Silans, A., Bruckler, L., Thory, J.L., and Vauclin, M. 1989. Numerical modelling of coupled heat and water flows during drying in a stratified bare soil—comparison with field observations. *Journal of Hydrology*, **105**: 109–138.
- Penman, H.L. 1948. Natural evapotranspiration from open water, bare soil and grass. *Proceedings of the Royal Society of London, Series A*, **193**: 120–146.
- Philip, J.R., and de Vries, D.A. 1957. Moisture movement in porous materials under temperature gradients. *Transactions, American Geophysical Union*, **38**(2): 222–232.
- Priestley, C.H.B., and Taylor, R.J. 1972. On the assessment of surface heat flux and evaporation using large-scale parameters. *Monthly Weather Review*, **100**: 81–92.
- Schildge, J.P., Kahle, A.B., and Alley, R.E. 1982. A numerical simulation of soil temperature and moisture variations for a bare field. *Soil Science*, **133**: 197–207.
- Shuttleworth, W.J., and Wallace, J. S. 1985. Evaporation from sparse crops—an energy combination theory. *Quarterly Journal of the Royal Meteorology Society*, **111**: 839–855.
- Sophocleous, M. A. 1979. Analysis of water and heat flow in unsaturated-saturated porous media. *Water Resources Research*, **15**(5): 1195–1206.
- Stannard, D.I. 1993. Comparison of Penman–Monteith, Shuttleworth–Wallace, and modified Priestley–Taylor evapotranspiration models for wildland vegetation in semi-arid rangeland. *Water Resources Research*, **29**(5): 1379–1392.
- Thornthwaite, C.W. 1948. An approach toward a rational classification of climate. *Geographical Review*, **38**: 55–94.
- van Bavel, C. H. M. 1967. Changes in canopy resistance to water loss from alfalfa induced by soil water depletion. *Agricultural Meteorology*, **4**: 165–176.
- Wilson, G. W. 1990. Soil evaporative fluxes for geotechnical engineering problems. Ph.D. dissertation, University of Saskatchewan, Saskatoon.
- Witono, H., and Bruckler, L. 1989. Use of remotely sensed soil moisture content as boundary conditions in soil-atmosphere water transport modelling 1. Field validation of a water flow model. *Water Resources Research*, **25**(12): 2423–2435.

48

Canadian
Geotechnical
CONFERENCE
Canadienne
de Géotechnique

*September 25-27, 1995
Vancouver, BC*



*Trends in Geotechnique
Tendances en Géotechnique*

Preprint Volume 2



Canadian Geotechnical Society
La Société Canadienne de Géotechnique

AN INTRODUCTION TO ANALYTICAL MODELLING OF PLANT TRANSPIRATION FOR GEOTECHNICAL ENGINEERS

D.J. Tratch¹, G.W. Wilson² and D.G. Fredlund²

¹ Clifton Associates Ltd., 101 - 108 Research Drive, Saskatoon, SK, S7N 3R3

² Department of Civil Engineering, University of Saskatchewan,
57 Campus Drive, Saskatoon, SK, S7N 5A9

ABSTRACT

Historically, geotechnical engineers have been concerned with groundwater flow, particularly within the saturated zone. More recently, geotechnical engineers have identified the importance of unsaturated flow and the flux boundary condition with respect to water flow across the soil-atmosphere interface. Plant transpiration is an important component of the surface flux rate.

This paper outlines a theoretical approach for the prediction of transpiration rates. A laboratory experiment was conducted to measure evapotranspiration rates and analytical modelling was performed to simulate the laboratory data. The experimental results identify the significance of including the transpiration flux in the surface flux boundary condition. The analytical modelling results show the proposed methodology for the prediction of transpiration to be reasonably accurate.

RESUME

INTRODUCTION

With an ever expanding knowledge base, the science of geotechnical engineering must continually apply theory developed by other disciplines. The evaluation of plant transpiration is one such area where the research has been conducted primarily by Soil Scientists. Geotechnical engineers often overlook the surface flux component related to the vegetative cover. The flux boundary condition at the soil surface is a critical factor for problems in geotechnical engineering related to soil cover system design, saturated/unsaturated groundwater flow, slope stability and volume change in expansive soils. In such engineered systems, the transpiration component may be critical in the success of the design.

The design of soil covers involves the placement of multiple soil layers over hazardous wastes. The arrangement allows for the control of oxygen diffusion and moisture percolation into the underlying waste to reduce leachate production. Vegetation is placed on the soil cover for aesthetic as well as design purposes. Vegetation promotes the integrity of the soil against erosion due to surficial runoff waters. The resulting influence of the vegetative cover on the performance of the cover system with respect to moisture flow must be evaluated. A review of literature on existing transpiration prediction methodologies identifies a science which although has had immense research conducted does not have consensus on an acceptable method to predict transpiration. Methods to predict transpiration vary between highly empirical (de Jong, 1974) to physically based models which are highly theoretical (Federer, 1979). Marker and Mein (1985) state that empirical based models lack accuracy whereas theoretical methods are too complicated for routine use.

METHODOLOGY TO PREDICT TRANSPIRATION

The computer program, SoilCover (MEND, 1993), was developed by a group of researchers at the University of Saskatchewan. SoilCover is a 1-dimensional, transient, heat and mass transfer finite element model. One of the special features of SoilCover is the ability to evaluate bare soil evaporation from unsaturated soil surfaces as given in eq. 1 by Wilson et al. (1994).

$$[1] \quad E = f(u) (e_s - e_a)$$

where: E = the actual evaporation from the saturated/unsaturated soil surface (mm/s),
 $f(u)$ = the turbulent mixing parameter (units),
 e_s = the vapour pressure at the soil surface (units), and
 e_a = the vapour pressure in the overlying atmosphere (units).

The partial differential equation describing mass movement through porous media, including its modification to include the transpiratory root uptake flux is presented in Eq. 2 (Wilson, 1990). Wilson (1990) also provides a heat transfer equation which is solved simultaneously with eq. 2.

$$[2] \quad \frac{\partial h_w}{\partial t} = C_w^1 \frac{\partial}{\partial z} \left(k_w \frac{\partial h_w}{\partial z} \right) + C_w^2 \frac{\partial}{\partial z} \left(D_v \frac{\partial P_v}{\partial z} \right) + S$$

where: h_w = the total hydraulic head (m),

- k_w = the coefficient of permeability as a function of matric suction (m/s),
 D_v = the coefficient of water vapour diffusion through the soil (kg·m/kN·s),
 C_w^1 = the modulus of volume change of water with respect to the liquid phase,

$$= \left(\frac{1}{\rho_w g m_w^2} \right),$$
 C_w^2 = modulus of volume change of water with respect to the vapour phase,

$$= \left(\frac{1}{(\rho_w)^2 g m_w^2} \right),$$
 m_w^2 = the slope to the moisture retention curve (1/kPa),
 ρ_w = the mass density of water (kg/m³),
 P = the total pressure in the bulk air phase (kPa),
 P_v = the actual vapour pressure in the bulk air phase (kPa),
 t = the time (s),
 z = the vertical position (m), and
 S = the root uptake sink term (m/s).

The first term on the right hand side of Eq. 2 describes the flow of liquid phase water according to Darcy's Law. The second term describes the flow of vapour phase water according to Fick's Law. The third term describes the root uptake sink term which occurs as a flux from each influenced node. The methodology to evaluate the sink term will be briefly discussed in the following paragraphs.

The methodology to predict transpiration has been based upon the method proposed by Feddes et al. (1978). The semi-empirical method to evaluate the transpiration flux was selected due to its ability to be adapted to bare soil and partitioned cover evaporation and evapotranspiration.

The first step in evaluating the transpiration flux involves determination of the potential evaporation rate. The term potential evaporation has been well defined in the past, hence only a brief discussion will be presented here. The exact definition of potential evaporation differs between disciplines and various authors. However it is generally agreed to be the maximum potential cumulative sum of bare soil evaporation and plant transpiration (Granger, 1989).

The second step in evaluating the transpiration flux involves determination of the potential transpiration flux. Because the evaporation and transpiration components must be evaluated individually, the potential evaporation flux must be distributed into its evaporation and transpiration components. Ritchie (1972) observed the transpiration component was dependent upon the leaf area index values of the plant canopy. From his research, three degrees of vegetative cover were identified with the resulting influence upon the potential transpiration flux presented in Eqs. 3, 4 and 5.

$$[3] \quad E_p = 0.0 \quad \text{LAI} < 0.1$$

$$[4] \quad E_p = E_o (-0.21 + 0.70 \text{ LAI}^{1/2}) \quad 0.1 < \text{LAI} < 2.7$$

[5]

$$E_p = E_o$$

2.7 < LAI

where, E_p = the potential transpiration rate per unit time (mm/day),
 LAI = the leaf area index of the vegetative cover, and

$$= \left(\frac{\text{surface area}_{\text{leaf}}}{\text{surface area}_{\text{soil}}} \right)$$

 E_o = the potential evaporation rate per unit time (mm/day).

Depending on the ratio of the surface area of the leaves to the soil surface area they cover, the surface flux condition described by either eqs. 3, 4 and 5 assume either: evaporation only, a combined evaporation and transpiration flux or solely transpiration flux conditions. The three phases of vegetative cover are identified as bare soil, partial cover and full cover conditions, respectively. Ritchie (1972) describes the leaf area index values which define lower and upper limits of the partial cover condition as 0.1 and 2.7 respectively.

The mass flux due to transpiration, being a surface potential flux, must be distributed through the soil profile which is occupied by the vegetative root structure. The proposed method of distributing the potential transpiration is presented in Figure 1 as a decreasing uptake rate with depth (Prasad, 1988).

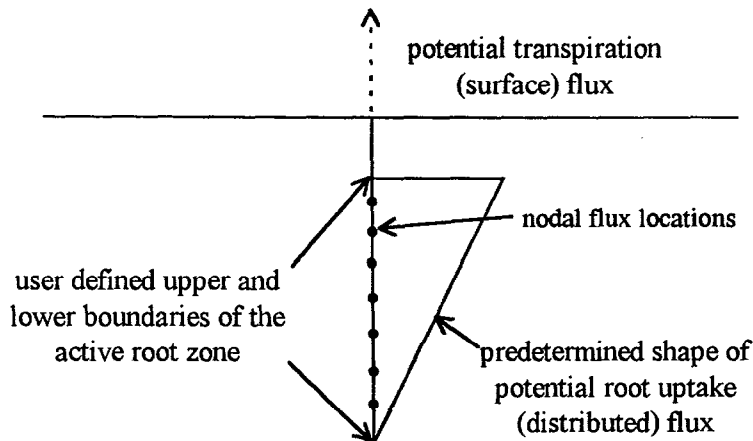


FIGURE 1. The shape function used to calculate the potential root uptake distribution through the active root zone (after Prasad, 1988).

The potential transpiration flux, defined in Figure 1, is distributed into nodal fluxes. The potential nodal flux rates are then dependent upon the potential transpiration flux, the location of the node with respect to the top and bottom of the active root zone and the node spacing. The potential nodal fluxes are then modified to determine the actual nodal root uptake flux as required in Eq. 2. The potential root uptake flux is modified by a reducing term given in Eq. 6, which is in turn based upon the matric suction at that nodal locations by the relationship presented in Figure 2.

[6]

$$S = PRU \cdot PLF$$

where, S = the actual nodal root uptake sink term, required in Eq. 1 (m/s),
 PRU = the potential root uptake flux (m/s), and

PLF = the plant limiting factor, dependent upon the nodal matric suction as defined in Figure 2.

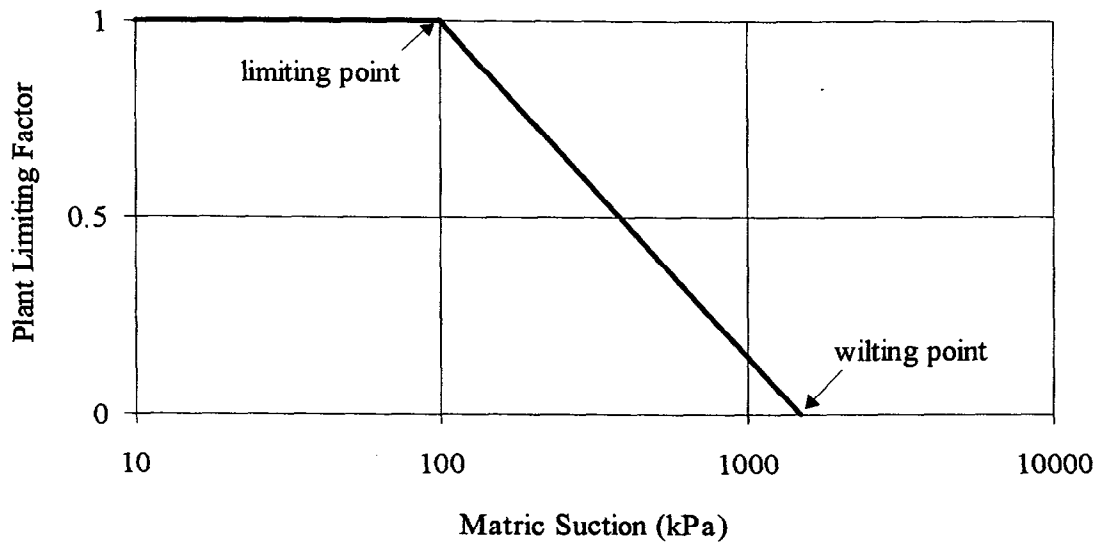


FIGURE 2. Definition of the plant limiting factor from the nodal matric suction. Generally accepted values for the limiting and wilting points range from 50 to 100 kPa and 1500 to 2000 kPa respectively (Feddes et al., 1978).

LABORATORY PROGRAM

A laboratory program was conducted to evaluate the physical responses of a soil profile to plant vegetation as well as to provide a data set for the verification of the transpiration equations presented in eqs. 2 through 6. The experiment consisted of 1-dimensional evapotranspiration from a soil column system placed within an environmental chamber. The soil column surface was vegetated and allowed to evapotranspire in the prevailing controlled atmospheric conditions. The surface flux as well as the subsurface moisture conditions were monitored to evaluate the influence of the vegetative cover. The soil column system, including some of the construction and instrumentation details, is presented in Figure 3.

The surface evapotranspiration flux condition was evaluated directly by measuring the flow of moisture into the soil column and the change in mass of the entire soil column system. The soil profile was instrumented for the measurement of matric suction using thermal conductivity sensors and tensiometers. The soil column was also instrumented for temperature using type T thermocouples. Manual water content profiles were evaluated using the PVC column port holes sealed with rubber stoppers. Climatic characterization included pan (potential) evaporation rates as well as ambient relative humidity and temperature. The vegetative canopy leaf area index was measured directly and the subsurface rooting characteristics were determined on the basis of water content profiles.

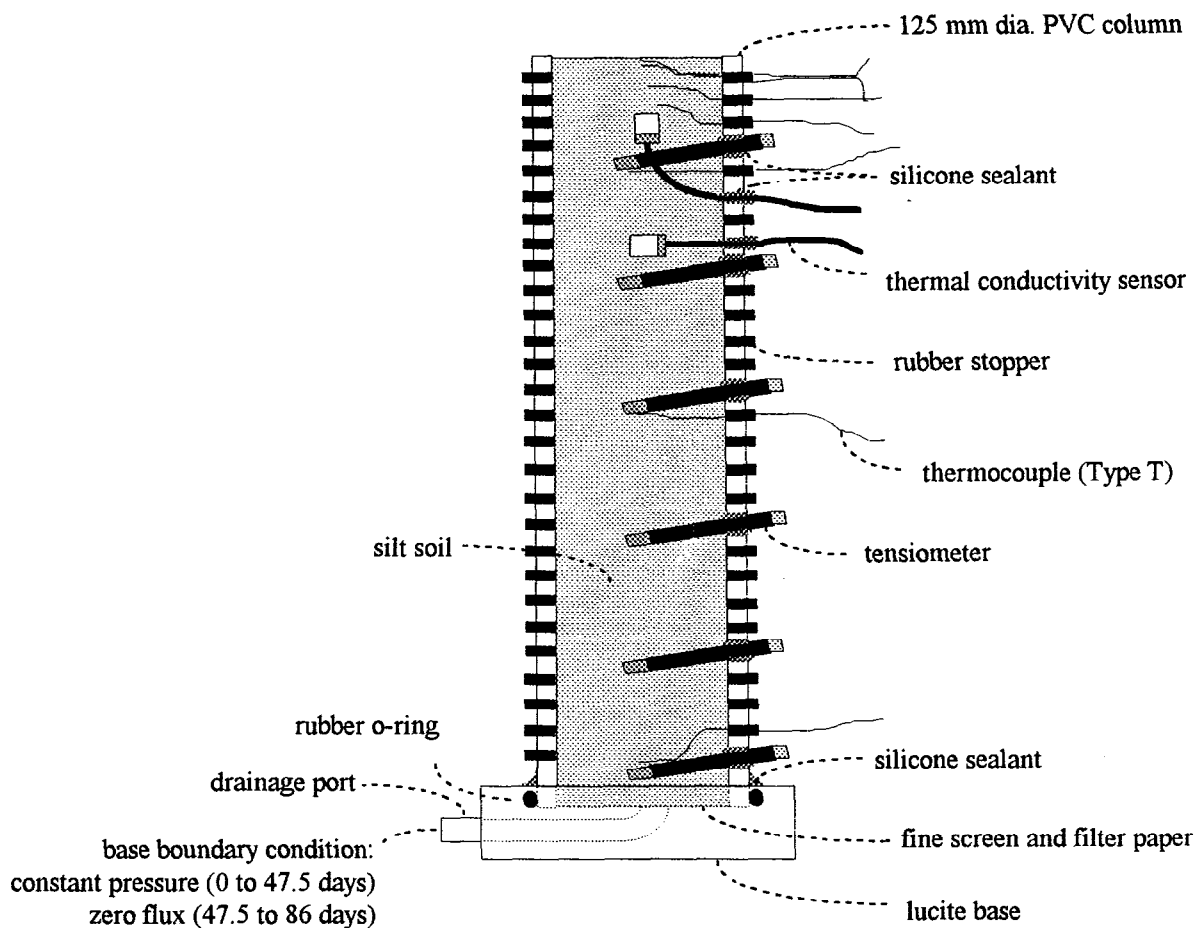


FIGURE 3. Diagram of the PVC column used in the evapotranspiration study, displaying the general construction and instrumentation details.

The soil used in the experiment was characterized as a low plasticity silt material. The soil water characteristic curve for the silt material is presented in Figure 4. The soil was observed to consolidate slightly under desiccation conditions, however was otherwise found to perform well through the experiment.

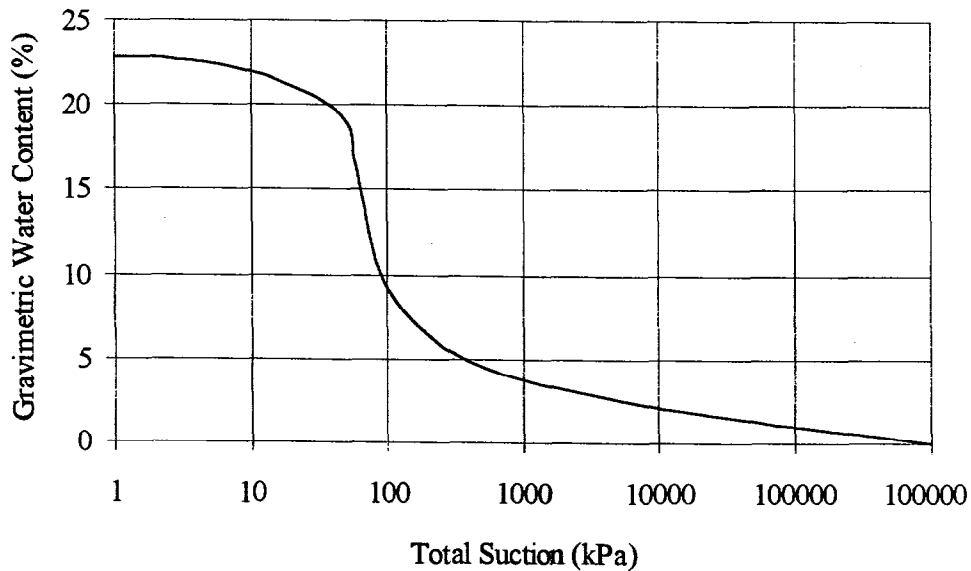


FIGURE 4. Soil-water characteristic curve for the silt material used in the soil column evapotranspiration study.

ANALYTICAL MODELLING RESULTS

The measured surface flux results obtained through the experimental program are presented in Figure 5. Figure 5 also shows the computed rate of evaporation, transpiration and evapotranspiration on the basis of eqs. 1 through 6. Good agreement is apparent between the measured and computed rates of evapotranspiration. The individual components of evaporation and transpiration were not measured, however the computed trends may be discussed in general terms.

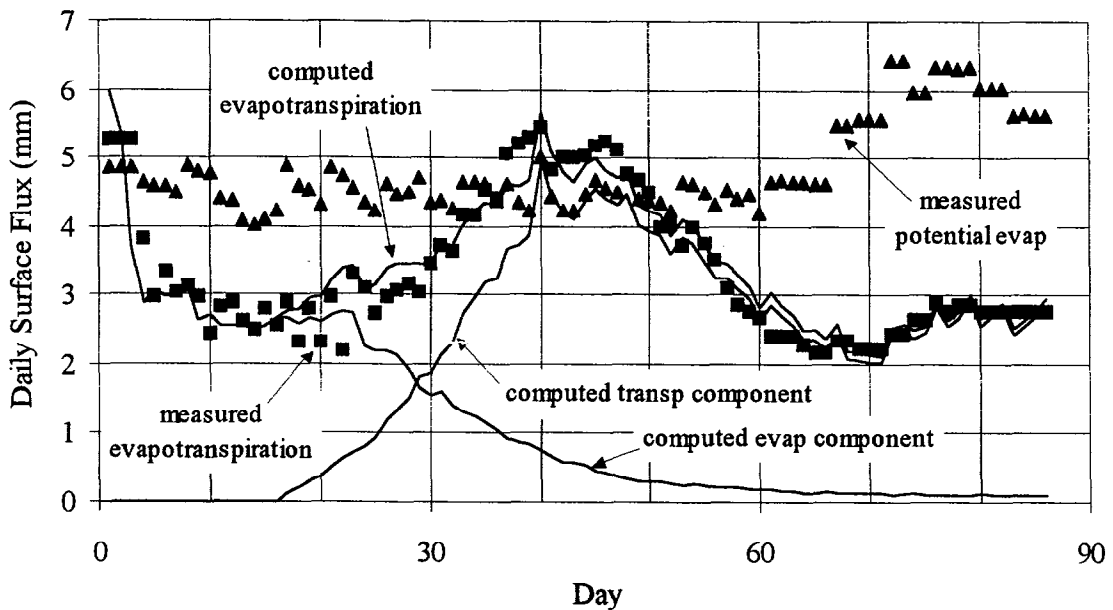


FIGURE 5. Comparison of the measured and predicted evapotranspiration fluxes. Also presented are the simulated evaporation and transpiration flux partitions.

Six surface flux stages were observed to occur through the experimental period, three involving evaporation only and three involving both evaporation and transpiration fluxes. During the first two days from initiation of the experiment, the soil surface was saturated and the flux continued at potential evaporation rates. Between days three and 10, the soil surface was desaturating and the evaporative flux continually decreased. Between days 10 and 17 the soil column system appeared to be near equilibrium for evaporative conditions. After day 17, the vegetative leaf area index exceeded 0.1, causing the transpiration flux to increase. On day 40, the vegetative canopy reached a leaf area index value of 2.7 and the potential transpiration flux was found to equal the potential evaporation flux. Between day 40 and day 47, the total evapotranspiration continued at potential evaporation rates. The flux supplying the column base was discontinued on day 47 which induced moisture limiting conditions. Almost immediately, the surface flux condition responded to the increased matric suctions caused by continuous drying conditions. The limiting conditions for evapotranspiration continued to the conclusion of the experiment on day 86. The increase in evapotranspiration after day 70 coincides with an increase in potential evaporation.

The simulated evaporation component in Figure 5 was found to continuously decrease with increasing transpiration fluxes. The decreasing evaporation flux was directly related to the desaturating surface due to the interception of moisture by the root system before it could reach the soil surface.

The measured and simulated water content profiles on select days are presented in Figure 6. The four days shown represent evaporation flux conditions only (day 16), non-limiting transpiration with full vegetative cover conditions (day 47), and evapotranspiration in moisture limiting conditions (days 72 and 86). The water content profile trends indicate the influence of transpiration and root water uptake. The water content profile on day 16 represents steady state conditions with an evaporative flux. Changes in the water content profiles after day 16 are related to the transpiration flux and the resulting root water uptake patterns.

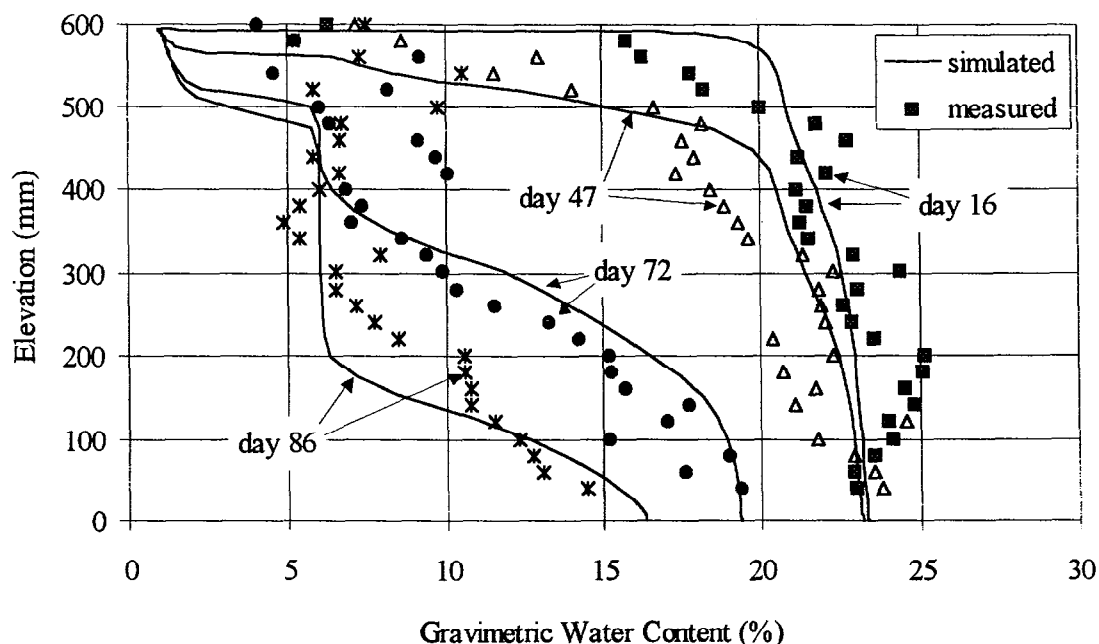


FIGURE 6. Simulated and measured water content profiles on days 16, 47, 72 and 86.

Comparisons of the simulated and measured water content results indicate the computed water uptake patterns were representative of the actual root uptake conditions. The computed root uptake trends on 10 day intervals are presented in Figure 7. The y-axis of Figure 7 are in units mm/day/mm, hence the uptake distribution must be integrated over the entire depth to determine the surface flux in units mm/day.

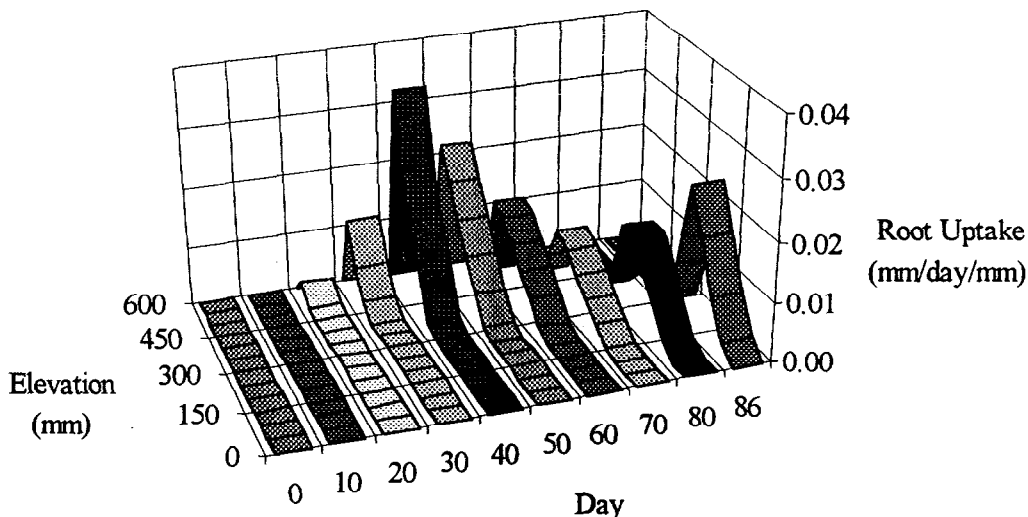


FIGURE 7. Presentation of the simulated root extraction patterns through the soil depth, displaying trends on 10 day intervals.

The various phases of the surface flux conditions are identified in Figure 7. Between initiation and day 17, the surface flux consisted totally of evaporation, hence root uptake was zero. Between days 20 and 40, the root uptake pattern is shown to increase substantially with increasing vegetative cover. After day 50, the matric suctions through the root system increase to moisture limiting conditions, hence the fluxes near the surface progressively decrease to the conclusion of the experiment. Also of interest is the increase in depth of the root system, indicating the progressive growth of the root system.

CONCLUSIONS

An experiment was conducted to evaluate the influence of transpiration on the surface flux and subsurface moisture conditions. The experiment was successful in evaluating the surface flux through six surface flux stages including bare soil evaporation and cumulative evaporation and transpiration fluxes. A good correlation was found between measured and computed evapotranspiration. Unfortunately, the evaporation and transpiration components of the surface flux could not be identified except by theoretical means. Moisture redistribution patterns under the influence of transpiration withdrawal of moisture were also successfully documented.

The proposed methodology to predict the transpiratory flux and root uptake rates appears to properly evaluate the measured data trends observed in the soil column experiment. The methodology follows a simple solution which conforms to geotechnical engineering nomenclature. The terms required for the transpiration flux solution are easy to define and measure and the results do not require a sophisticated biological interpretation.

Table 4.3 Compaction Test Results

Sites	w_{opt} Optimum water content (%)	γ_d Dry unit weight (kN/m ³)	e Resulting void ratios
Sigma	13.8	18.4	0.50
Bevcon	15.2	17.8	0.54
Senator - fine	13.3	18.7	0.49
Senator - coarse	13.0	18.6	0.51
Manitou-Barvue	14.2	18.1	0.56
Solbec-Cupra	12.0	20.75	0.57

Table 4.4 Main Results of Oedometer Tests

Sites	C_c	c_v (cm ² /s)	m_v (m ² /kN)	C_u	Range of "e"
Sigma	.046	5.01×10^{-3}	1.73×10^{-3}	.004	.48
	à .078	à 4.80×10^{-1}	à 1.40×10^{-2}		
Bevcon	.070	1.48×10^{-2}	1.91×10^{-3}	.003	.59
	à .096	à 5.44×10^{-1}	à 9.75×10^{-3}		
Senator - fine	.065	3.95×10^{-3}	1.69×10^{-3}	.003	.53
	à .100	à 6.94×10^{-1}	à 9.70×10^{-3}		
Senator - coarse	.088	2.01×10^{-3}	1.09×10^{-3}	.006	.54
	à .130	à 2.82	à 1.61×10^{-2}		
Manitou-Barvue	.048	1.04×10^{-3}	1.82×10^{-3}	.002	.53
	à .088	à 6.90×10^{-1}	à 3.90×10^{-3}		
Solbec-Cupra	.110	1.87×10^{-2}	1.61×10^{-3}	.003	.65
	à .160	à 1.22	à 1.31×10^{-2}		

Note: à = to

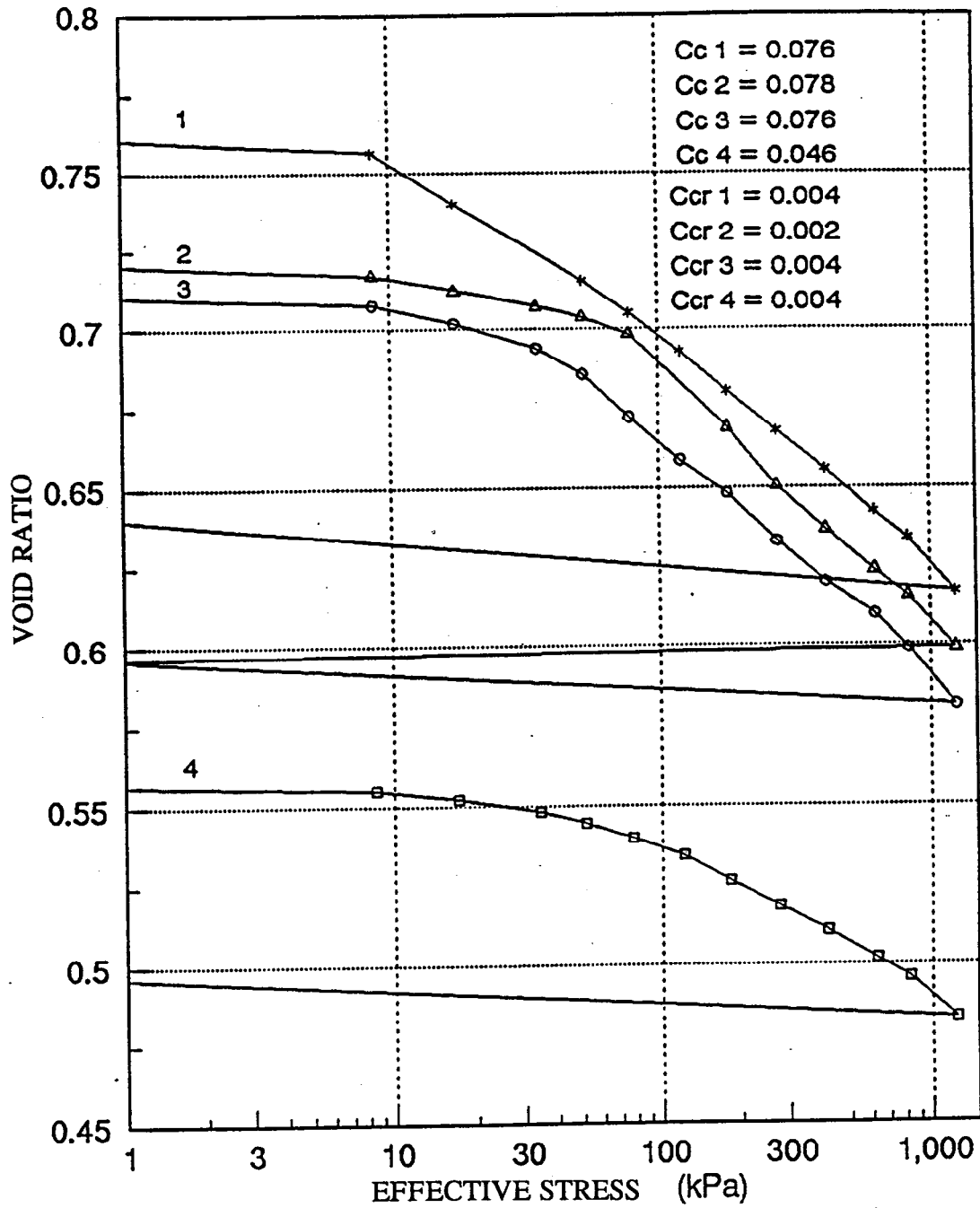


Figure 4.3a Consolidation Curves for the Sigma Tailings Sample

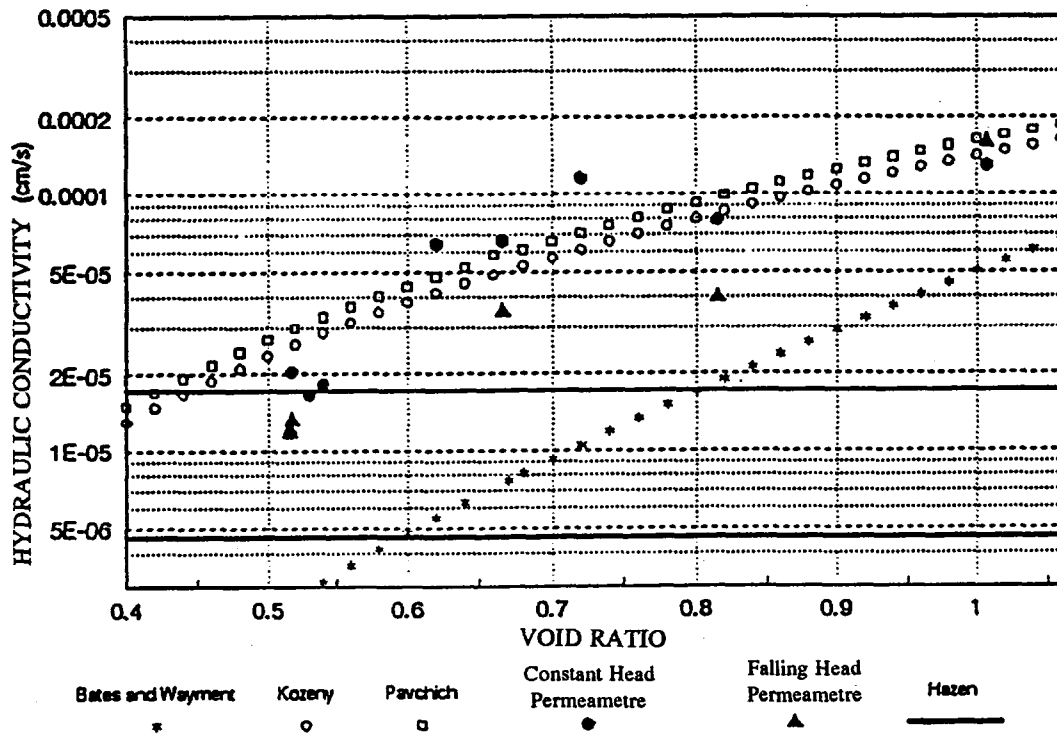


Figure 4.4a Correlation between the Measured Permeability using the Permeametre and the Calculated Value for the Sigma Tailings Sample

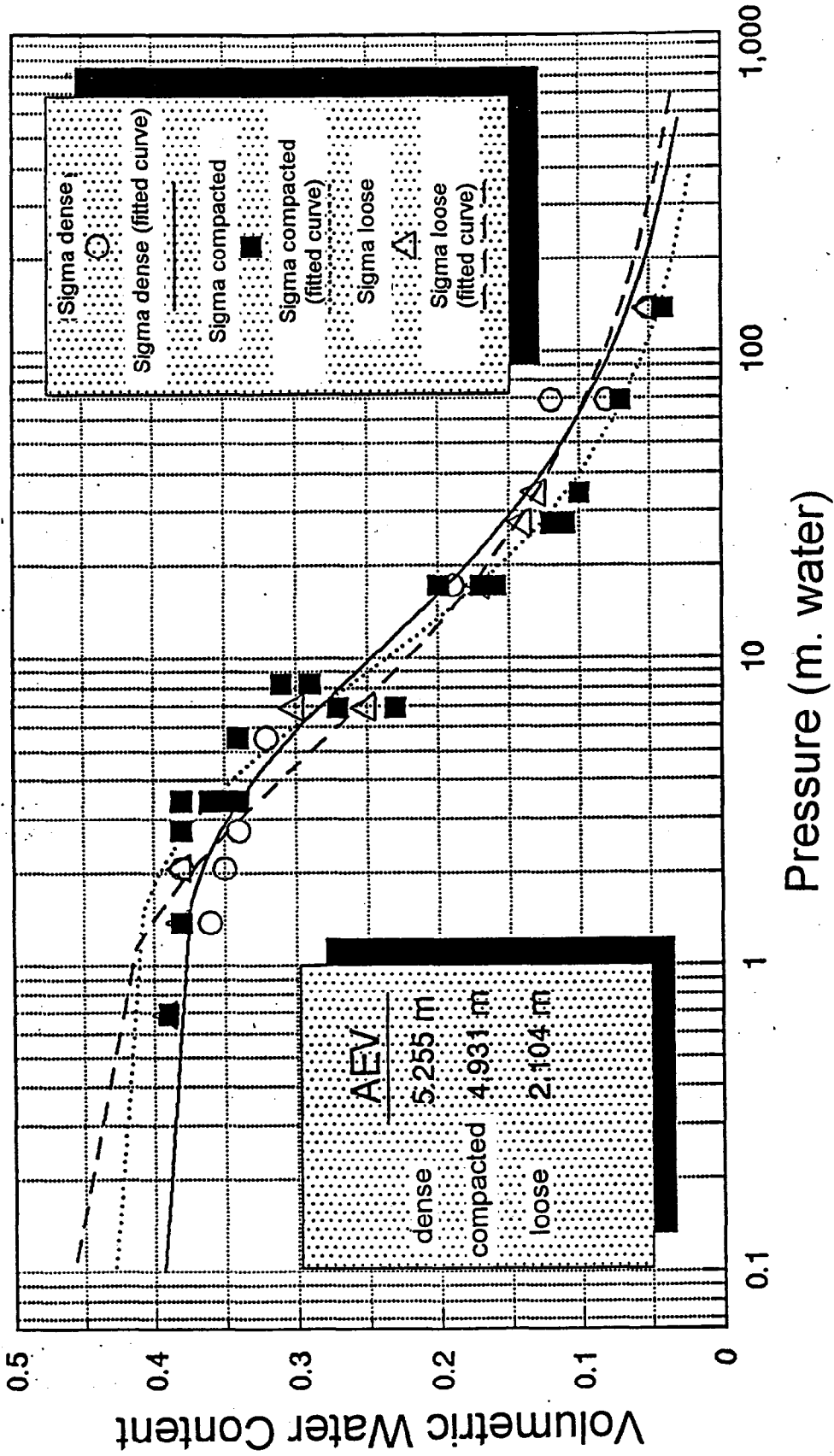


Figure 4.6a Suction Curves - Sigma

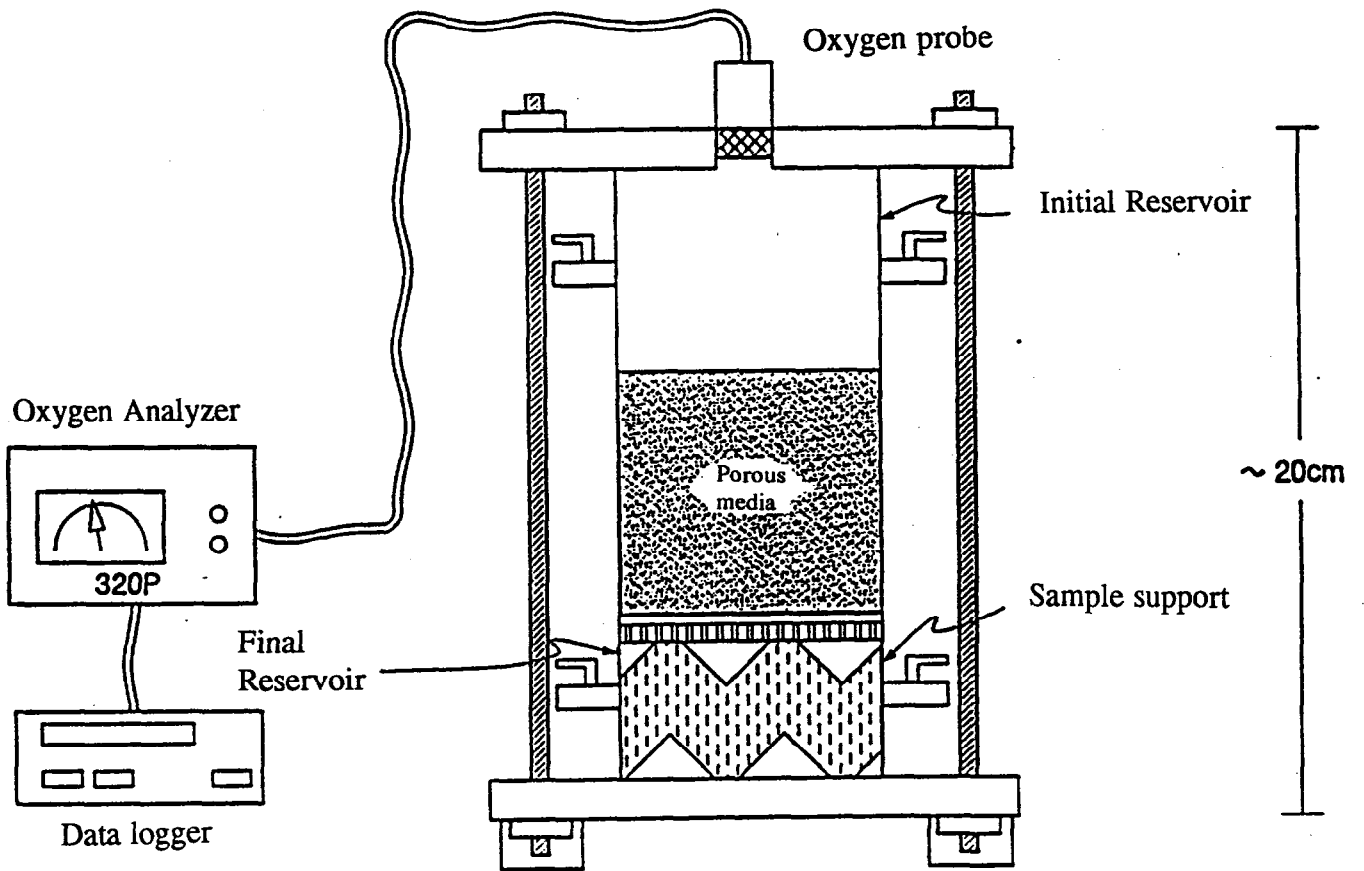


Figure 4.7 Experimental Setup to Measure Oxygen Diffusion Coefficient in A Porous Media

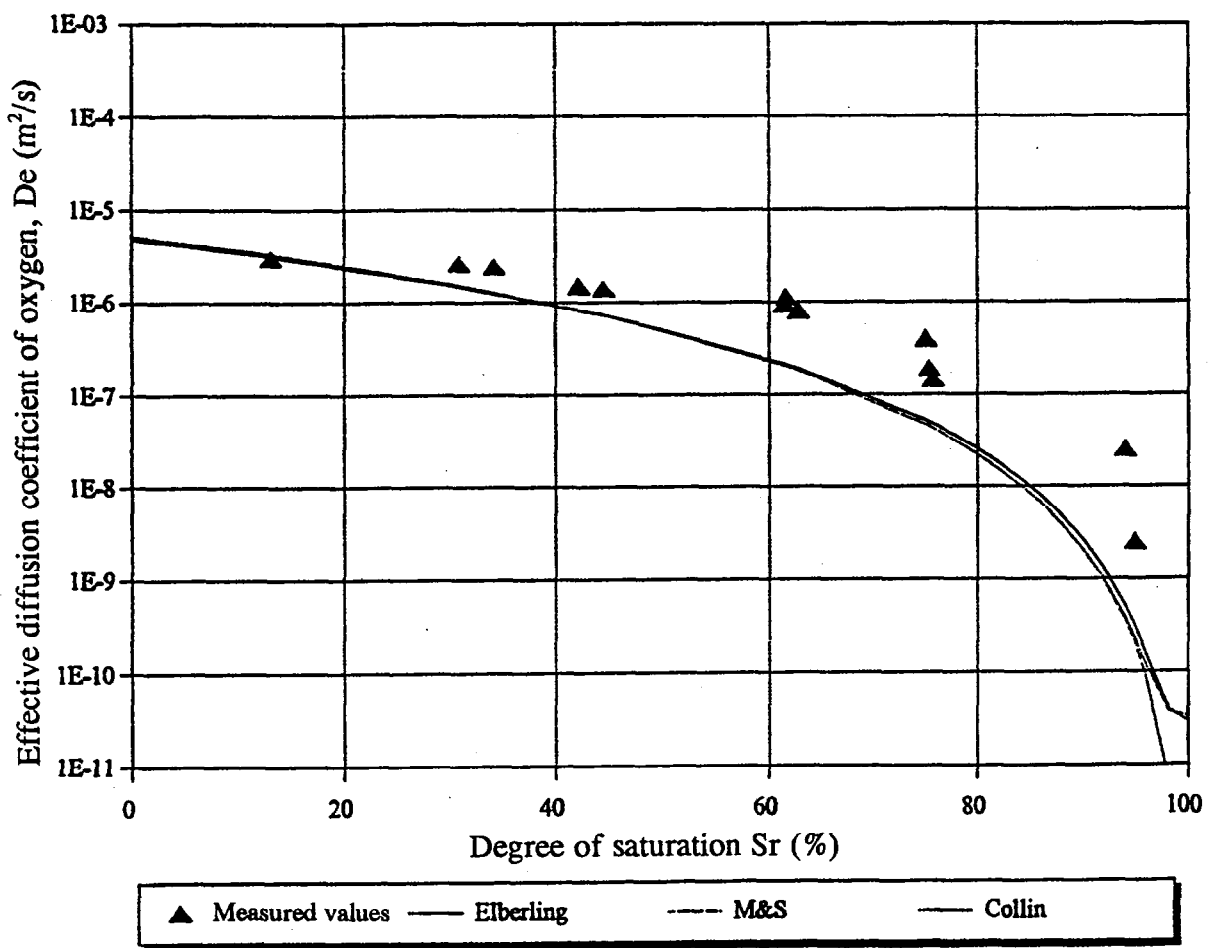


Figure 4.8a Results of Measured Effective Diffusion Coefficient Compared to Empirical Results for the Senator Tailings Site.

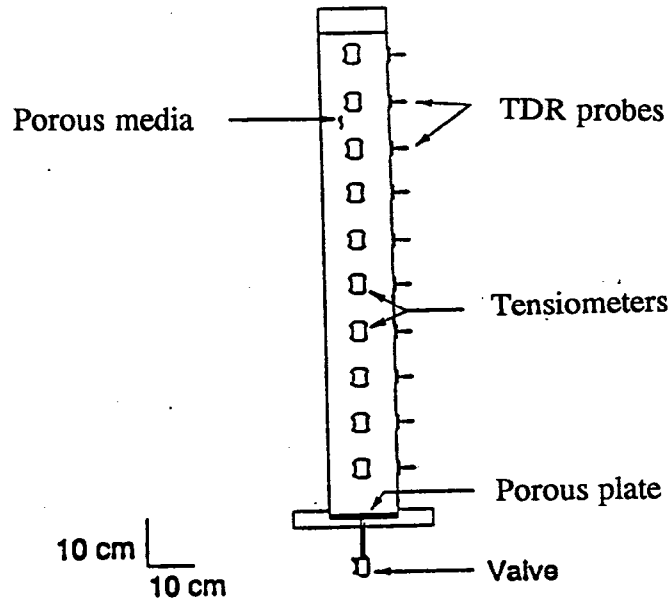


Figure 5.1 Schematic Diagram of the Drainage Column

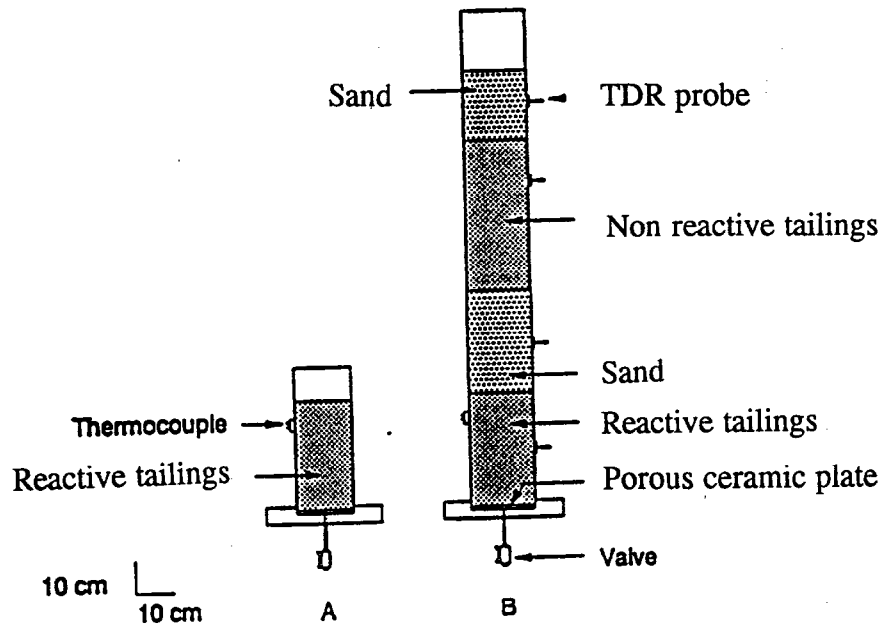


Figure 5.2 Schematic Diagram of the Control and Reference Columns

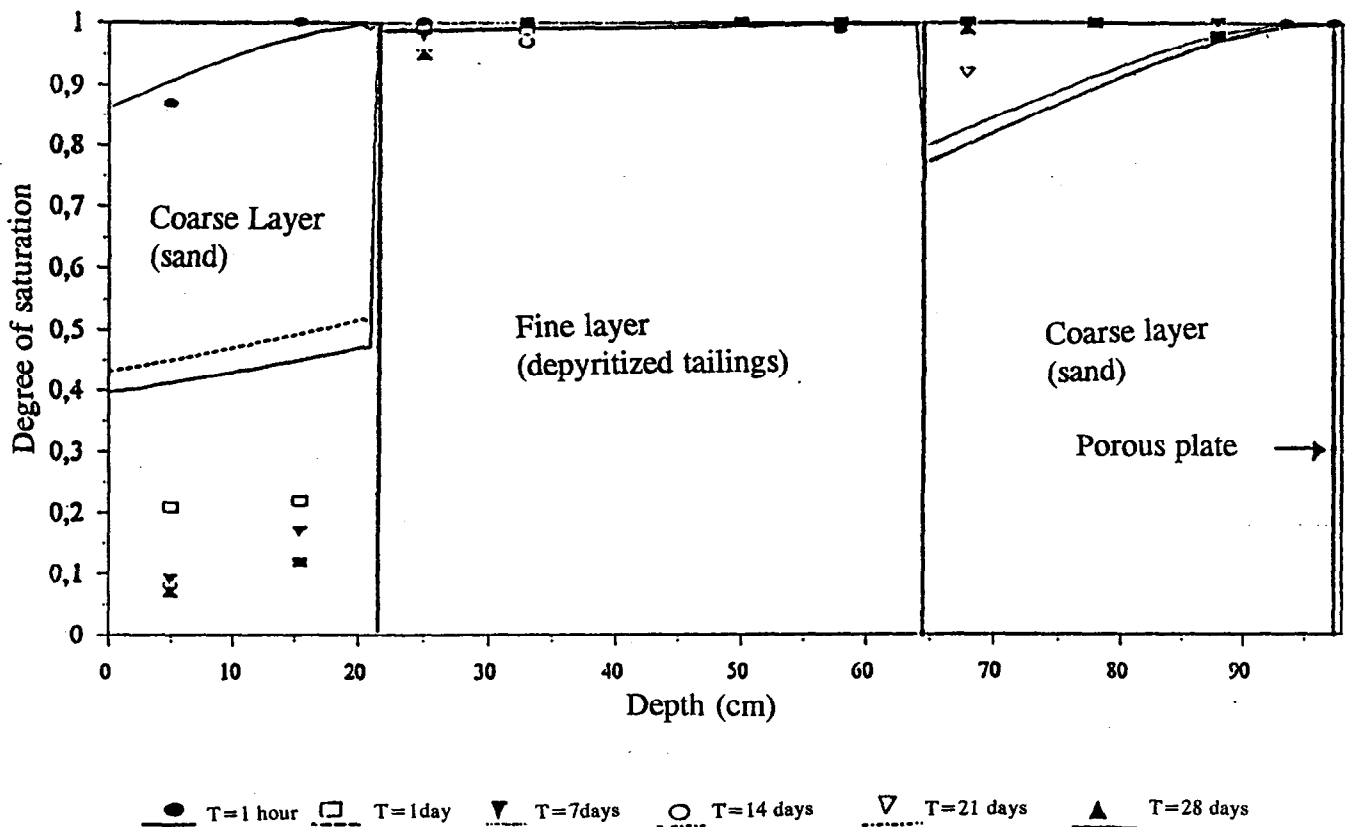


Figure 5.3b Test Results and Modelling of Drainage Conditions - Phreatic Surface and Bottom of Column

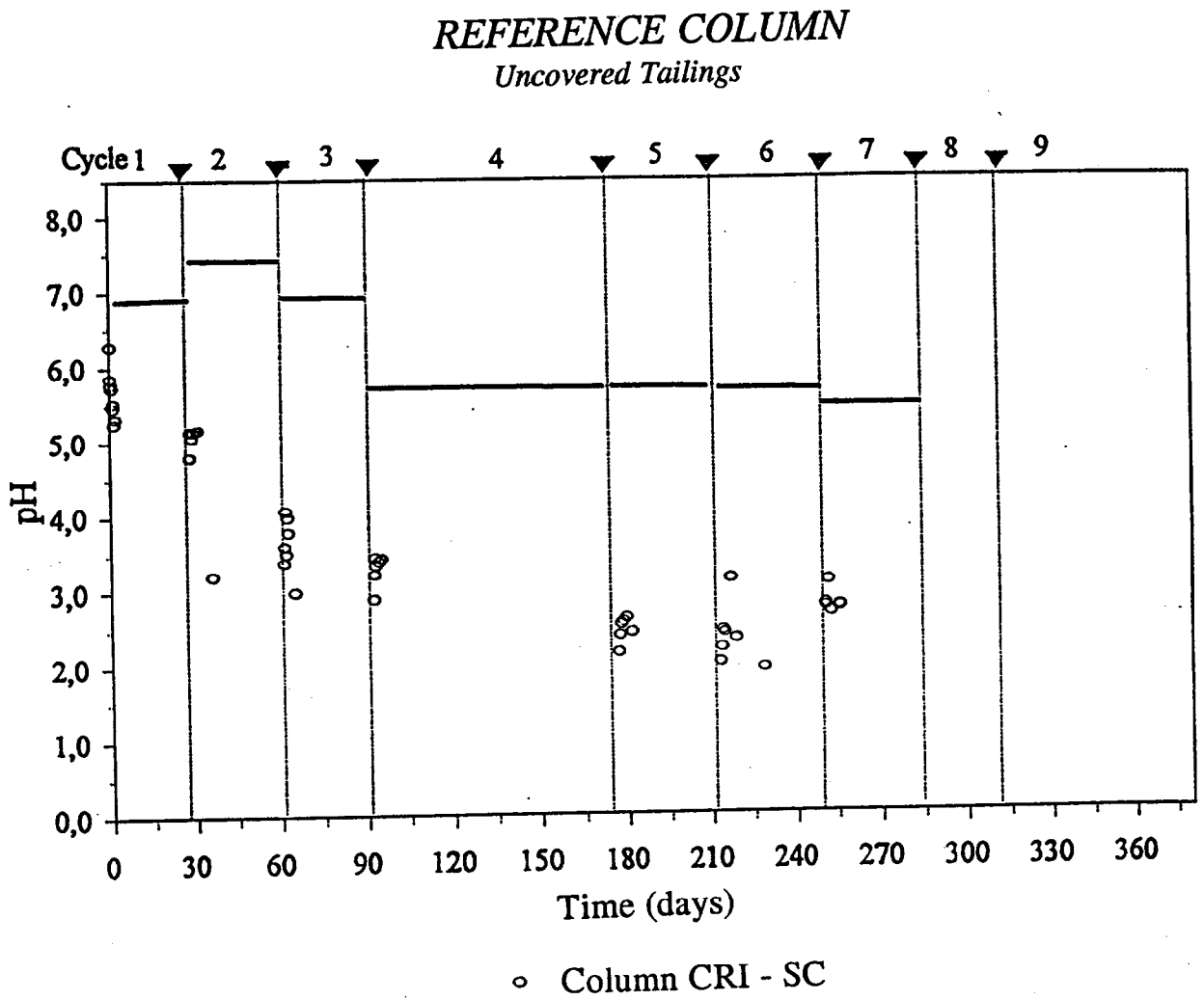


Figure 5.4a Change in pH (uncovered)

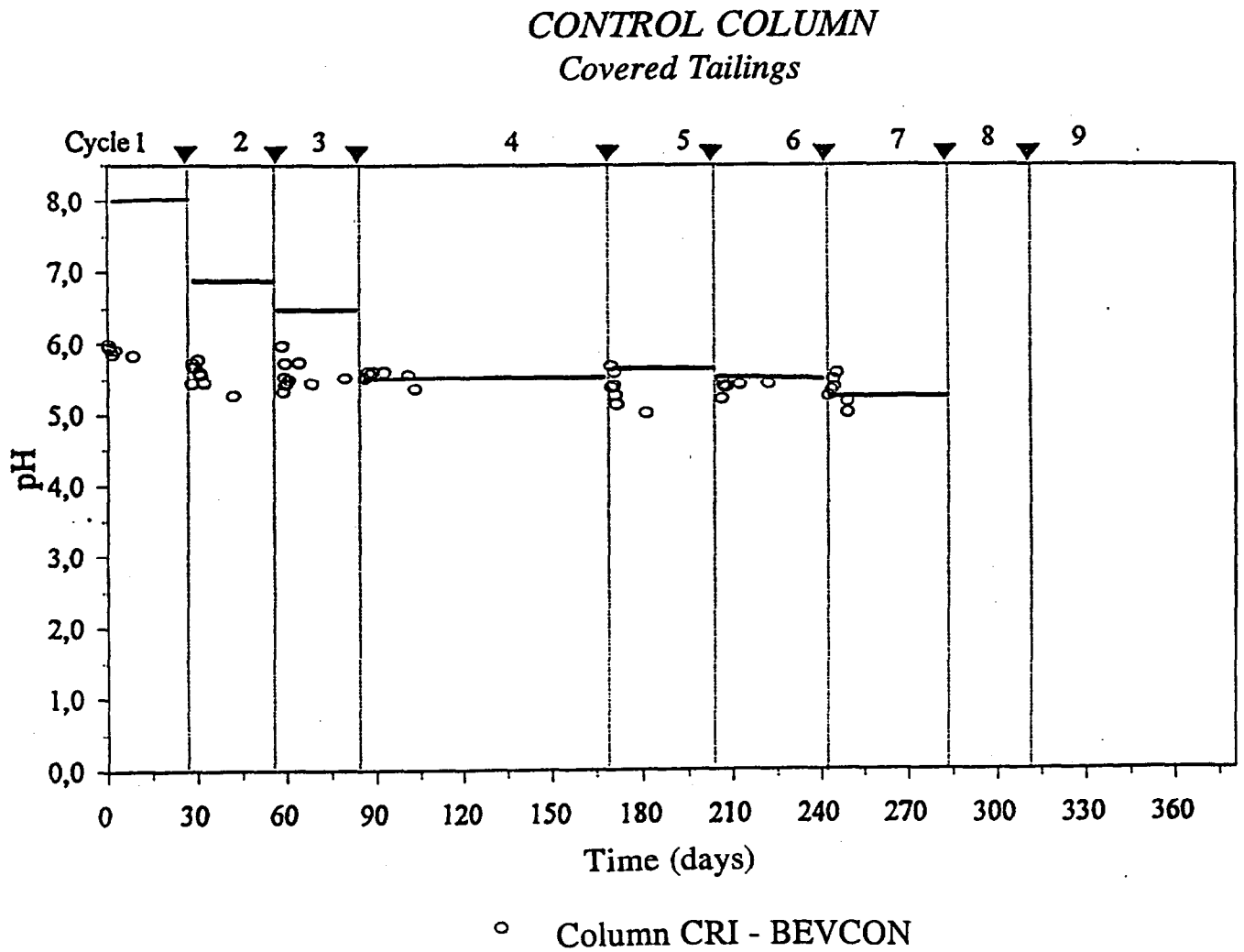


Figure 5.4b Change in pH (covered with Bevcon tailings)

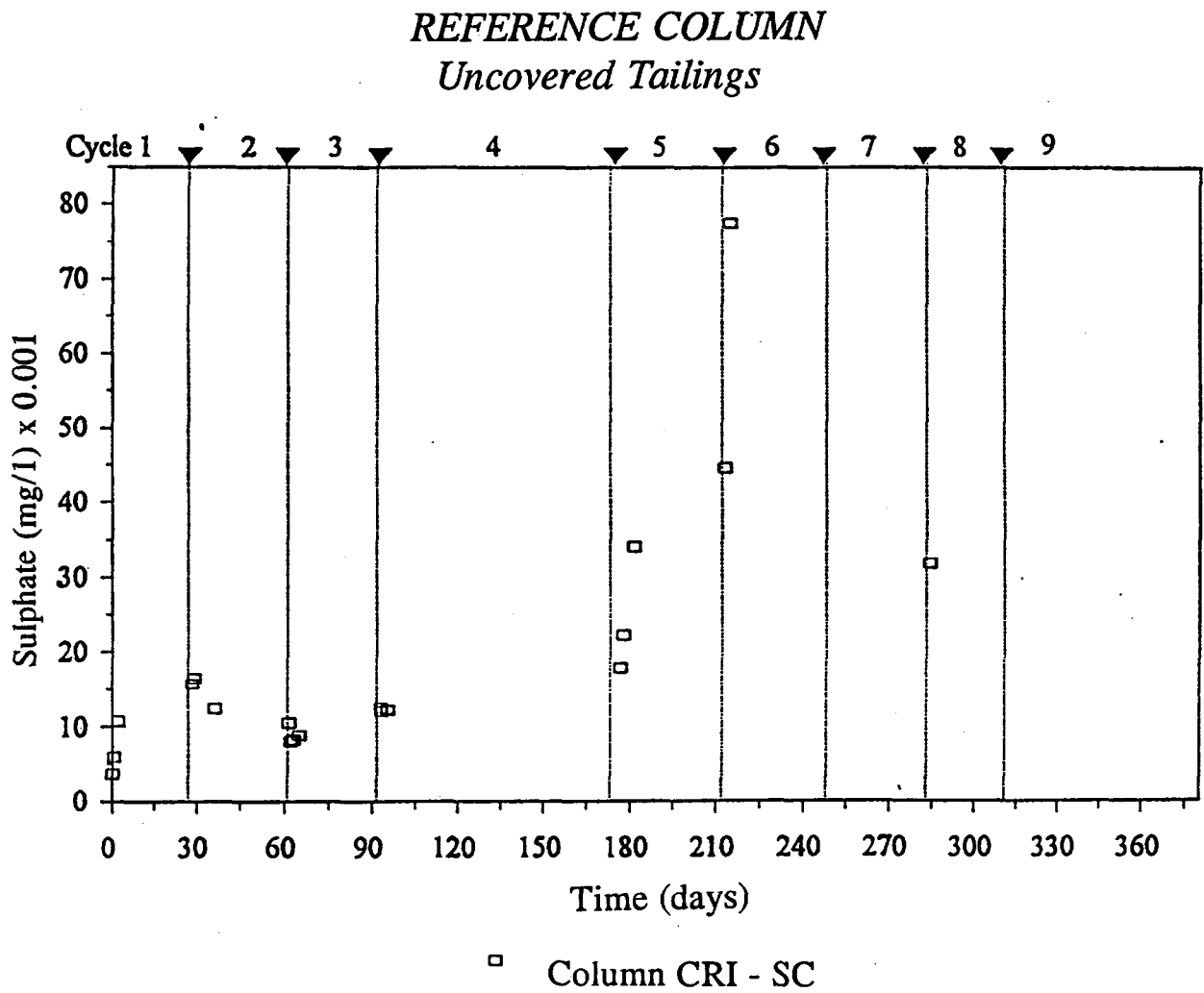


Figure 5.5a Changes in Sulphate Concentration (uncovered)

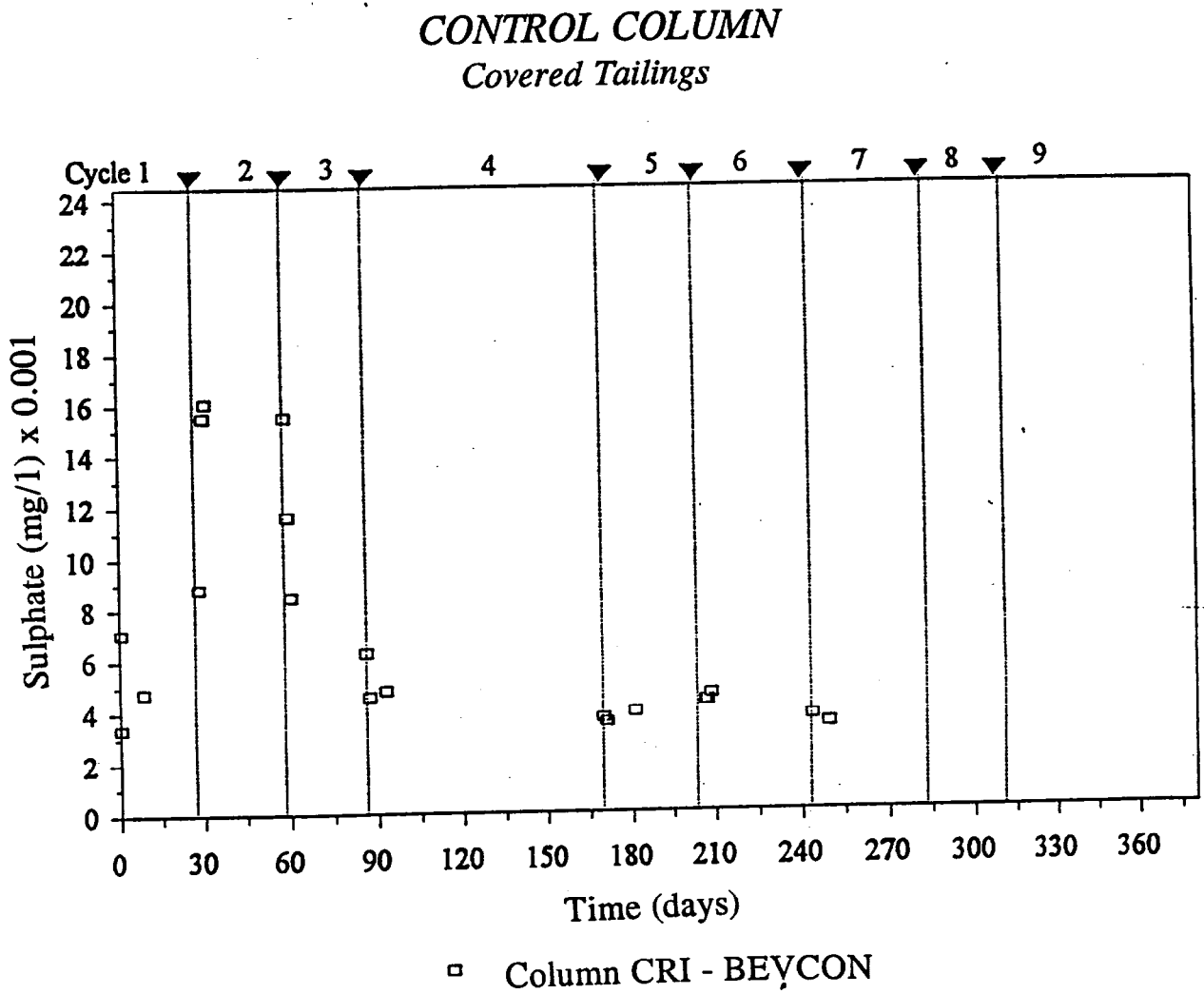


Figure 5.5b Changes in Sulphate Concentration (using Bevcon tailings as cover material)

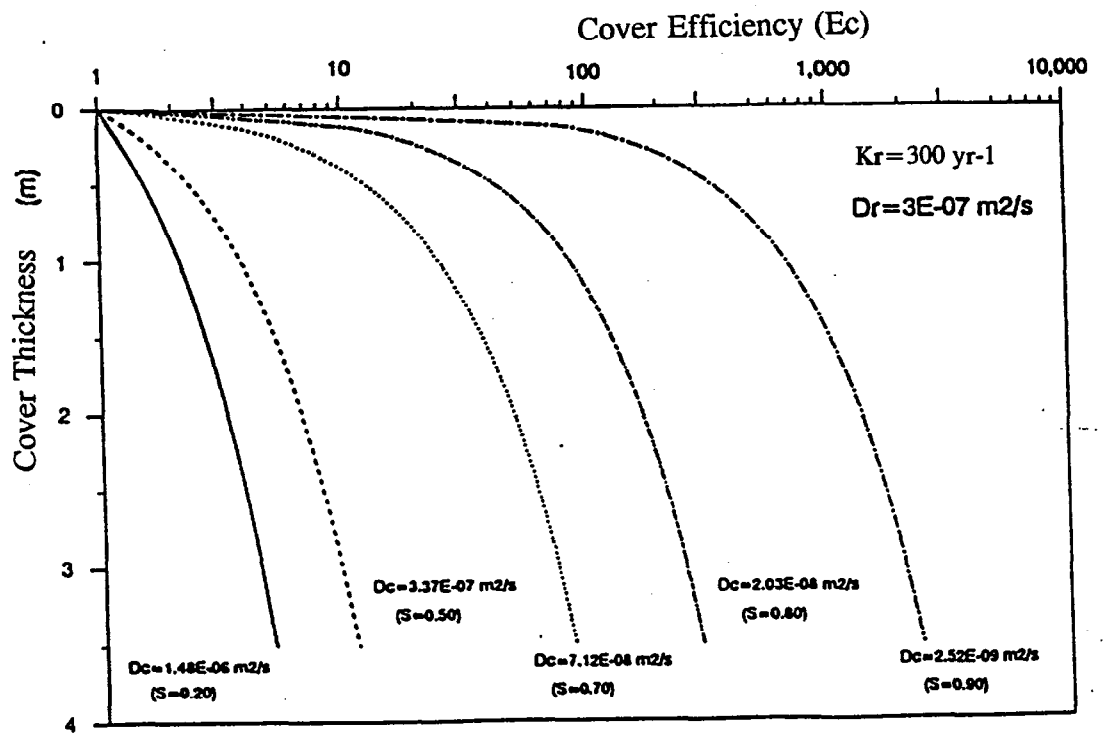


Figure 5.11 Relationship Between the Cover Thickness and its Efficiency to Reduce the Oxygen Flux (After Aachib and Al. 1993, 1994)

Unsaturated Flow Modeling of Covers for Reactive Tailings

Bruno Bussière

Unité de recherche et de service en technologie minérale (URSTM), Rouyn-Noranda, Québec

Michel Aubertin, Mostafa Aachib, Robert P. Chapuis, Rodolfo J. Crespo

Department of Mineral Engineering

École Polytechnique de Montréal, Montréal, Québec

ABSTRACT:

The installation of a cover is one of the main techniques to control the production of acid mine drainage by sulfide tailings. Such so called "dry covers" are used to restrict the flow of water and oxygen. A capillary barrier effect is usually created within covers to reach these objectives. Numerical simulations were done to evaluate the hydrogeological behavior of different types of cover with two and three layers. The results show that the main factors affecting the hydrogeological behavior are the suction properties contrast between the different materials and the thickness of the base layer that creates the capillary break. The simulations also show the large influence of the constitutive model used to evaluate the unsaturated hydraulic conductivity function.

RESUME:

L'installation de barrières de recouvrement constitue l'une des principales méthodes pour empêcher la génération de drainage minier acide de parcs à résidus miniers sulfureux. Ces recouvrements, appelés "barrières sèches", sont installés dans le but d'isoler les résidus de la migration de l'eau et de l'oxygène. Un effet de bris capillaire est habituellement créé dans le recouvrement pour atteindre ces objectifs. Des simulations numériques ont été réalisées afin d'évaluer le comportement hydrogéologique de recouvrements comprenant deux et trois couches. Les résultats obtenus démontrent que les principaux facteurs qui affectent le comportement hydrogéologique sont le contraste des propriétés de succion entre les différents matériaux et l'épaisseur de la couche grossière du bas qui crée le bris capillaire. Les simulations montrent également la grande influence qu'a le choix du modèle constitutif utilisé pour prédire la conductivité hydraulique non saturée.

INTRODUCTION

The most serious environmental problem facing the Canadian mining industry is the production of acid mine drainage (AMD) by sulfide tailings. The main methods used to prevent the production of AMD essentially aim at eliminating the interactions between the constitutive elements of the reactions, which are iron sulfides, water and oxygen. One of the most interesting way to do so is to use dry covers installed over reactive tailings in order to restrict the oxygen flow (SRK, 1989).

This paper deals with capillary effects created in covers to limit the oxygen and the water flow. A capillary barrier can exist when unsaturated flow occurs through a fine grained soil overlying a coarse grained soil. The paper also shows how numerical methods can be used to evaluate the performance of such capillary barriers. The formulation of the mathematical equations used by

the numerical model SEEP/W are presented. Then, simulations with different types of material and different configurations are analyzed and briefly discussed.

CAPILLARY BARRIERS

General description

Most covers used to isolate municipal and industrial wastes are constructed with natural (clay, till) and/or industrial (geosynthetics) materials. In the former case, the fine grain layer in the cover has to maintain a high degree of saturation in order to avoid cracking due to wet-dry cycles and to limit gas migration through the air filled pores. To maintain this high degree of saturation, a capillary barrier effect can be artificially created in the cover system.

Figure 1 shows a typical layered cover system. In such system, capillary barrier effect is created when a fine grain layer overlies a coarse grain layer, as for layers D and E in Figure 1. In this case, the water that infiltrates the surface flows through layer E (considered initially dry) only when the capillary tension in layer D is close zero, that is when it is nearly saturated. A similar effect can be created when a coarse material is placed over a fine material, as for layers C and D in Figure 1. Such configuration prevents rising of the water by capillary forces, from the fine to the coarse material.

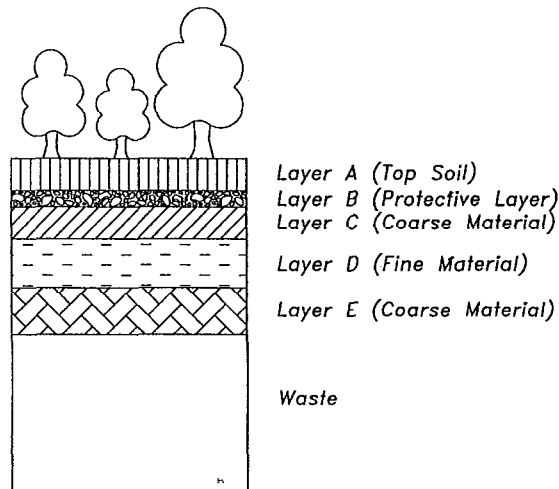


Figure 1. Typical configuration of a multi-layered cover (after Aubertin et al., 1993)

The cover system showed in Figure 1 thus includes a double capillary barrier effect, one on both sides of the fine layer. In this case, drainage of layers C and E inhibits the flow of water from the fine material layer and helps to maintain a high degree of saturation in layer D. More details on the description of capillary barrier effects have been presented by Morel-Scytoux (1992), Chiu and Shackelford (1994) and Aubertin et al. (1995).

Unsaturated flow

As previously mentioned, a capillary barrier effect results when unsaturated flow occurs through a relatively fine-grained soil overlying a relatively coarse-grained soil. When a soil is not saturated ($S_r < 100\%$, where S_r is the degree of saturation), air (or other gas) fills a fraction of the pores. The flux of water is then reduced in comparison with the one observed under saturated conditions (for a given hydraulic gradient).

It is not the objective of this paper to give a detailed presentation on the theory of unsaturated flow. It is nevertheless necessary to introduce the basic concepts

in order to understand the principles involved in the modeling of covers. More details on this theory can be found elsewhere (e.g. Hillel, 1980; Kovács, 1981; Mualem, 1986; Fredlund et Rahardjo, 1993).

The flow of water through a porous media can be estimated with the Darcy's law (presented here in a scalar form):

$$v = k \frac{\delta h}{\delta x} \quad (1)$$

where v is de Darcy's velocity, k is the hydraulic conductivity and $\delta h / \delta x$ is the hydraulic gradient commonly identified as i .

It is usually considered that Darcy's law is valid for both saturated and unsaturated conditions. In saturated conditions, the pore pressure is positive and the k value can be considered as a constant for a specific material. In unsaturated conditions, the water is maintained in the pores by capillary forces associated to the surface tension created at the water-air interface. Because the capillary forces depend on the radius of curvature of the surface at the water-air interface, small pores generates a larger capillary tension. Thus, fine materials will retain more water than coarse materials for a given pore pressure.

In unsaturated media, pore pressure changes with the degree of saturation (or the volumetric water content). The relationship between negative pore pressure (or suction) and volumetric water content (often called soil-water characteristic curve or ψ - θ relationship) can be used to estimate the unsaturated condition. Several mathematical models exist in order to describe (e.g. van Genuchten et al., 1991; Fredlund et Xing, 1994) or predict (e.g. Kovács, 1981; Aubertin et al., 1995b) the soil-water characteristic curve.

The hydraulic conductivity k of an unsaturated soil is not a constant. It depends on the volumetric water content θ , which, in turn, depends upon the soil suction ψ . Several functions have been developed over the years to relate permeability function (ψ - k relationship) to soil-water characteristic curve. These models can be empirical (e.g. Brooks and Corey, 1964) or statistical (e.g. Green and Corey, 1971; Mualem, 1976).

NUMERICAL MODELING

Numerical methods are used to solve mathematical models, which can be defined as a set of mathematical equations describing the physical process involved in

the real system. For a proper use of numerical methods, it is important that the resolution method used and the mathematical equations involved are known and understood.

The software used in this study is SEEP/W, from GEO-SLOPE International. This software uses the Finite Element Method (FEM) to solve the differential equations of the mathematical model. SEEP/W analyses the movement of water through porous media as soils and rock mass. Different types of problems can be simulated, including saturated and unsaturated flow analysis, steady-state and transient conditions, two dimensional and axisymmetric configurations.

The fundamental differential equation used by the software can be presented as follows (GEOSLOPE International, 1994):

$$\frac{\partial}{\partial x} \left[k_x \frac{\partial H}{\partial x} \right] + \frac{\partial}{\partial y} \left[k_y \frac{\partial H}{\partial y} \right] + Q = \frac{\partial \theta}{\partial t} \quad (2)$$

where H is the total head, k_x is the hydraulic conductivity in the x-direction, k_y is the hydraulic conductivity in the y-direction, Q is the applied boundary flux, θ is the volumetric water content and t is the time. More details on the fundamental aspects behind the software can be found elsewhere (GEOSLOPE International, 1994; Huyakorn and Pinder, 1983; Bathe, 1982; Zienkiewicz, 1977). The main characteristics of SEEP/W are presented in Table 1.

TABLE 1. General characteristics of SEEP/W

Type of elements	<ul style="list-style-type: none"> • Quadrilateral with or without secondary nodes (integration order 9 or 4) • Triangular with or without secondary nodes (integration order 3 or 1)
Interpolating functions	• Bathe's interpolating functions (Bathe, 1982)
Finite element equations	• Galerkin method
Time integration	• Backward difference method
Numerical integration	• Gauss numerical integration
Equation solver	• Gauss elimination techniques
Convergence	• Euclidean norm of the pressure head vector

The output files created by the software include: head file, velocity file, material properties, flux, convergence and initial head. With these files, it is possible to determine the water content profile, the pressure profile developed in the materials, the flux through a section and the permeability conditions.

NUMERICAL CALCULATIONS

In order to evaluate the hydrogeological behavior of layered covers, column tests were simulated. Similar calculations were performed by Akindunni et al. (1991). A comparison of calculated and measured conditions in column tests were also done by Yanful and Aubé (1993), Barbour and Yanful (1994) and Aubertin et al. (1995b) for different configurations of soils. Only the calculation results are presented here. The model is based on columns of 25 cm in diameter and of various height. The phreatic surface is initially placed at the top of the cover and gradually (3 600 s) lowered to the bottom of the column; such time function relaxes the constraint on the numerical model caused by a large and sudden change in the boundary conditions. Free drainage is allowed at the bottom. No function was used to simulate the effect of evaporation. The type of elements used for the generation of the finite element mesh was rectangular quadratic elements of the Lagrange family. The height of these elements were 0,25 and 0,5 cm with an integration order of 9. The iteration process stops if the difference of the vector norm between two successive iterations is less than 0,01%. The vector norm is a measure of the size of the pressure head vector.

Material Properties

The soil-water characteristic curves of the different materials studied are presented in Figure 2. Materials 1 and 2 are a sand (Crab Creek sand) and a silt (Touchet silt), which were taken from Akindunni et al. (1991). The characteristics of materials 3 and 4 (fine and coarse tailings) were evaluated by Bussière et al. (1994). The curves presented in Figure 2 were obtained with the van Genuchten model (van Genuchten, 1980); this commonly used model is different from the well-known Brooks and Corey model (1964), which can be expressed as follows:

$$\theta_e = \left(\frac{\psi_a}{\psi} \right)^\lambda \quad (3)$$

Where

$$\theta_e = \frac{\theta - \theta_r}{\theta_s - \theta_r} \quad (4)$$

θ_e is the volumetric water content in its normalized form, θ_s is the saturated volumetric water content, θ_r is the residual water content, ψ is the suction applied, ψ_a is the air entry value and λ is the pore-size distribution index. The equation of the van Genuchten model can be written as follows (van Genuchten, 1980):

$$\theta_e = \left[\frac{1}{1 + (\alpha\psi)^n} \right]^m \quad (5)$$

In equation (5) α , n and m are three different soil parameters, Model parameters for different types of soils are presented in van Genuchten and Nielsen (1985). In this case, parameter m is equal to $1 - 1/n$ and parameters n and α are fitted to experimental data. The relevant hydraulic parameters for the selected materials are presented in Table 2.

TABLE 2. Summary of the hydraulic and curve-fitting parameters for the selected materials

Materials	AEV (cm)	θ_r	θ_s	k_s (cm/s)	α (cm ⁻¹)	n
Crab Creek sand	24,0	0,141	0,448	$7,18 \times 10^{-3}$	0,029	10,21
Touchet silt	165,0	0,180	0,485	$5,83 \times 10^{-4}$	0,004	7,05
Coarse tailings	50,0	0,010	0,460	$3,00 \times 10^{-3}$	0,012	2,91
Fine tailings	140,0	0,054	0,430	$3,15 \times 10^{-4}$	0,0036	2,88

The permeability function (ψ - k relationship) must be specified for the numerical simulations. In this study, the permeability functions have been predicted using the soil-water characteristic curves. Two methods were used to evaluate the ψ - k relationship; the Mualem method (Mualem, 1976) and the Green and Corey method (Green and Corey, 1971).

The Green and Corey method is already included in SEEP/W, so one can directly calculate the permeability function from the soil-water characteristic. The Green and Corey equation can be expressed as (Green and Corey, 1971; GEOSLOPE International, 1994):

$$k(\theta)_i = \frac{k_s}{k_{sc}} \cdot \frac{30T^2}{\mu g \eta} \cdot \frac{\xi^p}{n^2} \cdot \sum_{j=i}^M [(2j+1-2i)h_i^{-2}] \quad (6)$$

where $k(\theta)_i$ is the calculated hydraulic conductivity for a specified water content or negative pore-water pressure, k_s is the measured saturated conductivity, k_{sc} is the

calculated saturated conductivity, i is the last water content class on the wet end, h_i is the negative pore-water pressure head for a given class of water filled pores, n is the total number of pore classes between the residual water content and the saturated water content, M is the pore class corresponding to the saturated water content, θ is the volumetric water content, T is the surface tension of water, ξ is the water-saturated porosity, η is the viscosity of water, g is the gravitational constant, μ is the density of water and p is a parameter that accounts for the interaction of pore classes (in our simulations, $p = 2$).

Elzefrawy and Cartwright (1981) have compared the experimental results obtained for different types of soils and those obtained from the Green and Corey relationship and concluded that the relationship is sufficiently accurate for most field applications. Yanful and Aubé (1993) also used the Green and Corey equation in their simulations and concluded that the method is applicable to predict the hydraulic conductivity of unsaturated media in most conditions. However, they also noted that the model seems inadequate for a sand at water contents close to the residual water content.

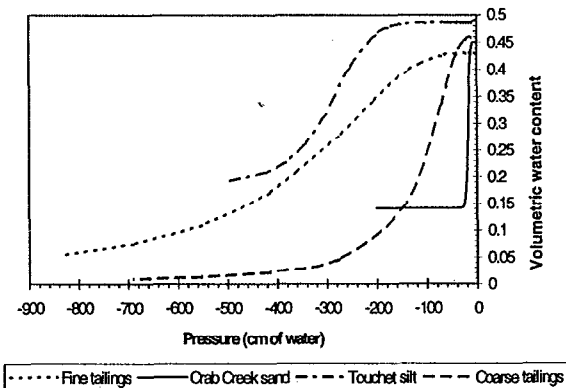


Figure 2. Soil-water characteristic curves for the selected materials

The Mualem equation, on the other hand, has become the most commonly used equation for predicting the permeability function using the soil-water characteristic curve (e.g. Wise et al., 1994; Yeh et al., 1994; Chiu and Shakelford, 1994; Marion et al., 1994; Akindunni et al.,

1991; Mishra and Parker, 1990). The software used in this study to evaluate the ψ -k relationship with the Mualem equation is the RETC program written by van Genuchten et al. (1991). Based on the Mualem equation, the relation between water content and hydraulic conductivity is given by (van Genuchten, 1980):

$$k(\theta) = k_s \left\{ 1 - \left[1 - \theta_e \left(\frac{V}{V_m} \right)^m \right]^2 \right\} \theta_e^\lambda \quad (7)$$

where k_s is the saturated hydraulic conductivity and θ_e is the volumetric water content in its normalized form. The parameters needed by the software are: data from a suction test (ψ - θ), the residual water content θ_r , the saturated water content $\theta_s (= n)$, the saturated hydraulic conductivity k_s and the curve fitting parameters (α and n , evaluated with $\lambda = 1/2$ and $m = 2/3$ as proposed by van Genuchten et al., 1991). With these values, the software fits a curve where the error between the experimental values and fitted values is minimized. It is this fitted curve, in the form θ vs ψ , that is inserted in the SEEP/W for the simulations.

Figure 3 shows the permeability functions of the different materials used in this study. The curves obtained by the RETC program are identified with the letters V-G while the Green and Corey curves are identified with the letters G-C. It can be seen that the Green and Corey equation gives, for Touchet silt, a greater value of k than the Mualem equation, especially at low pressure. For the Crab Creek sand, a relatively large difference exists between the two equations at the residual water content (k_r). For the Green and Corey equation, k_r is approximately 1×10^{-6} cm/s. instead of 6×10^{-9} cm/s with the Mualem equation. Finally, it is important to note that, for the two tailings studied, only the Mualem equation is used in the following to evaluate the permeability function.

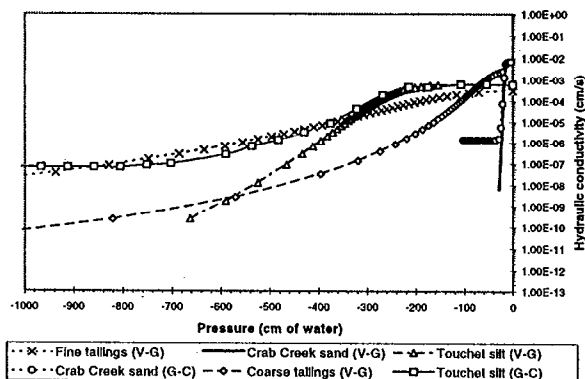


Figure 3. Permeability function curves for the selected materials

Modeling of bi-layered covers

Numerical simulation 1, The first simulation is similar to the one performed by Akindunni et al. (1991), which is 2,5 m of sand (Crab Creek sand) overlain by 1 m of silt (Touchet silt), with the use of the van Genuchten and Mualem models for the determination of the θ -k and ψ -k relationships. One of the objectives of this simulation is to validate the calculations. The system is initially saturated, and then allowed to drain.

One can see in Figure 4 that the degree of saturation goes down rapidly in the sand layer and reaches an equilibrium around the 14th day at 35% of saturation. During that time, the silt layer remains fully saturated over its entire thickness, for the total duration of the simulation. Figure 5 shows that a pressure equilibrium is reached after 14 days. It is also important to note that this equilibrium is not the hydraulic equilibrium (or static equilibrium) which would show a constant slope. The results obtained in this first simulation are very similar to those presented by Akindunni et al. (1991).

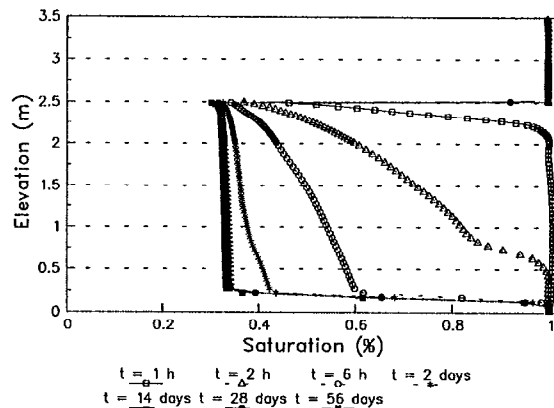


Figure 4. Variation in saturation with elevation at selected times for Numerical simulation 1

Numerical simulation 2, The second simulation evaluates the effect of using the Green and Corey model for the sand and silt instead of the Mualem model. In this simulation, the residual water content (θ_r) of the two soils was not fixed at a unique value (see Table 1). Rather, it is considered that the water content decreases progressively toward zero at a value of ψ of about 10^6 kPa as proposed by Fredlund and Xing (1994). Other parameters of this numerical simulation are identical to those used in the first simulation.

Figure 6 shows that the saturation profile is different of the one obtained for the Numerical simulation 1. The degree of saturation in the coarse layer goes down below the equilibrium value observed in Figure 4, which was about 35%. After 56 days, Figure 6 shows

that the top of the coarse layer is at a degree of saturation of approximately 17%. This is due to the fact that the residual water content is continues to decrease and, consequently, the shape of the soil-water characteristic and the permeability function are different at high pressure. Also, the degree of saturation of the fine layer decreases at the top of the layer to about 96%. The pressure applied at the top of this layer is - 20 kPa compared to - 14 kPa for Numerical simulation 1.

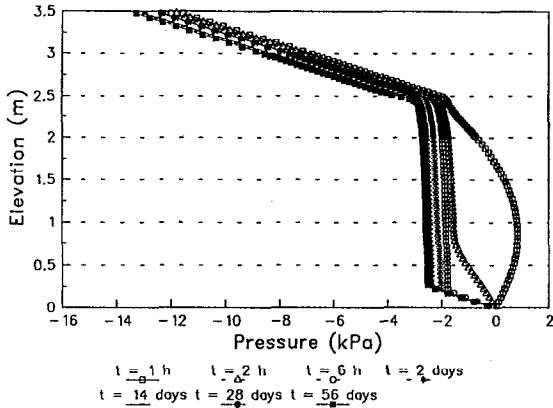


Figure 5. Variation in pressure with elevation at selected times for Numerical simulation 1

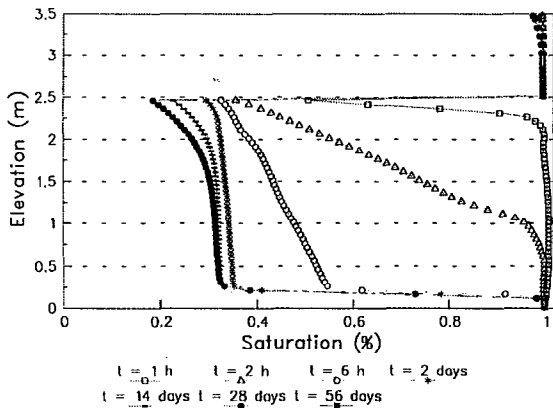


Figure 6. Variation in saturation with elevation at selected times for Numerical simulation 2

Numerical simulation 3, The objective of the third simulation is to evaluate the impact of reducing the thickness of the sand layer (to 1 m) on the global behavior of the cover. The permeability function used in this simulation is the one calculated with the Mualem function. The thickness of the fine layer is still the same, that is 1 m.

As it is the case with the results of Numerical simulation 1, the sand layer drains rapidly and reaches an equilibrium by the 14th day (at 35% of saturation) and the silt remains fully saturated over it's entire thickness for the total duration of the simulation (see Figure 7). In terms of pressure (not shown), the profile and the

values in the fine layer are similar to the ones obtained in Numerical simulation 1.

From this simulation, it can be said that the thickness of the sand layer can be reduced to 1 m without reducing the degree of saturation of the fine layer.

Numerical simulation 4, As shown in the previous simulation, the thickness of the coarse layer can be reduced to 1 m without affecting the behavior of the capillary barrier (in terms of water content in the fine layer). In Numerical simulation 4, the thickness is further reduced to 0,3 m; a value which is not much larger than the AEV of the sand. Others parameters are similar to the Numerical simulation 3.

The Figure 8 shows that the capillary break is still present, but that it could not be developed if the thickness was reduced below about 20 to 30 cm. The equilibrium is reached rapidly in the coarse layer (after 2 days). The fine layer remains fully saturated for the total duration of the simulation.

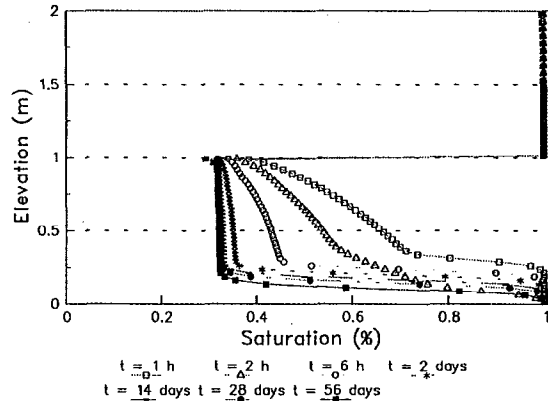


Figure 7. Variation in saturation with elevation at selected times for Numerical simulation 3

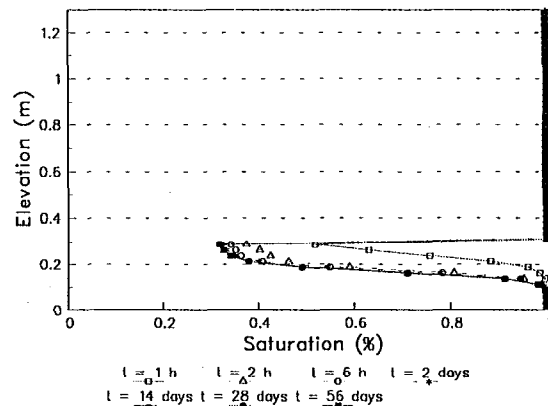


Figure 8. Variation in saturation with elevation at selected times for Numerical simulation 4

Numerical simulation 5. For all the numerical simulations presented above, free drainage was allowed at the bottom of the column by considering that the water table was located at elevation zero. In this next numerical simulation, a negative pressure is applied at the bottom of the column in order to evaluate the impact of placing the phreatic line 2 m below the bottom of the column. Other parameters are identical to those used in Numerical simulation 4.

The main difference between this simulation and the Numerical simulation 4 is that the degree of saturation of the coarse layer quickly reaches a constant value (approximately 35%) for the entire thickness. For the Numerical simulation 4, the bottom of the coarse layer has a degree of saturation of about 100%. Figure 9 also shows that, even if the phreatic line is located 2 m below the bottom of the column, the fine layer stays fully saturated. Again, the coarse sand layer act as a capillary barrier.

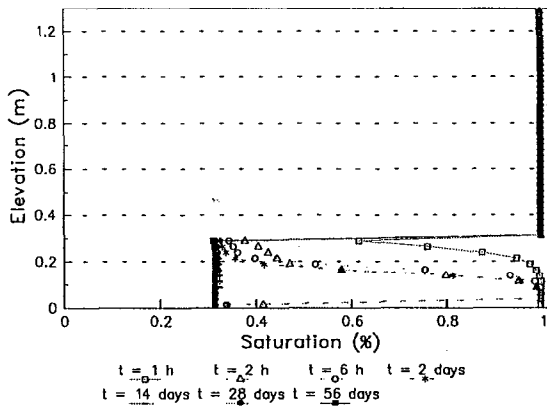


Figure 9. Variation in saturation with elevation at selected times for Numerical simulation 5

Modeling of three-layered covers

Numerical simulation 6. The main objective of this simulation is to evaluate the behavior of a cover made of three layers. The coarse layer at the bottom is made of 1 m of coarse tailings. The fine layer is 0,6 m thick, and is made of fine tailings. Finally, the coarse layer on top is made with the same material as the bottom layer, with a thickness of 0,4 m. The ψ -k relationship and ψ - θ relationship of these two materials are presented in Figures 2 and 3. Once again, the ψ -k relationships were evaluated with the Mualem equation.

One can see in Figure 10 that the degree of saturation of the three layers reaches an equilibrium by the 14th day. For the coarse layer on top, the final degree of saturation reaches about 20%; for the fine layer, it

remains around 90%; it is about 55% for the coarse layer of the bottom. To inhibit the oxygen diffusion, the degree of saturation should remain greater than about 90% (Aubertin et al., 1993), so the objective is attained (but the margin of safety is small).

The pressure profile of the layered cover is presented in Figure 11. It can be observed that an equilibrium is reached by 14th day and that it is close to the static equilibrium.

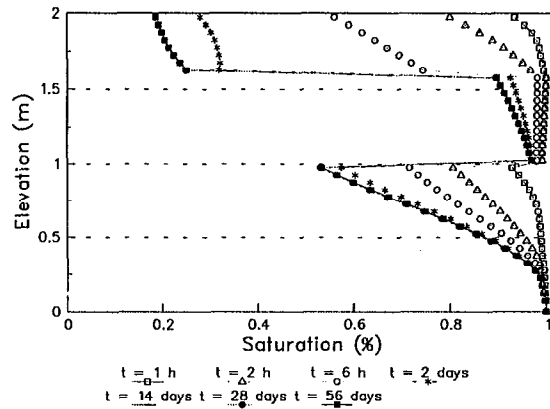


Figure 10. Variation in saturation with elevation at selected times for Numerical simulation 6

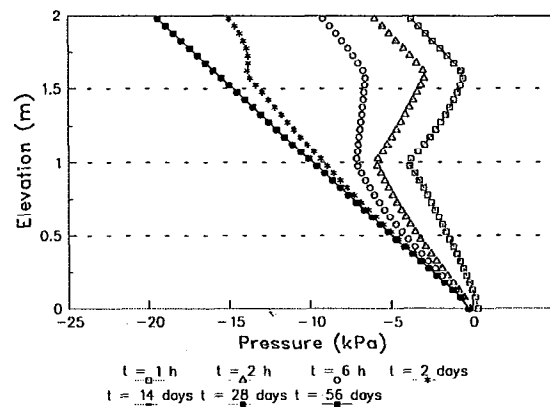


Figure 11. Variation in pressure with elevation at selected times for Numerical simulation 6

Numerical simulation 7. In order to improve the efficiency of the barrier system shown in Figure 11, the contrast in capillary properties between the fine and the coarse material layers is increased in the Numerical simulation 7. To do so, the authors have used Crab Creek sand instead of coarse tailings as the constituent of the coarse layers. As in Numerical simulation 6, the fine layer is fine tailings and the equation used to evaluate the permeability function is the Mualem equation.

One can see in Figure 12 that the end degree of saturation of the two coarse layers drops to approximately 35%, which represents the residual value, and the degree of saturation of the fine layer is over 95%. It seems evident that the increase of suction contrast has improved the effectiveness of the capillary barrier. This confirms the findings of Morel-Scytoux (1992).

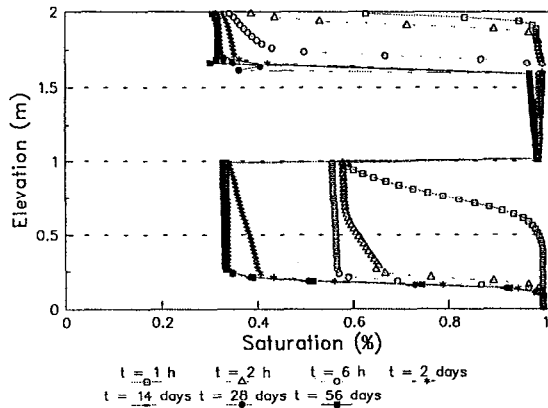


Figure 12. Variation in saturation with elevation at selected times for Numerical simulation 7

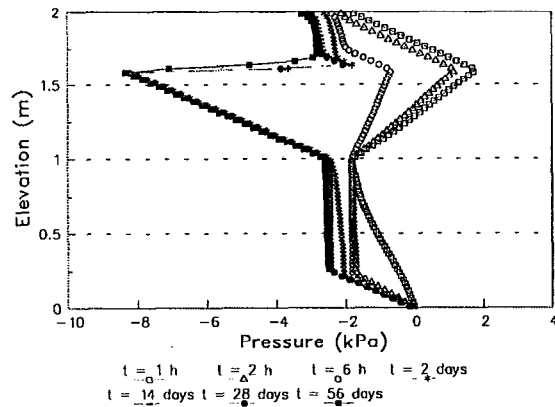


Figure 13. Variation in pressure with elevation at selected times for Numerical simulation 7

On the other hand, Figure 13 shows that the pressure in the fine layer is less in this simulation than in the Numerical simulation 6. This shows that the capillary break is more effective in this case.

CONCLUSION

The following conclusions can be deduced from the numerical simulations:

1. The model used for the determination of the permeability function from the soil-water characteristic curve can have a large influence on the results obtained from the numerical simulation.

In that regards, the value of the permeability function at high negative pressure has to be further investigated.

2. The thickness of the bottom coarse layer is an important parameter for the design of capillary barriers. The optimization of the thickness of this layer is highly dependent on the soil-water characteristic and the permeability function.
3. The suction contrast between the coarse layer and the fine layer is another important parameter for the efficiency of a capillary barrier.
4. The phreatic line position is not a critical parameter on the behavior of covers (in terms of water content in the fine layer) if the capillary break is well developed.

For a better understanding of the behavior of covers, numerical modeling can be used as a predictive tool. Nevertheless, some more work has to be done to better evaluate the practical significance of these results. Comparison between measured and predicted values in column tests (currently underway) is something that has to be investigated. The influence of slope (2 D and 3 D) and of *in situ* conditions will be also looked at in the near future.

REFERENCES

- AKINDUNNI, F.F., GILLHAM, R.W. and NICHOLSON, R.V. 1991. Numerical simulations to investigate moisture-retention characteristics in the design of oxygen-limiting covers for reactive mine tailings. *Canadian Geotechnical Journal*, 28 :446-451.
- AUBERTIN, M., CHAPUIS, R.P., BUSSIÈRE, B. and AACHIB, M. 1993. Propriétés des résidus miniers utilisés comme matériau de recouvrement pour limiter le drainage minier acide (DMA). *Geoconfine 93*, Arnould, Barrès and Côme (eds), Balkema, 299-308.
- AUBERTIN, M., RICARD, J.F. and CHAPUIS, R.P. 1995a. A study of capillary properties of mine tailings: measurements and modeling. *Proceedings of the 48th Canadian Geotechnical Conference*, Vancouver (to be published).

- AUBERTIN, M., CHAPUIS, R.P., AACHIB, M., BUSSIÈRE, B., RICARD, J.F. and TREMBLAY, L. 1995b.
Évaluation en laboratoire de barrières sèches construites à partir de résidus miniers. Final Report (Draft version), Prepared for CANMET, Report C.D.T. P1622, École Polytechnique de Montréal, 202 p.
- BARBOUR, S.L. and YANFUL, E.K. 1994.
A column study of static nonequilibrium fluid pressures in sand during prolonged drainage. Canadian Geotechnical Journal, 31 :299-303.
- BATHE, K-J. 1982.
Finite Element Procedures in Engineering Analysis. Prentice-Hall, 282 p.
- BROOKS, R.H. and COREY, J.C., 1964.
Hydraulic properties of porous medium. Colorado State University (Fort Collins), Hydrology Paper 3.
- BUSSIÈRE, B., LELIÈVRE, J., OUELLET, J. and BOIS, D. 1994.
Valorisation des résidus miniers : une approche intégrée. Rapport final soumis au Ministère des Ressources naturelles dans le cadre du volet Mines écologiques de l'Entente Auxiliaire du Développement Minéral, 194 p.
- CHIU, T-F. and SHACKELFORD, C.D.. 1994.
Practical aspects of the capillary barrier effect for landfills. Presented at the 17th International Madison Waste Conference, Septembre 21-22, 1994, 357-375.
- ELZEFATAWY, A. and CARTWRIGHT, K. 1981.
Evaluating the saturated and unsaturated hydraulic conductivity of soils. Permeability and Groundwater Contaminant Transport, ASTM STP, T.F. Zimmie and C.D. Riggs (eds), 168-181.
- FREDLUND, D.G. and XING, A. 1994.
Equations for the soil-water characteristic curve. Canadian Geotechnical Journal, 31: 521-532.
- FREDLUND, D.G. and RAHARDJO, H. 1993.
Soil Mechanics for Unsaturated Soils. John Wiley & Sons, inc., New York, 517 p.
- GEOSLOPE International, 1994.
SEEP/W User's Guide, Version 3.
- GREEN, R.E. and COREY, J.C. 1971.
Calculation of hydraulic conductivity : A further evaluation of some predictive methods. Soil Science Society of America Proceedings, 35: 3-8.
- HILLEL, D. 1980.
Fundamentals of Soil Physics, Academic Press, 413p.
- HUYAKORN, P.S. and PINDER, G.F. 1983.
Computational Methods in Subsurface Flow. Academic Press inc., San Diego, USA, 473 p.
- KOVÁCS, G. 1981
Seepage Hydraulics, Elsevier Scientific Pub.
- MARION, J.M., OR, D. ROLSTON, D.E., KAVVAS, M.L. and BIGGAR, J.W. 1994.
Evaluation of methods for determining soil-water retentivity and unsaturated hydraulic conductivity. Soil Science, Vol 158, 1: 1-13.
- MISHRA, S. and PARKER, J.C. 1990.
On the relation between saturated conductivity and capillary retention characteristics. Ground Water, Vol. 28, 5: 775-777.
- MOREL-SEYTOUX, H.J. 1992.
The capillary barrier effect at the interface of two soil layers with some contrast in properties. HYDROWAR Report 92.4, Hydrology Days Publications, 57 Shelby Lane, Atherton, CA 94027-3926, 109 p.
- MUALEM, Y. 1976.
A new model for predicting the hydraulic conductivity of unsaturated porous media. Water Resources Research, 12 : 513-522.
- MUALEM, Y. 1986.
Hydraulic conductivity of unsaturated soils : Prediction and formulas. In A. Klute (ed.). Methods of Soil Analysis. Part 1. Physical and Mineralogical Methods. Agron. Monogr. 9 (2nd ed.). American Society of Agronomy, Madison, Wisconsin, 799-823.

- SHACKELFORD, C.D., CHANG, C.K. and CHIU, T.F. 1994.
The capillary barrier effect in unsaturated flow through soil barriers. Proceedings of the First International Congress on Environmental Geotechnics, Edmonton, ISSMFE/CGS, 789-793.
- SHOUSE, P.J., RUSSELL, W.B., BURDEN, D.S., SELIM, H.M., SISSON, J.B. and van GENUCHTEN, M.Th. 1995.
Spatial variability of soil water retention functions in a silt loam soil. Soil Science, Vol. 159,1: 1-12
- SRK (Steffen, Robertson and Kirsten). 1989.
Draft Acid Rock Technical Guide. BC AMD Task Force, Vol. 1.
- van GENUCHTEN, M.Th., LEIJ, F.J. and YATES, S.R. 1991.
The RETC code for quantifying the hydraulic functions of unsaturated soils. Environmental Protection Agency, EPA/600/2-91/065.
- van GENUCHTEN, M.Th and NIELSEN, D.R. 1985
On Describing and predicting the hydraulic properties of unsaturated soils. Annales Geophysicae, 3: 615-628.
- van GENUCHTEN, M.Th. 1980.
A closed-form equation for predicting the hydraulic conductivity of unsaturated soils. Soil Science Society of America Journal, 44: 892-898.
- YANFUL, E.K. and AUBÉ, B. 1993.
Modelling moisture-retaining soil covers. Proceedings of the Joint CSCE-ASCE National Conference on Environmental Engineering, Montreal, Vol. 1, 373-380.
- YEH, T.-C. J, GUZMAN, A., SRIVASTAVA, R. and GAGNARD, P.E. 1994.
Numerical simulation of the wicking effect in liner systems. Ground Water, Vol. 32, 1: 2-11.
- WISE, W.R., CLEMENT, T.P. and MOLZ, F.J. 1994.
Variably saturated modeling of transient drainage : sensitivity to soil properties. Journal of Hydrology, 161 : 91-108.
- ZIENKIEWICZ, O.C. 1977. The Finite Element Method. McGraw-Hill Book Company (UK) Ltd, Maidenhead, England, 787 p.

PROCEEDINGS OF THE THIRD CANADIAN CONFERENCE ON COMPUTER
APPLICATIONS IN THE MINERAL INDUSTRY /MONTREAL /QUEBEC /22-25
OCTOBER 1995

COMPTES RENDUS DU TROISIÈME CONGRÈS CANADIEN SUR L'UTILISA-
TION DE L'INFORMATIQUE DANS L'INDUSTRIE MINIÈRE /MONTRÉAL /
QUÉBEC /22-25 OCTOBRE 1995



Computer Applications in the Mineral Industry

Utilisation de l'informatique dans l'industrie minière

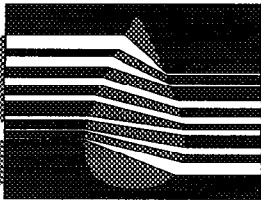
Edited by / Édité par

HANI SABRI MITRI

*Department of Mining and Metallurgical Engineering
McGill University, Montreal, Quebec, Canada*



*Le sans
sans frontières*



ICARD SHORT COURSE:

CONSTRUCTION AND PERFORMANCE MONITORING OF COVERS

Dr. Ernest Yanful, Professor

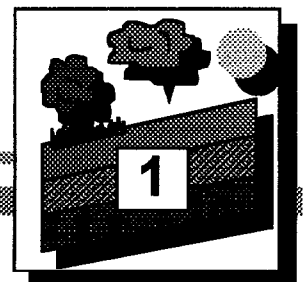
The University of Western Ontario

Tel. 519-661-4069

Fax 519-661-3942

E-mail: Eyanful@eng-ntadmin.engga.uwo.ca

Vancouver - June 1, 1997





Short-Course Content:

IV- CONSTRUCTION AND PERFORMANCE MONITORING OF COVERS

A- Introduction

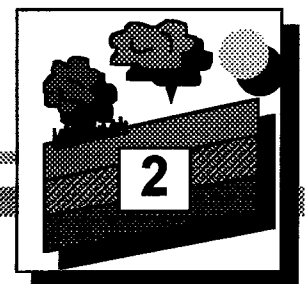
B- Placement Requirements

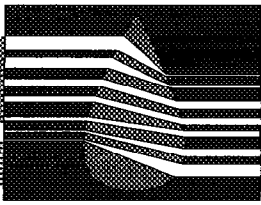
C- Definition of Problem Scale

D- Material Selection and Inventory

1- Freeze-Thaw Evaluation

2- Volumetric Calculations





Short-Course Content:

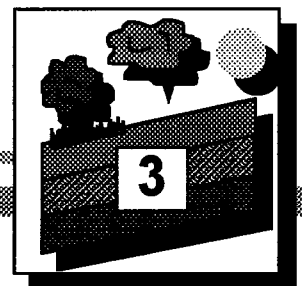
IV- CONSTRUCTION AND PERFORMANCE MONITORING OF COVERS

(continued)

E- Cover Placement

- 1- Construction Specifications**
- 2- Supervision and Communication**
- 3- Construction Scheduling**
- 4- Quality Control and Quality Assurance**

F- Performance Monitoring

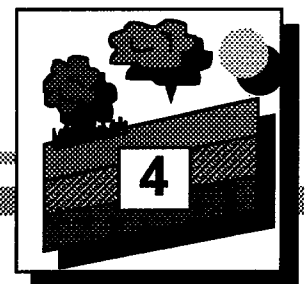




A- INTRODUCTION

■ Functions of an Effective Barrier

- Reduce Water Percolation
- Reduce Oxygen Flux → Acid Flux
- Control wind erosion (at tailings surface)
- Provide aesthetics through vegetation
-

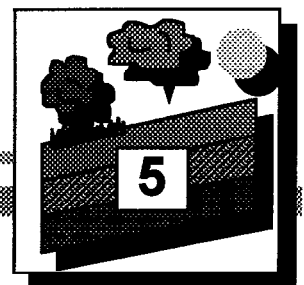




A- INTRODUCTION (con't)

■ Design Basis and Optimization

-
- Establish design criteria and expected performance (performance is related to cost).
 - rates of percolation and acid flux reduction
- Perform sensitivity analysis to determine optimal layer thickness
- the need to couple the environmental conditions to the physical behaviour of the cover
-

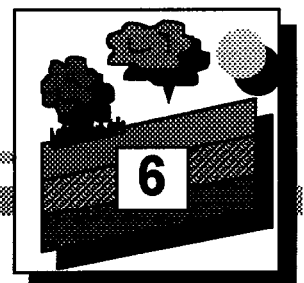




B- PLACEMENT REQUIREMENTS

■ Design Properties

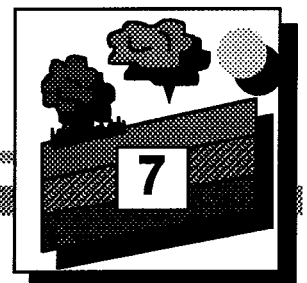
- Soil water characteristic curve (SWCC)
 - suction-water content relation →
suction-hydraulic conductivity relation.
- Saturated hydraulic conductivity, K_{sat}
 - generally higher in field than in laboratory because of presence of macro-fissures.
- Oxygen diffusion coefficient, D_e
 - controls oxygen flux and ultimately acid flux.
 - establish D_e -saturation relation, if possible.





B- PLACEMENT REQUIREMENTS (con't)

- Moisture Density Control
 -
 - Critical as it determines the performance of cover.
 -
 - Need to establish placement criteria and use proper equipment and method to achieve them.





C- DEFINITION OF PROBLEM SCALE

■ Area of waste to be covered  \$\$\$

- must be precisely known.

■ Technical feasibility

■ State of oxidation of waste

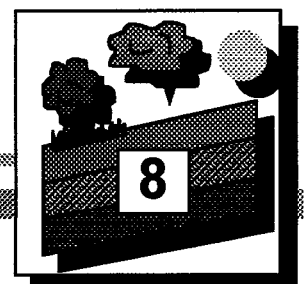
- environmental compliance monitoring

■ Hydrology and hydrogeology

- different climates and state of waste require different strategies (Indonesia, Canada, Australia)

Key Question: Is soil cover the best solution?

-
-

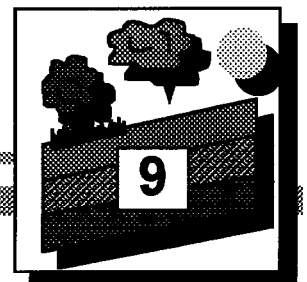




D- MATERIAL SELECTION AND INVENTORY

■ Material Availability and Handling

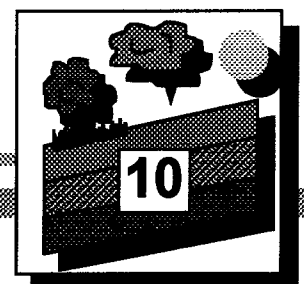
- material types and
availability → role of layers
 - hauling distances
 - selection criteria
 -





D- MATERIAL SELECTION AND INVENTORY (con't)

- Material types and availability
 - “back of the envelope”
calculations





D- MATERIAL SELECTION AND INVENTORY (con't)

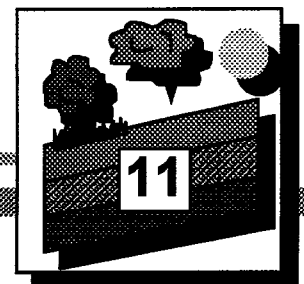
■ Laboratory and Field Testing

● Basic geotechnical testing

- hydraulic conductivity, grain size, Atterberg limits (plasticity can affect cracking resulting from freeze-thaw), compaction curve (standard Proctor is adequate), compressibility (consolidation?)
- Measurement of moisture retention → SWCC
- test as-placed material; clay OK but must exercise care with sand.

- -
 -
 -
 -
 -
 -
 -
 -

■



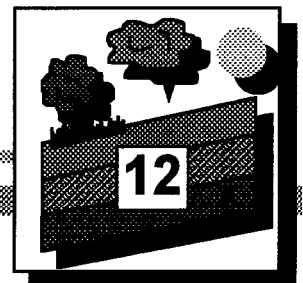


D- MATERIAL SELECTION AND INVENTORY (con't)

■ Laboratory and Field Testing

● Oxygen Diffusion

- Rate of oxidation \propto gaseous oxygen flux
- Rate of oxidation depends on rate constant, and
-
- diffusion coefficient
-
-





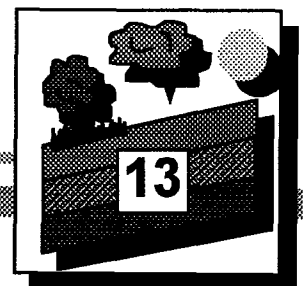
D- MATERIAL SELECTION AND INVENTORY (con't)

■ Freeze-Thaw: should be evaluated as follows:



- K_{sat}

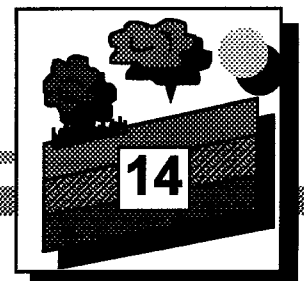
- (we are hoping to place compacted infiltration barrier as close to saturation as possible).
- reported increases in K_{sat} following freeze-thaw: 1-2 orders of magnitude on clays.





D- 1. Freeze-Thaw Evaluation

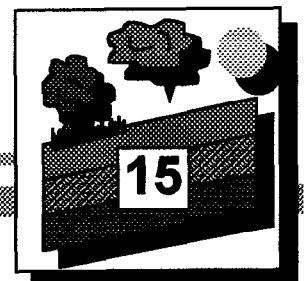
- SWCC → slope of curve can change for clays, tills and silts.
- D_e
-
- -
 -
 -
 - Will D_e and θ increase by 1-2 orders after freeze-thaw, just like K_{sat} ? If so, acid will probably also increase by 100 times.





D- 2. Volumetric Calculations

- Calculate volume of materials
 - take into account reductions due to compaction
 -
 - Experience/rule of thumb: volume of loose material required = twice final compacted volume for clays.
 -
 - Sandy materials (typically non oxygen barriers): compaction not critical.





E- COVER PLACEMENT

■ Criteria for Acceptable Performance

- What degree of saturation is acceptable?

- Placement affects cost

- labour and equipment costs

- Waite Amulet: 91%

- Equity Silver: 85% compacted layer

-

- Compaction: Is 2% wet of optimum achievable?

-

-

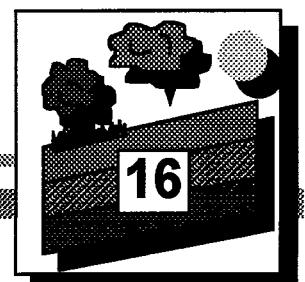
-

- What degree of saturation is acceptable?

Compaction: is 2% wet of optimum achievable

-

-





E- COVER PLACEMENT

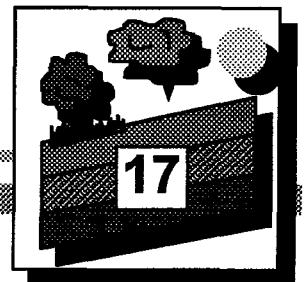
(con't)

■ Mechanical Compaction

- moisture-density relations for hydraulic and oxygen barriers
 - selection of suitable equipment (kneading compaction for clays; roller or vibratory compactor or even bulldozer adequate for sands)
 - technical aspects: control K and D_e
VERY IMPORTANT !

moisture content → saturation → diffusion → acid load

- economic aspects: is it affordable? Can we do it ourselves using a bulldozer/equipment on site?



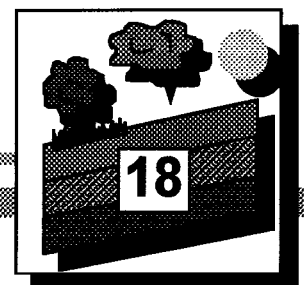


E- COVER PLACEMENT (con't)

■ Trial Compaction & Test Pad Design

- Ensuring good compaction is critical but can add to the cost.
 - Heath Steele site: pumping during compaction erosion on slopes; rest of cover acceptable because strength is not critical.
- Implementing a suitable test pad makes life easier and controls cost down the stretch →

of passes of compactor required for design moisture and density → use this in full scale installation.

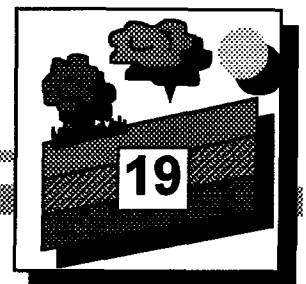




E- 1. Construction Specifications

- Instructions for construction should be clearly written out.
 - Specify grades, surface preparation work, number of passes, number of lifts, moisture control, density measurements etc.

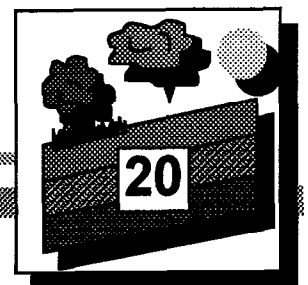
 - Specify various layers and thickness..





E- 2. Supervision and Communication

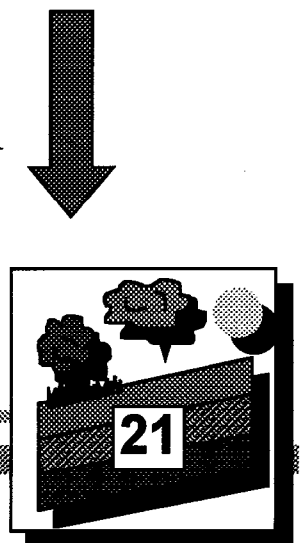
- Important to have a technical person on site to inspect all work according to the design, even if you are placing the cover yourself.
-
- Effective communication between engineer (on behalf of the client), contractor and other crew members is essential.
-





E-3. Construction Scheduling

- Schedule construction properly, taking into account
 - the weather (cost of compaction increased at Waite Amulet because of rainfall)
 - volume of material required and the need for stockpiling
 - equipment mobilization
 - the need to keep costs down

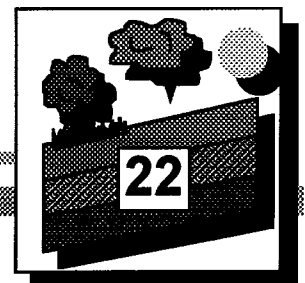




E- 4. Quality Control and Quality Assurance

■ Testing during placement

- perform moisture density test at a few locations on EACH LIFT → ensure good interlift bonding.
- check moisture-density relations carefully, as compaction-induced fractures can lead to increases in K
- need to measure density of compacted material and compare to Proctor curve → specified % compaction
- take a few samples for water content testing, using ASTM microwave method → yield results within a few hours.

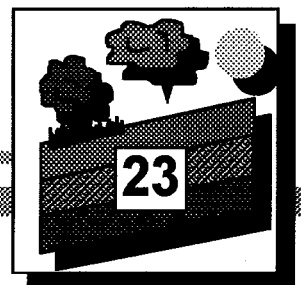




E- 4. Quality Control and Quality Assurance (con't)

■ Inspection of grades

- survey finished grades and slopes and ensure they conform to specified thickness.
-
- it may be necessary to compact again; this could add to the cost.

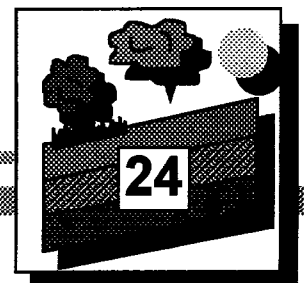




F- PERFORMANCE MONITORING

■ What will monitor and how?

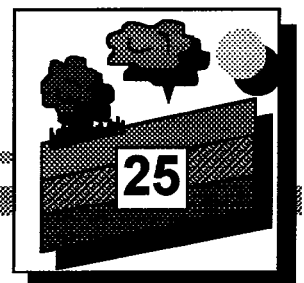
- answer depends on the type and scale of project → test plots and full scale or final covers have different requirements.
- will generally involve water percolation, involve oxygen, temperature, and water quality measurements
 - water quality for oxidized waste is not a very good indicator of cover effectiveness in the short term; better to use oxygen and temperature in the case of waste rock





F- PERFORMANCE MONITORING (con't)

- water quality of covered oxidized waste → oxidation products will take several months to flush out and may erroneously suggest cover is not effective
-
- Water percolation
 - very important; flow rate in ditch
 - may require a lysimeter and probably not feasible for a full scale final cover.



OXYGEN DIFFUSION THROUGH SOIL COVERS ON SULPHIDIC MINE TAILINGS

By Ernest K. Yanful,¹ Associate Member, ASCE

ABSTRACT: Engineered soil covers are being evaluated under Canada's Mine Environment Neutral Drainage (MEND) program for their effectiveness in preventing and controlling acid generation in sulphidic mill tailings. A critical parameter for predicting the performance of these covers is the diffusion coefficient of gaseous oxygen in the cover materials. Laboratory experiments conducted to determine the effective diffusion coefficient of a candidate cover material, a glacial till from an active mine site, are described. The diffusion coefficient is determined by fitting a semianalytic solution of the one-dimensional, transient diffusion equation to experimental gaseous oxygen concentration versus time graphs. Effective diffusion coefficients determined at high water saturations (85%–95%) were of the order of 8×10^{-8} m²/s. The diffusion coefficients decreased with increase in water saturation as a result of the low diffusivity of gaseous oxygen in water relative to that in air and the low solubility of oxygen in water. Placement of soil covers in high saturation conditions would ensure that the flux of oxygen into tailings underneath such covers is low, resulting in low acid flux. This is confirmed by combined laboratory, field, and modeling studies.

INTRODUCTION

The management of reactive sulphide tailings produced from milling of base metal ores is a major environmental challenge facing the mining industry. Sulphide minerals contained in these tailings oxidize upon contact with air and water, producing an acidic pore water with high concentrations of dissolved sulphate, iron, and heavy metals (Nordstrom 1982; Yanful and St-Arnaud 1992). In Canada, the problem has been estimated to involve some 12,000 ha of tailings and a rehabilitation cost of \$3 billion–\$5 billion over the next two decades (Wheeland and Feasby 1991). Current tailings management practices consist of water flooding to exclude gaseous oxygen, segregation, and blending of sulphidic and alkaline materials, and collection and treatment of acidic seepage from tailings impoundments by lime neutralization. Soil covers have not been extensively applied on tailings because of high cost and lack of reliable methods for predicting and evaluating their effectiveness. In recent years, however, there has been a resurgence of interest in developing reliable methods for designing and constructing effective soil covers in Canada, as part of the Mine Environment Neutral Drainage (MEND) program. The MEND program is a joint industry and government research consortium aimed at developing and applying technologies for decommissioning mine tailings and waste rock in a reliable, predictable, affordable, and environmentally acceptable manner. Detailed descriptions of the MEND program are presented elsewhere (Filion and Ferguson 1989; Wheeland and Feasby 1991).

The objective of this paper is to present laboratory and field measurements of gaseous oxygen diffusion into soil covers undertaken by Noranda

¹Sr. Sci., Mineral Sci. Lab., Noranda Tech. Ctr., 240 Hymus Blvd., Pointe-Claire, Quebec, H9R 1G5 Canada.

Note. Discussion open until January 1, 1994. To extend the closing date one month, a written request must be filed with the ASCE Manager of Journals. The manuscript for this paper was submitted for review and possible publication on April 23, 1992. This paper is part of the *Journal of Geotechnical Engineering*, Vol. 119, No. 8, August, 1993. ©ASCE, ISSN 0733-9410/93/0008-1207/\$1.00 + \$.15 per page. Paper No. 3784.

Technology Centre (NTC). Most of this work was conducted as part of MEND projects involving design, construction, and evaluation of soil covers on sulphidic tailings. The theory of oxygen diffusion through fine-grained geologic materials is briefly described in this paper. Laboratory column experiments conducted to provide a determination of oxygen diffusion coefficients at various degrees of water saturation are described and the resulting data discussed in detail. The paper also compares laboratory and field oxygen profiles observed in covered and uncovered tailings to demonstrate the fact that the flux of gaseous oxygen into a tailings deposit can be considerably reduced by the presence of an overlying, nearly fully saturated, soil cover.

THEORETICAL BACKGROUND

The transport of gaseous oxygen through fine-grained soil materials and mill tailings is mainly by molecular diffusion. The diffusive process occurs in response to concentration gradients usually established between the atmosphere and the pore spaces within the soil and tailings materials. The process may be assumed to be Fickian in behavior so that the flux can generally be written according to Fick's first law, as follows:

$$F(t) = -\theta_a D_e \frac{\delta C(t)}{\delta z} \dots \dots \dots (1)$$

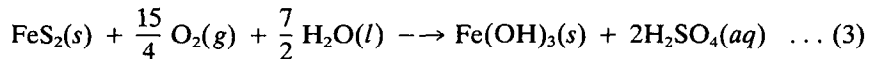
where $F(t)$ = mass flux ($ML^{-2}T^{-1}$); θ_a = air-filled porosity (L^3/L^3); D_e = effective diffusion coefficient (L^2T^{-1}); $C(t)$ = concentration at time t (ML^{-3}); and z = depth within the soil or tailings mass (L).

The air-filled porosity, θ_a , can be related to the degree of saturation, S_r , as follows:

$$\theta_a = \theta_t(1 - S_r) \dots \dots \dots (2)$$

where θ_t = the total porosity.

The mass flux is a measure of the amount of oxygen per unit area moving through the cover and into the uncovered tailings and is directly proportional to the theoretical maximum acid flux. This is the flux of acid that would be produced if all the oxygen entering the tailings is used up in sulphide mineral oxidation. The oxygen flux can be related to the theoretical maximum acid flux on the basis of the stoichiometry of the overall sulphide oxidation reaction:



This equation implies that 3.75 moles of gaseous oxygen (O_2) oxidizes 1 mole of pyrite (FeS_2) in the presence of water (H_2O) to produce 2 moles of sulphuric acid (H_2SO_4). The flux thus provides an indication of cover performance or effectiveness.

At any particular depth in the soil or tailings deposit, the rate of change in concentration can be determined from Fick's second law

$$\frac{\delta C}{\delta t} = D_e \frac{\delta^2 C}{\delta z^2} - KC \dots \dots \dots (4)$$

Eq. (4) is written in a general form to include a first-order reaction rate constant, K , assumed to describe oxygen consumption by sulphide oxidation

reactions occurring in the tailings. It is obvious that, in an unreactive soil cover, K is equal to zero.

MATERIALS AND METHODS

Soil Cover Materials and Tailings

Experiments were conducted at NTC to determine the diffusion coefficient of a natural till that was being considered as a candidate material for the design of a cover system for a waste rock pile at the Heath Steele Mines site, near Newcastle, New Brunswick, Canada. The Heath Steele till, sample HS-C, was a silty, sandy material collected from a trench excavated in the summer of 1989 in a deposit located in the vicinity of the mine. The sample contained a considerable amount of large stones that had to be removed by sieving prior to testing.

A second set of experiments was also conducted to evaluate the performance of a three-layer soil cover on tailings using laboratory columns. The soils used in the column evaluation consisted of a varved clay and sandy soils obtained from deposits located in the vicinity of the decommissioned Waite Amulet tailings impoundment near Rouyn-Noranda, Quebec. Varved clay, WA-C, used as part of a multilayered soil cover system, was sampled from the top 5 m of the Lake Ojibway clay plain. The geology, mineralogy, and geotechnical characteristics of the clay are described by Locat et al. (1984) and Quigley et al. (1985). The clay underneath the tailings impoundment is normally consolidated at depth but only slightly overconsolidated (with an overconsolidation ratio of 2.0) in the top 1 m (Yanful and St-Arnaud 1992). The upper zone has lower water contents and higher undrained shear strengths. The mineralogy of the clay consists of smectite, illite, chlorite, quartz, and feldspar. The soil cover also included sands S-1 and S-2, which were both obtained from borrow pits in the Rouyn-Noranda area. The clay and sands are similar to those used in the construction of field test plots at the Waite Amulet site (Yanful and St-Arnaud 1991). The sands were included in the cover system to provide a capillary barrier to the clay soil. The concept of the capillary barrier is described by Rasmuson and Eriksson (1986), Collin (1987), and Nicholson et al. (1989). The grain size distributions ("Standard" 1991a) of the soil materials are presented in Fig. 1.

The unoxidized tailings used in the laboratory tests were excavated from the deeper saturated zone of the Waite Amulet tailings impoundment. They are reactive and consist of pyrite, pyrrhotite, small amounts of chalcopyrite, sphalerite, and galena and gangue minerals (mostly silicates). A typical grain size distribution is also shown in Fig. 1.

Diffusion Cell Assembly and Measurements

The cell used for the determination of diffusion coefficient consisted of a clear polyvinyl chloride (PVC) tubing with an internal diameter of 10 cm and a height of 20 cm. Soil was thoroughly mixed with water to the desired water content and then compacted directly inside the column to the required density. Prior to placement of the soil, the interior wall of the cell was coated with vacuum grease to minimize side-wall leakage of oxygen. Rubber seals, also coated with vacuum grease, were placed between the ends of the cell and top and base plates. The plates were then clamped to the cell with threaded steel rods. Fig. 2 shows a schematic representation of the diffusion test arrangement.

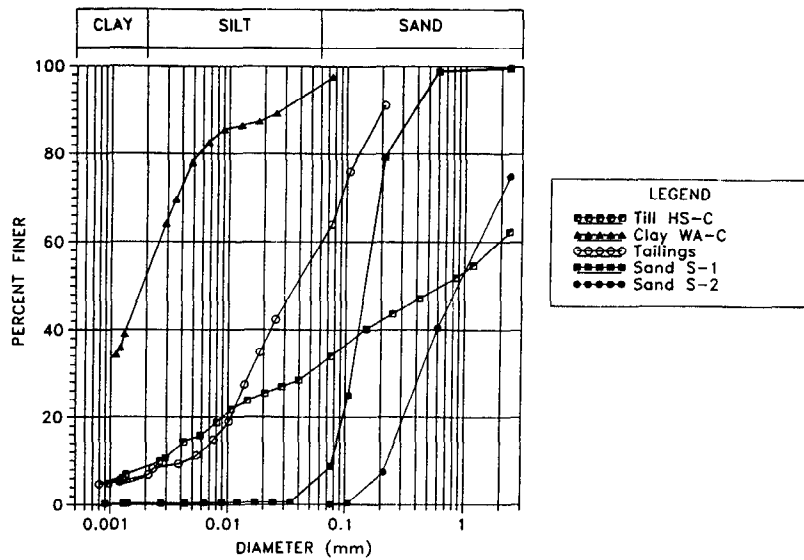


FIG. 1. Grain Size Distributions of Cover Materials and Mine Tailings (ASTM D 421 and 422)

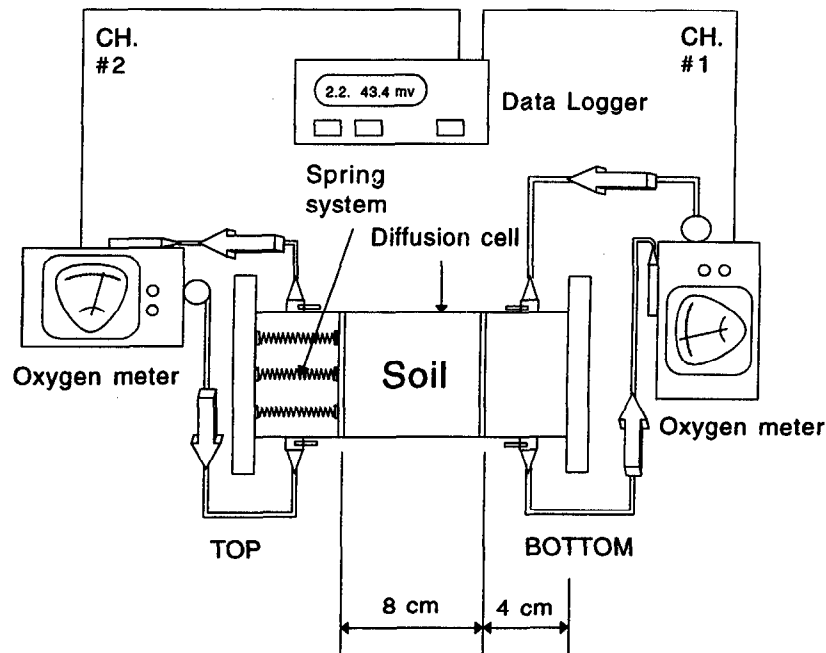


FIG. 2. Schematic Representation of Diffusion Test Arrangement

A finite mass of gaseous oxygen, initially equal to atmospheric value, was allowed to diffuse into the 10-cm long soil layer to determine diffusion coefficient (Fig. 2). Oxygen was supplied by humidified compressed air. The cell containing the packed soil was purged with humidified gaseous nitrogen prior to commencement of testing. The residual oxygen concentrations (after purging) at the top and base of the cell typically ranged from 0.2% to 0.5%. The source concentration (above the soil layer) was continuously monitored with a Teledyne Model 320P portable oxygen analyzer with a flow-through sensor. Gas leaving the column was drawn into the sensor by a built-in vacuum pump, which operated at a flow rate of 200 mL/min during the experiments. A similar analyzer was installed at the base to measure the base concentrations and to ensure that there was no pressure difference between the top and the base.

Several checks were conducted to confirm that the sensor itself did not consume a quantity of oxygen that could affect the changes in both source and base concentrations. This was accomplished by monitoring oxygen concentration above a solid polyethylene material finished to the same dimensions as the soil specimens. No measurable change in concentration was observed during a 72-hour period. At the end of each diffusion measurement, the soil was weighed again, sliced into two halves, and the gravimetric water content determined for each half. Generally, differences in the water contents between the top and bottom halves did not exceed 0.6%. The sample mass and water contents were used in the calculation of both the water-filled and gas-filled porosities of the soil.

The concentration-versus-time data were then simulated using the following boundary condition for the source:

$$C_T(z = 0, t) = C_0 - \frac{1}{H_g} \int_0^t F_T(z = 0, t) dt \dots\dots\dots (5)$$

where H_g = the height of gas space above the soil sample calculated as the volume of gas above the soil divided by the cross-sectional area of the soil, perpendicular to the direction of diffusion. The mass flux F_T can be further related to the concentration gradient across the top of the soil sample by Fick's law, as stated in (1).

Since the oxygen accumulating at the base was not flushed out during the test, the base concentration was simulated with a zero outflow velocity using the expression derived by Rowe and Booker (1990):

$$C(z = H_B, \tau) = \int_0^t \frac{f(z = H_B, C, \tau)}{n_b h_b} d\tau \dots\dots\dots (6)$$

where C = concentration of oxygen at the base of the soil (ML^{-3}); h_b = height of the space below the soil layer (L); n_b = porosity of the gas-filled space below the soil; τ = time variable (T); z = depth (L); and H_B = height of soil sample (L).

Laboratory Evaluation of Three-Layer Cover

Column experiments were conducted to provide a laboratory assessment of the effectiveness of the three-layer cover system. The experiments involved four Plexiglas square columns, each of which had an area of 28 cm² and a length of 105 cm. The top 15 cm of each column had a larger area (39 cm²) and was provided with holes along the perimeter. The columns were packed with tailings and soils as follows: (1) Two identical columns

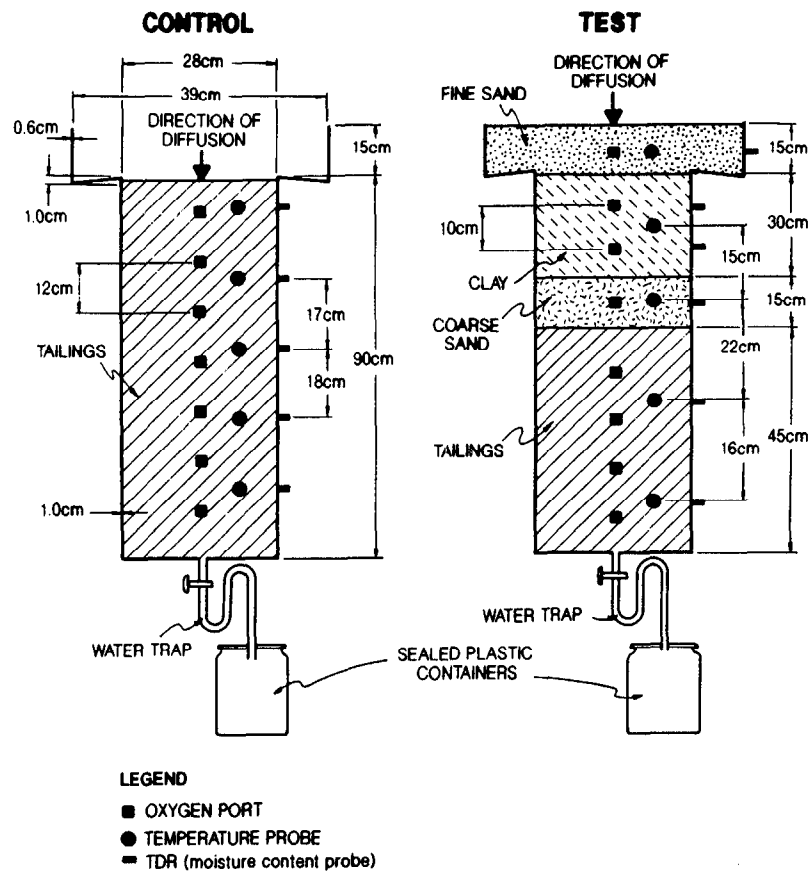


FIG. 3. Schematic Representation of Instrumented Laboratory Columns with Covered and Uncovered Mine Tailings

packed with 45 cm of unoxidized tailings overlain sequentially with 15 cm of coarse sand (S-2), 30 cm of compacted clay (WA-C), and 15 cm of fine sand (S-1); and (2) two other identical columns packed with 90 cm of unoxidized tailings. The upper sand filled the enlarged, top 15 cm of the column so that the fine sand/clay interface nearly coincided with the perimeter holes. A 4-mm thick woven geotextile underdrain was installed below the tailings in each column. Fig. 3 is a schematic representation of test and control installations.

The tailings and sands were packed to a bulk density of 1.90 Mg/m^3 . The fine and coarse sands were placed at residual saturation, which corresponded to volumetric water contents of 8% and 5%, respectively. The clay was compacted to a density of 1.53 Mg/m^3 and a water content of 25% (that is, 2% wet of the optimum water content). These compaction parameters corresponded to 93% of the modified Proctor compaction ("Standard" 1991b) and were the same as those specified for the field cover test plots.

Each column was instrumented to measure gaseous oxygen concentration in the pores and volumetric water content, θ_w . Sampling ports for oxygen,

equipped with rubber septa to provide automatic sealing after sampling, were installed at 10-cm spacings during packing of the columns. The ports were sampled and the samples analyzed with a percent oxygen analyzer (Teledyne Model 340 FBS), which required a sample volume of 2 mL and registered a stable reading within 20 s. After the reading, the sampled gas was released inside the port. The process was repeated twice and the average concentration recorded. The analyzer was calibrated in the atmosphere before sampling the next port. Water content was determined in place by time domain reflectometry (Topp et al. 1980).

Oxygen profiles obtained from the 28 cm^2 (Fig. 3) were simulated using

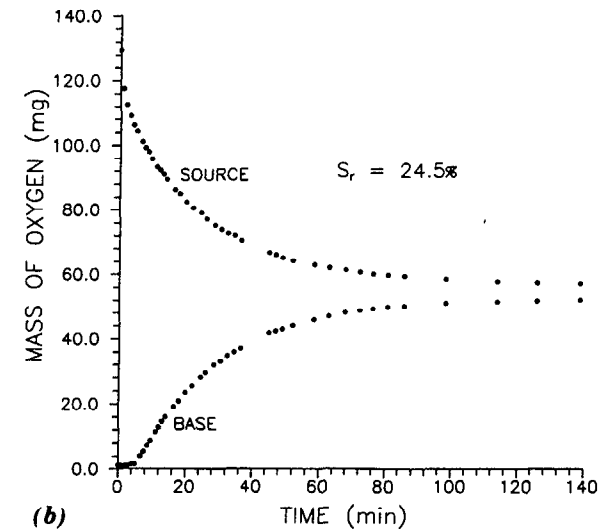
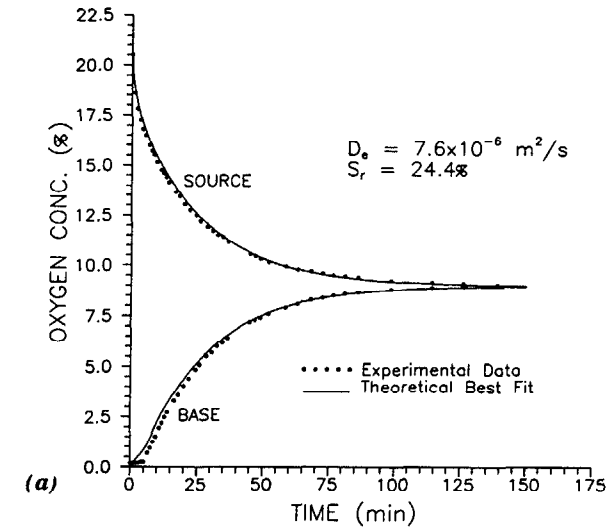


FIG. 4. Experimental and Predicted Oxygen Concentrations in Diffusion Cell Versus Time (Till HS-C, Water Saturation = 24.4%)

diffusion coefficients determined with the diffusion cell described previously. Oxygen fluxes estimated from the test columns (tailings with cover) and control columns (tailings without cover) were compared. The simulation assumed a constant source concentration of oxygen at the top of the column (open to the atmosphere) and a zero flux boundary at the base of the column, which are expressed as follows:

$$C(z = 0, t \geq 0) = C_0 \dots\dots\dots (7)$$

$$\frac{\delta C(z = H_B, t \geq 0)}{\delta z} = 0 \dots\dots\dots (8)$$

where C_0 = the source concentration, and H_B = the total length of soil layers. For the multilayered system, the solution also used continuity of flux at the interface of any two layers.

Semianalytic solutions to (1) and (4) incorporating the boundary conditions expressed in (5)–(8) are implemented in the computer program, POLLUTE, developed by Rowe and Booker (1990). This program was used for all simulations described in this paper.

RESULTS

Diffusion Tests

Gaseous oxygen concentrations and effective diffusion coefficients obtained in the laboratory experiments are presented in Figs. 4 to 11. Fig. 4(a) shows typical oxygen concentrations observed at the source and base of the diffusion cell. The data indicate a decrease in the source concentration as oxygen diffused through the soil and accumulated at the base. The experiment was run until steady-state conditions were attained, at which point the oxygen concentration was equal at all depths in the soil so that there was no concentration gradient for further diffusion. Thus, the source and base concentrations equalized at equilibrium, as shown in Fig. 4(a). The same data have been replotted as mass versus time in Fig. 4(b). The gap between the two profiles at equilibrium reflects the difference in the volumes of the gas space at the top and base of the cell. From a knowledge of the gas-filled porosity, mass balance calculations were performed to determine whether the till consumed or sorbed any gaseous oxygen. The following is a summary of typical calculations that indicate in this particular test about 5% of the initial mass of oxygen used in the test (or 8.1% of the diffused mass of oxygen) was taken up by the soil.

- Initial mass of oxygen (source)—129.5 mg
- Remaining mass of oxygen (source) at equilibrium—58.0 mg
- Mass of oxygen accumulated (base) at equilibrium—52.0 mg
- Net mass of oxygen (deficit)—19.5 mg
- Mass of oxygen in air required to fill soil voids—25.3 mg
- Amount taken up by soil—5.8 mg
- Predicted chemical uptake at equilibrium—0.28 mL per 100 g
- Calculated solubility in soil pore water, if free—0.011 mL per 100 g

where the following values apply:

- Air-filled porosity = 0.24

- Total porosity = 0.32
- Volumetric water content = 0.08
- Total volume of soil = 810.73 mL
- Oxygen concentration at equilibrium = 9.1%
- Density of oxygen = 1.43 g/L
- Henry's law constant at 22°C = 1.30 mmoles/L/atmos

This uptake, which amounted to about 4 µg per gram of dry soil, would represent the total mass of oxygen sorbed by the soil plus that used up by any soil microorganisms during the experiment plus the amount dissolved in the soil pore water. Mass balance calculations were performed for each of the 22 diffusion tests conducted. The results indicated that the maximum oxygen uptake was about 5% of the initial mass of oxygen.

The rate of oxygen consumption by chemical and biological processes within a soil mass is an important factor to consider in oxygen diffusion in soils (Papendick and Runkles 1965). These authors noted that oxygen uptake could be mostly attributed to microbiological processes in the soil. The work of Stevenson (1956) suggested that the rate of oxygen uptake, sometimes referred to as the *activity*, of a remoistened, previously air-dried soil is initially high and declines with time until it reaches a fairly constant rate. This burst in microbial activity immediately following remoistening was attributed to the utilization of increased amounts of nitrogenous materials released during air-drying.

The possible influence of soil microorganisms on the diffusion of oxygen was investigated during the present study. A sample of Heath Steele till was sterilized by autoclaving at a pressure of 103 kPa and a temperature of 120°C for an hour. Mineralogical analysis conducted on the samples, before and after sterilization, confirmed that the composition of the till did not change upon autoclaving. Oxygen diffusion tests were then run on specimens of the sterilized till moulded to a degree of saturation of 40%. Comparative tests were performed on unsterilized till samples. The results gave a diffusion coefficient of 4.6×10^{-6} m²/s for both the sterilized and unsterilized samples. It was inferred that the effect of microbial activity on the diffusion of oxygen in the Heath Steele till was probably minimal. This would suggest that the observed uptake was mostly a result of chemical processes. The pressure of organic substances in the till would use up oxygen in oxidation reactions.

The observed uptake can be expressed as a chemical activity rate, following the definition of Papendick and Runkles (1965). A typical oxygen activity rate for the Heath Steele till was calculated to be 1.70 µL/g/hr. It is interesting to note that Papendick and Runkles (1965) obtained oxygen activity rates in the range of 1.25–1.60 µL/g/hr for a natural soil. Their data indicated a decrease in activity rate with increase in moisture content for the same soil. It was determined that the amount of oxygen soluble in the soil pore water, if the water were free, would be 0.011 mL per 100 g of soil, or at least 20 times less than the observed uptake (presented previously). Thus, oxygen solubility in the soil pore water could not explain the observed uptake. It was also observed that, as the water content increased, the amount of oxygen uptake decreased. At high water contents (corresponding to degrees of saturation in excess of 50%), no uptake was observed. Runkles et al. (1958) made similar observations in their sorption tests.

Gaseous oxygen concentration profiles observed in the diffusion tests were simulated with POLLUTE using the calculated activity rate as an

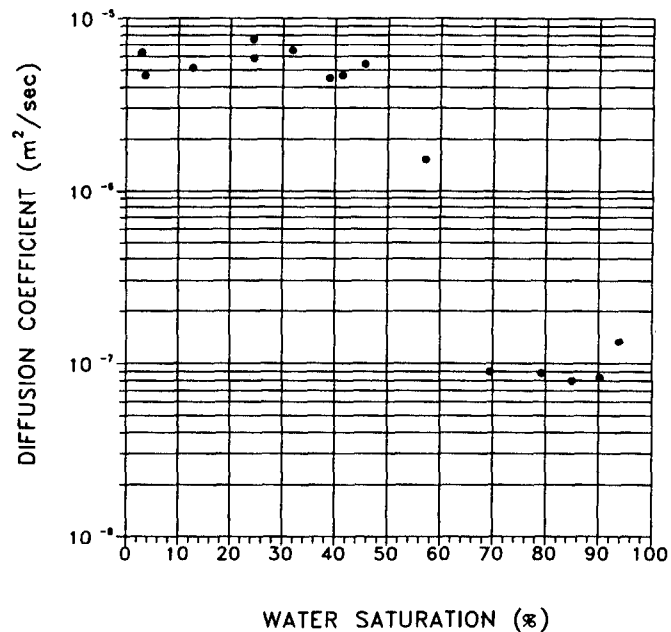


FIG. 5. Effective Diffusion Coefficient of Oxygen in Till HS-C versus Degree of Water Saturation

irreversible chemical reaction term, K [(4)]. For the orders of magnitude of diffusion coefficients observed in the tests, the inclusion of the activity rates in the POLLUTE simulations did not increase D_e by more than 5%.

Effect of Water Saturation on D_e

Effective diffusion coefficients determined for the Heath Steele till at different degrees of water saturation are presented in Fig. 5. The results generally indicate a decrease in diffusion coefficient with increase in water saturation, with greater decreases occurring in the 85%–95% saturation range. The diffusion coefficient determined for these high saturation states was of the order of $8 \times 10^{-8} \text{ m}^2/\text{s}$ and is lower than values reported by Papendick and Runkles (1965). These authors determined diffusion coefficients in the range of $1.20\text{--}1.75 \times 10^{-7} \text{ m}^2/\text{s}$ for a natural soil at high water contents. The data also show some scatter, which could be explained by differences in soil structure during packing. The diffusion coefficient versus water saturation relationship is further illustrated by the results of three diffusion tests run at different degrees of saturation plotted in Fig. 6. The data indicate the rate of decrease of the source concentration decreases with increase in water saturation. The values of D_e plotted in Fig. 5 represent concentration-independent diffusion coefficients, which include the coefficient of diffusion of oxygen in air and a tortuosity factor characteristic of the soil. As shown in (1), D_e does not include the air-filled porosity. This is consistent with the approach used by van Bavel (1951). Some authors [for example, Papendick and Runkles (1965)] combine the effective diffusion coefficient with the air-filled porosity, while others (van Brekel and Heertjes

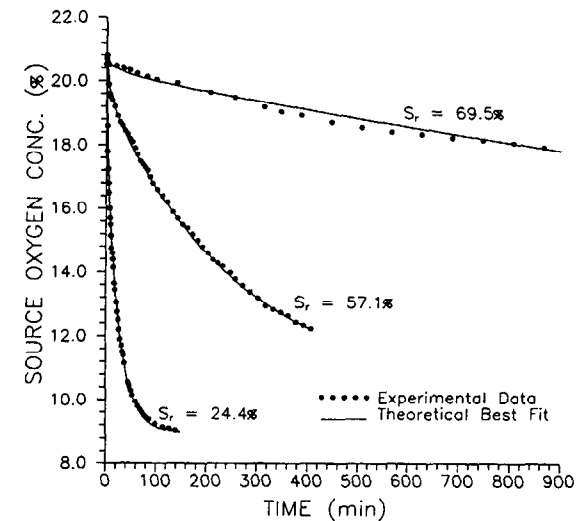


FIG. 6. Experimental and Predicted Source Oxygen Concentration in Diffusion Cell Versus Time and Degree of Water Saturation (Till HS-C)

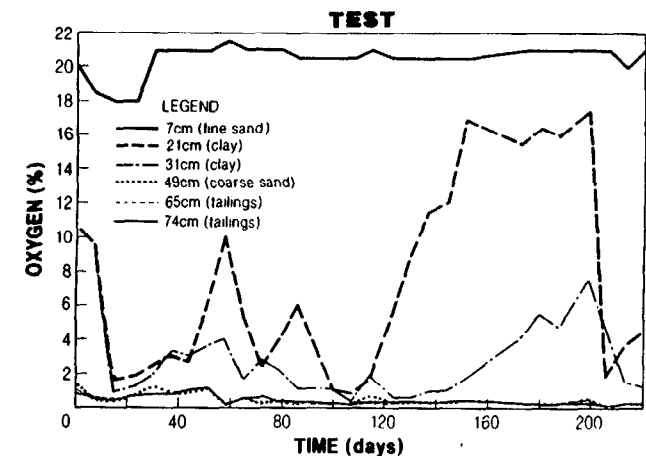


FIG. 7. Variation of Experimental Gaseous Oxygen Concentration in Soil Cover and Tailings with Time

1974) use empirical equations that combine both the porosity and tortuosity in a single diffusibility factor. Shackelford (1991) provides a review of the various definitions of the effective diffusion coefficient.

Laboratory Model of Covered and Uncovered Tailings

The variation of experimental gaseous oxygen concentration with time observed at various depths in the larger (28 cm^2) columns is presented in Fig. 7 for the soil cover and underlying tailings. The apparently erratic readings, observed in the uppermost sand layer (depth 7 cm) and the upper part of the clay layer (depth 21 cm) during the first 100 days, are believed

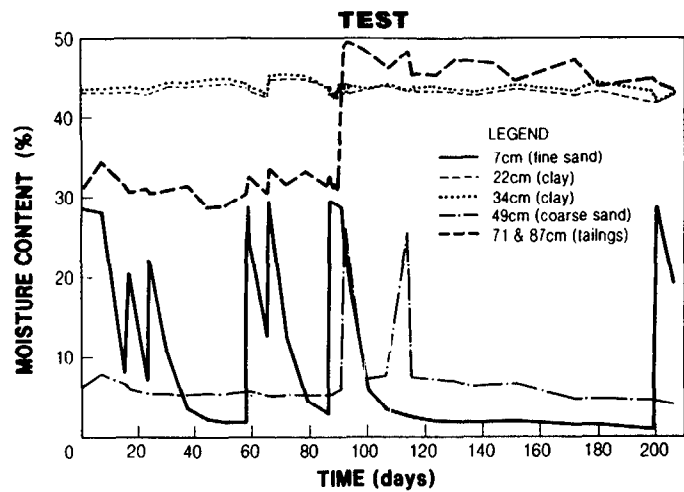


FIG. 8. Variation of Experimental Moisture Content in Soil Cover and Tailings with Time

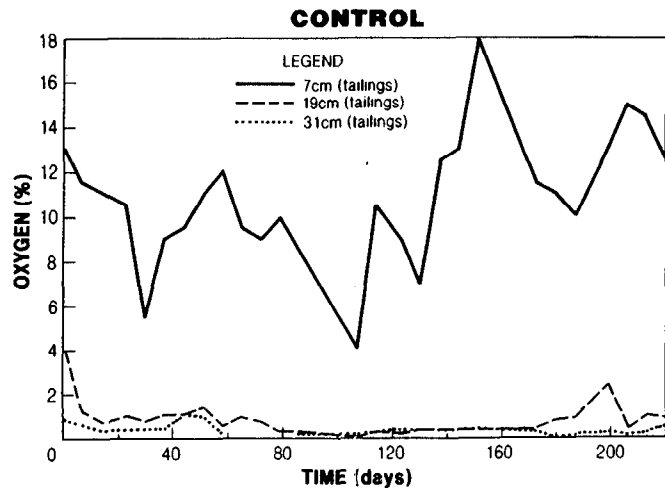


FIG. 9. Variation of Experimental Gaseous Oxygen Concentration in Uncovered Tailings with Time

to reflect changes in oxygen concentration resulting from wetting and drying cycles. This is confirmed by the corresponding moisture content data shown in Fig. 8. As expected, the oxygen level in the uppermost sand remained at atmospheric value (20.5%) during this period. Oxygen reaching the base of the uppermost sand diffused slowly into the nearly saturated clay at a rate determined by the diffusion coefficient. In the upper part of the clay, oxygen reached 16% at 140 days and decreased rapidly to 1% at the base of the clay layer at 220 days. The oxygen level in the deepest tailings was zero at all times. Similar data for the uncovered tailings are presented in

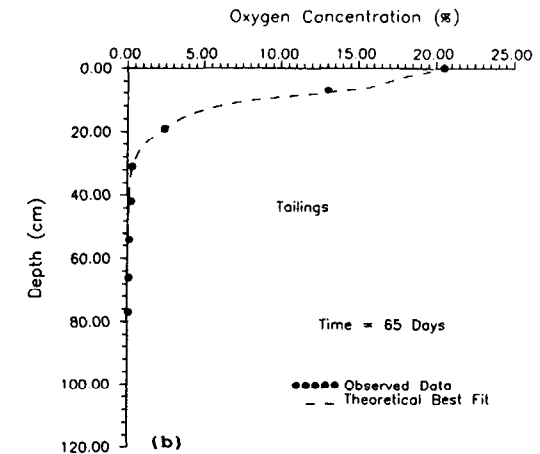
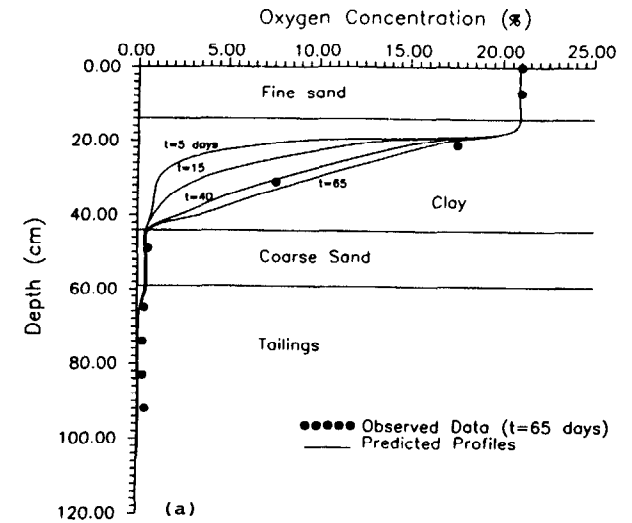


FIG. 10. Observed and Predicted Gaseous Oxygen Profiles in Covered and Uncovered Tailings (Laboratory Conditions)

Fig. 9. As in the covered tailings, the changes in concentration at the top could be attributed to fluctuations in moisture content resulting from wetting and drying. Fig. 9 indicates the oxygen concentrations in the uncovered tailings also decreased rapidly with depth as a result of consumption by sulphide oxidation reactions in the tailings.

Simulations with POLLUTE further elucidated the data shown in Figs. 7 and 8. Measured oxygen concentration profiles are presented in Fig. 10 along with the theoretical data. Effective diffusion coefficients used in the simulations were determined experimentally using the methods already described. In view of the fluctuations in the pore gas composition observed in the first 100 days of the tests, only data from part of the dry period (130–

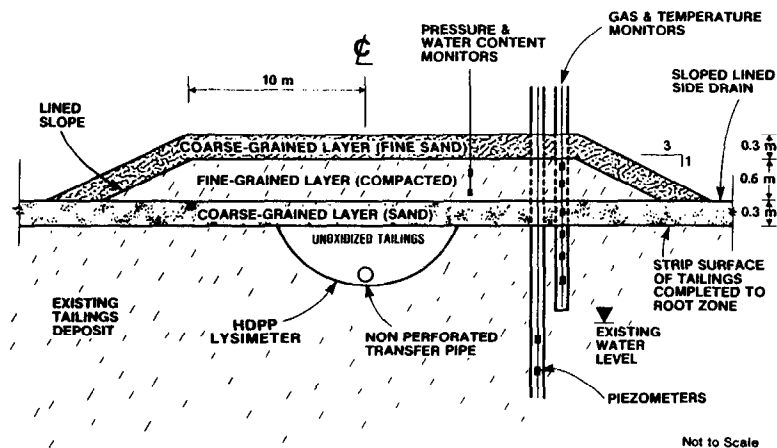


FIG. 11. Transverse Section through Composite Soil Cover Showing Instrumentation

195 days) were simulated. This was the period when moisture contents in the cover were minimum and steady and would represent the worst case. The concentration profile at time 130 days was input as initial concentrations and the data at time 195 days were simulated. The diffusion coefficients were assumed to remain constant during the modeled dry period. The moisture content data presented in Fig. 8 indicate that, with the exception of the tailings, this assumption was reasonable. Water- and gas-filled porosities used in the simulations were derived from the volumetric water content data. The tailings water contents were averaged over the modeled period. Reaction rate constants, K , used in the simulations were determined in the laboratory by an adaptation of the diffusion test arrangement. The effective diffusion coefficient of the clay layer, back-calculated from the theoretical best-fit profile to the experimental data from the large columns, was $3.35 \text{ cm}^2/\text{day}$ ($3.9 \times 10^{-9} \text{ m}^2/\text{s}$). Using the fitted parameters, the concentration profiles at earlier times were then predicted, as shown in Fig. 10(a). The experimental data (solid circles) shown in Fig. 10(a) represent oxygen profiles at 195 days and indicate good agreement between theory and actual observations. The predicted oxygen profiles at earlier times (5, 15, and 40 days) show increases in concentration in the middle part of the clay layer, as indicated by the experimental data at depths 21 and 31 cm (Fig. 7). The corresponding oxygen profile in the control (uncovered) tailings, presented in Fig. 10(b), was simulated by dividing the tailings into four separate layers to reflect the observed nonuniform moisture content profile resulting from drying of the tailings surface. The various layers were accordingly assigned different diffusion coefficients determined experimentally (Table 1). The laboratory column observations and associated simulations indicate oxygen attenuation by the clay layer. The predicted oxygen profiles in the covered tailings [Fig. 10(a)] suggest that concentrations at depths below 66 cm should be essentially zero. The 0.3% levels reported from the experimental observations below this depth are close to the detection limit (0.1%) of the oxygen analyzer used and could be an error. Fig. 10(b) shows that gaseous oxygen penetrated into the uncovered tailings to only 40 cm because of consumption by the tailings.

TABLE 1. Parameters Used in Simulation of Laboratory Diffusion

Layer (cm) (1)	D_e (cm^2/day) (2)	K (day^{-1}) (3)	θ_a (4)	θ_t (5)	θ_w (6)
(a) Control—No cover; time = 65 days ^a					
0–6 (tailings)	52.34	0.382	0.215	0.490	0.275
6–20 (tailings)	14.55	0.382	0.155	0.490	0.335
20–40 (tailings)	13.19	0.382	0.085	0.490	0.405
40–90 (tailings)	8.89	0.382	0.021	0.490	0.469
(b) Test—With cover; time = 65 days ^b					
0–15 (fine sand)	2,505.6	0	0.360	0.380	0.020
15–45 (clay)	3.348	0	0.018	0.455	0.437
45–60 (coarse sand)	1,382.4	0	0.265	0.320	0.055
60–105 (tailings)	8.89	0.382	0.021	0.490	0.469

^aOxygen flux = $2.105 \text{ g/m}^2/\text{day}$; acid loading in drainage water = $6.65 \text{ g CaCO}_3/\text{day}$.

^bOxygen flux = $0.059 \text{ g/m}^2/\text{day}$; acid loading in drainage water = $0.13 \text{ g CaCO}_3/\text{day}$.

Note: D_e = effective diffusion coefficient; K = reaction rate constant for oxygen consumption by tailings; and θ_a , θ_t , θ_w = air-filled and total porosity, and volumetric water contents, respectively.

Based on the simulations, the flux of oxygen into the covered tailings is estimated to be only 3% of the flux in the uncovered tailings, indicating a 97% effectiveness (Table 1). The theoretical maximum acid flux, assuming all the oxygen is consumed by the tailings, would be reduced by the same amount. The data therefore give an indication of the effectiveness of the compacted clay layer as an oxygen barrier. At the end of the dry period, the covered and uncovered tailings were flushed several times with deionized distilled water and the mass of acid produced during the dry period was quantified. The total acid production in the covered tailings was found to be only 2% of that observed in the uncovered tailings (Table 1), which is similar to the predicted value.

Field Oxygen Profiles

As part of the evaluation of the performance of soil covers, NTC designed and installed test plots at the Waite Amulet site in 1990. The design, construction, and instrumentation of the plots are described elsewhere (Yanful and St-Arnaud 1991). A cross section of one of the soil covers is presented in Fig. 11.

Fig. 12 presents gaseous oxygen profiles measured in the cover at different times in 1990 and 1991. The data indicate a rapid drop in oxygen concentrations in the clay layer from 12% to about 4%. During October and November 1990, there was heavy rainfall, which resulted in elevation of the water table and saturation of the entire tailings deposit. Thus, it was impossible to sample any pore gas. In July 1991, the oxygen profile penetrated the tailings with a concentration of about 2% near the surface.

The July 1991 field data were simulated with POLLUTE using the November 1990 data as initial concentrations. Since the period from December to April was mostly characterized by frozen ground conditions as well as rainfall and spring melting, it was assumed that the November data would persist until April 1991. Generally, significant lowering of the water table below the tailings

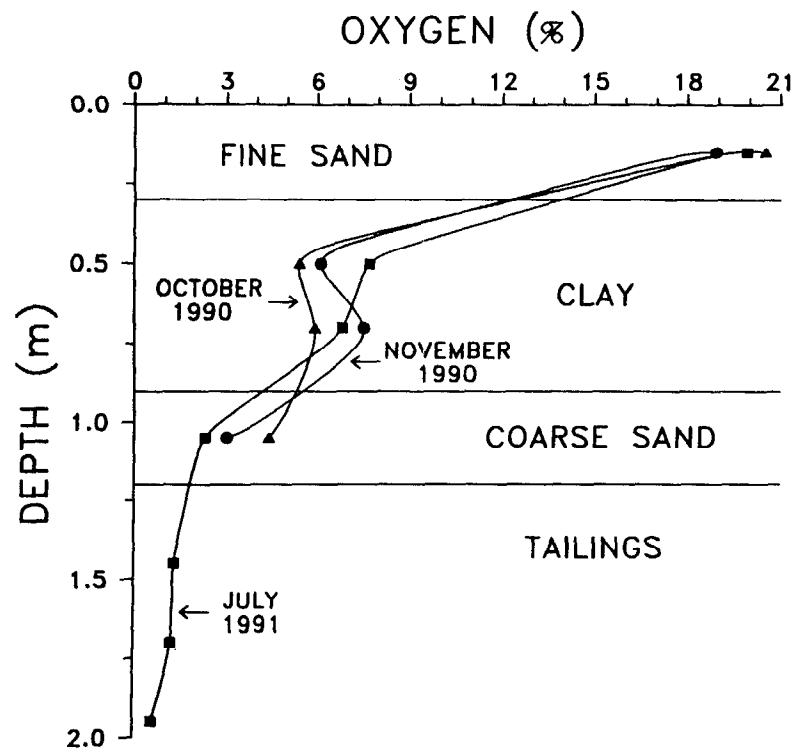


FIG. 12. Field Gaseous Oxygen Profiles in Composite Soil Cover and Tailings

surface after spring thaw would have commenced in May 1991. Thus, the oxygen data obtained in July were believed to have characterized three months of diffusion from May to July 1991. The observed and simulated profiles for July 1991 are presented in Fig. 13(a). The diffusion coefficient of the clay layer in the field was determined from the simulations to be $8.57 \text{ cm}^2/\text{day}$ ($9.9 \times 10^{-9} \text{ m}^2/\text{s}$). The corresponding data for the uncovered tailings are presented in Fig. 13(b), from which an effective diffusion coefficient of $24 \text{ cm}^2/\text{day}$ ($2.8 \times 10^{-8} \text{ m}^2/\text{s}$) was obtained for the tailings. The calculated flux of oxygen into the uncovered tailings is about 99% higher than the flux into the covered tailings (Table 2). Lysimeters, filled with unoxidized tailings (Fig. 11), were installed directly below the covers and also in a control test plot to provide a means for confirming the effectiveness of the cover in reducing acid flux. To date, the lysimeters underneath the covers have not reported water, whereas large volumes of acid water have been collected and analyzed in the control test plot. As explained here, the water flux through the cover is very low. The small amount of water that could infiltrate the clay is most likely exiting the slopes as runoff because of high net upward hydraulic gradients observed in the clay. Thus, it has not been possible to directly verify the predicted reduction in field acid flux.

ANALYSIS

The results of both laboratory and field studies of soil covers on sulphidic tailings presented here have indicated that gaseous oxygen is attenuated by

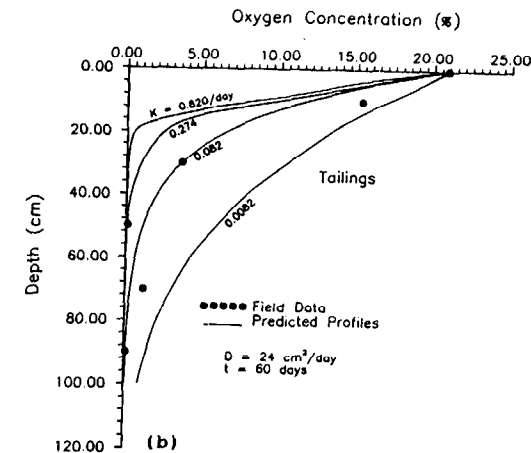
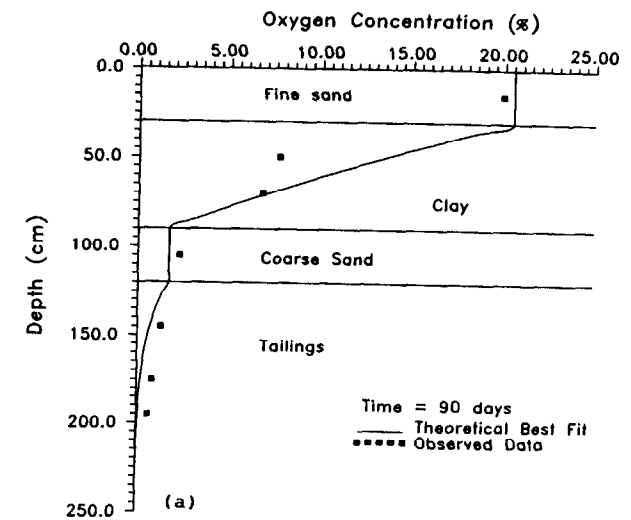


FIG. 13. Observed and Predicted Oxygen Profiles in Covered and Uncovered Tailings (Field Conditions)

the compacted clay layer in the three-layer cover system. Dissolved oxygen would play a minor role in oxidation of the tailings since the solubility of oxygen in water is only 11 mg/L at 11°C (Truesdale et al. 1955) and the diffusion coefficient of oxygen in water is nearly 10,000 times less than in air. Thus, the elimination or control of gaseous oxygen is the key requirement in any sulphidic tailings management strategy.

The cover described in this paper was designed using the capillary barrier concept. The lower sand layer drains rapidly to residual water saturation, at which point the hydraulic conductivity is so low that it is unable to transmit any more suction. The overlying clay is therefore prevented from draining. In laboratory column tests, full saturation was maintained for at least 100

TABLE 2. Parameters Used in Simulation of Field Diffusion

Layer (cm) (1)	D_e (cm^2/day) (2)	K (day^{-1}) (3)	θ_u (4)	θ_l (5)	θ_w (6)
(a) Control—No cover; time = 60 days ^a					
0–100 (tailings)	24	0.082	0.021	0.490	0.469
(b) Test—With cover; time = 90 days ^b					
0–30 (fine sand)	2,505.6	0	0.360	0.380	0.020
30–90 (clay)	8.57	0	0.018	0.455	0.437
90–120 (coarse sand)	1,382.4	0	0.265	0.320	0.055
>120 (tailings)	9.89	0.082	0.021	0.490	0.469

^aOxygen flux = 5.83 g/m²/day.

^bOxygen flux = 0.011 g/m²/day.

Note: D_e , K , θ_u , θ_l , and θ_w have the same meanings as in Table 1.

days. Numerical simulations conducted by Akindunni et al. (1991) showed that a fine-grained soil overlying a coarse-grained layer will remain saturated for at least 50 days without the need for recharge by infiltration. At most Canadian mine sites, 100 days would be the maximum dry period when no recharge would occur. Hence, it is critical to design and place the clay layer at a high water content. The design used called for field compaction of 93% modified Proctor and a moulding water content of about 2% wet of optimum. This would ensure close to 95% water saturation and a low hydraulic conductivity, if a good placement protocol [for example, destruction of soil clods and adequate interlift bonding (Elsbury et al. 1990)] is followed. Compaction tests conducted during construction gave an average dry density of 1.52 Mg/m³ and a water content of 24.3%, which corresponded to 92.5% of the maximum modified Proctor value.

Preconstruction laboratory tests had indicated a hydraulic conductivity of less than 1×10^{-7} cm/s was attainable under laboratory conditions. Using this conductivity value and a maximum hydraulic gradient of 0.3 the composite cover was designed to reduce the water flux into the tailings from 50 cm/year to less than 9 mm/year. In situ suction measurements made during May 1991 gave values ranging from a pF value of 2.35 (2.25 m of water) in the tailings to 3.32 (21.1 m of water) in the clay layer, in response to both downward drainage from the tailings and evaporation from the upper sand layer. The suction in the upper sand was found to be equal to a pF value of 2.94 (8.68 m of water). Moisture-drainage relationships suggest that, under such a high suction, the hydraulic conductivity of the sand would be low so that net flux of water from the underlying clay would be very small. Hydraulic gradients across the clay layer calculated from the field suction values were found to be upward with an average value of 14, which would reduce the net infiltration into the cover to essentially zero. The hydraulic conductivity of the compacted clay was measured in the field in June 1991 using an air-entry permeameter (Fernik and Haug 1990). The results indicated that the design saturated hydraulic conductivity of less than 1×10^{-7} cm/s was attained. The water-retention characteristics of the soils, determined prior to installation of the covers, suggest that even under these suction values, the clay could still remain nearly fully saturated. This was confirmed by in situ water content measurements using time domain re-

flectometry. The presence of the upper fine sand layer would reduce the evaporative fluxes, as was observed in the laboratory columns.

A comparison of fluxes in Tables 1 and 2 indicates that, in the case of the uncovered tailings, the calculated field flux is 2.8 times that of the laboratory flux. This may be explained by the difference in initial concentration gradients as the flux is directly proportional to the concentration gradient. The field data represent oxygen diffusion that would have begun in the month of May (at the end of spring thaw) and through to the end of June. During spring thaw, the tailings deposit is essentially saturated so that

TABLE 3. Calculated Oxygen Fluxes in Uncovered Tailings Deposit at Waite Amulet

Reaction rate constant K (day^{-1}) (1)	Gaseous oxygen flux (1-m depth) ($\text{g}/\text{m}^2/\text{day}$) (2)
0.0082	3.11
0.082	5.83
0.274	9.95
0.820	16.89

Note: Effective diffusion coefficient, $D_e = 24 \text{ cm}^2/\text{day}$; and time of diffusion (May–June, 1991), $t = 60$ days.

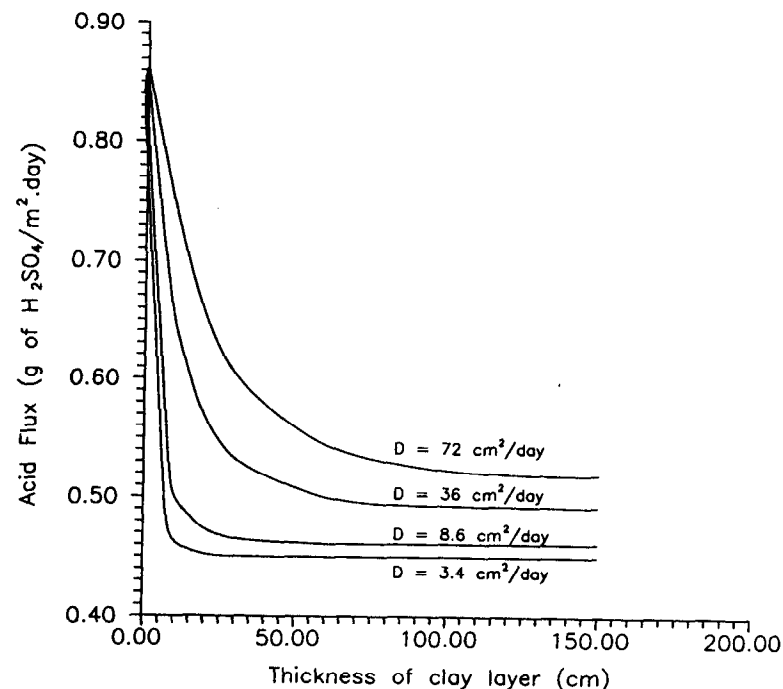


FIG. 14. Simulation of Composite Cover on Tailings Showing Variation of Acid Flux with Thickness and Effective Diffusion Coefficient of Clay Layer

the initial oxygen concentration is zero at all depths. In the case of the laboratory columns, however, a nonzero concentration profile existed at the end of the 130 days so that the initial gradient used in POLLUTE for the calculation of flux was higher than in the field. The same explanation can be given for the difference in fluxes computed for the covered tailings in which the laboratory gradient was higher than that of the field. In this case, however, the difference in the reaction rate constant, K , would also contribute to the difference in flux. The respective laboratory and field K values used in the simulations were 0.372 and 0.082 day⁻¹. The laboratory column tests were initiated with fresh, unoxidized tailings in which the sulphide minerals were largely preserved. The field case, on the other hand, involved oxidized tailings in which most of the sulphide minerals had been consumed in oxidation reactions (Yanful and St-Arnaud 1992). The rate of oxygen consumption would be higher in the laboratory than in the field. The observed and predicted field oxygen profiles [Fig. 13(b)] indicate that the less reactive the tailings (the lower the value of K), the deeper the penetration of gaseous oxygen. This would describe the case where the oxidation front advances into the tailings deposit as sulphide minerals are gradually consumed in the upper part. Calculated fluxes corresponding to the different values of K (Table 3) indicate higher K values would give higher fluxes.

The diffusion coefficient determined for the compacted clay layer was higher in the field than in the laboratory, as expected. During construction of the field cover, large tree roots present in the clay were manually removed by site personnel prior to compaction. The presence of smaller roots (which could not be removed), macropores and, probably, fractures induced by cracking would account for the higher field diffusion coefficient. The laboratory tests were conducted under controlled conditions that did not include most of these factors.

The thickness of the clay layer in the cover system was selected to provide the maximum reduction in gaseous oxygen flux. The flux of acid (as sulphuric acid), derived from the predicted oxygen flux using (3), is presented in Fig. 14 for various thicknesses and diffusion coefficients of the clay layer. The diffusion coefficients used include the laboratory and field values determined from the simulations (3.35 and 8.57 cm²/day, respectively) and a slightly high value of 72 cm²/day to characterize the clay under extreme drying or freezing and cracking conditions. The plots suggest that in both laboratory and field situations, a thickness of only about 30 cm (of clay) is required to minimize the acid flux. As shown in Fig. 11, a thicker layer (60 cm) of compacted clay was used in the field to forestall potential increases in the diffusion coefficient of the clay resulting from adverse climatic conditions. As the diffusion coefficient of the clay layer increases, the predicted acid flux increases and a thicker layer is required to minimize the flux. The effect of freezing and thawing on the diffusion coefficient is currently being investigated in the laboratory.

SUMMARY AND CONCLUSIONS

Laboratory experiments conducted to determine the diffusion coefficient of gaseous oxygen in a candidate natural till cover have been described. Effective diffusion coefficients, obtained from fitting a semianalytic solution of the one-dimensional, transient diffusion equation to experimental oxygen concentration versus time graphs, ranged from 8.3×10^{-8} m²/s to 6.2×10^{-6} m²/s at 3 and 90% degrees of water saturation, respectively. The

diffusion coefficients at the high saturation states are the most important as they are required for the design of effective covers for reducing the oxygen flux into sulphidic mill tailings. Placement of the cover in a high water saturation condition and close to the maximum compaction density also ensures a reasonably low hydraulic conductivity that would reduce infiltration into the cover.

The results of column tests designed to evaluate the effectiveness of a three-layer soil cover on sulphidic tailings from a decommissioned mine site are discussed. The cover consists of a compacted clay layer sandwiched between a fine and a coarse sand layer. The sands function as capillary barriers in preventing the clay from losing moisture by drainage and evaporation. This is corroborated by water content measurements. Theoretical fluxes, obtained from simulations of observed oxygen concentration profiles over a 65-day period, indicate a 97% reduction of the maximum acid flux by the cover. These results are found to be similar to those obtained from a comparison of drainage waters from covered and uncovered tailings in laboratory columns. In comparison, oxygen profiles measured in the covered field tailings gave a predicted flux that indicates a 99% effectiveness in the exclusion of gaseous oxygen. The effective diffusion coefficient of the clay layer is determined from the simulations to be 3.9 and 9.9×10^{-9} m²/s in the laboratory and field, respectively.

Further simulations confirm that, in both the laboratory and field, the thickness of the clay layer required to minimize the theoretical acid flux does not need to exceed 30 cm. However, a thicker layer (60 cm) was used in the field as a safety factor against possible increases in the diffusion coefficient of the clay due to adverse climatic conditions such as freezing and thawing.

ACKNOWLEDGMENTS

The work described in this paper has been funded by Noranda Inc., Canada Centre for Mineral and Energy Technology, Environment Canada and Centre de Recherches Minérales under Canada's Mine Environment Neutral Drainage (MEND) program. The experimental work and the computer simulations were conducted with the assistance of S. Payant, K. Shikatani and B. Aubé of Noranda Technology Centre (NTC), and G. Cotta and P. Tibble, students of the University of Waterloo. Initial fundamental research leading to the work described in this paper was undertaken in collaboration with R. Gillham and R. Nicholson of the University of Waterloo. The writer gratefully acknowledges telephone discussions with Kerry Rowe of The University of Western Ontario on the use of the computer program POLLUTE for the simulations. K. Wheeland and L. St-Arnaud (of NTC) provided editorial and technical reviews of this manuscript.

APPENDIX. REFERENCES

- Akindunni, F., Gillham, R. W., and Nicholson, R. V. (1991). "Numerical simulations to investigate moisture-retention characteristics in the design of oxygen-limiting covers for reactive mine tailings." *Can. Geotech. J.*, 28(3), 446-451.
- Collin, M. (1987). "Mathematical modelling of water and oxygen transport in layered soil covers for deposits of pyritic mine tailings." *Licentiate Treatise*, Dept. of Chemical Engrg., Royal Inst. of Tech., Stockholm.
- Elsbury, B. R., Daniel, D. E., and Anderson, D. C. (1990). "Lessons learned from compacted clay liner." *J. Geotech. Engrg.*, ASCE, 116(11), 1641-1660.

- Fernuik, N., and Haug, M. (1990). "Evaluation of in situ permeability testing methods." *J. Geotech. Engrg.*, ASCE, 116(2), 297-311.
- Filion, M. P., and Ferguson, K. (1989). "Acid mine drainage research in Canada." *Proc. of the Int. Symp. on Tailings and Effluent Management*, Pergamon Press, 61-72.
- Locat, J., Lefebvre, G., and Ballivy, G. (1984). "Mineralogy, chemistry and physical properties interrelationships of some sensitive clays from Eastern Canada." *Can. Geotech. J.*, 21, 530-540.
- Nicholson, R. V., Gillham, R. W., Cherry, J. A., and Reardon, E. J. (1989). "Reduction of acid generation in mine tailings through the use of moisture-retaining cover layers as oxygen barriers." *Can. Geotech. J.*, 16(1), 1-8.
- Nordstrom, D. K. (1982). "Aqueous pyrite oxidation and the consequent formation of iron minerals." *Acid Sulphate Weathering*, Soil Sci. Society of America, 37-56.
- Papendick, R. I., and Runkles, J. R. (1965). "Transient-state oxygen diffusion in soil: I. The case when rate of oxygen consumption is constant." *Soil Sci.*, 100(4), 251-261.
- Quigley, R. M., Seth, A. J., Boonsinsuk, P., Sherran, D. E., and Young, R. N. (1985). "Geologic control on soil composition and properties, Lake Ojibway clay plain, Matagami, Quebec." *Can. Geotech. J.*, 22, 491-500.
- Rasmuson, A., and Eriksson, J. C. (1986). "Capillary barriers in covers for mine tailings dumps." *Report 3307*, Nat. Swedish Envir. Protection Board, Solna, Sweden.
- Rowe, R. K., and Booker, J. R. (1990). "Pollute V5.0 1-D pollutant migration through a non homogenous soil, User Manual." *Report No. GEOP 90-1*, Geotech. Res. Ctr., Univ. of Western Ontario, London, Ontario, Canada.
- Runkles, J. R., Scott, A. D., and Nakayama, F. S. (1958). "Oxygen sorption by moist soils and vermiculite." *Soil Sci. Soc. Amer. Proc.*, 22, 15-18.
- Shakelford, C. D. (1991). "Laboratory diffusion testing for waste disposal—A review." *J. of Contaminant Hydrol.*, 7(3), 177-217.
- "Standard method for particle size analysis." (1991a). *Annual Book of ASTM Standards: Soil and Rock; Dimension Stone; Geosynthetics (ASTM D422)*, ASTM, Philadelphia, Pa.
- "Standard test methods for moisture-density relations of soils and soil-aggregate mixtures." (1991b). *Annual Book of ASTM Standards: Soil and Rock; Dimension Stone; Geosynthetics (ASTM D1557)*, ASTM, Philadelphia, Pa.
- Stevenson, I. L. (1956). "Some observations on the microbial activity in remoistened air-dried soils." *Plant Soil*, 8(2), 170-182.
- Topp, G. C., Davis, J. L., and Annan, A. P. (1980). "Electromagnetic determination of soil water content: Measurement in coaxial transmission lines." *Water Resour. Res.*, 16(3), 574-582.
- Truesdale, G. A., Downing, A. L., and Lowden, G. F. (1955). "The solubility of oxygen in pure water and sea water." *J. Appl. Chem.*, 5, Feb., 53-62.
- van Bavel, C. H. M. (1951). "A soil aeration theory based on diffusion." *Soil Sci.*, 72, 33-46.
- van Brekel, J., and Heertjes, P. M. (1974). "Analysis of diffusion in macroporous media in terms of a porosity, a tortuosity and a constrictivity factor." *Int. J. Heat Mass Transfer*, 17, 1093-1103.
- Wheeland, K. G., and Feasby, G. (1991). "Innovative decommission technologies via Canada's MEND program." *Proc. of the 12th Nat. Conf., Hazardous Mater. Control/Superfund '91*, Hazardous Mater. Control Res. Inst., 23-28.
- Yanful, E. K., and St-Arnaud, L. C. (1992). "Migration of acidic pore waters at the Waite Amulet tailings site near Rouyn-Noranda, Quebec, Canada." *Can. Geotech. J.*, 29(3) 466-476.
- Yanful, E. K., and St-Arnaud, L. C. (1991). "Design, instrumentation and construction of engineered reactive soil covers for reactive tailings management." *Proc. of the 2nd. Int. Conf. on the Abatement of Acidic Drainage*, Montreal, Canada, Vol. 1, Mine Envir. Neutral Drainage Program, Ottawa, Canada, 487-504.

1993: Yanful, E.K., Riley, M.D.,
Woyshner, M.R. and Duncan, J.

Construction and monitoring of a composite
soil cover on an experimental waste-rock
pile near Newcastle, New Brunswick, Canada.
Can. Geot. J., Vol. 30, pp. 588-599.

Construction and monitoring of a composite soil cover on an experimental waste-rock pile near Newcastle, New Brunswick, Canada

ERNEST K. YANFUL

Centre de technologie Noranda, 240 boulevard Hymus, Pointe-Claire (Québec), Canada H9R 1G5

MICHAEL D. RILEY

Nolan, Davis and Associates (N.B.) Limited, 403 Regent Street, Fredericton, N.B., Canada E3B 3X6

MARK R. WOYSHNER

2110 rue Clark, Unit 1, Montréal (Québec), Canada H2X 2R7

AND

JIM DUNCAN

Heath Steele Mines, P.O. Box 400, Newcastle, N.B., Canada E1V 3M5

Received September 15, 1992

Accepted March 30, 1993

A 130 cm thick composite soil cover was constructed on an experimental waste-rock pile at the Heath Steele mine site near Newcastle, New Brunswick. The cover consisted of a 30 cm thick sand base, a 60 cm thick compacted glacial till, a 30 cm thick granular layer, and a final 10 cm thick gravel layer for erosion protection. The till was compacted on the sand base in three finished lifts each of 20 cm thickness. Results of a preconstruction pad test indicated six passes of a 5-t vibratory compactor were required to attain the design specifications of 95% of the Modified Proctor maximum dry density at a moulding water content of 2–3% wet of the optimum. These compaction specifications also ensure that the till has a degree of water saturation of at least 95%, which is required to reduce oxygen and acid fluxes in the underlying pile. Quality control measures were taken during the construction to ensure the specifications were followed. Monitoring instrumentation was installed during the construction of the cover. Results indicate a reduction in gaseous oxygen concentrations in the pile from 20% before cover to about 3% after cover placement. The decreased oxygen penetration implies reduced oxygen flux and acid production. Volumetric water contents averaged about 32% in the till both immediately following cover installation and 7 months later. The water-content data are corroborated by soil-suction measurements. Temperatures in the pile have decreased following cover installation but appear to be more influenced by climatic variability than by a decrease in heat production and hence sulphide mineral oxidation. Observed discharge from two lysimeters, installed below the cover, indicates infiltration of 2–2.5% of precipitation during a 55-day period when rainfall was heavy. The quality of seepage from the pile has not changed since cover installation. Further monitoring will be required to confirm the reduction in acid production.

Key words: waste-rock pile, acid generation, soil cover, suction, oxygen flux, percolation.

Un couvert composite de sol de 130 cm d'épaisseur a été construit sur une pile expérimentale de stériles rocheux sur le site de la mine Heath Steele près de Newcastle, Nouveau-Brunswick. Le couvert consiste en une couche de fondation en sable de 30 cm d'épaisseur, une de till glaciaire compacté de 60 cm, une de sol granulaire de 30 cm, et finalement une couche de gravier de 10 cm d'épaisseur comme protection contre l'érosion. Le till a été mis en place sur la fondation de sable en trois couches compactées de 20 cm d'épaisseur. Les résultats d'une planche d'essai avant construction ont indiqué que six passes d'un compacteur vibrant de 5 tonnes étaient requis pour atteindre les spécifications de compactage de 95% de la densité sèche maximale du Proctor modifié à une teneur en eau de mise en place de 2–3% du côté mouillé de l'optimum. Ces spécifications assurent également que le till a un degré de saturation en eau d'au moins 95%, ce qui est requis pour réduire les flux d'oxygène et d'acide dans la pile sous-jacente. Des mesures de contrôle de qualité ont été prises au cours de la construction pour assurer le respect des spécifications. Une instrumentation pour fin de mesures a été installée durant la construction du couvert. Les résultats indiquent une réduction des concentrations d'oxygène gazeux dans la pile de 20% avant à 3% après la mise en place du couvert. La diminution de la pénétration d'oxygène implique une réduction du flux d'oxygène et de la production d'acide. Les teneurs volumétriques en eau étaient en moyenne de 32% dans le till, tant immédiatement après la mise en place du couvert que 7 mois plus tard. Les données de teneur en eau ont été corroborées par les mesures de succion dans le sol. Les températures dans la pile ont diminué suite à l'installation du couvert, mais semble être plus influencées par la variabilité climatique que par la diminution de la production de chaleur, et ainsi de l'oxydation du minéral de soufre. Le débit observé dans deux lysimètres installés sous le couvert indiquent une infiltration de 2–2,5% de la précipitation durant une période de 55 jours durant laquelle la pluie a été abondante. La qualité des liquides d'infiltration de la pile n'a pas changé depuis l'installation du couvert. Des mesures supplémentaires seront nécessaires pour confirmer la réduction dans la production d'acide.

Mots clés : pile de stériles rocheux, génération d'acide, couvert de sol, succion, flux d'oxygène, percolation.

[Traduit par la rédaction]

Introduction

A soil cover for controlling acidic drainage in waste rock must effectively retain high water saturation and also have a low hydraulic conductivity. These two requirements must be taken into account during design and construction of the cover.

TABLE 1. Construction specifications for composite soil cover

Surface preparation
Grade identified high areas on slide slopes (3H:1V), minimizing disturbance to pile
excavate two 3.5 × 2 × 1.2 m holes at identified monitoring stations at the top of the pile for lysimeters;
provide sand cushion at bottom of excavation and slope at 2% to promote drainage
Level top of pile filling voids and depressions with excavated waste rock or non-acid-generating crushed rock (-37.5 mm) or approved equivalent
Provide a tight seal between compacted till layer and pile
Sand base
Compact with several passes of a medium-size vibratory roller to 92% of maximum Modified Proctor density (ASTM 1987c)
Compact in two lifts to a finished total thickness of 30 cm
Ensure smooth surface of sand base to allow drainage
Ensure compacted surface is flat, with surface irregularity within ±25 mm of average grade
Finish final slopes at 3H:1V
Impermeable cover
Compact with medium-weight vibratory compactor or sheepsfoot roller (as approved by engineer) to achieve design specifications (Yanful et al. 1993)
Conduct preplacement test on a till pad using proposed equipment; pad to be compacted in a minimum of two layers and to measure at least 5 × 10 m in plan
Engineer to determine minimum number of passes of compactor (from test on pad) required for design densities
Compact till on sand base to at least 95% Modified Proctor density in three lifts (20 cm per lift) to a finished thickness of 60 cm
Apply water as necessary during compaction to maintain specified water content (-2 to +4% of optimum); if cover is excessively dried out, remove from site and replace
Engineer to perform field density tests on each lift before approving placement of next lift
In areas not accessible to rolling equipment, compact to specified density with approved mechanical tamper
Smooth top surface of cover to promote drainage
Granular cover
Place in maximum 15-cm lifts and compact to 92% of Modified Proctor to a finished thickness of 30 cm
Ensure compacted surface is flat, with irregularities within ±50 cm of average grade
Complete final slope at 3H:1V
Erosion protection
Particle size to be maximum of 75 mm and 15% by weight finer than 4.75 mm
Place uniformly over entire pile surface of granular cover to a minimum thickness of 10 cm

The design of a composite soil cover on a 0.25-ha experimental waste-rock pile located at Heath Steele mines near Newcastle, New Brunswick, is presented in Yanful et al. (1993). The design of the cover called for a three-layer system consisting of a 60-cm compacted till (impermeable cover) sandwiched between a 30 cm thick well-graded sand (sand base) and a 30 cm thick coarse-grained soil layer (granular cover).

This paper deals with the construction and instrumentation of the cover. A brief description of the geotechnical properties of the selected soils is presented. Monitoring data collected to date are also discussed.

Construction of cover

The design requirements for the cover presented by Yanful et al. (1993) and construction specifications outlined in Table 1 were developed into a request for a proposal that was submitted for costing. A contract was subsequently awarded for the construction of the cover in accordance with the specifications outlined in Table 1.

Surface preparation

The initial task in the placement of the cover was the preparation of the side slopes and the top of the pile. A Caterpillar 215 hydraulic excavator was used to level the top of the pile and remove high points on the side slopes.

Voids and depressions were filled with excavated waste rock and non-acid-generating crushed rock. A total of 50 t of crushed rock was used for surface preparation. Sand and gravel covering the edges of the impermeable membrane underlying the pile at the perimeter were excavated manually to expose the membrane. Additional membrane was joined to the existing one at the edges of the pile and then extended out to provide a lap that ensured a tight seal between the till layer and the waste rock.

Sand base

The prepared surface of the pile was covered with a 30 cm thick layer of medium to coarse sand. In areas near the base of the pile, the thickness of the sand had to exceed 30 cm to achieve the required grades. Grain-size data indicated the sand consisted of 4% gravel particles, 90% sand, and 6% silt- and clay-size particles. The sand was compacted with a minimum of four passes of a 5-t vibratory compactor to achieve the required densities. The final surface of the sand was sloped at a minimum gradient of 2%.

Impermeable cover

Source and properties of glacial till

A borrow source for the appropriate glacial till was located approximately 2.5 km east of pile 7/12. Preconstruction grain-size analysis (ASTM 1987a, 1987b) indicated the till

ASTM SIEVE SERIES NO.

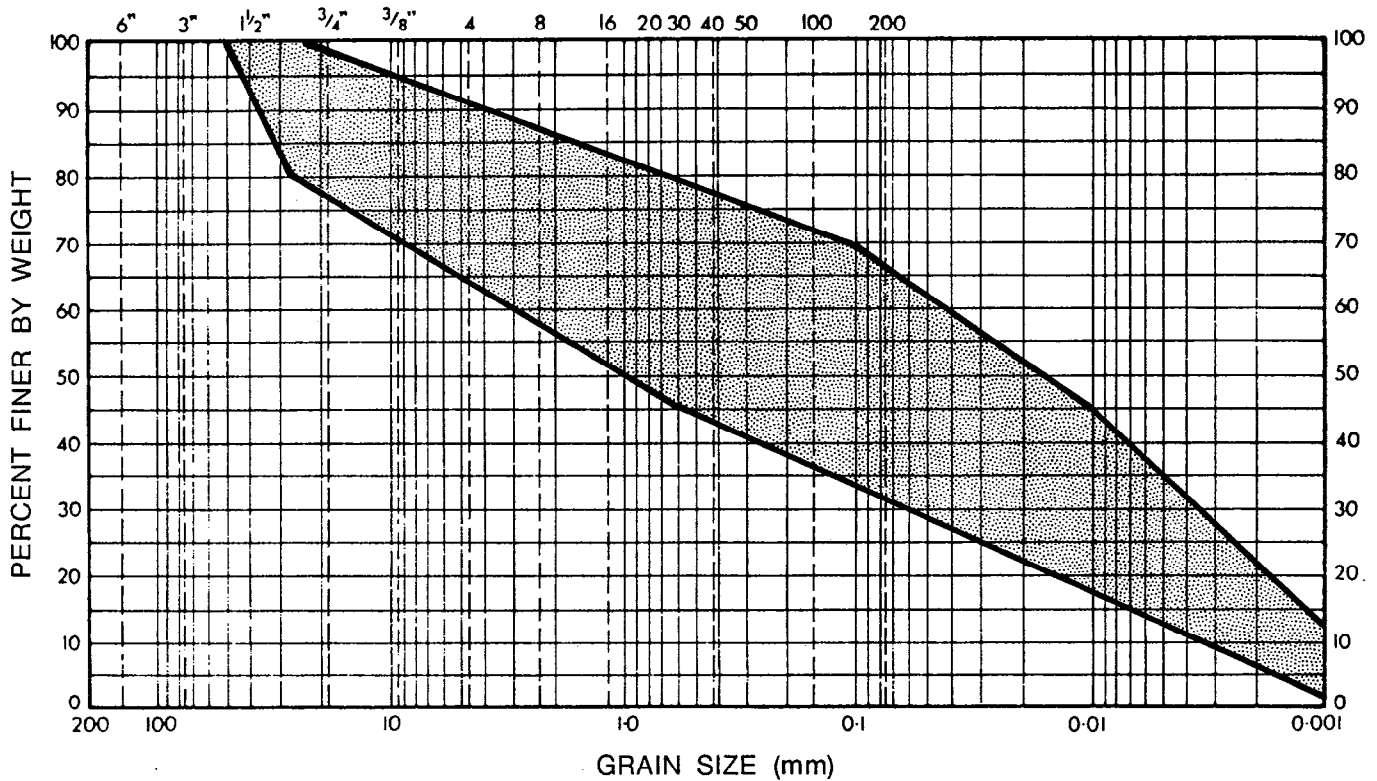


FIG. 1. Range of grain-size distributions of samples of impermeable cover (compacted glacial till).

consisted of 10–33% gravel, 18–45% sand, 28–44% silt, and 7–23% clay-size particles. The range of grain-size distributions obtained on several till samples is presented in Fig. 1. Modified Proctor compaction tests (ASTM 1987c) on representative samples gave an average optimum moisture content of 13.5% and a maximum dry density of 1.96 Mg/m³. Typical compaction curves are shown in Fig. 2. Atterberg limits were typically 27–28% for the liquid limit and 5–6% for the plasticity index.

Field test pad

Prior to placement on the sand base, the till was tested in a field pad in accordance with construction specifications (Table 1). The till was compacted in approximately 20 cm thick lifts using a 5-t vibratory compactor. In situ density tests were conducted after each pass of the compactor. A total of three layers of compacted till, with an approximate thickness of 60 cm, were placed in the test pad. The results of the test indicated a minimum of six passes of the 5-t vibratory compactor were required to achieve the design specification of 95% of the Modified Proctor maximum dry density.

Placement of till

On September 3, 1991, the till was excavated, trucked, and stockpiled at the base of the pile. Cobbles, boulders, and large tree roots were manually removed from the incoming material. The moisture content of the till at source was found to be generally 5% or more above the optimum which was too high for proper compaction. The till was therefore allowed to dry in the stockpile prior to placement. It was subsequently transported to the pile and spread in lifts. Each lift was compacted to a maximum final thickness of 20 cm,

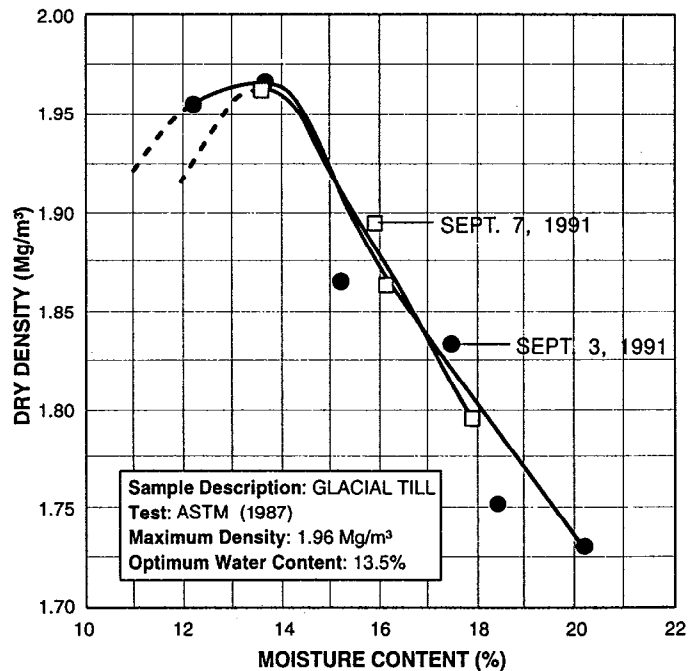


FIG. 2. Typical Modified Proctor compaction curves for impermeable cover (glacial till).

according to specifications (Table 1). Figure 3 shows the placement and compaction of the till.

Quality control

In situ density tests were conducted at various locations during the placement of each lift using a nuclear density apparatus. Sufficient tests (average of 30) were performed on



FIG. 3. Placement and compaction of impermeable cover (glacial till).

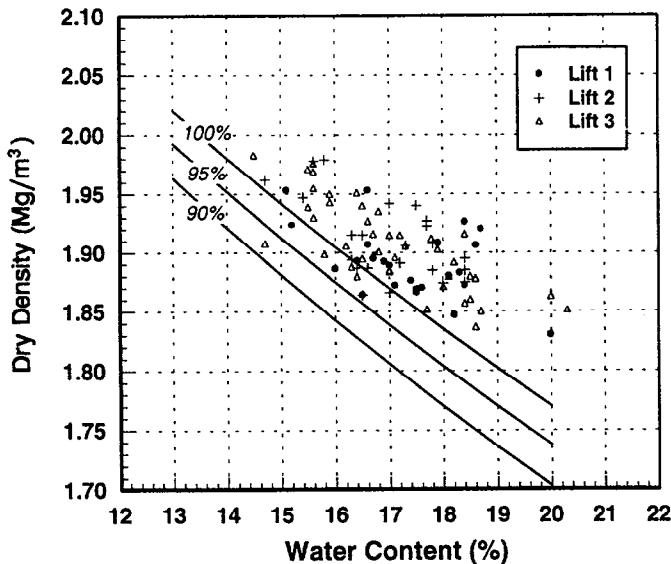


FIG. 4. In situ density vs. water content for compacted till.

each lift to ensure that the entire area (50×50 m in plan) was well covered. The next lift was placed only when the results of the density tests indicated that the till was being placed within an acceptable range of densities and water contents (-2 to $+4\%$ wet of the optimum water content). A total of 94 density tests were conducted. Figure 4 presents the dry densities and water contents obtained during the placement of each lift. The data indicate at least 95% of water saturation was achieved after compaction of each lift. The placement water content was, however, too high at some locations where an excessive number of passes of the smooth-wheeled, vibratory compactor may have been used to achieve the specified densities. The implication of this

overcompaction (Holtz and Kovacs 1981) is a reduction in shear strength. For this cover where the overburden stress due to the granular cover is small (less than 10 kPa), stability may not have been unduly compromised by the overcompaction. The results of the tests are further illustrated in Fig. 5 for the first lift. The degree of compaction achieved for the three lifts ranged from 93 to 99%. Moulding water contents were from 15 to 19.5%, giving an average of about 17.3%, which was 3.5% above optimum.

The till was placed on the entire pile during September 4–14, 1991. Placement was completed on the west, south, and east side slopes during September 3–10, 1991 when the weather was generally sunny with moderate temperatures. On the top part of the pile, however, only the first lift was completed during this period. A major rainstorm on September 10, 1991 resulted in wetting of the first lift. The wet till was subsequently excavated, allowed to dry, and recompacted prior to the placement of the second lift on September 14. Placement of the cover on the north side slope was completed last. Precautions were taken during placement to ensure that no damage was done to existing piezometer installations located in the top and north side of the pile.

Following the installation of the final lift, field hydraulic conductivity tests were performed in the till using a single ring infiltrometer similar to the type described by Fernuik and Haug (1990). Hydraulic conductivity values, obtained at two locations on the top of the pile, were of the order of 1.0×10^{-7} and 1.0×10^{-6} cm/s.

Granular cover

A granular cover consisting of clean sand and gravel was placed over the entire pile. Grain-size analysis indicated the granular cover to consist of 40% gravel, 58% sand, and 2% silt- and clay-size particles. Modified Proctor compaction

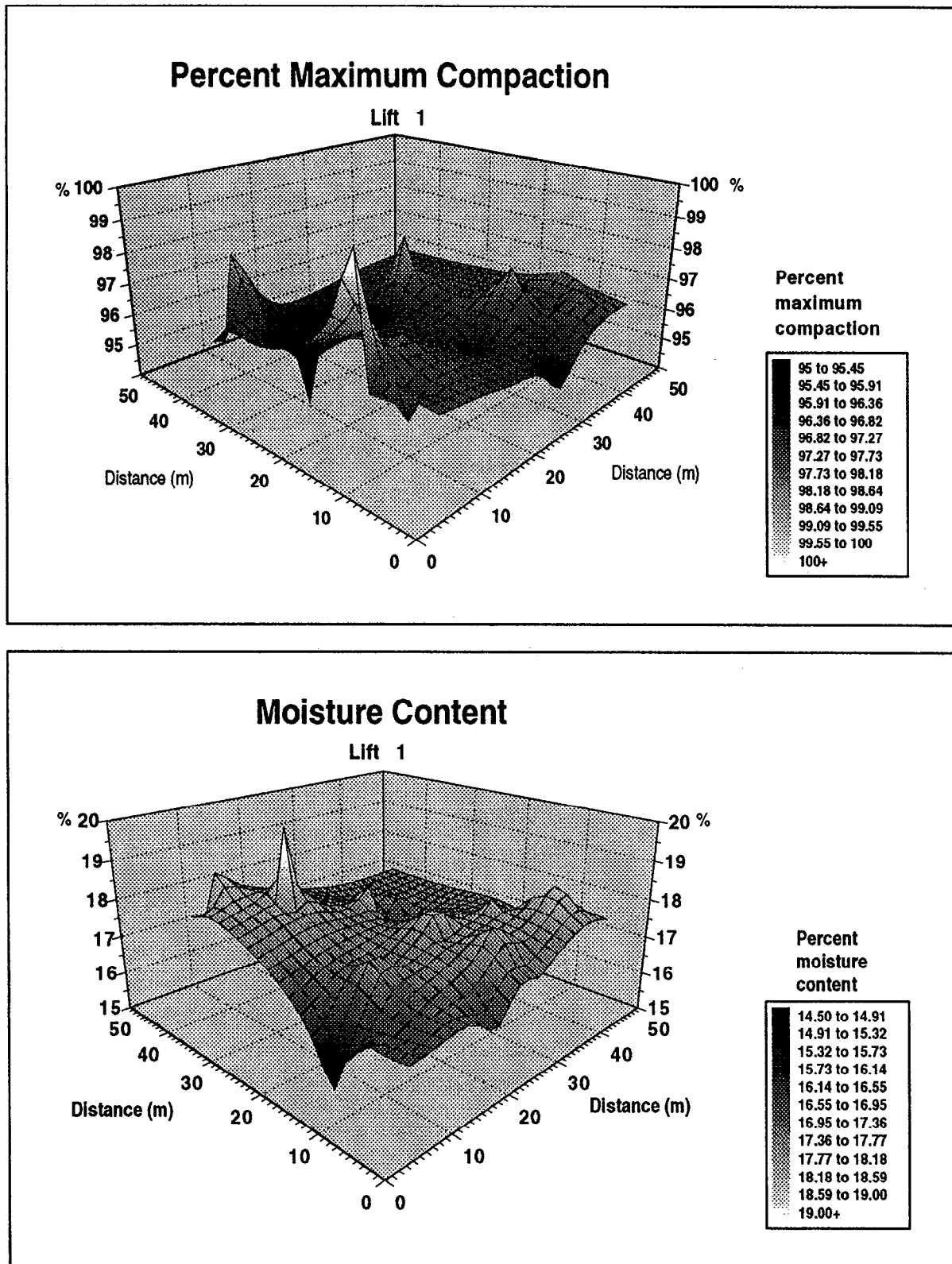


FIG. 5. Percent compaction densities and water content for first lift of impermeable cover.

tests gave a maximum dry density of 2.24 Mg/m^3 and an optimum water content of 6.5%.

The granular cover was placed in 15–20 cm thick lifts and compacted to at least 92% of the maximum dry density. This gravelly sand arrived on site in a dry condition

and had to be wetted during placement to achieve the desired compaction. The results of 29 in situ density tests conducted on the compacted granular cover indicated field densities ranged from 91 to 95% of the Modified Proctor maximum dry density and water contents were 3.0–6.4% of optimum.

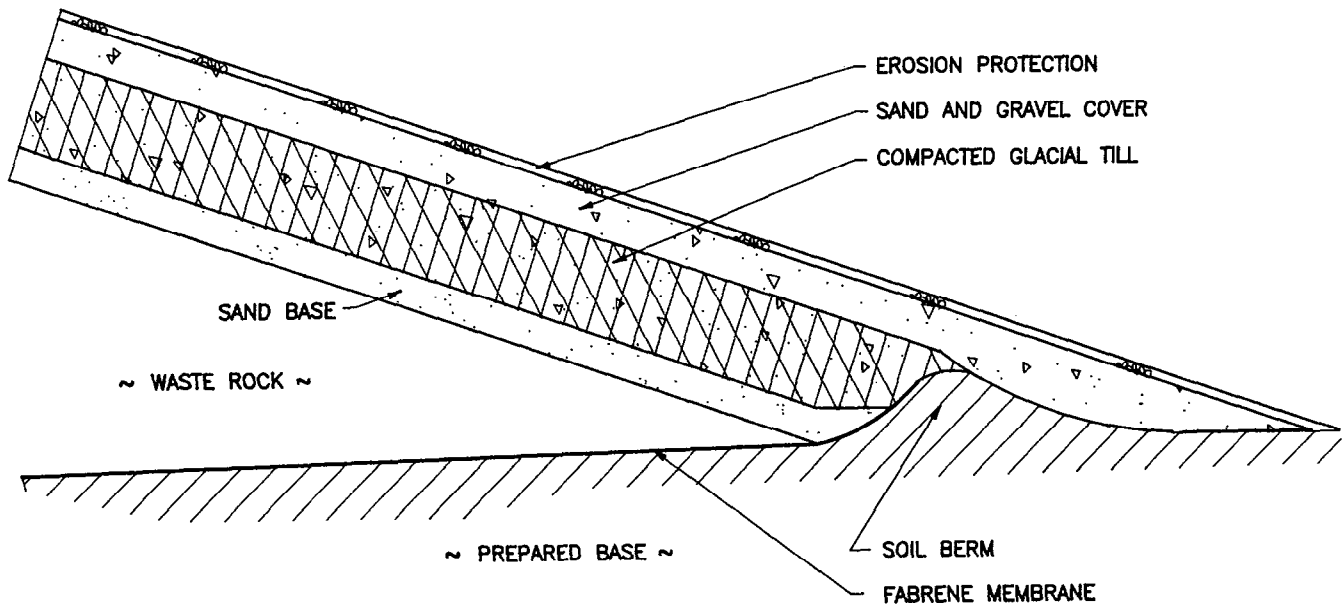


FIG. 6. A cross section of completed composite cover.



FIG. 7. Waste rock pile 7/12 before cover installation.



FIG. 8. Waste rock pile 7/12 after cover installation.

Erosion protection

A final 100-mm layer consisting of a well-graded gravel was added to the covered pile to provide erosion protec-

tion. This material was compacted with several passes of the vibratory compactor. A cross section of the completed composite cover is shown in Fig. 6. Photographs of the

TABLE 2. Instrumentation installed in cover and waste rock pile

Cover and pile parameters	Method
Soil suction	(1) Heat-dissipation sensors (2) Electrical-resistance sensors (gypsum blocks)
Moisture content	Time-domain reflectometry (TDR)
Gaseous oxygen	Portable oxygen meter and permanently emplaced sampling tubes
Temperature	Thermocouple sensors
Percolation through cover	Two collection-basin lysimeters, each 2.0 × 3.1 m, 6.2 m ² surface area, 9.8 m ³ volume, semicylindrical, acid-resistant, high-density polyethylene
Water quality	Outflow collection and laboratory analysis: (i) Lysimeters (percolation through cover) (ii) Pile perimeter drain (pile runoff, through the sand base) (iii) Pile base (percolation through the pile)
Meteorological parameters	
Rainfall	Tipping-bucket rain gauge
Evaporation	U.S. Class A evaporation pan
Air temperature	Thermistor
Relative humidity	Surface resistivity (of impervious solid) sensor
Wind	Three-cup anemometer
Automated monitoring system	
Parameters measured	Soil suction, moisture content, soil and air temperature, relative humidity, wind, rainfall, and pan evaporation
Data acquisition	Two Campbell Scientific, model CR10 data loggers Three Campbell Scientific multiplexers: (i) AM416 multiplexer for soil suction sensors, (ii) AM416 multiplexer for thermocouple sensors, (iii) SDMX50 multiplexer for TDR probes.
TDR measurement	Tektronix 1502B TDR metallic cable tester
Data retrieval	Telephone modem
Power	12 V dc (110 V ac source)

uncovered and covered piles are shown in Figs. 7 and 8, respectively.

Instrumentation

As part of the performance evaluation of the cover, instrumentation was installed to monitor four key parameters: (i) gaseous oxygen concentration in the pile and cover, (ii) the hydraulic properties of the cover, (iii) pile temperature, and (iv) the quality of the seepage from the pile. Table 2 lists the monitoring systems installed in the cover and the pile. The importance of these parameters is discussed in Yanful et al. (1993).

Two monitoring stations were established at the top of the pile, one on the east side and the other on the west side, about 10 m apart. Each station consisted of a lysimeter and a vertical profile nest of five monitoring units (Fig. 9). Gas-sampling probes were used to sample gaseous oxygen. Heat-dissipation sensors and electrical-resistance sensors (gypsum blocks) were used to measure soil suction. Time-domain reflectometry (TDR) was used to measure water content, and thermocouple sensors were used to measure temperature. The lysimeters were used to collect water that percolated through the cover. Drains were installed beneath the pile and along the perimeter of the pile to collect seepage and runoff, respectively.

Prior to the design and construction of the cover, several monitoring stations were established in the waste rock pile. Each station consisted of gaseous oxygen probes, temperature sensors, and piezometers. Monitoring of these stations began 2 years before and continued after the construction of the cover.

Lysimeter installation

Collection-basin lysimeters were installed at the two monitoring stations directly below the cover to measure the quantity of percolated water. Each lysimeter was designed to have a collection surface of 6.2 m² and a total volume of approximately 9.8 m³. These dimensions were chosen based on the assumption that less than 25% of the annual precipitation of about 1100 mm will infiltrate the cover.

A 3.8 mm diameter threaded outlet drain installed at the bottom of each lysimeter was connected to an extended transfer pipe that terminated at the base of the pile in an outfall structure. The lysimeter drain was lined with fine woven geotextile to prevent clogging. One lysimeter (on the east) was filled with gravel, whereas the other (on the west) was filled with the same sand as that used for the sand base. After the lysimeters were placed, the excavations were backfilled with sand (Fig. 10) and compacted with a hand compactor. The installed lysimeters cleared the surface of the pile by at least 25 mm on all four sides. The sand and gravel contained in the lysimeters were saturated with water prior to placement of the cover to ensure that no postconstruction infiltrated water was taken up in storage.

Outfall structure

A fabricated steel outfall structure was installed at the base of the pile on the north side to which all collection pipes from within the pile were connected. A total of four 3.8-mm collection pipes were connected to separate chambers in the outfall structure, with two pipes draining the lysimeters, one pipe from a perimeter ditch at the base of the pile and another from the centre of the pile. The separate

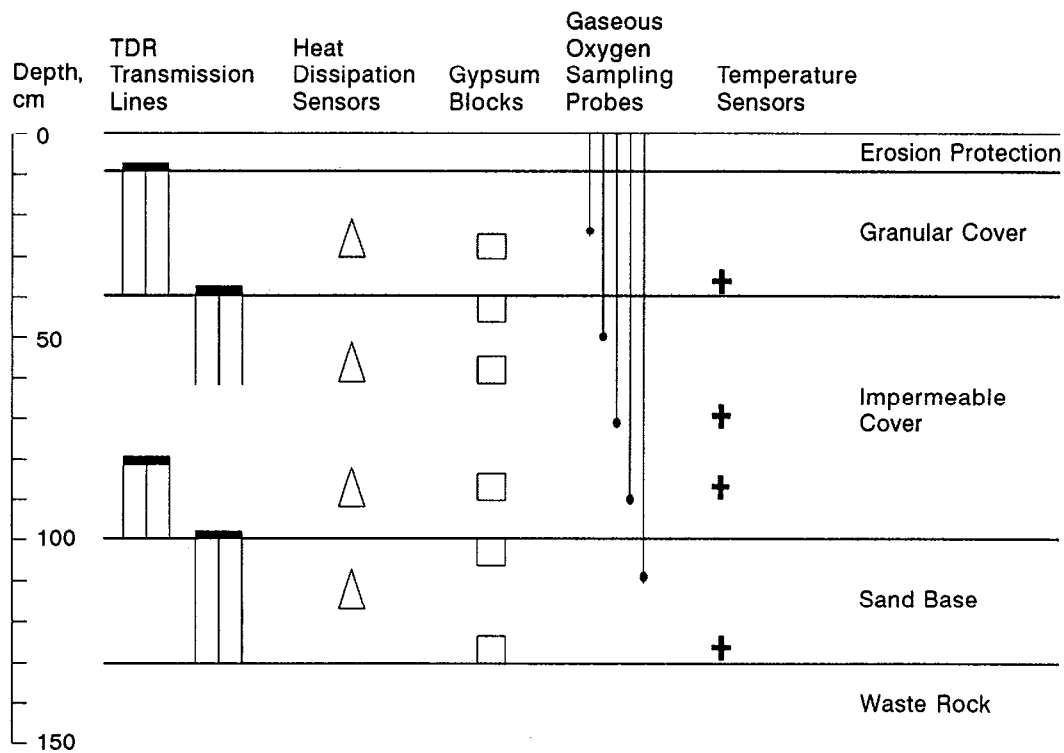


FIG. 9. Schematic representation of a vertical profile at an instrumented station.



FIG. 10. Backfilling of northeast lysimeters following installation.

chambers allow flow and water quality to be monitored individually. The cover of the outfall structure was insulated with 50-mm styrofoam, and all internal exposed surfaces were covered with fiberglass epoxy. Overflow from the outfall structure is directed to 100-mm drainage pipes sloping away from the site to a settling pond located nearby.

Gaseous oxygen

The gaseous oxygen concentration within the cover was determined with a Teledyne portable oxygen meter. A gas sample was extracted from a 6.3 mm diameter stainless steel tube permanently installed at the depth of interest. Five sampling tubes extending vertically to the centre of each

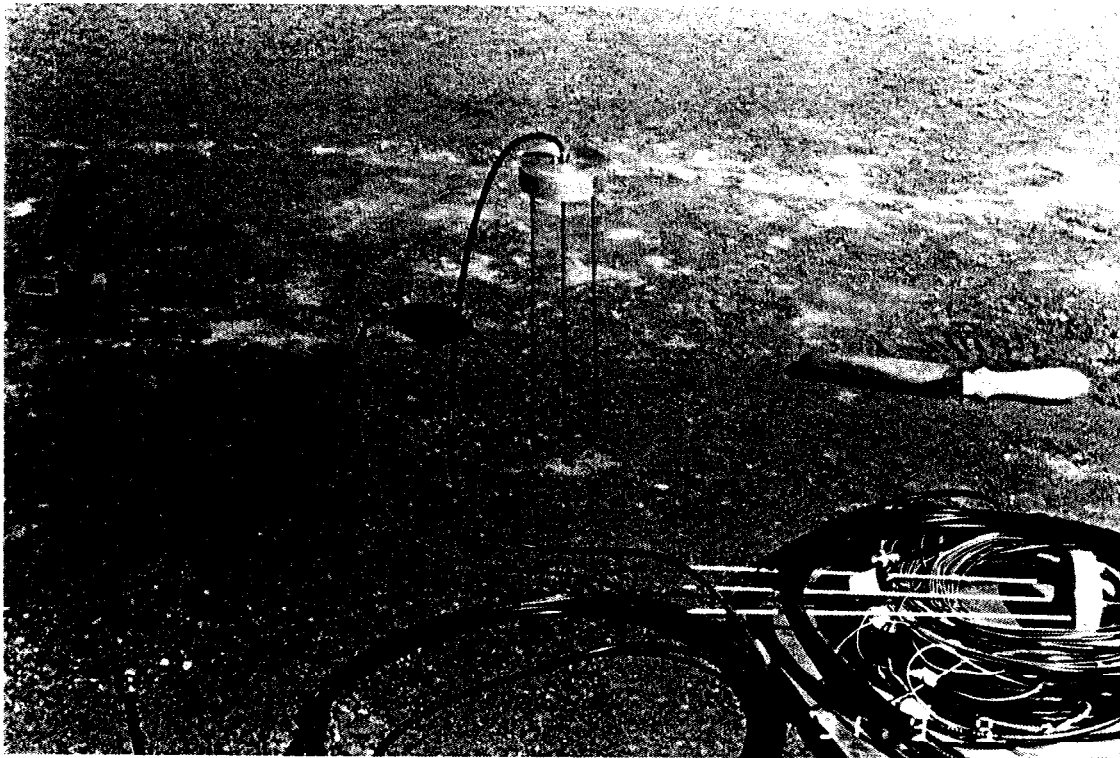


FIG. 11. A typical three-rod time domain reflectometry system for water-content measurements.

lift of the impermeable cover were installed at each station. The buried end of each tube was wrapped with fine, woven geotextile and placed in sand at the bottom of an augered hole. The hole was then backfilled by sealing to the surface with bentonite. The exposed sampling end of each tube was sealed with a rubber septum. A syringe was used to extract the gas sample, which was then immediately analyzed for oxygen on the meter.

Gas samplers installed in the waste rock, prior to the construction of the cover, were composed of 6.4 mm diameter, flexible, acid-resistant, noncollapsing, noprrene tubing. Each set of tubing was attached to a piezometer installed at the appropriate depth. The sampling ports were located at approximately 1.0, 1.5, 2, 3, 4, and 5 m below the top of the pile surface. Pore gas was pumped to the surface and measured with a Teledyne portable oxygen meter. When not being sampled, clamps were used to seal the surface ports from ingress of atmospheric oxygen.

Soil suction

Soil suction was measured by two methods: heat dissipation and electrical resistance. These methods measure a specific physical property of an absorbent or a porous block in equilibrium with the soil of interest. From these measurements, matric (or pressure) potential produced from the soil-water capillary forces can be determined. Soil suction, being the negative of matric potential, is defined in terms of the soil phase and is therefore a positive number. It is generally expressed as pressure (kPa or bars) or hydraulic head (metres of water or pF).

A heat-dissipation sensor measures the rate at which heat dissipates in a porous ceramic block. The development of the sensor is presented in Rahardjo et al. (1989). A sensor based on a design developed by Phene et al. (1971), which consists of a miniature heater and a thermocouple encased in

a porous ceramic block, was adapted. The thermal conductivity of the ceramic block is sensitive to its water content and can be related to soil suction. The temperature of the block is measured before and after a known quantity of heat is delivered to the block. More heat will dissipate through the block at higher water contents, resulting in a smaller increase in temperature (ΔT). If the soil loses water and the suction increases, then the water content of the sensor decreases and ΔT increases. Consequently, ΔT is proportional to the soil suction. Each sensor is unique in its relation to soil suction; therefore, a calibration is required prior to installation. Calibration procedures similar to those presented by Fredlund and Wong (1989) were followed.

An electrical-resistance sensor measures the electrical resistance of an absorbent block, commonly composed of gypsum (Bouyoucos and Mick 1940). Resistance is sensitive to the water content of the block; high water contents yield low resistance. When the block is in contact with soil, the electrical resistance varies inversely with soil suction. Electrical resistance, however, also varies with pore-water chemistry. Gypsum is used for two reasons: (i) its relatively low solubility contributes to the longevity of the sensor, and (ii) a saturated solution containing Ca^{2+} and SO_4^{2-} ions provides effective buffering at low pH. As a result, the variance of the resistance of a gypsum block, resulting from small changes in soil chemistry, has less significance than that of a block composed of an inert material. In general, individual gypsum blocks have similar response to soil suction; therefore a generalized calibration provided by the manufacturer was used.

Four heat-dissipation sensors were installed at each monitoring station, one in each sand layer and two in the till; and six gypsum blocks were installed, one in each sand layer, two in the till, and one at each sand-till contact. All sensors were installed as each lift was placed. Following

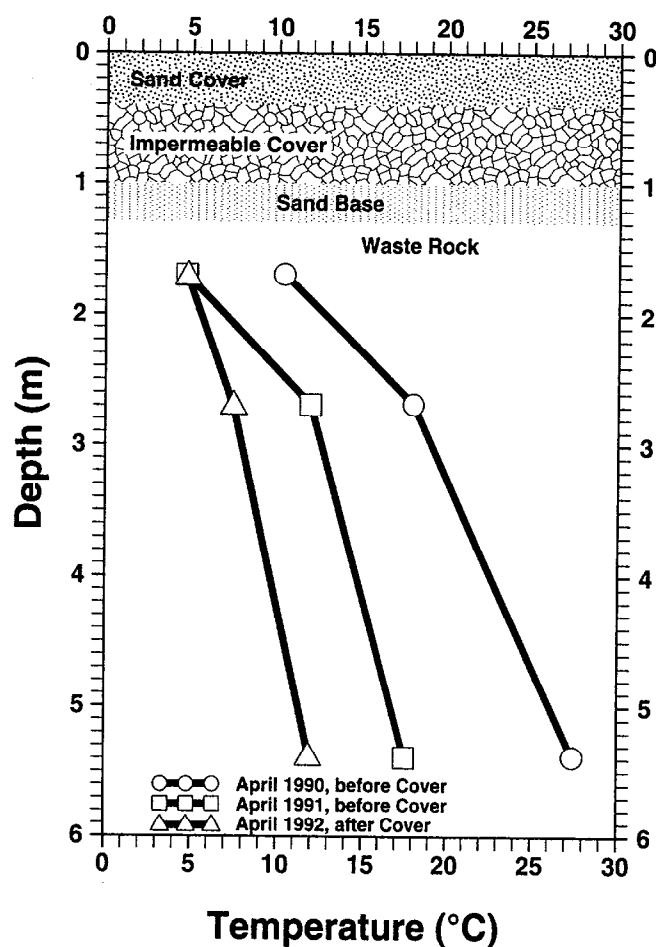
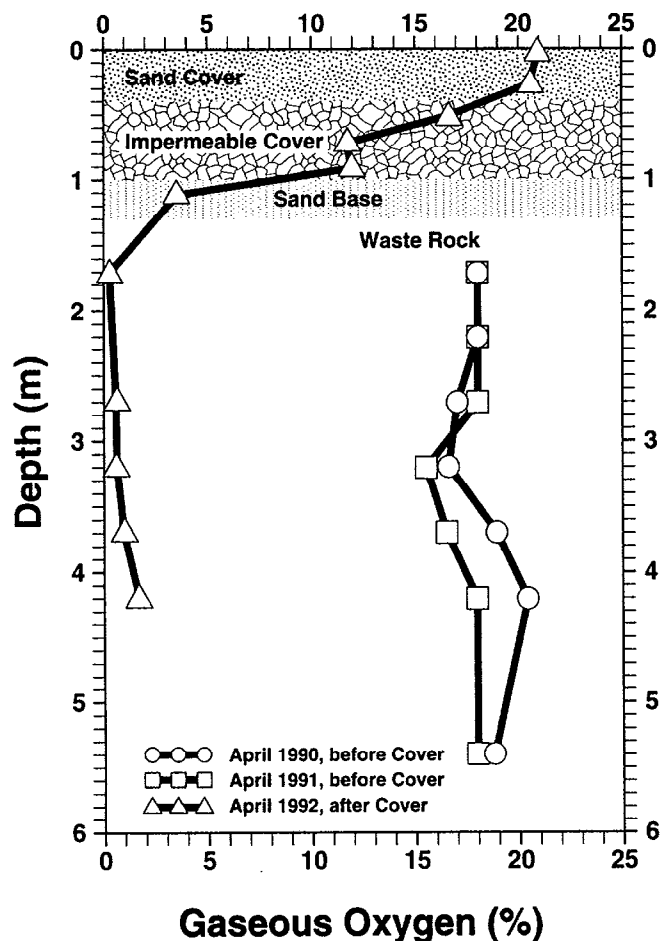


FIG. 12. Gaseous oxygen concentrations in pile 7/12 before and after cover installation.

FIG. 13. Temperature profiles in pile 7/12 before and after cover installation.

TABLE 3. Comparison of the quality of seepage from the pile before and after construction of the cover

Date	pH	Acidity (mg/L CaCO ₃)	Total Fe (mg/L)	SO ₄ ²⁻ (mg/L)
Before construction of the cover				
July 1989	2.4	44 000	5 100	43 440
Sept. 1989	2.8	30 500	2 800	28 000
May 1990	2.4	16 400	5 510	12 700
Sept. 1990	2.2	73 250	7 920	32 970
Oct. 1990	2.1	64 400	3 700	—
After construction of the cover				
Oct. 30 1991	2.3	54 450	19 590	71 042
June 29, 1992	2.4	35 000	10 500	5 140
Aug. 17, 1992	—	14 400	3 720	14 800
Sept. 29, 1992	2.9	15 800	5 250	15 400

NOTE: Construction of the cover was completed in October 1991.

compaction, a small-diameter (25 mm) hole was augered, the sensor installed in a soil slurry, and the hole backfilled and sealed to the surface with bentonite.

Moisture content

The moisture content of each layer of the soil cover was measured by time-domain reflectometry (TDR). TDR is a radar technique in which a fast rise time voltage pulse is propagated through the soil and its reflection measured. The pulse is guided through the soil by stainless-steel rods of

known dimensions. The measurement of travel time (Δt) yields an estimate of "apparent" dielectric constant (K_a) of the soil. The volumetric soil-moisture content (θ_v) is then calculated using a relation developed by Topp et al. (1980), or other soil-specific relations. A good review of the method can be found in Topp and Davis (1985).

A three-rod TDR probe system (Fig. 11) was adapted from Zegelin and White (1989). The rods were 30 cm long in the sand layers and 20 cm long in the till. The probes were placed in each layer horizontally as the cover was being constructed. Probes were installed in the top and bottom lifts of the till layer. The application of the voltage pulse and measurement of Δt were performed with a Tektronix 1502B TDR metallic cable tester. The unit was attached to a data logger to automate measurements.

Results to date

The effectiveness of the cover in reducing sulphide oxidation and acid generation can be assessed with the data collected to date:

- (i) gaseous oxygen concentrations in both cover and pile,
- (ii) moisture contents and suctions developed in the cover,
- (iii) temperatures within the pile, and
- (iv) quality and quantity of the runoff and percolated water reporting to the bottom of the pile (underdrain).

Gaseous oxygen concentrations measured before and after the placement of the cover (Fig. 12) clearly indicate the presence of the cover reduces oxygen penetration into the

TABLE 4. Hydraulic characteristics of the cover following construction

Layer	31 Oct. 1991		31 May 1991		26 Aug. 1992	
	West	East	West	East	West	East
Volumetric moisture content by TDR method (%)						
Granular cover	12	8	8	7	9	8
Impermeable layer, top 30 cm	30	32	25	30	nd	36
Impermeable layer, bottom 30 cm	34	30	27	26	31	30
Sand base	12	12	12	11	13	12
Matric suction by gypsum block method (kPa)						
Granular cover	10	10	60	40	30	30
Impermeable layer, 15 cm from top	30	10	30	30	100	30
Impermeable layer, 15 cm from bottom	10	10	30	20	20	20
Sand base	10	10	20	20	20	20

NOTE: Construction of the cover was completed in October 1991.
nd, no data available at this time.

TABLE 5. Rainfall and discharge of water from lysimeters underneath the cover

Date	Rainfall (mm)	West lysimeter		East lysimeter	
		Volume (L)	Depth (mm)	Volume (L)	Depth (mm)
24 June–14 July 1992	82	16.25	2.6	12.25	2.0
14 July–18 Aug. 1992	116	9.7	1.6	12.1	2.0
24 June–18 Aug. 1992	198	25.9	4.2	24.35	3.9

NOTE: The lysimeter surface area is 6.2 m².

waste rock. The oxygen levels in the pile decreased from a maximum of about 20% to less than 3% after placement of the cover. This substantial reduction in concentration implies a decrease in the oxygen flux which should, in turn, lead to a decrease in the mass of iron sulphide minerals (principally, pyrite and pyrrhotite) being oxidized. The quantity of acid produced is expected to decrease which will, in the long run, be reflected in the quality of seepage leaving the pile. The seepage will be characterized by reduced concentrations of iron and sulphate and less acidic pH levels. The transition period (elapsed time for the improvement in the seepage quality) will depend on the mass of stored acidity and flushing rates in the pile. The flushing rate is a function of the rate of percolation of precipitation through the cover. The transition period for the pile could be a few years because of the relatively low hydraulic conductivity of the compacted till. Thus, monitoring of gaseous oxygen concentrations is a useful tool for performance evaluation in the short term.

Table 3 compares the quality of seepage from the base of the pile before and after construction of the cover. The data indicate no significant change in water quality at the present time.

Temperatures in the pile decreased after the placement of the cover (Fig. 13). Oxidation of sulphide minerals is an exothermic reaction; therefore if it were not for the apparent climatic variability, this decrease in temperature would suggest a decrease in the rate of waste rock oxidation. Harries and Ritchie (1987) calculated heat sources from temperatures measured in White's dump located at the Rum Jungle mine site in Northern Australia. They correlated the heat sources to the rate of oxidation of pyrite in the dump: a heat source of 1 W m⁻³ was found to correspond to the

oxidation of 7×10^{-7} mol m⁻³ s⁻¹ of pyrite and the use of 2.4×10^{-6} mol m⁻³ s⁻¹ of gaseous oxygen. Heat sources calculated for active regions of the dump were in the range of 0.2–1.4 W m⁻³, prior to covering with a compacted clay. After placement of the cover, they found heat sources in the dump to be effectively zero at all depths, which was attributed to a zero oxidation rate. Future evaluation of the performance of the cover on pile 7/12 would include an analysis of temperature data with a heat-transfer model similar to the one used by Harries and Ritchie (1987).

Table 4 shows the soil-moisture data. Water contents of the till, measured in August of 1992, were generally similar to those taken immediately following construction of the cover, in October of 1991. The results do not show a trend of desaturation. The apparent decrease in moisture content of the impermeable layer, observed on May 31, 1992, is an artifact of the measurement technique. The TDR method measures unfrozen water content only. Part of the cover was still frozen in May which resulted in an artificially lower water content. The suction measurements show expected evaporation from the surface of the cover.

The lysimeter discharge data (Table 5) indicate that only a small portion of rainfall percolates through the cover. The lysimeter discharge for the period June 24 to August 18, 1992 was 2% of rainfall. This suggests that water is available to replenish evaporative losses from the cover. Thus, the impermeable cover is less likely to desaturate and oxygen fluxes are more likely to be low. The water-content data confirm the high saturation state of the impermeable cover.

Since the pile has a small surface area and steep slopes that are exposed to wind, little snow would tend to accumulate over winter. Indeed, during the winter of 1992, snow accumulation was observed to be most enhanced at the base of the

slope and on the leeward side of the cover. In addition, the cone shape minimizes ponding of water on the impermeable layer, thereby reducing percolation to the till. Water would, instead, tend to flow through the granular cover, down slope. These hydrologic conditions are more enhanced on top of the pile and could result in a low replenishment of water to the cover, thereby providing a worst-case scenario for this study.

Summary and conclusions

A composite soil cover was constructed on an acid-generating waste-rock pile located at the Heath Steele mine site near Newcastle, New Brunswick. The cover was constructed by compacting a glacial till in three lifts of 20 cm each on a sand base prepared on the levelled surface of the waste-rock pile. The compaction energy used yielded a minimum field dry density of at least 95% of the maximum Modified Proctor value. Moulding water contents were about 3% higher than the optimum value. A 30 cm thick gravelly sand layer was placed on the till followed by a final 10 cm thick erosion-protection layer.

Instrumentation was installed to measure the following parameters:

- (i) gaseous oxygen concentrations in both cover and pile,
- (ii) moisture contents and suctions developed in the cover,
- (iii) temperatures within the pile, and
- (iv) quality and quantity of the runoff and percolated water reporting to the bottom of the pile (underdrain).

Based on the monitoring results obtained to date, the following can be concluded.

- (1) The cover has reduced gaseous oxygen concentration in the pile from 20% to less than 3%.
- (2) The volumetric water content of the compacted till layer has remained essentially the same at about 32% since cover installation. The till continued to remain nearly fully saturated.
- (3) Infiltration through the cover observed during a 55-day wet period was about 2–2.5% of precipitation.
- (4) Reduced temperatures observed in the pile since cover installation appear to be a result of seasonal fluctuations. Continued monitoring will be required to confirm these data.
- (5) No significant change in the water quality of the seepage from the pile has been noted since cover installation.

These conclusions indicate that the placement of the cover has reduced the flux of oxygen and water to the waste rock, which suggests a reduction in oxidation and acid production in the pile. Long-term monitoring of quality of the seepage from the pile will be required to confirm the reduction in acid production because of the presently stored acidity and low percolation of water through the cover.

Acknowledgements

The project is being conducted as part of Canada's Mine Environment Neutral Drainage (MEND) program. Funding

is provided by Noranda Minerals Inc., New Brunswick Department of Natural Resources, and Canada Centre for Mineral and Energy Technology (CANMET).

- ASTM 1987a. Standard practice for dry preparation of soil samples for particle-size analysis and determination of soil contents. (D421-85). In 1987 Annual Book of ASTM Standards, Sect. 4. Vol. 04.08. ASTM, Philadelphia. pp. 113–114.
- ASTM 1987b. Standard method for particle-size analysis of soils. (D422-63). In 1987 Annual Book of ASTM Standards, Sect. 4. Vol. 04.08. ASTM, Philadelphia. pp. 115–125.
- ASTM 1987c. Standard test methods for moisture-density relations of soils and soil aggregate mixtures using 10–16 (4.54 kg) rammer and 18 in (457-mm) drop (D1557-78). In 1987 Annual Book of ASTM Standards, Sect. 4. Vol. 04.08. ASTM, Philadelphia. pp. 280–290.
- Bouyoucous, G.J., and Mick, A.H. 1940. An electrical resistance method for continuous measurement of soil moisture under field conditions. Michigan Agricultural Experiment Station, Technical Bulletin No. 172.
- Ferriuk, N., and Haug, M.D. 1990. Evaluation of *in situ* permeability testing methods. ASCE Journal of Geotechnical Engineering, **116**(2): 297–311.
- Fredlund, D.G., and Wong, D.K.H. 1989. Calibration of thermal conductivity sensors for measuring soil suction. Geotechnical Testing Journal, **12**(3): 188–194.
- Harries, J.R., and Ritchie, A.I.M. 1987. The effect of rehabilitation on the rate of oxidation of pyrite in a mine waste rock dump. Environmental Geochemistry and Health, **9**(2): 27–36.
- Holtz, R.D., and Kovacs, W.D. 1981. An introduction to geotechnical engineering. Prentice-Hall, Inc., Englewood Cliffs, N.J.
- Phene, C.J., Hoffman, G.H., and Rawlins, S.L. 1971. Measuring soil matric potential *in situ* by sensing heat dissipation within a porous body: I. Theory and sensor construction. Soil Science Society of America, Proceedings, **35**: 27–33.
- Rahardjo, H., Loi, J., and Fredlund, D.G. 1989. Typical matric suction measurements in the laboratory and the field using thermal conductivity sensors. Proceedings of the Indian Geotechnical Conference, 14–16 Dec. 1989, Visakhapatnam, India. Vol. 1. pp. 127–131.
- Topp, G.C., and Davis, J.L. 1985. Time domain reflectometry (TDR) and its application to irrigation scheduling. In Advances in irrigation. Vol. 3. Academic Press, Inc., New York. pp. 107–127.
- Topp, G.C., Davis, J.L., and Annan, A.P. 1980. Electromagnetic determination of soil moisture content by TDR: Measurements in coaxial transmission lines. Soil Science Society of America Journal, **46**: 672–678.
- Yanful, E.K., Bell, A.V., and Woyshner, M.R. 1993. Design of a composite soil cover for an experimental waste rock pile near Newcastle, New Brunswick, Canada. Canadian Geotechnical Journal, **30**: 578–587.
- Zegelin, S.J., and White, I. 1989. Improved field probes for soil water content and electrical conductivity measurement using time-domain reflectometry. Water Resources Research, **25**(11): 2367–2376.

1993: Yanful, E.K., Bell, A.V. and
Woyshner, M.R.

Design of a composite soil cover for an
experimental waste rock pile near
Newcastle, New Brunswick, Canada.
Can. Geot. J., Vol. 30, pp. 578-587.

Design of a composite soil cover for an experimental waste rock pile near Newcastle, New Brunswick, Canada

ERNEST K. YANFUL

Noranda Technology Centre, 240 Hymus Boulevard, Pointe-Claire (Québec), Canada H9R 1G5

ALAN V. BELL

Nolan, Davis and Associates (NS) Limited, 7020 Mumford Road, Halifax, N.S., Canada B3L 4S9

AND

MARK R. WOYSHNER

2110 rue Clark, Unit 1, Montréal (Québec), Canada H2X 2R7

Received September 15, 1992

Accepted March 30, 1993

The Heath Steele Waste Rock Project was initiated in 1989 under Canada's Mine Environment Neutral Drainage (MEND) Program to develop and test strategies for managing acid-generating waste rock. The multiphase project involved the identification and selection of a few waste rock piles for field evaluation at the Heath Steele mine site located at about 50 km northeast of Newcastle, New Brunswick. As part of the evaluation, a 0.25-ha acid-generating pile, pile 7/12, was relocated and reconstructed on an impermeable synthetic membrane by end dumping from the perimeter and pushing into the middle section. The pile, which contains about 14 000 t of mine waste rock, has been producing an acidic seepage characterized by high dissolved iron (3.5–13.5 g/L) and sulphate (12.7–43.4 g/L) concentrations. Following the definition of the baseline acid-generating characteristics of the pile and laboratory investigation of potential soil cover materials in the vicinity of the site, a three-layer cover design is proposed. The design calls for a 60 cm thick saturated impermeable cover sandwiched between a 30 cm thick sand base and a 30 cm thick, overlying granular layer. The principal objectives of the design are to obtain a low gas diffusion coefficient to minimize oxygen fluxes and, also, to attain a low hydraulic conductivity to reduce infiltration into the pile. Both objectives can be achieved by compacting the impermeable cover at a density of 95% of Modified Proctor or greater and a water content slightly higher than the optimum value. The design of the cover and the anticipated resulting low gaseous-oxygen fluxes are confirmed by one-dimensional diffusion modelling. The potential for the impermeable layer to remain nearly fully saturated, even under an evaporative flux, is demonstrated by flow modelling. It is noted that the assessment of the durability of the cover with respect to variable climatic conditions (drying, freezing, and thawing) is a critical component of the performance evaluation.

Key words: acid rock drainage, soil cover, capillary barrier, oxygen flux, infiltration.

Le projet Heath Steele Waste Rock a été amorcé en 1989 dans le cadre du programme Neutralisation des eaux de drainage dans l'environnement minier (NEDEM) du Canada pour développer et tester des stratégies pour la gestion des stériles de roches générateurs d'acide. Le projet multiphase a impliqué l'identification et la sélection de quelques piles de stériles rocheux pour une évaluation du site minier de Heath Steele localisé à environ 50 km au nord-est de Newcastle, Nouveau-Brunswick. Comme partie de l'évaluation, une pile de 0,25 ha de stériles générateurs d'acide, pile 7/12, a été relocalisée et reconstruite sur une membrane synthétique par déversement arrière à partir du périmètre et en poussant les stériles vers la section centrale. La pile qui contient environ 14 000 tonnes de stériles rocheux produisait une infiltration acide caractérisée par des concentrations élevées de fer (3,5–13,5 g/L) et de sulfate (12,7–43,4 g/L) en solution. À la suite de la définition des caractéristiques de génération d'acide à la base de la pile, et d'investigation en laboratoire de sols qui ont un potentiel comme matériau de couvert à proximité du site, une conception de couvert à trois couches est proposée. La conception fait appel à un couvert imperméable saturé de 60 cm d'épaisseur en sandwich entre une fondation de sable de 30 cm d'épaisseur et une couche granulaire susjacente de 30 cm d'épaisseur. Les principaux objectifs de la conception sont d'obtenir un faible coefficient de diffusion du gaz pour minimiser le flux d'oxygène et aussi pour atteindre une faible conductivité hydraulique de façon à réduire l'infiltration dans la pile. Les deux objectifs peuvent être atteints en compactant le couvert imperméable à une densité de 95% du Proctor modifié ou plus grande, et à une teneur en eau légèrement inférieure à la valeur optimale. La conception du couvert et le faible flux gazeux d'oxygène anticipé qui en résulte sont confirmés au moyen d'un modèle unidimensionnel de diffusion. Le potentiel pour la couche imperméable de demeurer presque complètement saturée, même sous un flux d'évaporation, est démontré par une modélisation d'écoulement. L'on note que l'évaluation de la durabilité du couvert dans des conditions climatiques variables (séchage, gel et dégel) est une composante critique de l'évaluation de la performance.

Mots clés : drainage de roche acide (ARD), couvert de sol, barrière capillaire, flux d'oxygène, infiltration.

[Traduit par la rédaction]

Can. Geotech. J. 30, 578–587 (1993)

Introduction

The management of waste rock produced from the mining of sulphidic base-metal ores in underground and open-pit operations poses an environmental challenge to mining com-

panies. Iron sulphide minerals (principally pyrite and pyrrhotite) contained in the rock may oxidize upon contact with oxygen and air to produce an acidic solution containing high concentrations of dissolved ferrous iron and sulphate:

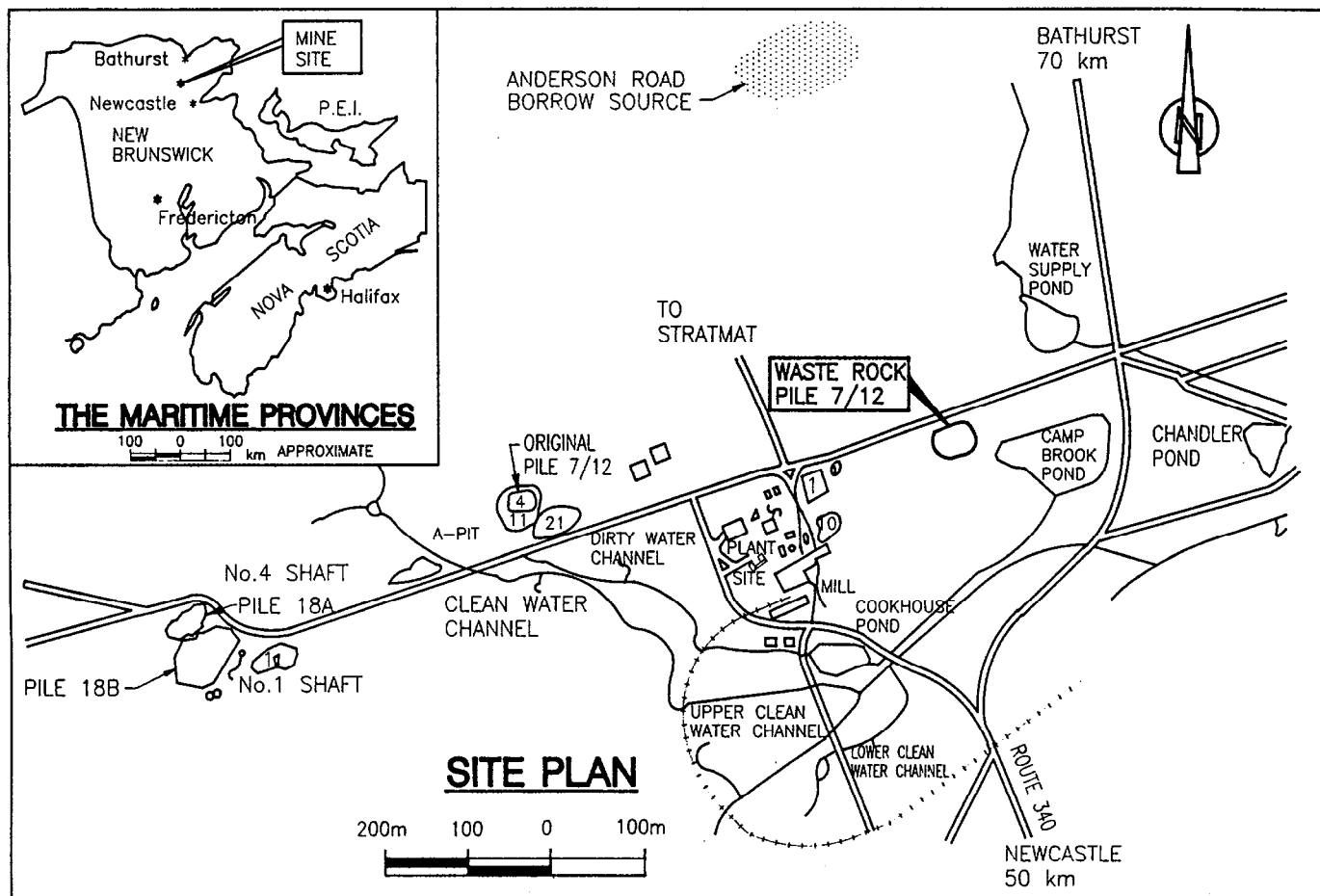
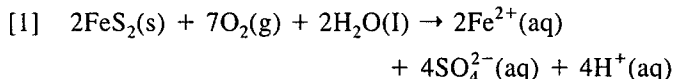


FIG. 1. Location of Heath Steele mine site and waste rock pile 7/12.



The ferrous iron (Fe^{2+}) may in turn oxidize to ferric iron (Fe^{3+}) under bacterial mediation at low pH (1.5–3.5) conditions. The ferric iron released into solution can oxidize other heavy-metal sulphides present, such as galena (PbS), sphalerite (ZnS), and chalcopyrite (CuFeS_2). The final acidic solution seeping from the rock may therefore also contain high concentrations of heavy metals. This solution is generally referred to as acid rock drainage (ARD) and is considered the single largest environmental problem facing the mining industry (Filion and Ferguson 1989).

Generally, the waste rock is left underground after mining, or in the case of open pits it is piled on the ground surface and any acidic seepage produced is collected and treated by lime neutralization. At cessation of mining operations, the pile may be decommissioned either by covering or by continuing the collection and treatment of the seepage. In recent years, waste-rock decommissioning practices have also involved moving the rock back into the pit and flooding. Flooding requires successfully maintaining a certain depth of water above the acid-generating rock in the pit. This may be difficult if the bedrock in the pit area is fractured or if excessive drought conditions occur. Sometimes the residual iron sulphide minerals in the exposed pit walls oxidize, requiring further treatment of the pit water. Most cases of waste rock covering involve the use of engineered soil

covers. The principal function of these covers is to minimize the transport of oxygen and water into the rock.

In 1989 a program was initiated by Brunswick Mining and Smelting Corporation Limited to develop and test strategies for long-term management of several acid generating waste rock piles located at the Heath Steele mine site. The program was conducted in four phases under the auspices of Mine Environment Neutral Drainage (MEND), Canada's national task force for ARD research (Filion and Ferguson 1989; Wheeland and Feasby 1991). The four phases comprised the selection of a few rock piles for field trials, definition of physicochemical characteristics of the selected piles; identification and evaluation of suitable candidate soils for a cover; and the design, installation, and monitoring of the cover on a selected pile.

This paper deals with the design of the composite soil cover installed on the selected waste rock pile, pile 7/12. Modelling results used in the design are discussed along with the geotechnical specifications for the cover materials. The physicochemical characteristics of the waste rock pile, prior to cover installation, and the history of mining and milling operations at the Heath Steele mine are briefly discussed. The construction, instrumentation, and monitoring of the cover are described in Yanful et al. (1993).

Site location and history

The Heath Steele mine site is located approximately 50 km northwest of Newcastle, New Brunswick, and about 60 km

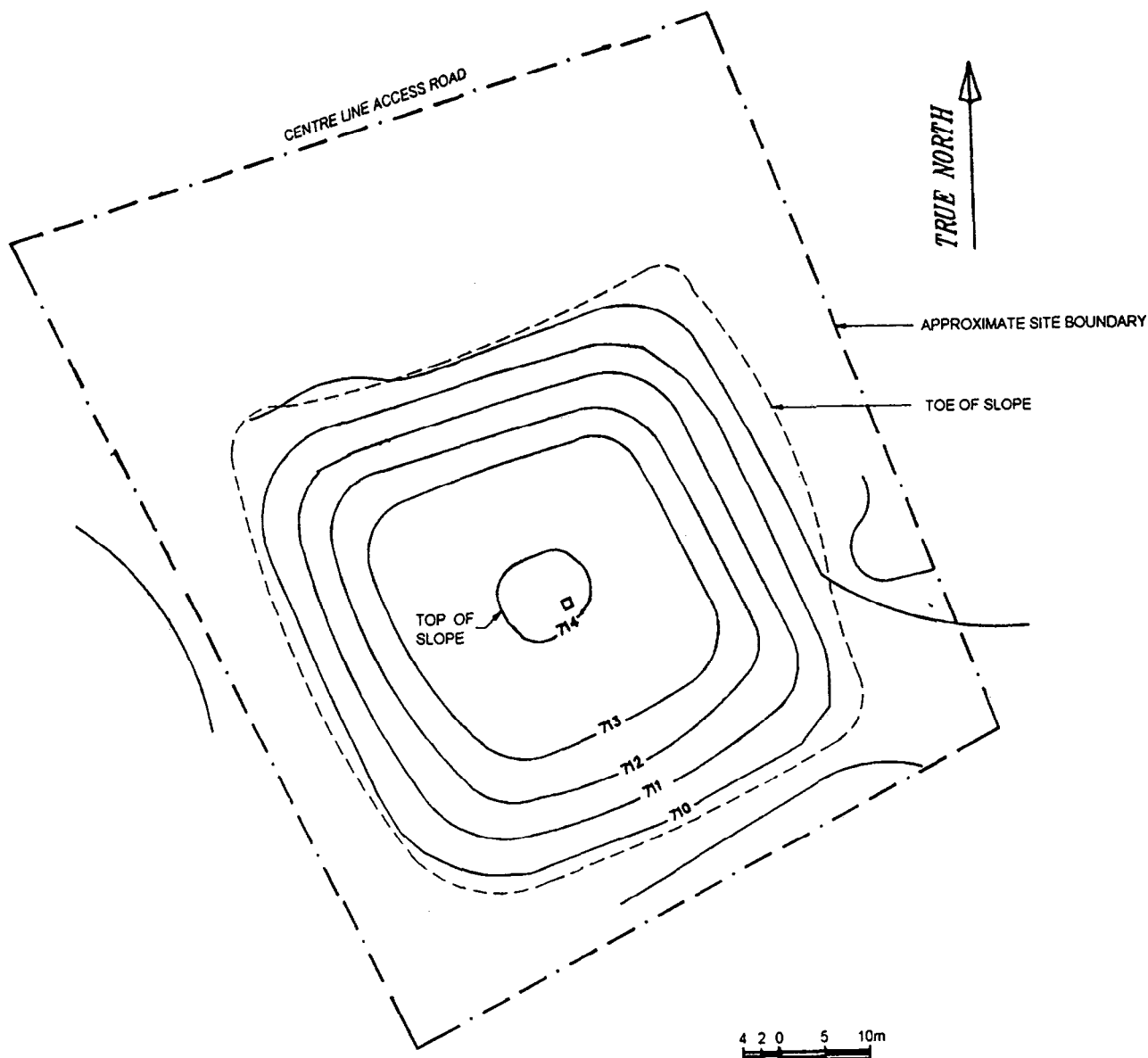


FIG. 2. Configuration of pile 7/12. Contours are in metres.

southwest of Bathurst, within the drainage basin of the Northwest Mirimichi River (Fig. 1). Massive sulphide ore deposits at the site were discovered in 1953. Mine development commenced in 1955 and ore beneficiation in 1957. Operations were suspended twice between 1958 and 1984 as a result of low base-metal prices and metallurgical problems encountered in the processing of oxidized portions of the ore. During suspension of production in May 1983, milling was continued with a modification of the concentrator to process silver-gold gossan ore that had been stockpiled on site for over 20 years. Processing of the gossan ore continued until October 1984. Following a lengthy shut-down, operations resumed in September 1989. Surface water and mine drainage from the site are collected by means of a comprehensive site-drainage collection system and pumped either to the mill for recycling or to the tailings pond for treatment.

In total, some 750 000 t of potentially acid-generating waste rock and reject ore are currently stockpiled in more than 20 piles at the site. The total projected waste-rock

TABLE 1. Physicochemical characteristics of relocated waste-rock pile 7/12

Surface area	2100 m ²
Average depth	2.9 m
Maximum depth	5.0 m
Estimated volume	6200 m ³
Estimated tonnage ^a	14 700 t
Sulphide mineralogy	
Pyrite	7-10%
FeS	5-7%
Pyrrhotite	<1%
Other sulphides (galena, sphalerite, etc.)	<1%
Total sulphur	5%
Theoretical acid production (as CaCO ₃)	210.7 kg/t
Acid consumption (as CaCO ₃)	0.4 kg/t

^aBased on a rock density of 2.35 t/m³.

inventory at closure in 1994 (including waste rock from active operations) is 2.3 Mt.

TABLE 2. Summary of water-quality data for pile 7/12 from the period July 1989 – October 1990

	Surface runoff	Underdrains
pH	2.0–3.0	2.1–2.8
Acidity (as CaCO ₃) (mg/L)	22 000 – 67 850	15 800 – 73 250
Sulphate (mg/L)	22 970 – 70 500	12 700 – 43 440
Dissolved iron (mg/L)	3600 – 18 800	3510 – 13 767

Waste-rock pile 7/12

Pile 7/12 was one of the four acid-generating waste rock piles at Heath Steele mine selected for monitoring and evaluation of remedial measures. It is located approximately 1 km from the Heath Steele mill complex off the main haul road (Fig. 1). The pile was moved to its present location and reconstructed in June 1989 as part of an ongoing test program to evaluate soil covers. It was placed on a prepared sand base, underlain by an impermeable membrane, by truck end dumping from the perimeter and pushing into the middle section with a loader. Placement on the impermeable membrane would permit the collection of leachate at the base of the pile before and after placement of the soil cover. Reconstruction included recontouring the pile to a maximum slope of approximately 3:1 (*H:V*). It was also isolated from the influence of any neighbouring topographical features. The reconstruction resulted in a more uniform pile configuration that was likely to minimize any shape-induced effects on the monitoring results and also facilitate the placement of monitoring instrumentation. A perimeter ditch was also constructed to allow for separate collection of surface runoff. The pile configuration prior to installation of the cover is presented in Fig. 2.

The relocated pile contains approximately 14 000 t of pyritic waste rock with maximum depth of 5 m. The predominant constituent sulphide mineral is pyrite (FeS₂), and total sulphur content averages about 5%. The physico-chemical characteristics of the pile are presented in Table 1. The pile was instrumented with seven sets of thermocouples and six sets of pore-gas samplers. It is the only pile at the mine for which a water and contaminant balance can be determined and was therefore selected for cover placement and monitoring.

Although pile 7/12 has a maximum height of only 5 m, pre-cover temperature and gaseous oxygen data indicated behaviour similar to large waste rock dumps (of average height of 20 m) at the Rum Jungle site in Australia (Harries and Ritchie 1981, 1985). For instance, oxygen concentrations within the pile were found to be high enough (up to 19%) to allow oxidation to occur. Elevated temperatures tended to occur at locations where low oxygen concentrations were observed, confirming the exothermic nature of the oxidation process. In addition, thermal convection was found to be an important mechanism for oxygen transport into the pile through the base.

Waste-rock oxidation and cover requirements

Pile 7/12, like the other acid-generating waste-rock piles at Heath Steele mine, has already started oxidizing and presumably contains a large volume of stored acidity. Water quality of underdrain flows reported for the period April–October 1990 showed pH values in the range of 2.1–2.5, sulphate levels of 17 000 – 33 000 mg/L, and dissolved-

iron levels of 3000 – 17 000 mg/L. Acidity, which is a measure of the total concentration of dissolved species capable of consuming alkaline materials, ranged from 16 000 to 73 000 mg/L. Surface runoff was also characterized by low pH and high acidity, sulphate, and iron (Table 2). These chemical characteristics are definitely indicative of acidic conditions. The mineralogical data (Table 1) also indicate that there is a substantial amount of unoxidized sulphide minerals left in the pile. Therefore, the two key aspects of an effective cover system are the control or mitigation of water infiltration and oxygen ingress into the pile. High infiltration rates would flush out large volumes of stored acid, resulting in high treatment costs. Residual iron sulphide minerals left in the pile will oxidize if the pile is exposed to air and moisture. Placement of an effective soil cover will decrease both infiltration and oxygen flux into the pile. Although the cover could decrease further oxidation to an insignificant level, release of stored acidity would continue, probably at a reduced rate, for a few years.

For the cover to be effective, it should have a low hydraulic conductivity and a high degree of water saturation. The high saturation results in a low oxygen diffusion coefficient which, in turn, leads to a low oxygen flux, since the flux F is proportional to the effective diffusion coefficient D_e according to Fick's first law:

$$[2] \quad F = -D_e \frac{\delta C}{\delta z}$$

where C is the gaseous oxygen concentration in the pores, and z is the distance in the direction of diffusion.

The cover will remain effective as long as it retains the properties of low hydraulic conductivity and high saturation. In adverse climatic conditions such as drying, freezing and thawing, these requirements may not be met in a single-layer cover. Moisture losses by evaporation and drainage will lead to desaturation and, possibly, cracking. Covers constructed from soils with high plasticities may develop shrinkage cracks upon freezing (Chamberlain and Gow 1979). The integrity of such covers could also be adversely affected by differential settlement of the underlying waste rock. Differential settlement may not be a major problem in pile 7/12 because of its small size. However, other aspects of the performance evaluation of the cover (such as the effects of freezing and thawing and reductions in temperature following cover placement) would still be applicable to other waste-rock piles. Vick (1983) noted that mill tailings, because of their low cohesion, could tolerate up to 1 m of settlement without fracturing. This would seem to suggest that covers constructed from soils with low cohesion such as silts would undergo less cracking as a result of differential settlement in the underlying waste.

In mill tailings where the grain-size distribution is finer than in waste rock, the water table can occur close to the

ground surface and could result in a substantial portion of a cover being saturated by capillarity. In a waste-rock pile, the large pores would preclude this possibility; therefore, maintenance of high saturation in the cover becomes a major design and construction challenge.

Another important factor that has to be considered is the upward transfer of heat generated in the pile as a result of sulphide oxidation. High temperatures (up to 56°C) have been observed in waste-rock piles in Australia (Harries and Ritchie 1981). Much higher temperatures (in excess of 80°C) have been reported for dumps of low-grade copper in Bulgaria (Groudev et al. 1978) and in the United States (Beck 1967). Temperature monitoring in Heath Steele pile 7/12, prior to the placement of the cover, indicated values up to 48°C within the pile. These elevated temperatures can be attributed to the heat released by sulphide oxidation reactions within the piles. The presence of an effective oxygen barrier such as a cover on the pile may curtail sulphide oxidation and heat production. On the other hand, if the cover becomes ineffective as a result of desaturation or cracking, heat released from oxidation may be available for upward transfer to the overlying cover and lead to further deterioration.

These foregoing requirements put severe constraints on the availability of suitable candidate cover materials. It would seem that the most desirable material for a waste-rock pile cover will be a silty soil with a low clay content. An important design consideration for such soils will be the potential for frost heaving. One approach will be to place the cover below the zone of frost penetration and overlay it with a coarse-grained soil layer. The depth of frost penetration can reach 2 m in parts of eastern Canada. In New Brunswick, the expected frost penetration is about 1.2 m (Crawford 1968). In most waste rock rehabilitation projects, placement of the entire cover below the depth of frost penetration will be economically unacceptable, since it will require a fairly thick (of the order of 2 m) and therefore expensive cover system. Therefore, a field pilot study such as described in this paper provides a good opportunity to assess the effects of freezing and thawing on the durability of a soil cover, at least for the scale under consideration.

Design of composite soil cover

Moisture drainage characteristics

As part of the Heath Steele Waste Rock Project, several soil-cover design scenarios were investigated. The design philosophy was based on the concept of the capillary barrier. In a capillary barrier, a coarse-grained soil layer underlying a fine-grained layer is relied upon to reduce moisture loss in the latter by drainage. The coarse layer has a higher air-entry pressure ψ_a and is the first to start draining as the pressure head in the system becomes negative. The air-entry pressure is the pressure required to initiate drainage, and any soil initially saturated will not drain unless the applied suction exceeds ψ_a (Rasmuson and Eriksson 1986; Nicholson et al. 1989). Figure 3 shows moisture drainage curves for a till and a sand obtained from the Heath Steele mine site used in the design of the cover. The curve for the sand was obtained from laboratory measurements. Attempts to obtain a reliable drainage curve for the till were unsuccessful because of consolidation of the sample during testing. The curve for the till was therefore derived from the literature (Gillham 1984; Nicholson et al. 1989) and by estimating

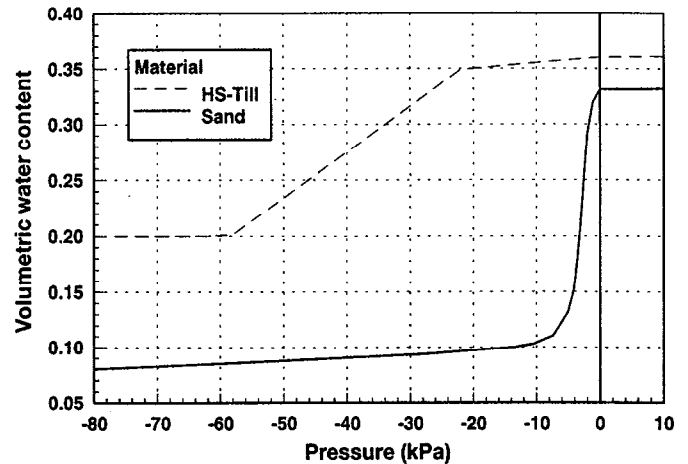


FIG. 3. Moisture drainage characteristics of Heath Steele till (HS-Till) and sand.

the air-entry value from data presented by Lambe and Whitman (1969).

In a fully saturated cover system consisting of the Heath Steele till underlain by sand, the sand will begin to drain as the suction exceeds -10 cm. As more suction is applied the sand will continue to drain until it attains its residual water content θ_r of about 10%. As shown, this will occur at a pressure head close to -50 cm. Since ψ_a of the till is higher than -50 cm, it will remain saturated at this pressure head. The thickness of the till, H_i , that will remain saturated in this simple two-layer cover system, ignoring evaporation for the time being, can be estimated as follows:

$$[3] \quad H_i = \theta_r - \psi_a$$

To reduce evaporation from the till, it may be overlain by a coarse-grained layer. Following rainfall and considerable infiltration, the rate of moisture loss by evaporation is initially high but decreases with time. Work done by Wilson (1990) and ongoing laboratory measurements at the Noranda Technology Centre confirmed this phenomenon. Unpublished data obtained from another site with a similar three-layer cover system by Noranda Technology Centre personnel have indicated suction values in the range of 8 m of water (78.5 kPa) in an upper sand layer. Laboratory measurements at lower evaporation rates gave much lower suctions, typically 3 m of water (29 kPa). These suctions are higher than that of the upper coarse layer at residual saturation. Wilson (1990) made empirical calculations to show that, at suctions exceeding 10 kPa the unsaturated hydraulic conductivity of a sandy soil is lower than 1×10^{-8} cm/s. The low hydraulic conductivity of the sand, and the fact that that of the compacted underlying till is also low will result in a low net flux of water from the till.

Figure 4 depicts the results of saturated-unsaturated flow modelling of the three-layer cover design proposed for pile 7/12. The underlying and overlying sands were each assigned a thickness of 30 cm, whereas a thickness of 60 cm was used for the till. An evaporative flux function consisting of a maximum of about 5 mm/day, which dropped gradually to almost zero over a period of 60 days (Fig. 5), was stipulated for the upper sand surface. The evaporation function was obtained from laboratory column measurements. As shown in Fig. 4, although very high suctions are developed in the upper sand (up to 30 m of water), the till layer

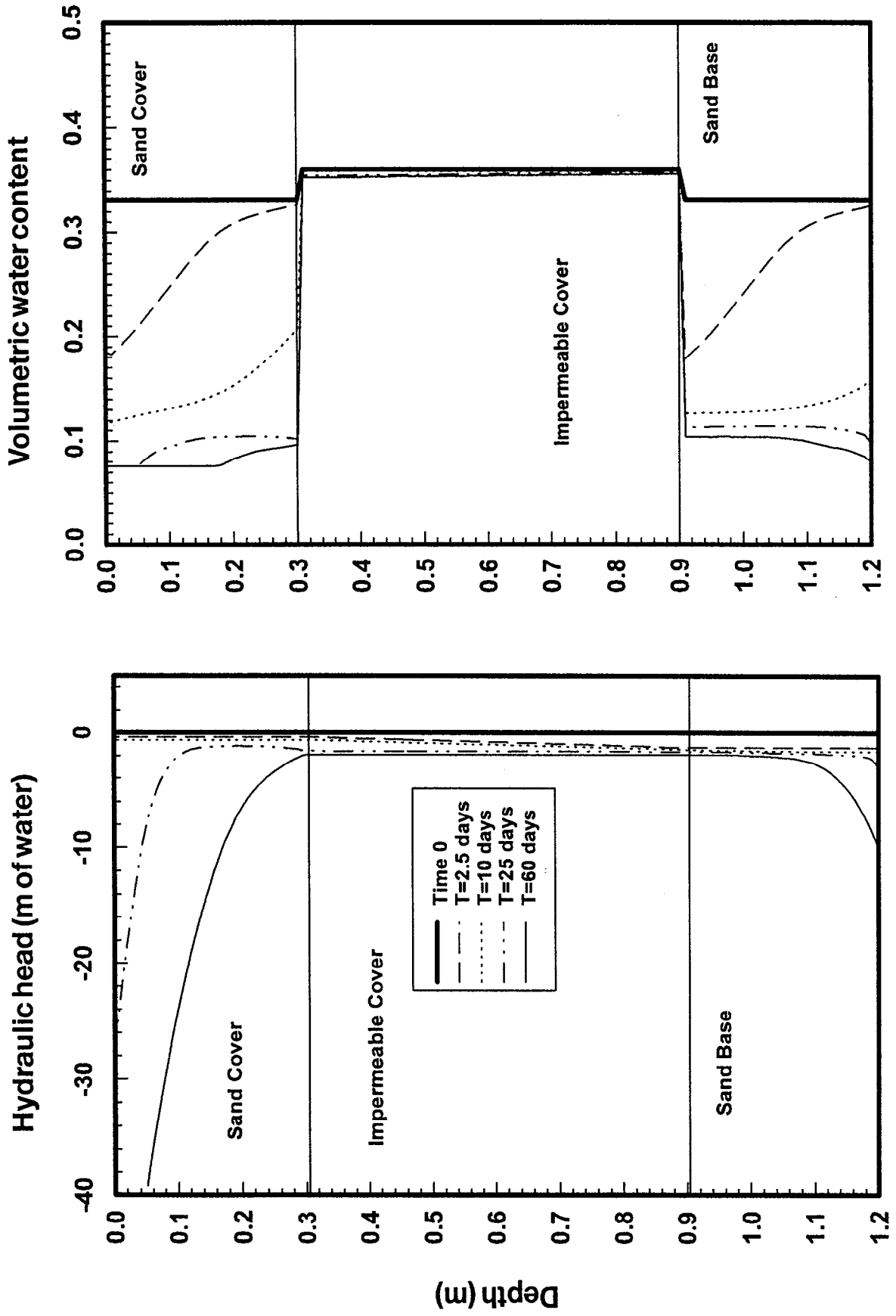


FIG. 4. Modelled hydraulic heads and water contents in composite soil cover.

remains nearly fully saturated, with only a marginal decrease in the water content. The modelling assumes that during the 60-day period no precipitation would occur to replenish the cover (Fig. 5). For the Heath Steele mine site area, where the average annual precipitation is about 1100 mm of which 750 mm is rainfall, 60 days is a reasonable maximum period without precipitation.

In addition to being an evaporation barrier, the upper sand will also promote replenishment of moisture to the till. During infiltration, the sand provides storage of water and reduces runoff, thus allowing more water to reach the till.

Prediction of oxygen flux

Continual saturation of the till will result in a low oxygen flux because the diffusion coefficient of gaseous oxygen through the till is low. The effective diffusion coefficient of oxygen determined in the laboratory on till HS-C at varying degrees of water saturation from 75 to 92% was typically 9×10^{-9} m²/s. Diffusion coefficients for sand HS-D were higher and ranged from 2.2×10^{-6} to 1.2×10^{-5} m²/s at water saturations of 50 and 0.6%, respectively.

Predicted oxygen fluxes in the three-layer cover system using different diffusion coefficients of the till are plotted against thickness in Fig. 6. A diffusion coefficient of 1×10^{-5} m²/s was assigned to the sand layers to reflect conditions at residual water saturation. The plot indicates that at a diffusion coefficient of 1×10^{-7} m²/s, a till layer with a thickness of less than 60 cm is required to reduce the flux to a minimum value. As expected, the flux is lower and a much smaller thickness is required when the diffusion coefficient is 1×10^{-8} m²/s. The key to the design of an effective cover, therefore, is to specify that it be placed under maximum water saturation conditions in the field without compromising on its capacity to withstand high shear forces. This can be achieved by placing the cover at a water content slightly above the optimum compaction value. As an approximation, the shear strength c_u (in kPa) of the compacted till can be predicted from the following relationship (Leroueil et al. 1992):

$$[4] \quad c_u = 140 \exp \left[-5.8 \frac{(w - w_{opt})}{I_p} \right]$$

where w_{opt} is the optimum water content, w the moulding water content, and I_p is the plasticity index of the till.

Design specifications

On the basis of the results of the computer modelling presented above, the design of the cover for the pile called for a 60 cm thick saturated till layer sandwiched between two sand layers, each of a thickness of 30 cm. The predicted oxygen concentrations in the composite cover are presented in Fig. 7 along with the profile for a single cover. As shown by the plots, oxygen penetration into the cover is effectively contained in the till layer because of its lower diffusion coefficient. A deeper oxygen profile is obtained in the single cover because of the higher diffusion coefficient. The depth of oxygen penetration is not as important as the flux in assessing cover effectiveness.

To be effective as an oxygen barrier, the till layer has to be placed at conditions as close to full saturation as practicable. A secondary requirement is that the till also be an effective water barrier to reduce infiltration into the waste rock pile. The hydraulic conductivity of a clay soil com-

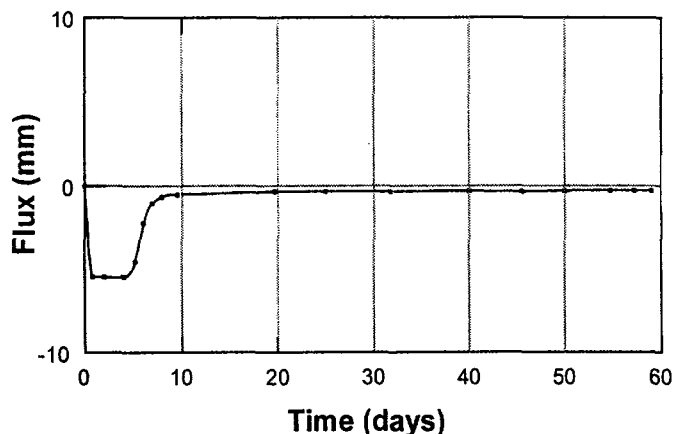


FIG. 5. Evaporation function used in flow modelling.

acted at water contents higher than the optimum value would be low, provided a good placement protocol (for example, destruction of soil clods and adequate interlift bonding; Elsbury et al. 1990) is followed. It was therefore specified in the design that the till be moulded at a field water content of 2–3% higher than its optimum water content and compacted at a density of about 95% of the maximum Modified Proctor compaction. It can be shown from moisture–density relations that this compaction specification results in a degree of saturation close to 95% and satisfies the first requirement noted above. The high saturation would also lead to low oxygen fluxes across the cover. The geotechnical specifications for the three-layer cover system are presented in Table 3. The sand base refers to the bottom sand layer required to be placed directly above the prepared surface of the waste rock pile and would function as a capillary barrier minimizing moisture drainage from an overlying finer material. The fine-grained layer (compacted till), referred to as the impermeable cover, was required to function both as an oxygen and water barrier, while the overlying granular cover would reduce evaporation. From [4] and the preconstruction geotechnical properties obtained on the soils, a shear strength in the range of 7–13 kPa was predicted for the impermeable cover at the specified placement water content. This shear strength is higher than the overburden stresses expected from the granular cover. The pile is located in an isolated area where vehicular traffic on the cover is expected to be minimal; thus, the shear strength of the till would be adequate.

The capillary-barrier concept used in the three-layer cover design has been evaluated in a series of detailed laboratory investigations at the Noranda Technology Centre. Results have shown that the three-layer cover system effectively reduces moisture and oxygen fluxes. Earlier work involving fundamental research on the hydraulic behaviour and gaseous oxygen diffusion were conducted in collaboration with the University of Waterloo. Numerical modelling was later conducted that confirmed the laboratory observations (Akindunni et al. 1991; Nicholson et al. 1991). A field evaluation of the design was initiated in September 1990 in a test program at the Waite Amulet tailings site (Yanful and St-Arnaud 1991). Results obtained to date are in agreement with the laboratory observations and model predictions and do indicate 90–98% reduction in acid production (Yanful 1993). The Heath Steele Waste Rock Project provides a unique

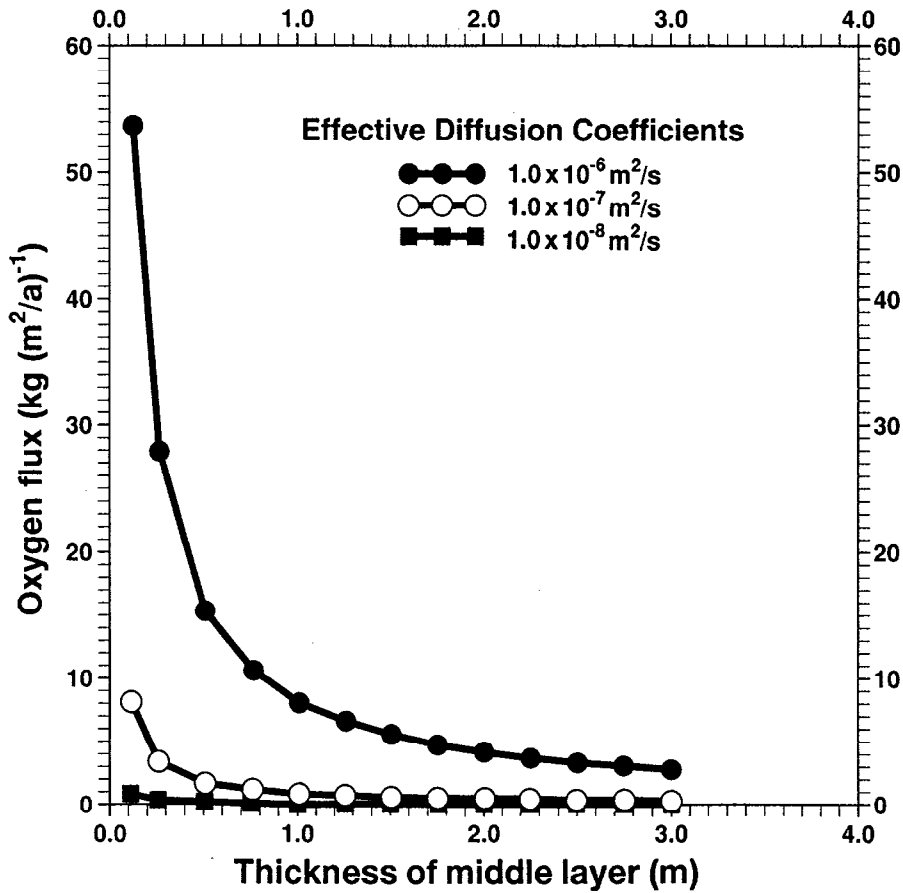


FIG. 6. Predicted oxygen flux vs. thickness of compacted till layer as a function of oxygen diffusion coefficient.

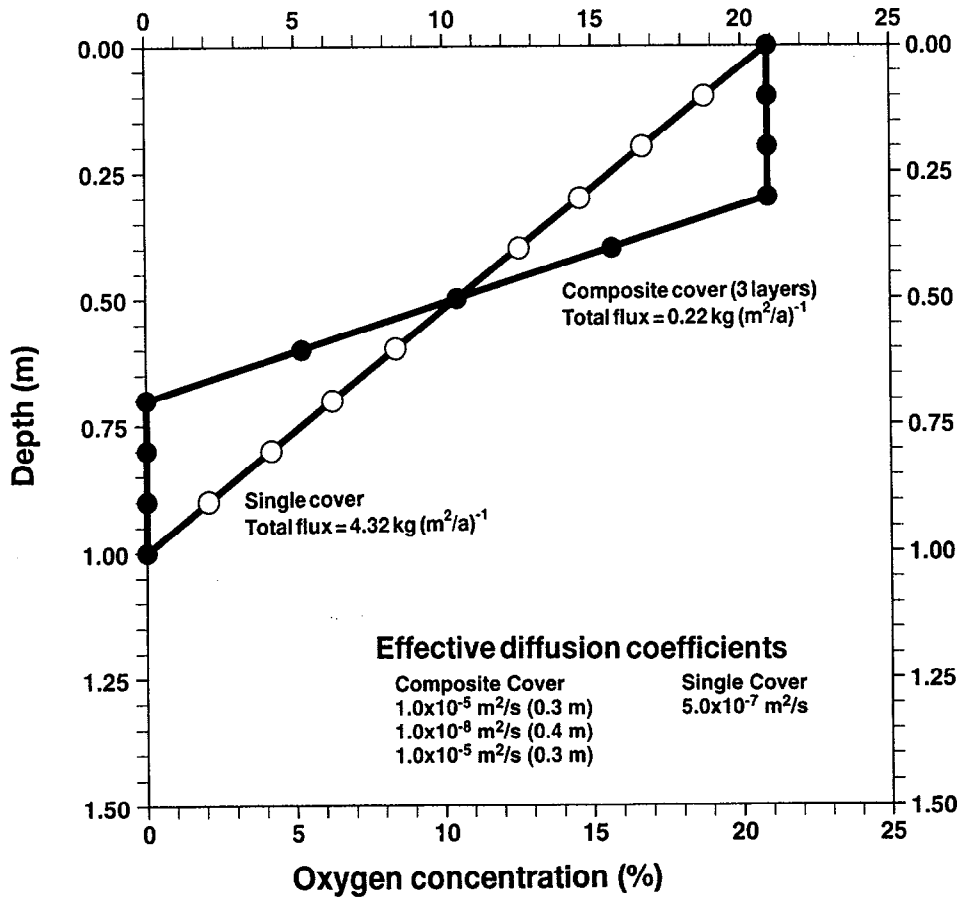


FIG. 7. Predicted depth of oxygen penetration in a composite soil cover compared with the penetration in a single cover.

TABLE 3. Specifications for cover materials

Layer	Specifications
Sand base	Non-acid-generating, well-graded, coarse-grained material meeting the following requirements: 60% ranging between 0.5 and 4.0 mm particle diameter D_{10} ranging between 0.35 and 0.40 mm compaction to 92% of maximum Modified Proctor density in 15-cm thick lifts to a finished thickness of 30 cm
Impermeable cover	Non-acid-generating glacial till meeting the following requirements: (i) Percent finer than 0.075 mm greater than 40% (dry wt). (ii) Maximum particle size of 30 mm. (iii) Percent finer than 0.002 mm greater than 10% (dry wt). (iv) D_{10} ranging between 0.001 and 0.003 mm. (v) Moulding moisture content of -2 to 4% of optimum moisture content. (vi) Compaction to at least 95% of maximum Modified Proctor density in 20-cm thick lifts to a finished thickness of 60 cm. (vii) Liquid limit greater than 30% and plasticity index greater than 15%. (viii) Hydraulic conductivity of 1×10^{-7} cm/s or less.
Granular cover	Non-acid-generating, well-graded pit run sand and gravel or equivalent crushed rock meeting the following requirements: (i) Percent finer than 0.075 mm less than 8% (dry wt). (ii) Maximum particle size of 50 mm. (iii) Compaction to 92% maximum Modified Proctor density in 15-cm thick lifts to a finished thickness of 30 cm

opportunity to evaluate the design concept on an acid-generating waste rock pile in a Canadian climate.

Summary

The development of strategies for managing acid generation in waste rock produced from the mining of base-metal ores is receiving attention in the MEND program. As part of the program, several waste-rock piles located at Heath Steele mines, near Newcastle, New Brunswick, were selected for baseline physicochemical characterization. An engineered soil cover was subsequently proposed for one of the acid-generating rock piles, pile 7/12. The objective was to design a cover that was effective in reducing gaseous oxygen flux and water infiltration into the underlying pile. The final design was a three-layer cover system consisting of a 60 cm thick saturated fine-grained soil layer sandwiched between two 30 cm thick, coarse-grained soil layers. The coarse layers serve as capillary barriers to minimize moisture losses in the fine layer due to evaporation and drainage. Modelling of gaseous oxygen transport, using laboratory-measured diffusion coefficients, suggests flux through such a cover would be low because of potentially high water saturation of the fine layer. The potential for the fine layer to remain nearly fully saturated, even under an evaporative flux, is confirmed by flow modelling. The requirements of high water saturation and low hydraulic conductivity for the fine layer can both be achieved by placing and compacting it at a water content slightly higher than the optimum value and about 95% of the maximum Modified Proctor density.

The three-layer cover system has been extensively evaluated in laboratory, modelling, and field studies involving acid-generating mill tailings. The results of these evaluations all indicate that the system is effective in reducing acid generation by at least 90%. The Heath Steele Waste Rock Project provides an opportunity to assess the performance of the cover for an acid-generating waste-rock pile.

Although differential settlements in the 5 m high pile could be much smaller than those associated with large piles (of several metres high), other aspects of the performance evaluation of the cover (such as the effects of freezing and thawing and reductions in temperature resulting from cover placement) would be applicable to other piles.

Acknowledgements

The work described in this paper was funded by Brunswick Mining and Smelting Corporation Limited, New Brunswick Department of Natural Resources and Energy, and the New Brunswick Department of Commerce and Technology under the MEND program. B. Aubé assisted with the modelling. C. Ferron of Heath Steele Mines Ltd. and K. Wheeland and L. St-Arnaud of Noranda Technology Centre reviewed the manuscript.

- Akindunni, F.F., Gillham, R.W., and Nicholson, R.V. 1991. Numerical simulations to investigate moisture-retention characteristics in the design of oxygen-limiting covers for reactive mine tailings. *Canadian Geotechnical Journal*, **28**: 446-451.
- Beck, J.V. 1967. The role of bacteria in copper mining operations. *Biotechnology and Bioengineering*, **9**: 487-497.
- Chamberlain, E.J., and Gow, A.J. 1979. Effect of freezing and thawing on the permeability and structure of soils. *Engineering Geology (Amsterdam)*, **13**: 73-92.
- Crawford, C.B. 1968. Frost action—construction hazard. *Engineering and Contract Record*, **81**: 51-57.
- Elsbury, B.R., Daniel, D.E., Sraders, G.A., and Anderson, D.C. 1990. Lessons learned from compacted clay liner. *ASCE Journal of Geotechnical Engineering*, **116**: 1641-1660.
- Filion, M.P., and Ferguson, K. 1989. Acid mine drainage research in Canada. *In Tailings and Effluent Management. Proceedings of the International Symposium on Tailings and Effluent Management, Aug. 20-24, Halifax. Edited by E.M. Chalkley, B.R. Conard, V.I. Lakshmanan, and K.G. Wheeland. Pergamon Press, New York. pp. 61-72.*

- Gillham, R.W. 1984. The capillary fringe and its effect on water table response. *Journal of Hydrology*, **67**: 307-324.
- Groudev, S.N., Genchev, F.N., and Gaidarjiev, S.S. 1978. Observations on the microflora in an industrial copper dump leaching operation. *In Metallurgical applications of bacterial leaching and related microbiological phenomena. Edited by L.E. Murr, A.E. Torma, and J.A. Brierley.* Academic Press, New York. pp. 253-274.
- Harries, J.R., and Ritchie, A.I.M. 1981. The use of temperature profiles to estimate the pyritic iron oxidation rate in a waste rock dump from an open cut mine. *Water, Air and Soil Pollution*, **16**: 405-423.
- Harries, J.R., and Ritchie, A.I.M. 1985. Pore gas composition in waste rock dumps undergoing pyritic oxidation. *Soil Science*, **140**: 143-152.
- Lambe, T.W., and Whitman, R.V. 1969. *Soil mechanics.* John Wiley & Sons, New York.
- Leroueil, S., Le Bihan, J.P., and Bouchard, R. 1992. Remarks on the design of clay liners used in lagoons as hydraulic barriers. *Canadian Geotechnical Journal*, **29**: 512-515.
- Nicholson, R.V., Gillham, R.W., Cherry, J.A., and Reardon, E.J. 1989. Reduction of acid generation in mine tailings through the use of moisture-retaining cover layers as oxygen barriers. *Canadian Geotechnical Journal*, **26**: 1-8.
- Nicholson, R.V., Akundunni, F.F., Sydor, R.C., and Gillham, R.W. 1991. Saturated tailings covers above the water table: the physics and criteria for design. *Proceedings of the 2nd International Conference on Abatement of Acidic Drainage*, 16-18 Sept. 1991, Montréal. Mine Environment Neutral Drainage (MEND) Program, Ottawa. pp. 443-460.
- Rasmuson, A., and Eriksson, J.-C. 1986. Capillary barriers in covers for mine tailings. National Swedish Environmental Protection Board, Report 3307.
- Vick, G. 1983. *Planning, design and analysis of tailings dams.* Wiley Interscience, New York.
- Wheeland, K.G., and Feasby, G. 1991. Innovative decommission technologies via Canada's MEND Program. *In Proceedings of the 12th National Conference, Hazardous Materials Control/Superfund '91*, 3-5 Dec. 1991, Washington, D.C. *Edited by G.F. Bennett.* Hazardous Materials Control Resources Institute, Green Belt, Md. pp. 24-28.
- Wilson, G.W. 1990. Soil evaporative fluxes for geotechnical engineering problems. Ph.D. thesis, Department of Civil Engineering, University of Saskatchewan, Saskatoon.
- Yanful, E.K. 1993. Oxygen diffusion through soil covers on sulphidic mill tailings. *ASCE Journal of Geotechnical Engineering*, Vol. 119, No. 8.
- Yanful, E.K., and St-Arnaud, L.C. 1991. Design, instrumentation and construction of engineered soil covers for reactive tailings management. *In Proceedings of the 2nd International Conference on Abatement of Acidic Drainage*, 16-18 Sept. 1991, Montréal. Mine Environment Neutral Drainage (MEND) Program, Ottawa, pp. 487-504.
- Yanful, E.K., Riley, M.D., Woysner, M.R., and Duncan, J. 1993. Construction and monitoring of a composite soil cover on an experimental waste rock pile near Newcastle, New Brunswick, Canada. *Canadian Geotechnical Journal*, **30**: 588-599.

Modelling and field measurements of water percolation through an experimental soil cover on mine tailings

Mark R. Woyshner and Ernest K. Yanful

Abstract: A composite soil cover constructed on acid-producing tailings was evaluated for its ability to retain a high degree of water saturation and low hydraulic conductivity. The cover consisted of a 60 cm thick, compacted, nearly saturated, varved clay placed between two sand layers, each 30 cm thick. A final 10 cm thick gravel layer was placed on the upper sand layer to minimize erosion. The Hydrologic Evaluation of Landfill Performance (HELP) model and a finite-element flow model (SEEP/W) were applied, and the results corroborated with field measurements of percolation and soil-water content. Modelling predictions indicate that 4% of precipitation will percolate through the cover and that the intermediate clay layer will retain a high degree of saturation after a 20 year simulation. Four years of field monitoring also indicate that 4% of precipitation percolates through the cover and that the clay retains its high saturation. These results suggest that a properly designed and constructed soil cover can be effective in reducing acid production in reactive mine tailings.

Key words: acid-producing tailings, soil cover, water saturation, capillary barrier, hydrologic processes.

Résumé : Une couverture composite de sol construite sur des stériles miniers produisant de l'acide a été évaluée en fonction de sa capacité de maintenir un fort degré de saturation en eau et une faible conductivité hydraulique. La couverture consiste en une argile varvée compactée, presque saturée, de 60 cm d'épaisseur, placée entre deux couches de sable de 30 cm d'épaisseur. Une couche de gravier de 10 cm a finalement été placée sur la couche supérieure de sable pour minimiser l'érosion. L'on y a appliqué le modèle d'évaluation de la performance hydrologique d'un enfouissement (HELP) et un modèle d'écoulement en éléments finis (SEEP/W), et les résultats ont été corroborés par des mesures de percolation et des teneurs en eau du sol sur le terrain. La prédiction au moyen des modèles indique que, après 20 ans de simulation, 4% de la précipitation va percoler à travers la couverture et que la couche intermédiaire d'argile va retenir un fort degré de saturation. Quatre années de mesure sur le terrain ont aussi indiqué que 4% de la précipitation percole à travers la couverture et que l'argile retient un fort degré de saturation. Ces résultats laissent supposer qu'une couverture de sol conçue et construite de façon adéquate peut réduire de façon efficace la production d'acide dans les stériles miniers réactifs.

Mots clés : stériles producteurs d'acide, couverture de sol, saturation en eau, barrière capillaire, processus hydrologique.

[Traduit par la rédaction]

Introduction

A soil cover for controlling acid production in sulphide-bearing mill tailings effectively must retain a high degree of water saturation and also have a low hydraulic conduc-

tivity (Yanful et al. 1993). One method of achieving these two objectives above the water table is by incorporating a capillary barrier in the design of the cover. In a capillary barrier, a saturated, fine-grained soil layer with a low hydraulic conductivity is placed on top of a coarse-grained soil layer (Rasmuson and Eriksson, 1986; Nicholson et al. 1989; Yanful 1991). The coarse layer, having larger pores, drains to residual saturation where a high suction is developed, and the resulting hydraulic conductivity of the coarse layer is very low. The coarse layer is therefore not able to transmit a significant amount of moisture downward from the overlying fine layer and essentially prevents the fine-grained layer from draining, thereby retaining a high degree of saturation.

Received August 12, 1994. Accepted March 28, 1995.

M.R. Woyshner, Hydrology, Hydrogeology, and Environment, P.O. Box 37, Eastman, QC J0E 1P0, Canada.

E.K. Yanful, Geotechnical Research Centre, Department of Civil Engineering, The University of Western Ontario, London, ON N6A 5B9, Canada.

Table 1. HELP model input data.

Layer:	Sand cover	Clay	Sand base
Layer type	Lateral drainage	Barrier	Vertical percolation
Layer thickness (cm)	30	60	30
Porosity ^a	0.33	0.445	0.39
Field capacity ^a	0.08	0.43	0.05
Wilting point	0.03	0.35	0.025
Initial water content ^a	0.08	0.44	0.05
Saturated hydraulic conductivity (cm/s) ^a	2.6×10^{-3}	1.0×10^{-7}	8.4×10^{-3}
Slope (%)	0		
Maximum drainage length (m)	10		
Cover area (m ²)	400		
SCS runoff curve number	81		
Evaporative zone depth (cm)	20		
Maximum leaf area index	0; bare ground		
Initial snow water content (mm)	50.8 (2 in.)		
Growing season	June–September; not applicable to bare ground		

^aLaboratory measured soil parameters.

The phenomenon was illustrated in a combined experimental and modelling study by Yanful and Aubé (1993).

Two experimental soil covers, incorporating the capillary-barrier concept, were constructed on acid-generating tailings at the Waite Amulet site, near Rouyn-Noranda, Quebec. The design, construction, and instrumentation details are documented in two papers by Yanful and St-Arnaud (1991) and Yanful (1993) and are only briefly described here. The test plots were 20 by 20 m in plan and consisted of a 60 cm compacted clay layer placed between a 30 cm sand base and a 30 cm sand cover. A 10 cm gravel crust blanketed the sand cover to control erosion. A collection basin lysimeter was placed below each cover. Lysimeters are commonly used to assess evapotranspiration in water-balance studies, but in this study they were used to collect water percolating through the cover. They consisted of semicylindrical, acid-resistant, high-density polypropylene laid horizontally along the axis of the cylinder. Each lysimeter had an exposed, receiving surface area of 2.2 m² and a volume of ~2 m³. The water content of each layer of the covers was also measured.

Percolation through the cover was predicted using two computer models. This paper compares predicted amounts with those measured in the lysimeter. The predicted level of saturation is also compared with field measurements. Overall, the capillary-barrier concept is illustrated and clarified through hydrologic flow modelling.

Hydrologic evaluation and prediction

The Hydrological Evaluation of Landfill Performance (HELP) model is a deterministic water balance model, developed by the United States Environmental Protection Agency (EPA), which uses climatic, soil, and design data to determine the water budget of a landfill (Schroeder et al. 1984). The HELP model for windows (HMfW) utilizes the EPA computer code and incorporates meteorological

data from Environment Canada (Grace Dearborn Inc. 1993). Since the soil covers at Waite Amulet are similar in design to landfill covers, HMfW was used to evaluate the magnitude of the water balance components at the field site.

The amount of annual infiltration predicted with HMfW was used as the soil surface boundary condition in SEEP/W, a finite-element flow model used to solve the two-dimensional equation of flow for steady-state saturated and unsaturated flow at the site.

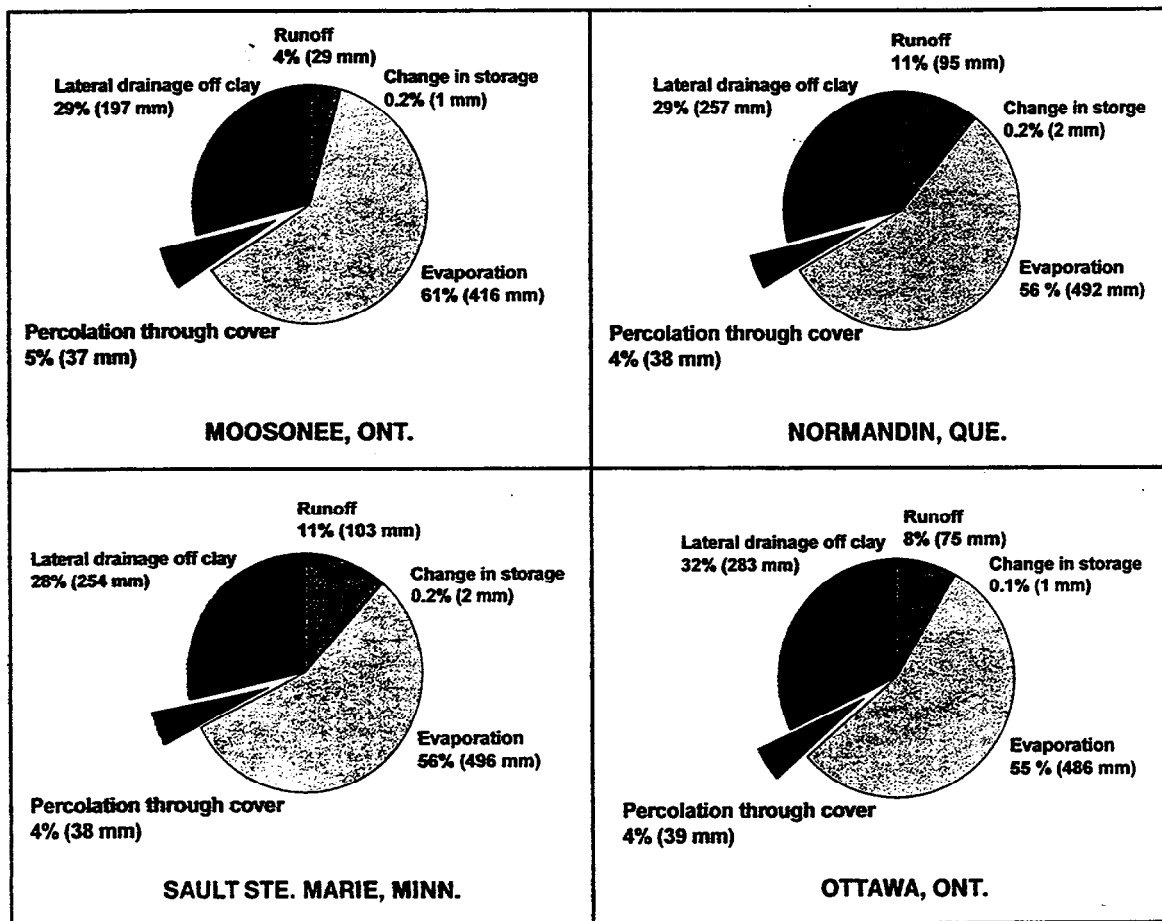
HELP model

The HELP model simulates 4 hydrologic processes on a daily account: (i) runoff, and hence infiltration, is computed using the United States Soil Conservation Service (SCS) Curve Number method; (ii) percolation (i.e., saturated and unsaturated vertical flow) is modelled using Darcy's law; (iii) lateral drainage is computed using the Boussinesq equation; and (iv) evaporation is estimated with a modified Penman method. Other components of the water budget are deduced from these results.

Cover design specifications consist of the thickness and soil type of each layer. There are four types of layers that are defined by the HELP model: (i) a vertical percolation layer that allows only vertical flow; (ii) a lateral drainage layer that allows vertical flow but also horizontal flow through drainage pipes; (iii) a barrier soil layer that restricts vertical flow; and (iv) a waste layer (not used in this soil cover application).

Table 1 lists the input data used to apply HMfW to the composite soil covers at Waite Amulet. Laboratory measured soil parameters were used where possible. The SCS runoff curve number was chosen using a relationship to the minimum infiltration rate and vegetative cover (Schroeder et al. 1984). The default SCS curve number for fine sand and bare ground was used. In the present study, the impact of vegetation was negligible and bare ground values were used when applicable.

Fig. 1. HELP modelling results, average annual totals.



HELP modelling was conducted for four locations available in the HMfW data base: Moosonee, Ontario (51.26N 80.65W); Normandin, Quebec (48.85N 72.53W); Ottawa, Ontario (45.38N 75.71W); and Sault Sainte Marie, Minnesota (46.60N 84.36W). These meteorological stations surround the Waite Amulet site (48.32N 79.08W) within a 500 km radius. At each site the model was run for 20 years, inputting daily data of total precipitation, average temperature, and total solar radiation.

Results of HELP modelling

Figure 1 shows the annual results of the HELP modelling. All four simulations responded similarly, with results from the Normandin and Sault Sainte Marie runs being nearly identical. In general, the modelling predicts that 4% of precipitation percolates through the cover, which implies the clay receives water for saturation. In addition, since percolation (38 mm/a) is higher than the hydraulic conductivity of the clay (10^{-7} cm/s or 32 mm/a), free water is available (ponded) at the surface of the clay. The monthly results indicate these conditions exist for all months of the year. Therefore, the HELP modelling exercise concludes that the clay will not desaturate. Indeed, the soil moisture content at the end of the 20 year modelling simulation is identical to its initial value of 44 vol.%.

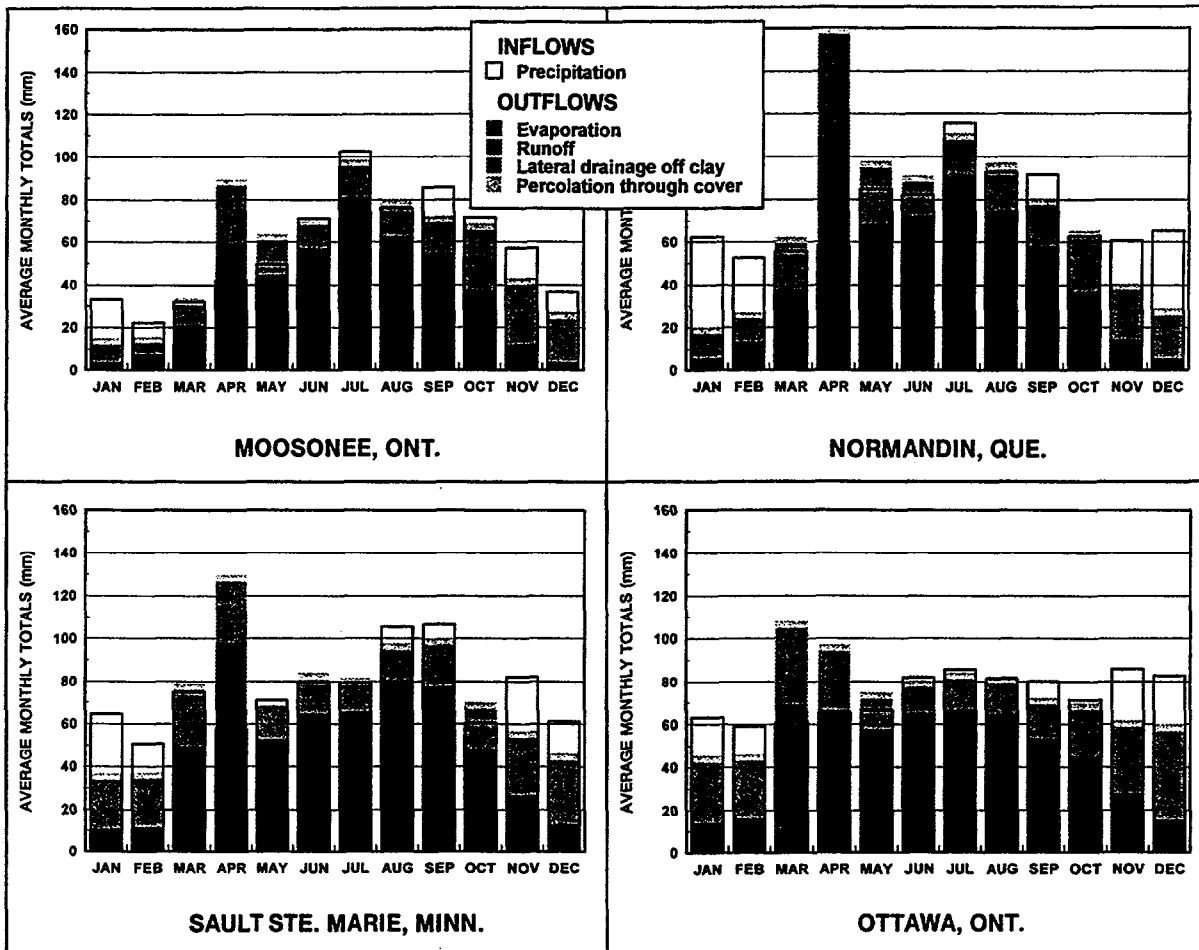
The monthly results of the HELP modelling are illustrated in Fig. 2. The difference in the inflows and outflows

depicts two hydrologic processes: (i) the accumulation and melting of snowfall; and (ii) the change in soil moisture storage from month to month, chiefly in the sand cover. On the raised and exposed experimental plots at Waite Amulet, however, wind would reduce the accumulation of snow during winter. Wind erosion is therefore a third process contributing to the difference in inflows and outflows on the experimental covers, but not depicted in Fig. 1. The model assumes the cover surface is smooth and without topographic irregularities.

In general, the snow pack that accumulates over winter melts in April and contributes heavily to runoff. During the summer months, runoff diminishes to a negligible amount and lateral flow off the surface of the clay stabilizes around 13 mm per month. The soil moisture losses during the summer months are replenished during August, September, and October, accompanied by an increase in runoff and lateral drainage. Although most components vary throughout the year, percolation remains relatively steady, averaging 3.25 mm/month. In reality, however, during winter the cover freezes, thereby reducing percolation during those months. The HELP model does not accommodate frozen soil.

Since the saturated hydraulic conductivity (K_s) of the clay layer is the principal control on the flow of water through the cover, a sensitivity analysis of the Normandin simulation was conducted to determine the effect of the water-

Fig. 2. HELP modelling results, average monthly totals.



balance components with varying levels of K_s (Fig. 3). The hydraulic gradient (i) across the clay was calculated by dividing flow through the clay by K_s . Percolation increased with K_s values greater than 1×10^{-7} cm/s, while runoff, lateral drainage, and hydraulic gradient decreased. Percolation was most sensitive at K_s values between 2×10^{-7} and 2×10^{-6} cm/s, and i at values greater than 4×10^{-7} cm/s. When K_s is less than 7×10^{-7} cm/s, i is greater than 1, which indicates that free water is available at the surface of the clay. The percolation for this value of K_s is 220 mm/a or 25% of mean annual precipitation. This would be the maximum amount of percolation to expect while still retaining free water conditions at the surface of the clay, and therefore a high degree of saturation of the clay. Monthly results from this run confirm these conditions are sustained from April through December, with no loss in the degree of saturation of the clay at the end of the 20 year simulation. From January through March, the cover is frozen; precipitation accumulates as a snow pack and there is no gain or loss of water and hence no change in the degree of saturation.

Flow modelling

To enhance the HELP modelling, the flow model SEEP/W (Geo-slope International 1992) was used to simulate flow through the composite soil cover at Waite Amulet. The test plot was modelled as a two-dimensional system and

under steady-state conditions. SEEP/W is formulated to analyze both saturated and unsaturated flow. Pressure head versus water content functions (Fig. 4), used in the flow modelling, were adapted from pressure plate and column studies conducted by McGill University and Noranda Technology Centre. Pressure head versus hydraulic conductivity functions (Fig. 5) were developed with a routine in SEEP/W that utilized the drainage curves and other soil properties. The top boundary condition was specified as a constant flow of water, equivalent to 303.6 mm/a, which was infiltration deduced from the HELP modelling. The sides of the covered tailings domain were specified as a constant head boundary set to piezometer head measurements. The base of the tailings, which generally sits on clay, was defined as impermeable. All other soil properties were similar to those used in the HELP modelling.

Modelling the test plot as a steady-state system simulates the flow conditions as if precipitation and evaporation were constant throughout the year, which yields equilibrium conditions of flow with steady infiltration. Realistically, precipitation would fluctuate throughout the year; runoff and infiltration would therefore also fluctuate. Evaporation is greatest during the summer and least during the winter. The cover would also freeze during winter and limit percolation. Results of the flow modelling therefore represent the average flow conditions. It is similar to a system with

Fig. 3. Sensitivity analysis of HELP modelling, Normandin, Quebec.

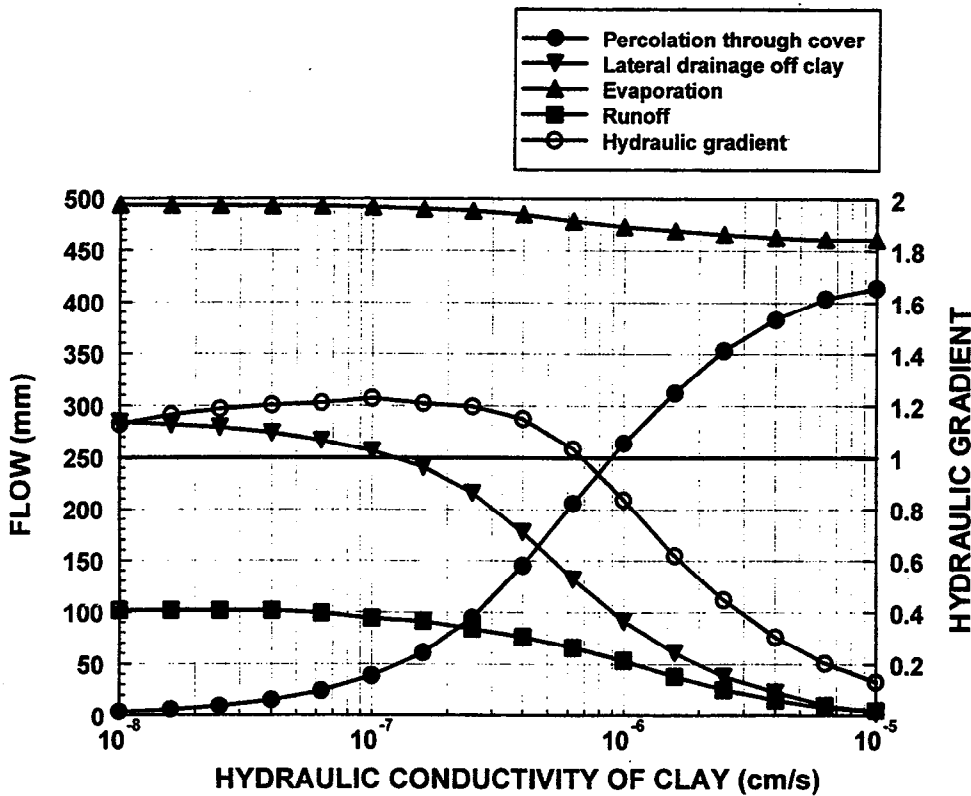
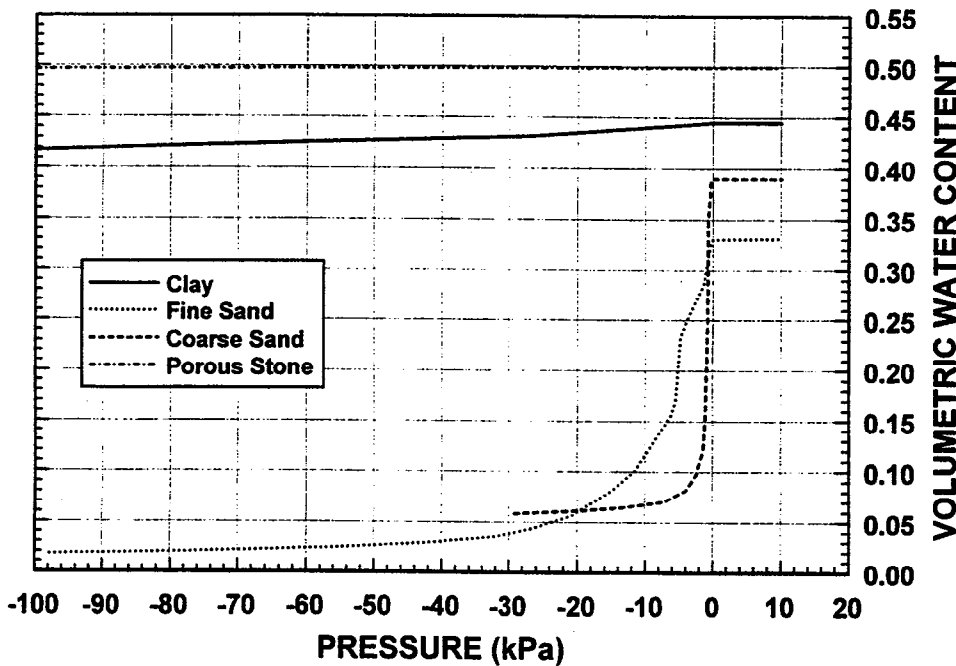


Fig. 4. Pressure head versus water content functions used in SEEP/W modelling.



constant infiltration but without evaporation. The dynamics of the system are not considered in these assumptions.

Results of flow modelling

Figure 6 shows the results obtained with SEEP/W. Zero elevation is taken at sea level, and the surface of the cover

is at 317.45 m. The flow vectors, illustrated in the longitudinal view at the bottom of page, indicate that most of the flow travels off the top of the clay, laterally through the sand cover. This result, which is consistent with the HELP modelling, is due to the high hydraulic conductivity (K_s) of the sand layer. As a generalized rule of thumb, in layered

Fig. 5. Pressure head versus hydraulic conductivity functions used in SEEP/W modelling.

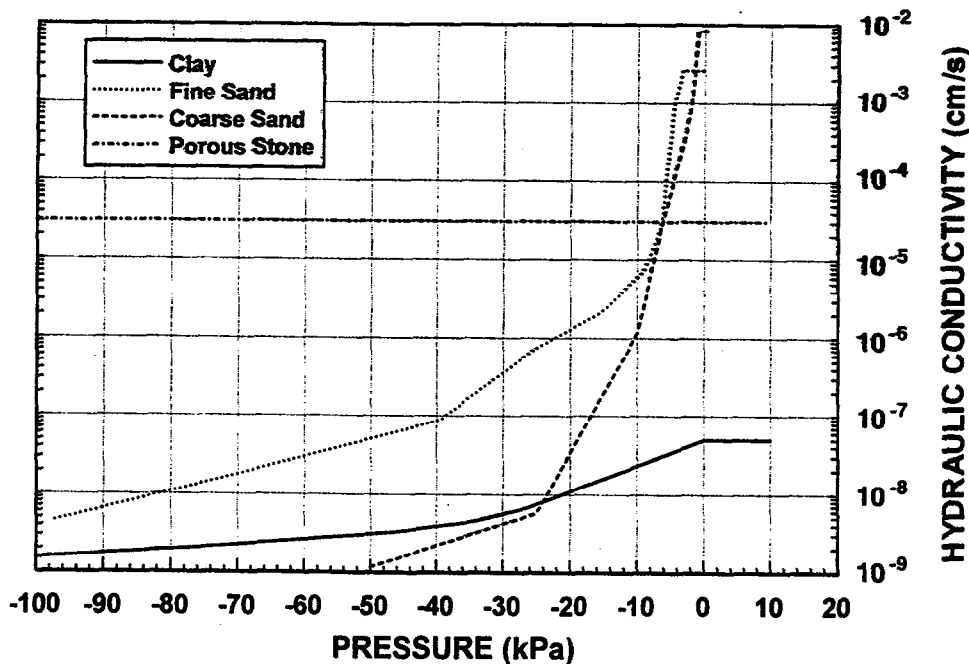


Table 2. Observed percolation through the experimental clay cover at Waite Amulet.

Period	Oct. 26 to Nov. 20, 1992 (Fall)	Nov. 20 to May 21, 1993 ^a (Winter to early spring)	May 21 to June 11, 1993 ^b (Spring)	June 11 to Aug. 19, 1993 (Summer)	Aug. 19 to Sept. 22, 1993 (Late summer to fall)	Oct. 26, 1992 to Sept. 22, 1993 (Annual)
Precipitation (mm)	75	440	82	257	105	958
Lysimeter discharge (L)	10	0	30	20	22	82
Lysimeter discharge (mm)	5	0	14	9	10	37
Lysimeter discharge (% of precip.)	6	0	17	4	10	4

^aPrecipitation measured at Duparquet, Quebec.

^bThe spring thaw appeared to percolate to the lysimeter between site visits on May 21 and June 11, thus showing a time lag.

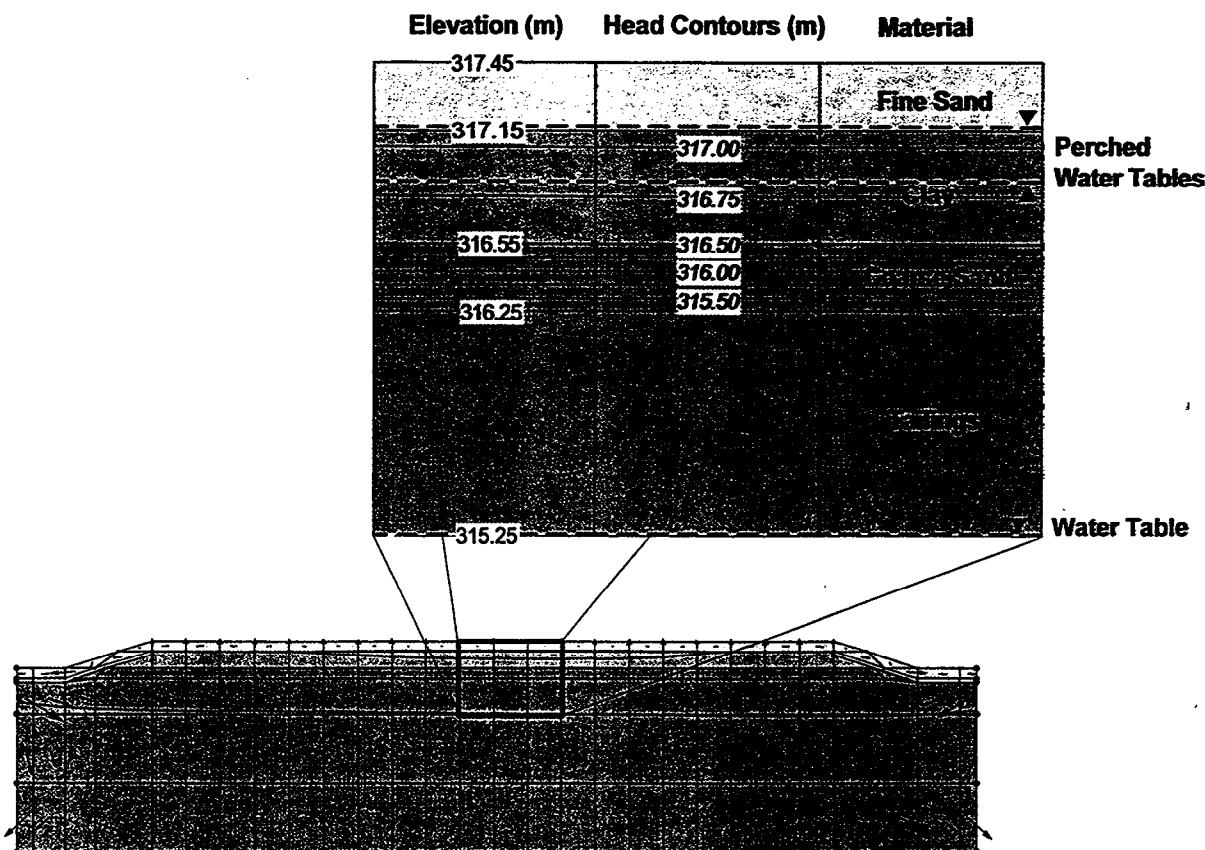
systems consisting of soils with contrasting grain-size distributions, such as a composite soil cover, a high K_s implies horizontal flow and a low K_s , a vertical flow.

The water that enters the clay flows vertically, as indicated by the hydraulic head contours; flow is perpendicular to the head contours. The flow continues vertically across the sand base, suggesting a low unsaturated hydraulic conductivity, K . The head contours also concentrate across the sand base, illustrating the larger gradient needed to push the flow through the sand. Since the flux is constant and the gradient across the sand base is greater than that across the clay, the K of the sand must be less than the K_s of the clay, in accordance with Darcy's law. Thus, the sand base, being unsaturated, has a lower hydraulic conductivity than the clay, which is saturated. The flow modelling therefore confirms the sand base as a capillary barrier that restricts drainage from the clay. This result is

consistent with the HELP modelling. Flow modelling results predicted vertical flow through the cover to be 34.3 mm of water, which is also consistent with the HELP modelling (Fig. 1).

The water table indicates where the pressure head equals zero ($\psi = 0$); this is also called the free water surface. When ψ is less than zero, water is under tension (or suction), and when ψ is greater than zero, water is under pressure. Unsaturated soils contain water under tension. The water table occurs in the tailings at 1 m below the cover and in the clay, as shown by the modelling results in Fig. 6. The fact that the clay has a perched water table indicates it is saturated, which is consistent with the HELP modelling. The extent of saturation or the size of the perched water table envelope is not actual, its presence is simply an indication of saturation. The sand layer below the clay is unsaturated.

Fig. 6. Results of SEEP/W steady-state flow modelling.



Field measurements

The covers were installed in the autumn of 1990. Each cover was placed above a 2.2 m² collection basin lysimeter filled with unoxidized tailings. The lysimeters were used to collect water percolating through the covers. The lysimeters did not report water until the fall of 1992. Table 2 shows the observed percolation through one of the clay covers. Percolation was observed to be 4% of precipitation, which is consistent with the results from the HELP modelling.

The HELP modelling results can also be corroborated with field measurements of evaporation and precipitation. In 1993, pan evaporation and precipitation were measured at the site from June 11 to September 22. Pan evaporation was observed to be 431 mm, and precipitation was observed to be 361 mm. The HELP model predicted evaporation from the cover to be 71% of precipitation from June through September. Since 71% of the measured precipitation is 256 mm, or 59% of the measured pan evaporation, the actual evaporation is 59% of pan evaporation, which is reasonable for a well-drained nonvegetated soil in the Abitibi region of Quebec. For example, evaporation from nonvegetated tailings at the Kidd Creek thickened tailings deposit near Timmins, Ontario, was observed to be 56% of pan evaporation during the months June through September (Woyshner and St-Arnaud 1994). Therefore, field observations of evaporation confirm the results of the HELP modelling exercise.

Water content of the cover was periodically measured using time-domain reflectometry (TDR) method.

TDR probes were installed in each layer of the cover during the construction of the cover. Measurements were conducted with a Tektronix model 1502B TDR metallic cable tester, and water content values were determined with an empirical relation developed by Topp et al. (1980). Results from 4 years of monitoring (Fig. 7) indicate that the clay has essentially maintained its placement water content of ~41% by volume (degree of saturation > 93%) and that the sand base is still at residual saturation. The tailings also show a high degree of water saturation. These results are supported by gravimetric water content measurements, conducted in June 1993 (Fig. 8). The winter TDR data (February 1991 and March 1992) appear to indicate low saturation but are actually attributed to the formation of ice; TDR interprets ice as a solid phase.

Figure 8 also shows a higher degree of saturation of the tailings mass as compared with that of the lysimeter tailings. In the lysimeter, the tailings are isolated from the tailings mass and drain to residual saturation, which appears to be about 17% by weight. In the tailings mass, water extends above the water table, due to surface tension, manifesting in a zone of higher saturation called the "capillary fringe." The tailings in the lysimeter in the control test plot are not at residual saturation because, being not covered, they are exposed to influx of water by precipitation.

Summary and conclusions

Two computer models were used in the hydrologic analysis of a composite soil cover constructed on the Waite Amulet

Fig. 7. Water content of the composite soil cover at Waite Amulet, Quebec.

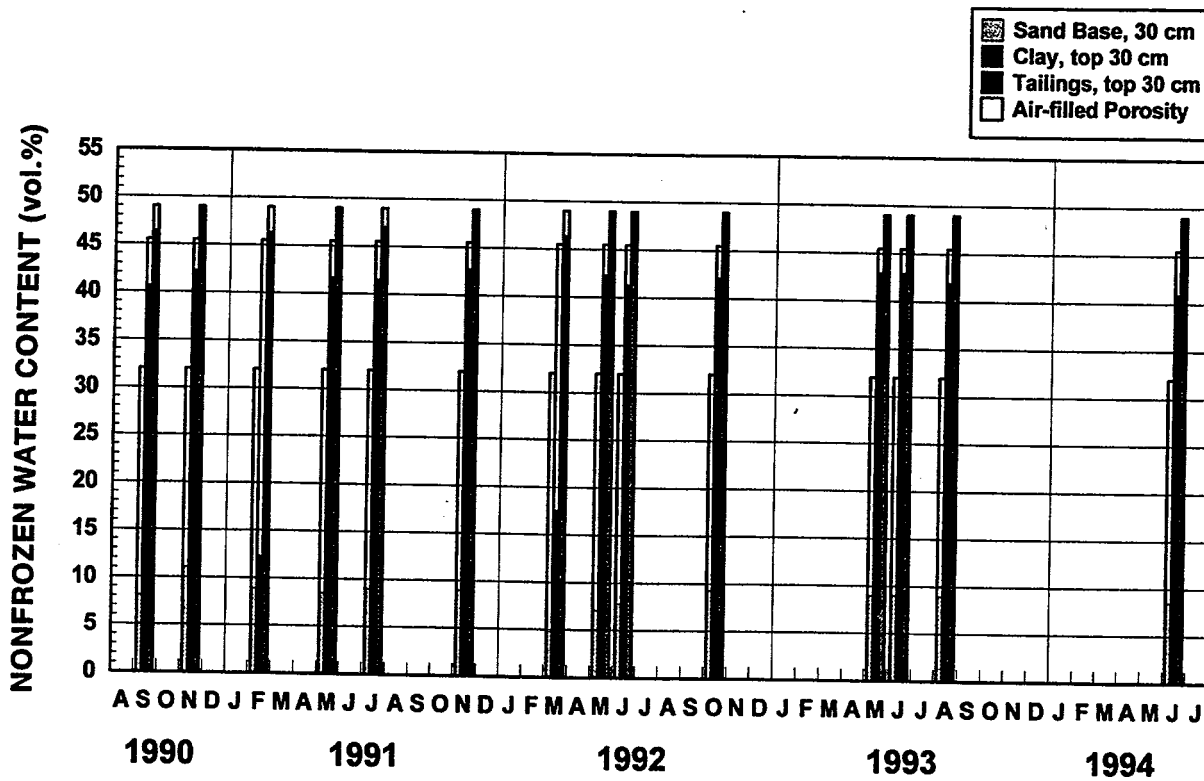
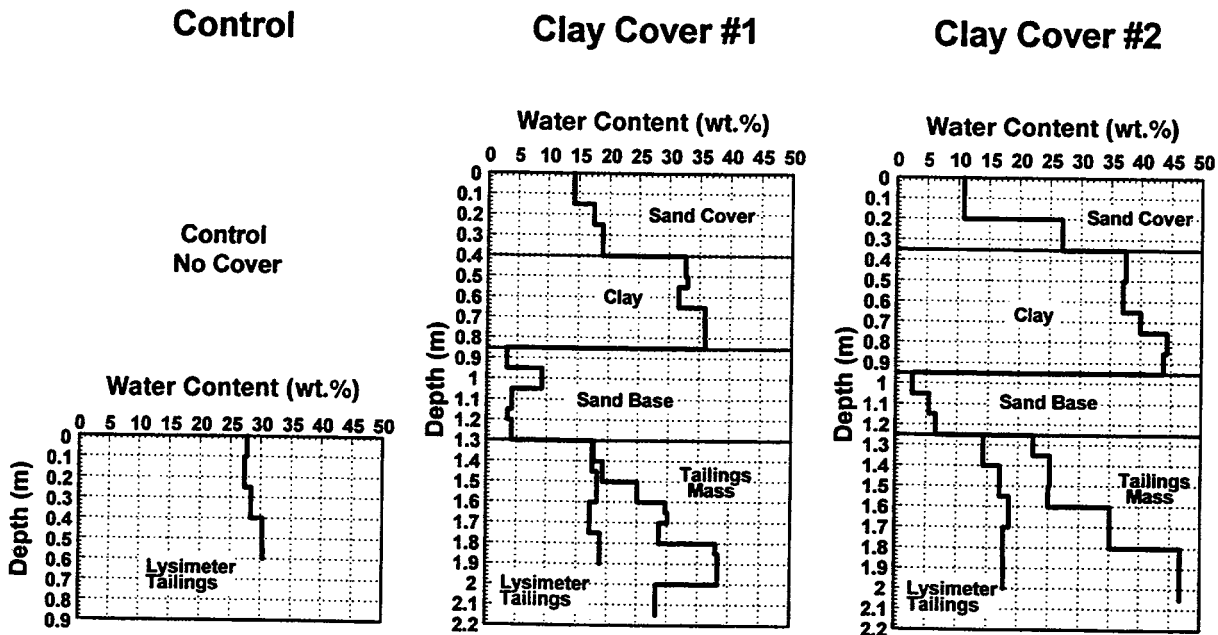


Fig. 8. Gravimetric water content measurements in June 1993.



tailings, near Rouyn-Noranda, Quebec. The model predictions were corroborated by field measurements of percolation, evaporation, and soil water content. The Hydrologic Evaluation of Landfill Performance (HELP) model was used to evaluate the effectiveness of the cover at four meteorological stations surrounding the site, within a 400–500 km radius. The HELP modelling showed that approximately 56% of average annual precipitation evaporates and 11% runs off. The amount available for subsurface flow is therefore

33% of precipitation. Using 33% of the precipitation at Amos, Quebec, as a surface boundary condition in saturated–unsaturated flow modelling, it was determined that 34.4 mm of water would percolate through the cover. HELP modelling determined that 38 mm would percolate through the cover. The modelling exercises predict that 4% of precipitation percolates through the cover. Field lysimeter measurements indicate that 4% of precipitation percolates through the cover. Both modelling methods also

indicate the sand base will drain and the clay will remain at a high water saturation. Four years of monitoring data confirm the modelling results. Field measurements of hydraulic conductivity over 3 years did not reveal any increase in the hydraulic conductivity of the clay (Yanful et al. 1993). These results suggest that a properly designed and constructed soil cover can reduce acid production in sulphide-bearing mine tailings located in the region of eastern Ontario and western Quebec. The modelling and field experiments were conducted with a nonvegetated cover; therefore, the effect of revegetation was not evaluated. Reclamation of tailings ponds using soil covers may, however, require the inclusion of a sustainable vegetation. This could affect the overall water percolation and should be considered in the analysis.

Acknowledgements

This project has been funded by Noranda Minerals Inc., Canada Centre for Mineral and Energy Technology (CANMET) and the Centre de recherches minérales under the MEND (Mine environment Neutral Drainage) program. B. Aubé of Noranda Technology Centre (NTC) performed the SEEP/W modelling. The authors also gratefully acknowledge discussions with L. St-Arnaud of NTC, who also reviewed the manuscript.

References

- Geo-slope International. 1992. SEEP/W version 2. Geo-slope International Ltd., Calgary, Alta.
- Grace Dearborn Inc. 1993. HELP model for windows, version 2.05. Grace Dearborn Inc., Mississauga, Ont.
- Nicholson, R.V., Gillham, R.W., Cherry, J.A., and Reardon, E.J. 1989. Reduction of acid generation in mine tailings through the use of moisture-retaining cover layers as oxygen barriers. *Canadian Geotechnical Journal*, 26: 1-8.
- Rasmuson, A., and Eriksson, J.-C. 1986. Capillary barriers in covers for mine tailings. National Swedish Environmental Protection Board, Report 3307.
- Schroeder, P.R., Morgan, J.M., Walski, T.M., and Gibson, A.C. 1984. The Hydrologic Evaluation of Landfill Performance (HELP) Model. U.S. Environmental Protection Agency, Office of Solid Waste and Emergency Response, Washington, D.C.
- Topp, G.C., Davis, J.L., and Annan, A.P. 1980. Electromagnetic determination of soil water content: measurement in coaxial transmission lines. *Water Resources Research*, 16(3): 574-582.
- Woyschner, M.W., and St-Arnaud, L.C. 1994. Hydrological evaluation and water balance of a thickened-tailings deposit near Timmins, ON. *In Proceedings of the International Land Reclamation and Mine Drainage Conference and 3rd International Conference on the Abatement of Acidic Drainage. Vol. 2, Mine Drainage. United States Bureau of Mines, Special Publication SP 06B-94, pp. 198-207.*
- Yanful, E.K. 1991. Engineered soil covers for reactive tailings management: Theoretical concepts and laboratory development. *In Proceedings of the 2nd International Conference on the Abatement of Acid Drainage, Sept. 16-18, 1991, Montréal. Sponsored by MEND (Mine Environment Neutral Drainage) Program. Vol. 1, pp. 461-485.*
- Yanful, E.K. 1993. Oxygen diffusion through soil covers on sulphidic mill tailings. *ASCE Journal of Geotechnical Engineering*, 119(8): 1207-1228.
- Yanful, E.K., and Aubé, B. 1993. Modelling moisture-retaining soil covers. *Proceedings of the Joint Canadian Society of Civil Engineers - American Society of Civil Engineers National Conference on Environmental Engineering, 12-14 July, Montréal, Canada, pp. 273-280.*
- Yanful, E.K., and St-Arnaud, L.C. 1991. Design, instrumentation and construction of engineered soil covers for reactive tailings management. *In Proceedings of the 2nd International Conference on the Abatement of Acid Drainage, Sept. 16-18, 1991, Montréal. Sponsored by MEND (Mine Environment Neutral Drainage) Program. Vol. 1, pp. 487-504.*
- Yanful, E.K., Woyschner, M.R., and Aubé, B.C. 1993. Field evaluation of the effectiveness of engineered soil covers for reactive tailings. *Submitted to MEND (Mine Environment Neutral Drainage) program. Supply and Services Canada contract number 23440-0-9061/01-SQ.*